НАУЧНО-ПРАКТИЧЕСКИЙ ЖУРНАЛ

БСМ

ISSN 1682-0363 (print)
ISSN 1819-3684 (online)

БЮЛЛЕТЕНЬ СИБИРСКОЙ МЕДИЦИНЫ

BULLETIN OF SIBERIAN MEDICINE

BSM

Том 23
№ 1. 2024

300 ЛЕТ РОССИЙСКОЙ АКАДЕМИИ НАУК

В 2024 г. Российская академия наук отмечает 300-летие. За три столетия истории академии менялись ее состав, государственный статус, научная направленность. Но одно оставалось неизменным — роль академии наук как главного научного учреждения страны.

За годы своего правления последний царь и первый император Петр Первый сделал многое для России: создал флот, основал академию наук, построил на болотистой местности целый город! Академия наук стала родоначальницей всей системы научной деятельности в стране. Россия взяла курс на науку и образование.

Лаврентий Лаврентьевич Блюментрост

Еще до официального открытия академии наук император стал активно разрабатывать элементы будущей инфраструктуры. Первым делом Петр Первый сделал общедоступным свое личное собрание книг и нанял библиотекаря, который должен был следить за собранием и пополнять его. Также в 1714 г. Петр организовал публичный музей – Кунсткамеру, фонды которого содержали различные редкости. В документах об учреждении Академии наук и художеств Кунсткамера рассматривалась как неотъемлемая часть академии наук, а фонд — как инструмент, способствующий деятельности академиков.

В наши дни мы отмечаем день основания академии наук как День российской науки — 8 февраля. Именно 8 февраля 1724 г. (28 января по старому стилю) Сенат опубликовал указ об учреждении «Академии, или Социетета художеств и наук». Однако сам Петр Первый не успел торжественно открыть академию. Это сделала его вторая жена императрица Екатерина I в декабре 1725 г.

Первым президентом академии наук стал лейб-медик Лаврентий Блюментрост. Несмотря на свои иностранные корни, Блюментрост первое время оставался единственным из академиков, родившимся в России. При подготовке документов об учреждении академии наук он руководствовался установками императора и успешно вел дела от его имени, а затем и от имени императрицы Екатерины.

Спустя 12 лет после основания академии наук известный французский физик Дорту де Меран писал: «Петербургская академия со времени своего рождения поднялась на выдающуюся высоту науки, до которой академии Парижская и Лондонская добрались только за 60 лет упорного труда».

Во все времена академическое сообщество осознавало главную цель академии наук: расширять пределы человеческих знаний, развивать науки, обогащать их новыми открытиями и просвещать человечество. Ведь наука была и остается двигателем прогресса.

Информация взята с портала «Научная Россия» (https://scientificrussia.ru/)

BULLETIN OF SIBERIAN MEDICINE

Peer-reviewed scientific-practical journal
Issued quarterly

Volume 23, No. 1, 2024

ISSN 1682-0363 (print)
ISSN 1819-3684 (online)

FOUNDER AND PUBLISHER:
Siberian State Medical University, Ministry of Healthcare of the Russian Federation

Registered by the Ministry of Mass Media and Communications of the Russian Federation
Certificate of registration
No. 77-7366 of 26.03.2001

The journal "Bulletin of Siberian Medicine" is included in the list of peer-reviewed scientific journals and publications issued in the Russian Federation, which should publish main scientific results of doctoral and Candidate of Sciences theses

Bulletin of Siberian Medicine is indexed in:
Scopus
Web of Science (WoS (ESCI))
Science Index
RSCI
Ulrich's International Periodicals Directory
Cyberleninka
DOAS

Editorial Board Office:
107, Lenina Av., Tomsk, 634050, Russian Federation
Telephone: +7-(382-2)-51-41-53.
http://bulletin.ssmu.ru
E-mail: bulletin.tomsk@mail.ru

Publisher: Siberian State Medical University.
2, Moscow Trakt, Tomsk, 634050,
Russian Federation.
Editors: E.E. Stepanova, Yu.P. Gotfrid
Translators: M.E. Orlova, K.Yu.Skvortsova
Electronic makeup, cover design
L.D. Krivtsova

Printed in Litburo LLC,
4, Koroleva Str., Tomsk, 634055, Russian Federation

Signed to print on 29.03.2024
Format 60 × 84/8. Offset print.
Coated paper. Times font.
P.s. 21,9. C.p.s. 21,0.
500 copies. Order No. 123.

The price – free.
Date of publication 29.03.2024.

БЮЛЛЕТЕНЬ СИБИРСКОЙ МЕДИЦИНЫ

Научно-практический журнал
Выходит 4 раза в год

Том 23, № 1, 2024

ISSN 1682-0363 (print)
ISSN 1819-3684 (online)

УЧРЕДИТЕЛЬ И ИЗДАТЕЛЬ:
ФГБОУ ВО «Сибирский государственный медицинский университет» Минздрава России

Журнал основан в 2001 году
Зарегистрирован в Министерстве РФ по делам печати, телерадиовещания и средств массовых коммуникаций
Свидетельство регистрации ПИ № 77-7366 от 26.03.2001 г.

Журнал входит в Перечень ведущих рецензируемых научных журналов и изданий, выпускаемых в РФ, в которых должны быть опубликованы основные научные результаты диссертаций на соискание ученой степени доктора и кандидата наук

Индексация:
Scopus
Web of Science (WoS (ESCI))
РИНЦ (Science Index)
RSCI
Ulrich's International Periodicals Directory
Cyberleninka
DOAS

Редакция:
634050, г. Томск, пр. Ленина, 107.
Тел.: (382-2)-51-41-53.
http://bulletin.ssmu.ru
E-mail: bulletin.tomsk@mail.ru

Оригинал-макет:
Издательство СибГМУ.
634050, г. Томск, Московский тракт, 2.
Редакторы: Е.Е. Степанова, Ю.П. Готфрид
Перевод: М.Е. Орлова, Дж. Палацца
Электронная верстка, дизайн обложки Л.Д. Кривцова

Отпечатано в ООО «Литбюро»,
634055, г. Томск, ул. Королёва, 4.

Подписано в печать 29.03.2024 г.
Формат 60 × 84/8. Печать офсетная.
Бумага мелованная. Гарнитура «Times».
Печ. л. 21,9. Усл. печ. л. 21,0.
Тираж 500 экз. Заказ 123.

Цена – свободная.
Дата выхода в свет 29.03.2024.

СОДЕРЖАНИЕ

CONTENTS

ОБЗОРЫ И ЛЕКЦИИ

REVIEWS AND LECTURES

Dear authors and readers of the journal,

Olga I. Urazova
Editor-in-Chief, Dr. Sci. (Med.), Professor,
Corresponding Member of RAS,
Head of the Pathophysiology Division

In 2024, we continue to follow through on the priorities of the state policy in developing domestic science and technology by publishing articles on advanced areas of medical and biological research in Russia and globally.

Following the effective government strategy on attracting talented youth to research and development, we expect growing interest of young scientists and doctors in research and an increase in their publication activity, including publications in this journal.

The journal will strive to keep its international format and a leading position in modern biomedical science. Moreover, we set ambitious goals to get in the list of world's top high impact factor journals. But to achieve this goal, we will certainly need your interest and experience. In addition, your work and desire to share the results of your research will serve as a good example for students and young researchers who do not yet have significant scientific achievements and awards but already show great potential in science.

I wish all authors and readers success and new meaningful and interesting publications! I express my deepest gratitude to the members of the editorial board and the staff of the journal for their commitment to the traditions of the journal and their invaluable contribution to its development!

УДК 616.24-002-039.57-036.88-07-037
https://doi.org/10.20538/1682-0363-2024-1-7-14

Comparative analysis of the prognostic value of CURB-65 and CRB-65 scores and their modifications in assessing in-hospital mortality in patients with community-acquired pneumonia

Vinokurova D.A.[1], Kulikov E.S.[1], Fedosenko S.V.[1], Gubareva A.M.[1], Pshevorskaya E.V.[1], Osipov P.V.[1], Arzhanik M.B.[1], Starovoitova E.A.[1], Arzhanik A.A.[2]

[1] *Siberian State Medical University*
2, Moscow Trakt, Tomsk, 634050, Russian Federation

[2] *Credit Bank of Moscow*
Build. 1, 2, Lukov Lane, Moscow, 107045, Russian Federation

ABSTRACT

Background. Mortality associated with community-acquired pneumonia (CAP) continues to be a crucial health problem worldwide. Correct assessment of CAP severity and the level of care is pivotal in the disease outcome.

Aim. To evaluate the prognostic value of the CURB-65 and CRB-65 scores and their modifications in determining the risk of in-hospital mortality in patients with CAP.

Materials and methods. The retrospective study included 1,412 patients with CAP aged over 18 years. In a population of 1,020 patients, which was subsequently split into test (n = 676) and training (n = 344) samples in the ratio 2 : 1, we compared the predictive value of the CURB-65 (confusion, urea > 7 mmol / l, respiratory rate ≥ 30 / min, low blood pressure (BP), and age ≥ 65 years) and CRB-65 (confusion, respiratory rate ≥ 30 / min, low blood pressure (BP), and age ≥ 65 years) scores in identifying patients at high risk of in-hospital death. The specified scoring systems were modified by changing the cut-offs for each criterion to increase their accuracy. For comparison, we used the ROC analysis with the calculation of the area under the curve (AUC).

Results. The modified CURB-65 score with new cut-off values (age > 72 years, respiratory rate > 21 / min, urea level > 9.5 mmol / l, systolic blood pressure ≤ 105 mm Hg, and diastolic blood pressure ≤ 65 mm Hg) was more accurate than the original one in predicting death and was named CURB-72. The AUC for CURB-72 and CURB-65 was 0.946 (95% confidence interval (CI): 0.916–0.967) and 0.905 (95% CI: 0.869–0.934), respectively (p = 0.0034). The modified CRB-65 (CRB-72) score also outperformed the original model, but showed no statistically significant difference. While comparing the modified scoring systems, the new CURB-72 score surpassed the CRB-72 score and demonstrated maximum accuracy in identifying CAP patients at risk of in-hospital mortality (p = 0.0347).

Conclusion. The modified CURB-65 (CURB-72) and CRB-65 (CRB-72) scores demonstrated potential for assessing the prognosis of CAP and are superior to classical scoring systems. CURB-72 showed the highest sensitivity and specificity.

Keywords: community-acquired pneumonia, pneumonia, CRB-65, CURB-65, mortality, prognosis, pneumonia, scores

Conflict of interest. The authors declare the absence of obvious or potential conflicts of interest related to the publication of this article.

Source of financing. The authors state that they received no funding for the study.

Conformity with the principles of ethics. All patients signed an informed consent to participate in the study. The study was approved by the Ethics Committee at Siberian State Medical University (Protocol No. 5789 of 26.02.2018).

For citation: Vinokurova D.A., Kulikov E.S., Fedosenko S.V., Gubareva A.M., Pshevorskaya E.V., Osipov P.V., Arzhanik M.B., Starovoitova E.A., Arzhanik A.A. Comparative analysis of the prognostic significance of the CURB-

✉ *Vinokurova Daria A.,* vinokurovadarial@gmail.com

65 and CRB-65 scores and their modifications in hospital mortality assessment in patients with community-acquired pneumonia. *Bulletin of Siberian Medicine.* 2024;23(1):7–14. https://doi.org/10.20538/1682-0363-2024-1-7-14.

Сравнительный анализ прогностической значимости шкал CURB-65, CRB-65 и их модификаций в оценке госпитальной летальности у пациентов с внебольничной пневмонией

Винокурова Д.А.[1], Куликов Е.С.[1], Федосенко С.В.[1], Губарева А.М.[1], Пшеворская Е.В.[1], Осипов П.В.[1], Аржаник М.Б.[1], Старовойтова Е.А.[1], Аржаник А.А.[2]

[1] *Сибирский государственный медицинский университет (СибГМУ)*
Россия, 634050, г. Томск, Московский тракт, 2

[2] *ПАО «Московский кредитный банк»*
Россия, 107045, г. Москва, Луков переулок, 2, стр. 1

РЕЗЮМЕ

Введение. Смертность от внебольничной пневмонии (ВП) остается серьезной проблемой систем здравоохранения разных стран. Правильная оценка тяжести и места лечения больного имеет решающее значение в исходе заболевания.

Цель. Оценить прогностическую значимости шкал CURB-65 и CRB-65 с их модификацией в определении риска смерти у госпитализированных больных с ВП.

Материалы и методы. В ретроспективное исследование включили 1 412 пациентов с ВП старше 18 лет. На популяции 1 020 больных, с последующим разделением на тестовую (n = 676) и обучающую (n = 344) выборки 2 : 1, выполнено сравнение прогностической ценности шкал CURB-65 (спутанность сознания, мочевина > 7 ммоль/л, частота дыхания ≥ 30/мин, низкое артериальное давление (АД) и возраст ≥ 65 лет) и CRB-65 (исключена мочевина) в идентификации пациентов с высоким риском госпитальной смерти. Проведена модификация указанных шкал с изменением точек разделения по каждому из критериев для повышения их точности. Для сравнения использовался анализ ROC-кривых с вычислением AUC (площади под кривой).

Результаты. Модифицированная шкала CURB-65 с новыми точками разделения (возраст > 72 лет, частота дыхания > 21/мин, уровень мочевины > 9,5 ммоль/л, систолическое АД ≤ 105 мм рт. ст. и диастолическое АД ≤ 65 мм рт. ст.) оказалась точнее исходной в прогнозировании смерти и названа CURB-72. Для CURB-72 и CURB-65 AUC составила 0,946 (95%-й доверительный интервал (95% ДИ) 0,916–0,967) и 0,905 (95% ДИ 0,869–0,934) соответственно (p = 0,0034). Измененная модель CRB-65 (CRB-72) также превзошла исходную, но статистически значимо они не различались. При сравнении модифицированных шкал между собой новая шкала CURB-72 продемонстрировала максимальную точность в выявлении пациентов с ВП с риском госпитальной летальности, превзойдя CRB-72 (p = 0,0347).

Заключение. Модифицированные CURB-65 (CURB-72) и CRB-65 (CRB-72) демонстрируют потенциал в оценке прогноза ВП и превосходят классические шкалы, при этом CURB-72 демонстрирует наибольшую чувствительность и специфичность.

Ключевые слова: внебольничная пневмония, CRB-65, CURB-65, смерть, прогноз, пневмония, шкалы

Конфликт интересов. Авторы декларируют отсутствие явных и потенциальных конфликтов интересов, связанных с публикацией настоящей статьи.

Источник финансирования. Авторы заявляют об отсутствии финансирования при проведении исследования.

Соответствие принципам этики. Все пациенты подписали информированное согласие на участие в исследовании и обработку персональных данных. Исследование одобрено этическим комитетом СибГМУ (заключение № 5789 от 26.02.2018).

Для цитирования: Винокурова Д.А., Куликов Е.С., Федосенко С.В., Губарева А.М., Пшеворская Е.В., Осипов П.В., Аржаник М.Б., Старовойтова Е.А., Аржаник А.А. Сравнительный анализ прогностической значимости шкал CURB-65, CRB-65 и их модификаций в оценке госпитальной летальности у пациентов с внебольничной пневмонией. *Бюллетень сибирской медицины.* 2024;23(1):7–14. https://doi.org/10.20538/1682-0363-2024-1-7-14.

INTRODUCTION

Community-acquired pneumonia (CAP) remains one of the main causes of high morbidity, mortality, and high costs for healthcare systems in different countries [1, 2]. According to the 2016 Global Burden of Disease Study, more than 336 million episodes of lower respiratory tract infections (LRTIs) were reported worldwide, corresponding to 65.9 million hospitalizations and 2,377,697 deaths [3]. Despite modern advances in medicine, a deep understanding of the etiology and pathogenesis of the disease, and possibilities of antibacterial therapy, according to the World Health Organization, LRTIs ranked fourth among all causes of death in 2019 [4].

One of the key stages for a favorable outcome in CAP is an initial assessment of the severity and prognosis of the disease, allowing the doctor to determine the level of care, the volume of necessary research, and the intensity of therapy.

There are a number of systems for assessing the prognosis of CAP in the world. The most popular among them are the Pneumonia Severity Index (PSI) [5] and the CURB-65 score (confusion; urea > 7 mmol / l; respiratory rate ≥ 30 / min; systolic blood pressure (SBP) (< 90 mm Hg) or diastolic blood pressure (DBP) (< 60 mm Hg); and age ≥ 65 years) [6].

Both scoring systems were developed to facilitate decisions on the level of care based on the risk of a poor outcome in CAP. At the same time, PSI consists of 20 variables, including such laboratory tests as blood pH, which, in some cases, complicates its practical application. This scoring system classifies patients into five risk classes depending on the severity of the disease (based on the score) and assumes outpatient treatment for patients of risk classes I–II, short-term hospitalization for patients of risk class III, and full hospitalization for risk classes IV and V (with a high probability of resuscitation and intensive care (ICU) for the latter).

The CURB-65 score classifies patients into low-, intermediate-, and high-risk groups based on only five parameters, each of which is attributed one point. Patients with score 0–1 should be treated as outpatients, with score 2 are indicated short-term hospitalization, with score 3–5 – hospitalization with a high probability of transfer to the intensive care unit (ICU) with the maximum score [6]. The CRB-65 score, a simplified version of the CURB-65, does not include blood urea assessment and can be determined in just a few minutes at any stage of care. In this case, low-risk group is assigned to patients with score 0, intermediate-risk group – to patients with score 1–2, and high-risk group – to patients with score 3 and 4 [6].

There is no doubt that emergency room doctors with high work intensity and patient flow do not always resort to predictive models to make decisions on where to treat a patient. So, according to S.A. Rachina et al. (2016), doctors in Russian hospitals use both scores in routine practice only in isolated cases [7]. Foreign colleagues also come to disappointing conclusions. So, in the study by D.J. Serisier et al. (2013) involving practicing doctors, only 11.8% of pulmonologists and 21% of emergency room doctors were able to correctly determine severity classes on the PSI score. 20.4% of pulmonologists and 15% of emergency room doctors were able to perform the CURB-65 assessment successfully [8]. Thus, it is obvious that more complex scores, which include many parameters for assessment, are more likely to remain unclaimed in real clinical practice.

The aim of this study was to assess the prognostic value of the CURB-65 and CRB-65 scoring systems in hospitalized patients with CAP in determining the risk of an unfavorable outcome of the disease, followed by modification of these scoring systems to improve their accuracy.

MATERIALS AND METHODS

A retrospective study using a continuous sampling method included data obtained from 1,412 patients aged 18 years and older, hospitalized in emergency hospitals in Tomsk with a diagnosis of CAP in 2017. The study did not include patients with nosocomial pneumonia, pulmonary tuberculosis, malignant tumors of the lungs, and radiologically confirmed septic pneumonia. All patients signed an informed consent to participate in the study and for personal data processing. The study was approved by the Ethics Committee at Siberian State Medical University (Protocol No. 5789 of 26.02.2018).

Within this study, we assessed > 200 parameters, including features of the CAP development, data on the socio-demographic status, complaints, medical history, objective status, results of laboratory and instrumental studies, information about treatment at the pre-hospital and in-hospital stages, and information about the course of the disease during hospitalization and outcomes. The article provides a comparative assessment of the prognostic value of the CURB-65 and CRB-65 scores in identifying patients with an increased risk of in-hospital death. Modification of these scoring systems was also carried out with

changes in the cut-off value for each of the criteria to increase their accuracy. To evaluate parameters for each of the scoring systems, we included physical examination data, blood urea level (for CURB-65), and age determined at the time of patient admission to the emergency room.

The analysis of the obtained data was carried out using the statistical software package MedCalc, version 18.9.1. Quantitative variables were presented as the median and the interquartile range *Me* (Q_{25}; Q_{75}), qualitative variables – as absolute and relative frequencies *n* (%). To analyze the prognostic value of the CURB-65 and CRB-65 scores, the ROC analysis was used with calculating the area under the curve (AUC) and 95% confidence interval (CI) for AUC, determining the cut-off value using the Youden index and sensitivity and specificity for this point, as well as establishing the statistical significance of differences between AUCs for scoring systems and their modifications. The results were considered statistically significant at $p < 0.05$.

RESULTS

The study analyzed data obtained from 1,412 people (790 men (55.9%) and 622 women (44.1%)). The age of the patients was 61 (40; 76) years (from 18 to 103 years). In-hospital mortality was registered for 128 (9.1%) patients. A comparative assessment of the CURB-65 and CRB-65 scoring systems was carried out on the population of 1,020 patients with CAP.

The risk of death increased directly with an increase in scores for each scoring system (Table 1).

Table 1

Relationship between the number of unfavorable factors (score) and the risk of in-hospital death, *n* = 1,020

	Score	Discharged, *n* (%)	Died, *n* (%)
CURB-65	0	137 (100)	0 (0)
	1	98 (97.0)	3 (3)
	2	64 (87.7)	9 (12.3)
	3	13 (56.5)	10 (43.5)
	4	2 (25.0)	6 (75.0)
	5	0 (0)	2 (100)
CRB-65	0	170 (99.4)	1 (0.6)
	1	121 (93.8)	8 (6.2)
	2	21 (65.6)	11 (34.8)
	3	1 (11.1)	8 (88.9)
	4	1 (33.3)	2 (64.7)

Next, the general sample (*n* = 1,020) was split into test (*n* = 676) and training (*n* = 344) subsets in the ratio 2:1. No statistically significant differences were observed between them.

To compare the predictive value of the scoring systems, ROC curves were constructed for the general sample (Fig. 1) and for the test sample (Fig. 2). In both cases, AUC for the CURB-65 score was greater than for the CRB-65 score and was 0.870 (95% CI: 0.848–0.890) for CURB-65 and 0.839 (95% CI: 0.815–0.861) for CRB-65 ($p = 0$ .0036) in the general sample, and 0.905 (95% CI: 0.869–0.934) and 0.889 (95% CI: 0.851–0.920) in the test sample, respectively ($p = 0.3692$). In the test sample, the differences between the curves were subtle and not significant.

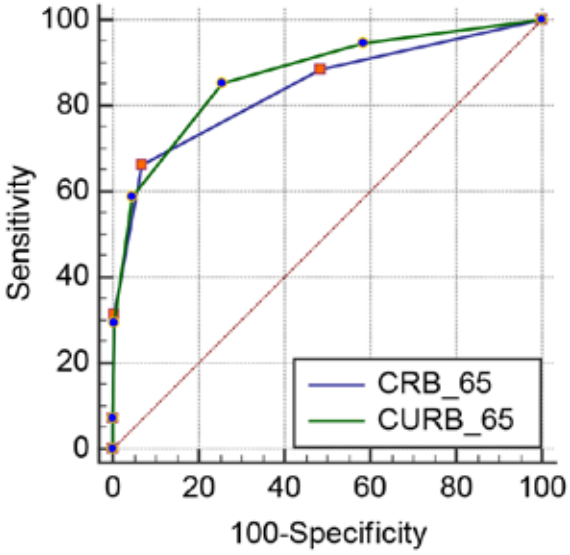

Fig. 1. Comparison of the ROC curves for the CURB-65 and CRB-65 scores in the general sample

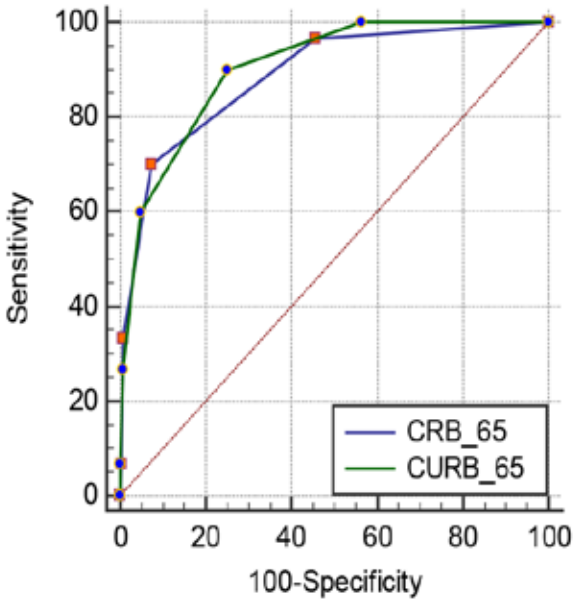

Fig. 2. Comparison of the ROC curves for the CURB-65 and CRB-65 scores in the test sample

The study hypothesized that modification of the scoring systems would increase their diagnostic value. To test this hypothesis on the test subset, the ROC analysis was performed for each of the factors, searching for the most accurate cut-offs. As a result, new cut-off values for each parameter were obtained in the study population (Table 2).

Table 2

Cut-off values in the classical and modified CURB-65 and CRB-65 scoring systems

Parameter	Classical CURB-65/ CRB-65 scores	Modified s CURB-72*/ CRB-72* scores
Age, years	> 65	> 72
Cognitive impairment	Yes	Yes
Blood urea, mmol / l	> 7	> 9.5
Respiratory rate, min	> 30	> 21
Systolic blood pressure, mm Hg	< 90	< 105
Diastolic blood pressure, mm Hg	< 60	< 65

*due to the new cut-off value based on age > 72 years, the modified scores were given the names CURB-72 and CRB-72.

ROC curves were constructed for each of the modified scoring systems in the test sample and compared with the ROC curves constructed for the classical scores (Fig. 3, 4)

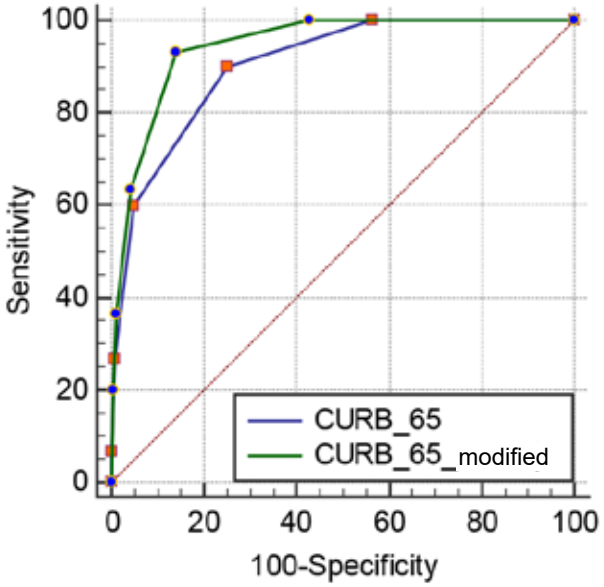

Fig. 3. Comparison of the ROC curves for the CURB-65 and modified CURB-65 (CURB-72) scores

AUC for the modified CURB-72 score surpassed the one for the classical CURB-65 model and was 0.946 (95% CI: 0.916–0.967) and 0.905 (95% CI: 0.869–0.934), respectively (p = 0.0034). When CRB-65 was modified to CRB-72, AUC increased from 0.889 (95% CI: 0.851–0.920) to 0.910 (95% CI: 0.874–0.938) but was not significantly different (p = 0.0724).

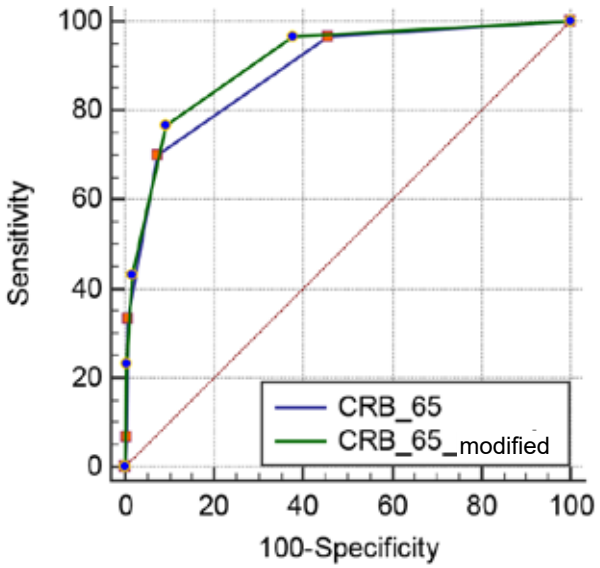

Fig. 4. Comparison of the ROC curves for the CRB-65 and modified CRB-65 (CURB-72) scores

The new CURB-72 score demonstrated maximum accuracy in identifying patients with CAP at risk of in-hospital mortality, surpassing CRB-72 (p = 0.0347) (Fig. 5).

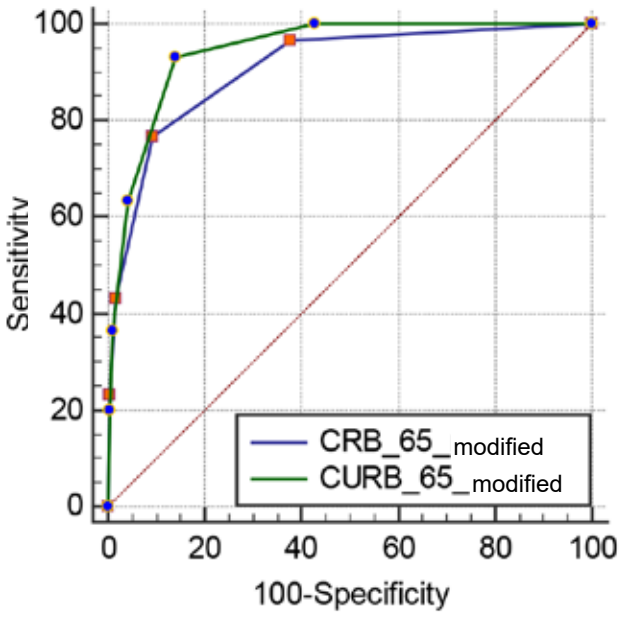

Fig. 5. ROC curves comparing the modified CURB-65 (CURB-72) and CRB-65 (CRB-72) scores

The cut-off value for both scoring systems (both modified and classical) was > 1 point. As a result, the modified CURB-65 score (CURB-72) with the

modified cut-off values showed the highest sensitivity and specificity (Table 3), which allowed for the most accurate identification of not only patients at high risk of death, but also patients with a favorable prognosis of the disease. Implementation of the proposed modified scoring system in routine clinical practice can reduce the burden on hospitals by redistributing low-risk patients to outpatient treatment.

Table 3

Characteristics of the ROC curves for the classical and modified CRB-65 and CURB-65 scores

Score	AUC, 95% CI	Sensitivity	Specificity
CRB-65	0.889 (0.851–0.920)	70.00	92.68
CURB-65	0.905 (0.869–0.934)	90.00	74.84
Modified scores			
CRB-72	0.910 (0.874–0.938)	76.67	90.76
CURB-72	0.946 (0.916–0.967)	93.33	85.99

DISCUSSION

W.S. Lim et al. (2003) developed and validated the CURB-65 and CRB-65 scoring systems for predicting 30-day mortality in patients with CAP. In the study population (n = 1,068), 9% of patients died [6].

The present study assessed outcomes only during hospitalization, which lasted 11 (9; 13.6) days, and did not track the health status of discharged individuals (n = 1,412). Among the patients included in the study, 9.1% died.

In the general sample in the present study, the mortality rate in patients with the CURB-65 score of ≥ 2 was slightly higher than in the study by W.S. Lim et al. [6]. Scientists demonstrated that among CAP patients with the CURB-65 score of 2, death occurred in 9.2% of cases (intermediate risk of death), with the score of ≥ 3 – in 22% (high risk of death). In our work, in patients with the score of 2, mortality was 12.3%, with the score of 3 – 43.5%. There were only two patients with the score of 5, and both of them died (Table 1).

In addition, W.S. Lim et al. concluded that low-risk patients (CURB-65 score of < 2 and CRB-65 score of < 1) can be provided with outpatient care. At the same time, according to our data, among patients with the CURB-65 score of 1, three (3%) died, and in the group with the CRB-65 score of 0, death was registered in one case, and, according to the decision-making strategy, these patients had to be treated in the outpatient setting [6]. Our results suggest that the predictive ability of the CURB-65 and CRB-65 scoring systems is not perfect. The opinions of other scientists on the significance of these scoring systems in identifying patients with mild CAP are ambiguous, and a number of studies question their accuracy [9, 10].

Thus, according to A. Ilg et al. (2019), among patients with the CURB-65 scores of 0 and 1, 15.6% were hospitalized in the intensive care unit, and 0.6% died [10]. At the same time, according to the meta-analysis by M.H. Ebell et al. (2019), the authors concluded that the CRB-65 score is effective in identifying patients at low risk of death and demonstrated that when this scoring system is applied to stratify patients, the risk of outpatient mortality in this group of patients is no more than 0.5% [11].

In the study, we came to the conclusion that the cut-off value for both scoring systems is > 1, and if at least one criterion in both the CURB-65 and CRB-65 scores is identified, the patient undoubtedly requires hospitalization. When comparing the CURB-65 and CRB-65 scores with each other, the former outperformed the latter in the general sample, but in the test sample, no differences were found.

The question of the significance of urea in the CURB-65 score remains open. According to various researchers, the CURB-65 and CRB-65 models demonstrate comparable value [12, 13]. So, in the meta-analysis by J.D. Chalmers et al. (2010), it was concluded that there are no significant differences between the scores in predicting death from CAP [14].

The present study demonstrated the maximum accuracy of the modified scales (CURB-72 and CRB-72) at higher blood pressure values and lower respiratory rates, which could result in an underestimated risk of death in classical scoring systems. In general, while the importance of assessing respiratory rate (as a sign of respiratory failure) is beyond doubt, the role of hypotension is the subject of debates and has been questioned by some scientists. So, H.Y. Li et al. (2015) demonstrated that CURB-65 can be simplified by excluding low blood pressure, which improves the prediction of mortality in patients with CAP [15]

In the population we studied, a decrease in SBP to a level of < 90 mm Hg was detected only in 34 (26.6%) of deceased patients. In turn, a decrease in DBP to a value of < 60 mm Hg was registered in 38 (29.7%) of the deceased. In addition, only 36 patients had a respiratory rate ≥ 30 / min. Moreover, out of 128 deceased patients, this criterion was identified only in 22 cases (17.2%). The data obtained were comparable to the results in the work by Q. Guo et al. (2023), where respiratory rate ≥ 22 / min and SBP ≤ 100 mm

Hg demonstrated higher odds ratio and greater reliability than generally accepted parameters of classical scoring systems (AUC 0.823 versus 0.519; 0.688 versus 0.622, respectively) [16].

Thus, respiratory rate ≥ 21 / min, SBP ≤ 105 mm Hg, and DBP ≤ 65 are more suitable for predicting mortality, as evidenced by significant improvements in AUC values for both scores. For urea, we concluded that the most accurate cut-off values should be higher than in the classical scores and amount to 9.5 mmol / l instead of 7 mmol / l.

The modified CURB-65 (CURB-72) score exhibited not only higher sensitivity in determining the risk of death, but also higher specificity, which allows to more accurately identify low-risk patients who can be treated in the outpatient setting, thus reducing the burden on hospitals. According to our data, the cut-off value for both modified scoring systems was > 1. That is, patients with the score of 1 or more should be hospitalized.

CONCLUSION

Given the high mortality associated with CAP, search for new ways to assess the risk of in-hospital death remains an important goal in modern science. The study proposed a new methodological approach to improve the predictive value of the CURB-65 and CRB-65 scores. We obtained results indicating that the modified CURB-65 (CURB-72) and CRB-65 (CRB-72) scores demonstrate potential in assessing the prognosis of CAP and surpass the classical scoring systems. At the same time, the CURB-72 score has maximum sensitivity and specificity. Further prospective studies with larger cohorts in different populations and settings are required.

REFERENCES

1. Prina E., Ranzani O.T., Torres A. Community-acquired pneumonia. *Lancet*. 2015;386(9998):1097–1108. DOI: 10.1016/S0140-6736(15)60733-4.
2. Torres A., Cillóniz C., Blasi F., Chalmers J.D., Gaillat J., Dartois N. et al. Burden of pneumococcal community-acquired pneumonia in adults across Europe: A literature review. *Respiratory Medicine*. 2018;137:6–13. DOI: 10.1016/j.rmed.2018.02.007.
3. GBD 2016 Lower Respiratory Infections Collaborators. Estimates of the global, regional, and national morbidity, mortality, and aetiologies of lower respiratory infections in 195 countries, 1990–2016: a systematic analysis for the Global Burden of Disease Study 2016. *Lancet Infect. Dis*. 2018;18(11):1191–1210. DOI: 10.1016/S1473-3099(18)30310-4..
4. World Health Organization. The top 10 causes of death. World Health Organization: Geneva, Switzerland, 2019 (in Russ.). URL: https://www.who.int/news-room/fact-sheets/detail/the-top-10-causes-of-death (accessed on 1 Dec 2023).
5. Fine M.J., Auble T.E., Yealy D.M., Hanusa B.H., Weissfeld L.A., Singer D.E. et al. A prediction rule to identify low-risk patients with community-acquired pneumonia. *The New England Journal of Medicine*. 1997;336(4):243–250. DOI: 10.1056/NEJM199701233360402.
6. Lim W.S., van der Eerden M.M., Laing R., Boersma W.G., Karalus N., Town G.I. et al. Defining community acquired pneumonia severity on presentation to hospital: an international derivation and validation study. *Thorax*. 2003;58(5):377–382. DOI: 10.1136/thorax.58.5.377.
7. Rachina S.A., Dekhnich N.N., Kozlov R.S., Bobylev A.A., Batishcheva G.A., Gordeeva S.A., et al. Severity assessment of community-acquired pneumonia in real clinical practice in a multiprofile hospital in Russia. *Pulmonologiya*. 2016;26(5):521–528 (in Russ.). DOI: 10.18093/0869-0189-2016-26-5-521-528.
8. Serisier D.J., Williams S., Bowler S.D. Australasian respiratory and emergency physicians do not use the pneumonia severity index in community-acquired pneumonia. *Respirology (Carlton, Vic.)*. 2013;18(2):291–296. DOI: 10.1111/j.1440-1843.2012.02275.x.
9. Ilg A., Moskowitz A., Konanki V., Patel P.V., Chase M., Grossestreuer A.V. et al. Performance of the CURB-65 Score in predicting critical care interventions in patients admitted with community-acquired pneumonia. *Annals of Emergency Medicine*. 2019;74(1):60–68. DOI: 10.1016/j.annemergmed.2018.06.017.
10. Hincapié C., Ascuntar J., León A., Jaimes F. Community-acquired pneumonia: comparison of three mortality prediction scores in the emergency department. *Colombia Medica (Cali, Colombia)*. 2021;52(4):e2044287. DOI: 10.25100/cm.v52i4.4287.
11. Ebell M.H., Walsh M.E., Fahey T., Kearney M., Marchello C. Meta-analysis of Calibration, Discrimination, and Stratum-Specific Likelihood Ratios for the CRB-65 Score. *Journal of General Internal Medicine*. 2019;34(7):1304–1313. DOI: 10.1007/s11606-019-04869-z.
12. Al Hussain S.K., Kurdi A., Abutheraa N., Al Dawsari A., Sneddon J., Godman B. et al. Validity of Pneumonia Severity Assessment Scores in Africa and South Asia: A Systematic Review and Meta-Analysis. *Healthcare (Basel, Switzerland).* 2021;9(9):1202. DOI: 10.3390/healthcare9091202.
13. Fernandes L., Arora A.S., Mesquita A.M. Role of semi-quantitative serum procalcitonin in assessing prognosis of community acquired bacterial pneumonia compared to PORT PSI, CURB-65 and CRB-65. *Journal of Clinical and Diagnostic Research: JCDR*. 2015;9(7):OC01–OC4. DOI: 10.7860/JCDR/2015/12468.6147.
14. Chalmers J.D., Singanayagam A., Akram A.R., Mandal P., Short P.M., Choudhury G. et al. Severity assessment tools for predicting mortality in hospitalised patients with community-acquired pneumonia. Systematic review and meta-analysis. *Thorax*. 2010;65(10):878–883. DOI: 10.1136/thx.2009.133280.
15. Li H.Y., Guo Q., Song W.D., Zhou Y.P., Li M., Chen X.K. et al. CUR-65 Score for community-acquired pneumonia predicted mortality better than CURB-65 score in

low-mortality rate settings. *The American Journal of the Medical Sciences*. 2015;350(3):186–190. DOI: 10.1097/MAJ.0000000000000545.
16. Guo Q., Li H.Y., Song W.D., Li M., Chen X.K., Liu H. et al. Updating cut-off values of severity scoring systems for community-acquired pneumonia to orchestrate more predictive accuracy. *Annals of Medicine*. 2023;55(1):62202414. DOI: 10.1080/07853890.2023.2202414.

Authors' contribution

Vinokurova D.A., Kulikov E.S. – conception and design; collection, analysis and interpretation of data; justification of the manuscript and critical revision of the manuscript for important intellectual content; final approval of the manuscript for publication. Fedosenko S.V., Starovoitova E.A. – critical revision of the manuscript for important intellectual content; final approval of the manuscript for publication. Gubareva A.M.., Pshevorskaya E.V., Osipov P.V. – collection, analysis, and interpretation of the data. Arzhanik A.A., Arzhanik M.B. – statistical processing of the data, analysis and interpretation of the data.

Authors' information

Vinokurova Daria A. – Head of the Internal Medicine Clinic, Teaching Assistant, Division of Intermediate-Level Therapy with a Course in Clinical Pharmacology, Siberian State Medical University, Tomsk, vinokurovadarial@gmail.com, http://orcid.org/0000-0002-8422-8349

Kulikov Evgeny S. – Dr. Sci. (Med.), Associate Professor, Professor, Division of General Medical Practice and Outpatient Therapy, Rector of Siberian State Medical University, Tomsk, evgeny.s.kulikov@gmail.com, http://orcid.org/0000-0002-0088-9204

Fedosenko Sergey V. – Dr. Sci. (Med.)., Associate Professor, Professor, Division of General Medical Practice and Outpatient Therapy, Siberian State Medical University, Tomsk, s-fedosenko@mail.ru, http://orcid.org/0000-0001-6655-3300

Gubareva Anastasia M. – Pulmonologist, Internal Medicine Clinic, Siberian State Medical University, Tomsk, anmigu@mail.ru, http://orcid.org/0009-0001-2576-3106

Pshevorskaya Ekaterina V. – Resident, Division of Intermediate-Level Therapy with a Course in Clinical Pharmacology, Siberian State Medical University, Tomsk, pskatlin@gmail.com, http://orcid.org/0009-0005-1250-0752

Osipov Pavel V. – Student, Siberian State Medical University; Tomsk, pirs50000@gmail.com, http://orcid.org/0009-0002-3760-1400

Arzhanik Marina B. – Cand. Sci. (Pedagogics), Associate Professor, Division of Medical and Biological Cybernetics, Siberian State Medical University, Tomsk, arzh_m@mail.ru, http://orcid.org/0000-0003-4844-9803

Starovoitova Elena A. – Dr. Sci. (Med.), Head of the Division of General Medical Practice and Outpatient Therapy, Siberian State Medical University, Tomsk, elena-starovoytova@yandex.ru, http://orcid.org/0000-0002-4281-1157

Arzhanik Alexandra A. – Developer, Credit Bank of Moscow, Moscow, arzh_sasha@mail.ru, http://orcid.org/0000-0003-4378-272X

(✉) **Vinokurova Daria A.,** vinokurovadarial@gmail.com

Received 12.12.2023;
approved after peer review 18.12.2023;
accepted 21.12.2023

УДК 616.895.8–085.214-073.97
https://doi.org/10.20538/1682-0363-2024-1-15-22

Comparative analysis of EEG in patients with schizophrenia receiving various atypical antipsychotics

Galkin S.A.[1], Kornetova E.G.[1, 2], Ivanova S.A.[1, 2]

[1] *Mental Health Research Institute, Tomsk National Research Medical Center (NRMC) of the Russian Academy of Sciences*
4, Aleutskaya Str., Tomsk, 634014, Russian Federation

[2] *Siberian State Medical University*
2, Moscow Trakt, Tomsk, 634050, Russian Federation

ABSTRACT

Aim. To conduct a comprehensive analysis of EEG recordings of schizophrenia patients receiving atypical antipsychotics as monotherapy.

Materials and methods. We examined 94 patients with schizophrenia aged 33 [28; 40] years with a disease duration of 10 [4; 15] years. The patients were divided into 5 groups depending on the antipsychotic drugs they took: 1) risperidone – 31 patients; 2) quetiapine – 20 patients; 3) aripiprazole – 11 patients; 4) olanzapine – 13 patients; 5) clozapine – 19 patients. EEG was recorded during wakefulness with closed eyes (background test), 3-minute hyperventilation, and rhythmic photostimulation in all patients. To describe and interpret the received recordings, the EEG classification according to J. Micoulaud – Franchi et al. was used.

Results. EEG modifications (score > 1A) were observed in 61.7% (n = 58) of patients. In the group of patients receiving risperidone, EEG modifications were found in 48.4% of cases, in patients taking quetiapine – in 70% of cases, aripiprazole – in 63.6% of cases, olanzapine – in 61.5% of cases, clozapine – in 73.7% of cases. The frequency of epileptiform patterns in patients receiving olanzapine was significantly higher than in those taking risperidone (p = 0.033) and clozapine (p = 0.032). Slowing in the EEG (score > 1) was more often observed in patients taking clozapine – 63.2% (n = 12), olanzapine – 61.5% (n = 8), and quetiapine – 60% (n = 12). Slower EEG waves were less common in patients receiving aripiprazole – 45.5% (n = 5) and risperidone – 45.2% (n = 14). In the group of patients with EEG slowing (score > 1), the dose of chlorpromazine equivalent was significantly greater compared to patients with normal EEG (p = 0.00046).

Conclusion. The data obtained demonstrate changes in EEG parameters during monotherapy with atypical antipsychotics and indicate their dose-dependent effect on the bioelectrical activity of the brain.

Keywords: schizophrenia, antipsychotics, therapy, electroencephalography, slowing, paroxysmal activity

Conflict of interest. The authors declare the absence of obvious or potential conflicts of interest related to the publication of this article.

Source of financing. The study was conducted within the state assignment No. 075–01392–23–00 “Personalized diagnosis and therapy of patients with co-occurring schizophrenia and affective spectrum disorders”, registration number 123041900006–4.

Conformity with the principles of ethics. All patients signed an informed consent to participate in the study and have their personal data processed. The study was approved by the local Ethics Committee at Mental Health Research Institute of Tomsk NRMC (Protocol No. 157 of 18.11.2022).

✉ *Galkin Stanislav A.,* s01091994@yandex.ru

For citation: Galkin S.A., Kornetova E.G., Ivanova S.A. Comparative analysis of EEG in patients with schizophrenia receiving various atypical antipsychotics. *Bulletin of Siberian Medicine.* 2024;23(1):15–22. https://doi.org/10.20538/1682-0363-2024-1-15-22.

Сравнительный анализ электроэнцефалограммы у больных шизофренией, получающих различные атипичные антипсихотики

Галкин С.А.[1], Корнетова Е.Г.[1, 2], Иванова С.А.[1, 2]

[1] Научно-исследовательский институт (НИИ) психического здоровья, Томский национальный исследовательский медицинский центр (НИМЦ) Российской академии наук
Россия, 634014, г. Томск, ул. Алеутская, 4

[2] Сибирский государственный медицинский университет (СибГМУ)
Россия, 634050, Томск, Московский тракт, 2

РЕЗЮМЕ

Цель. Провести комплексный анализ записей электроэнцефалограммы (ЭЭГ) больных шизофренией, получавших атипичные антипсихотики в режиме монотерапии.

Материалы и методы. Обследованы 94 больных шизофренией в возрасте 33 [28; 40] лет с длительностью заболевания 10 [4; 15] лет. Сформировано пять групп пациентов на основании принимаемых ими антипсихотических препаратов: 1) рисперидон – 31 пациент; 2) кветиапин – 20; 3) арипипразол – 11; 4) оланзапин – 13; 5) клозапин – 19 пациентов. ЭЭГ регистрировалась во время бодрствования с закрытыми глазами (фоновая проба), 3-минутной гипервентиляции и ритмической фотостимуляции у всех пациентов. Для описания и интерпретации полученных записей использовалась классификация ЭЭГ по J. Micoulaud-Franchi и соавт.

Результаты. Изменения (модификации) на ЭЭГ (класс > 1А) наблюдались у 61,7% (n = 58) пациентов. В группе пациентов, принимавших рисперидон, модификации ЭЭГ были обнаружены у 48,4%, кветиапин – 70%, арипипразол – 63,6%, оланзапин – 61,5%, клозапин – 73,7%. Частота эпилептиформных паттернов у пациентов была статистически значимо выше при приеме оланзапина по сравнению с рисперидоном (p = 0,033) и клозапином (p = 0,032). Замедление ЭЭГ (класс > 1) чаще наблюдалось у больных, принимавших клозапин – 63,2% (n = 12), оланзапин – 61,5% (n = 8) и кветиапин – 60% (n = 12). Реже медленные волны на ЭЭГ встречались у больных, принимавших арипипразол – 45,5% (n = 5) и рисперидон – 45,2% (n = 14). В группе больных с замедлением ЭЭГ (класс > 1) хлорпромазиновый эквивалент оказался статистически значимо выше по сравнению с пациентами с нормальной ЭЭГ (p = 0,00046).

Заключение. Полученные данные демонстрируют изменения показателей ЭЭГ в процессе терапии отдельными атипичными антипсихотиками и свидетельствуют об их дозозависимом эффекте на биоэлектрическую активность мозга.

Ключевые слова: шизофрения, антипсихотики, терапия, электроэнцефалография, замедление, пароксизмальная активность

Конфликт интересов. Авторы декларируют отсутствие явных и потенциальных конфликтов интересов, связанных с публикацией настоящей статьи.

Источник финансирования. Исследование проведено в рамках выполнения госзадания № 075–01392–23–00 «Персонализированная диагностика и терапия больных полиморбидными расстройствами шизофренического и аффективного спектра», № 123041900006–4.

Соответствие принципам этики. Все пациенты подписали согласие на участие в исследовании и обработку персональных данных. Исследование одобрено локальным этическим комитетом при НИИ психического здоровья Томского НИМЦ (протокол № 157 от 18.11.2022).

Для цитирования: Галкин С.А., Корнетова Е.Г., Иванова С.А. Сравнительный анализ электроэнцефалограммы у больных шизофренией, получающих различные атипичные антипсихотики. *Бюллетень сибирской медицины.* 2024;23(1):15–22. https://doi.org/10.20538/1682-0363-2024-1-15-22.

INTRODUCTION

The study of the effect of psychotropic drugs on the human electroencephalogram (EEG) began in the first half of the 20th century. In 1933, the founder of electroencephalography H. Berger described the changes in the EEG caused by barbiturates and morphine [1]. The first studies that reported anomalies caused by antipsychotic drugs appeared in the early 1970s and used phenothiazine as an example [2]. In 1970–1971, H. Dasberg and S. Robinson described changes related to the toxic effects of drugs, which turned out to be secondary to pre-existing cerebral disorders [2, 3]. Phenothiazine antipsychotics caused slight slowing, an increase in amplitude, synchronization, and expansion of alpha activity in the EEG [2, 3]. H. Dasberg [3] explained that human behavior changes through the effect of antipsychotics in the EEG.

As is known, many patients with mental disorders have various changes in the EEG [4–8]. Approximately 20–40% of patients with mood disorders and 20–60% of patients with schizophrenia have persistent disturbances in the bioelectric activity of the brain [8, 9]. In a relatively big proportion of patients with schizophrenia, changes in the EEG are detected in the form of generalized slowing (delta and theta waves), asymmetry, the presence of sharp waves and spike-and-wave complexes (paroxysmal patterns) [9].

However, a meta-analysis by S. O'Sullivan et al. suggested that most of the changes in the EEG in patients with mental disorders can be explained by taking psychotropic drugs and in this case the EEG cannot be used for the diagnosis of mental disorders [10]. However, EEG can help in determining whether patients suffering from mental disorders are taking prescribed medications, or whether different doses of medications cause side effects in the central nervous system (CNS) [10, 11].

One way or another, taking antipsychotics of different classes is accompanied by changes in the EEG. The literature mainly reports generalized slowing in background activity, an increase in paroxysmal theta or delta activity, and the development of epileptiform discharges [12–14]. Despite the appearance of various new antipsychotics over the past thirty years, only a few studies have been devoted to changes in the EEG caused by atypical antipsychotics [13, 15–18]. Some authors suggest that changes in the EEG caused by taking certain antipsychotics are associated with a good therapeutic response [14].

F. Centorrino et al. [15] showed that EEG changes were more severe when using second-generation antipsychotics than the first-generation ones, with a high risk of EEG modifications when using clozapine (47.1%) and olanzapine (38.5%), and a moderate risk when using risperidone (28%). In their study, severe modifications (spike discharges) were observed in patients taking clozapine (5.9%), olanzapine (7.7%), and risperidone (4.0%), but not in individuals taking haloperidol [15]. Risk factors contributing to significant changes in the EEG were the presence of arterial hypertension, the use of an atypical antipsychotic, the presence of bipolar affective disorder, and old age.

F. Pillmann et al. [16] analyzing the EEG in 43 patients treated with olanzapine showed an increase in diffuse slowing (48.8%), intermittent slowing (34.9%), and epileptiform activity in some patients (9.3%). A study involving 54 patients treated with olanzapine found significant slowing in the EEG (70.4%), the appearance of sharp waves (22.2%), and paroxysmal discharges of slow waves (14.8%) [17]. The combination of olanzapine with other antipsychotics increased the number of EEG modifications, while co-treatment with benzodiazepines reduced the number of EEG changes [17].

In another study, EEG was evaluated in 81 patients receiving quetiapine, olanzapine or haloperidol as monotherapy [18]. Adverse EEG changes were detected in one patient (5%) receiving quetiapine, in 13 (35%) patients receiving olanzapine, and in 5 (22.8%) patients receiving haloperidol. Epileptiform activity was observed only in 4 patients (10.8%) treated with olanzapine [18].

Thus, the prevalence of EEG modifications seems to vary depending on the type of antipsychotic drug taken. According to studies, the prevalence of EEG changes in people taking clozapine ranges from 25 to 53% [13, 15]. Quetiapine causes fewer changes in the EEG [18]. However, the number of EEG studies is very limited.

In this regard, the aim of the study was to conduct a comprehensive analysis of EEG recordings in patients with schizophrenia receiving atypical antipsychotic as monotherapy. We suggested that changes in the EEG may depend on the dose of antipsychotics taken.

MATERIALS AND METHODS

The study was conducted in accordance with the ethical principles set out in the Declaration of Helsinki of the World Medical Association in 1964, as amended in 1975–2013, and approved by the local Ethics Committee at Mental Health Research Institute of Tomsk NRMC (Protocol No. 157 of 18.11.2022).

All the examined patients signed an informed consent to participate in the study and have their personal data processed.

The selection of patients to participate in the study was carried out at the clinic of the Mental Health Research Institute of Tomsk NRMC of the Russian Academy of Sciences. The study included 94 patients with schizophrenia (50 men and 44 women) aged 33 [28; 40] years; the duration of the disease was 10 [4; 15] years, and the age of schizophrenia onset was 23 [20; 28] years. The inclusion criteria were: age of patients 18–60 years, a verified diagnosis of schizophrenia according to the criteria of ICD–10, and an informed consent to participate in the study. The exclusion criteria were: the presence of pronounced organic, neurological, and somatic symptom disorders leading to organ failure, and refusal to participate in the study.

All patients at the time of inclusion in the study received basic antipsychotic therapy at therapeutic doses approved by the Ministry of Health of Russia; the therapy lasted for 4 [1; 9] years. We formed 5 groups of patients based on the antipsychotic drugs they took: 1) risperidone – 31 patients, 2) quetiapine – 20 patients, 3) aripiprazole – 11 patients, 4) olanzapine – 13 patients, 5) clozapine – 19 patients. All doses of medications taken were brought to uniformity in terms of a chlorpromazine equivalent (CPZeq).

Electroencephalography was performed in an electrically shielded room with dim lighting. During the study, patients were sitting in a state of calm, relaxed wakefulness. The EEG was recorded using the NEUROFAX EEG–1200K encephalograph (Nihon Kohden, Japan) according to the International 10–20 system, with monopolar connections in 16 standard leads: Fp_1, Fp_2, F_3, F_4, F_7, F_8, C_3, C_4, P_3, P_4, O_1, O_2, T_3, T_4, T_5 and T_6, with a sampling frequency of 1 kHz, Fz as a grounding electrode and reference electrodes on the earlobes. EEG of all patients was recorded during wakefulness with closed eyes (background test), 3-minute hyperventilation, and rhythmic photostimulation. EEGs were recorded in the morning (between 9 and 12 o'clock), after breakfast. The total duration of the EEG recording was at least 15 minutes.

All patients during the EEG recording were under the supervision of a functional diagnostics doctor, and in case of signs of falling asleep or EEG signs of drowsiness, the recording was stopped. The analysis and interpretation of EEG data was carried out separately by two experienced certified neurophysiologists. In case of disagreement in the interpretation of the data, the EEGs were re-evaluated and discussed to reach a consensus. The EEG Classification by Micoulaud–Franchi et al. was used to describe and interpret the obtained recordings [19], developed to assess the effect of psychotropic drugs (Table 1).

Table 1

EEG modifications using the classification of Micoulaud – Franchi et al.

Slowing score		Excitability score	
Class	Description	Class	Description
1	Absent (predominant alpha)	A	Absent
2	Theta slowing	B	Sporadic epileptiform discharges or sharp waves during hyperventilation or photostimulation
3	Theta slowing with delta bursts	C	Sporadic epileptiform discharges or sharp waves throughout the recording
4	Delta slowing	D	Long lasting epileptiform discharges

The statistical analysis was performed using the Statistica for Windows V. 12.0 software (Statsoft Inc.). Compliance with the law of normal distribution was checked using the Lilliefors-corrected Kolmogorov – Smirnov test and the Shapiro–Wilk test. Data with a normal distribution were presented as the mean and the standard deviation $M \pm SD$. In the absence of a normal distribution, data were presented as the median and the interquartile range Me [Q_1; Q_3]. Qualitative variables were represented by frequency parameters in absolute and relative units n (%). To compare EEG parameters (EEG types according to the EEG classification of Micoulaud–Franchi et al.), the $\chi 2$ test was used. Average daily doses of antipsychotics were compared in accordance with EEG changes using the Student's t-test. The Spearman's rank correlation coefficient was used to identify the relationships between the studied parameters. The threshold level of statistical significance p was assumed to be 0.05.

RESULTS

According to the data obtained, EEG modifications (class >1A) were observed in 61.7% (n = 58) of the patients included in this study. In the group of patients receiving risperidone, EEG modifications were found in 48.4% of cases, in patients taking quetiapine – in 70% of cases, aripiprazole – in 63.6% of cases, olanzapine – in 61.5% of cases, clozapine – in 73.7% of cases (Table 2).

Epileptiform patterns (class B and C) were more often detected in the group of patients taking olanzapine – 30.7% (n = 4). Less frequently, paroxysmal activity was detected in 20% of patients taking quetiapine (n = 4), in 18.2% of patients taking aripiprazole (n = 2), in 12.9% of individuals taking risperidone (n = 4), and in 10.5% of patients taking clozapine (n = 2). The frequency of epileptiform patterns was significantly higher in patients taking olanzapine compared with risperidone (p = 0.033) and clozapine (p = 0.032).

EEG slowing (class >1) was more often observed in patients taking clozapine – 63.2% (n = 12), olanzapine – 61.5% (n = 8), and quetiapine – 60% (n = 12). EEG slowing was less common in patients taking aripiprazole – 45.5% (n = 5) and risperidone – 45.2% (n = 14). However, according to the $\chi 2$ test, these differences did not reach statistical significance ($p > 0.05$). Extremely severe EEG modifications (class 4C or 4D) were not found in the study sample.

We also failed to find correlations between the presence (class >1A) and severity of EEG changes (classes 2 and 3, B and C) and clinical data (age, duration of the disease, age of schizophrenia onset and the duration of therapy) collected from patient clinical records ($p > 0.05$).

The results of comparing the average daily doses of antipsychotics, depending on the presence or absence of EEG changes, are presented in Table 3.

Table 2

Percentage of EEG changes (class >1A) depending on the type of the atypical antipsychotic taken in patients with schizophrenia

Antipsychotic	n	Age of patients, Me [Q_1; Q_3]	Dose CPZeq, mg/day, $M \pm SD$	EEG modifications (class >1A)	
				n	%
Risperidone	31	35 [29; 39]	290.3 ± 89.8	15	48.4
Quetiapine	20	33 [25; 45]	598.6 ± 455.3	14	70
Aripiprazole	11	30 [21; 35]	193.9 ± 80	7	63.6
Olanzapine	13	34 [27; 40]	307.7 ± 171.8	8	61.5
Clozapine	19	33 [32; 44]	163.3 ± 79.9	14	73.7

Table 3

Comparison of average daily doses of atypical antipsychotics in accordance with the presence (class >1A) and absence of EEG changes in patients with schizophrenia

Antipsychotic	EEG modifications (class >1A)		Absent (class = 1A)		p
	n	Dose (CPZeq, mg/day), $M \pm SD$	n	Dose (CPZeq, mg/day), $M \pm SD$	
Risperidone	15	296.7 ± 81.2	16	284.4 ± 99.5	0.452
Quetiapine	14	657.9 ± 503.4	6	460.3 ± 310	0.291
Aripiprazole	7	190.4 ± 103.1	4	199.9 ± 101.2	0.993
Olanzapine	8	262.5 ± 178.8	5	380 ± 148.3	0.754
Clozapine	14	168.1 ± 82.4	5	150 ± 79.5	0.909
All	58	335.3 ± 272.6	36	298.9 ± 176.1	0.00029*

Here and in Table 5, * the reliability of statistical differences at $p < 0.05$.

There were no statistically significant differences in the average daily doses (mg per day) of atypical antipsychotics between patients without and with EEG modifications (risperidone: p = 0.452; quetiapine: p = 0.291; aripiprazole: p = 0.993; olanzapine: p = 0.754; clozapine: p = 0.909). However, when the doses of all antipsychotics were averaged, it could be seen that in patients with EEG changes (class >1A), the dose of chlorpromazine equivalent was significantly greater (p = 0.00029).

Tables 4 and 5 contain the results of comparing the average daily doses depending on the assessment of paroxysmal activity and EEG slowing.

The average daily doses of antipsychotics did not significantly differ in patients depending on the presence or absence of paroxysmal activity (risperidone: p = 0.191; quetiapine: p = 0.261; aripiprazole: p = 0.177; olanzapine: p = 0.848; clozapine: p = 0.725) (Table 4), as well as on the presence or absence of EEG slowing (risperidone: p = 0.386; quetiapine: p = 0.154; aripiprazole: p = 0.374; olanzapine: p = 0.754; clozapine: p = 0.588) (Table 5). However, taking into account the average doses of all atypical antipsychotics, it was found that in the group of patients with EEG slowing (class >1), the dose of the chlorpromazine equivalent was significantly higher (p = 0.00046).

Table 4

Comparison of average daily doses of atypical antipsychotics depending on the assessment of paroxysmal activity

Antipsychotic	EEG modifications (class >A)		Absent (class = A)		*p*
	n	Dose CPZeq, mg/day, *M* ± *SD*	*n*	Dose CPZeq, mg/day, *M* ± *SD*	
Risperidone	4	250 ± 129.1	27	296.3 ± 84.3	0.191
Quetiapine	4	631.9 ± 132.5	16	590.3 ± 126.8	0.261
Aripiprazole	2	199.9 ± 41.4	9	170.3 ± 45.5	0.177
Olanzapine	4	200 ± 141.4	9	225.5 ± 168.5	0.848
Clozapine	2	121.8 ± 39.8	17	168.2 ± 82.7	0.725
All	16	323.2 ± 153.8	78	320.9 ± 156.3	0.171

Table 5

Comparison of average daily doses of atypical antipsychotics depending on the assessment of paroxysmal activity

Antipsychotic	EEG modifications (class >1)		Absent (class = 1)		*p*
	n	Dose CPZeq, mg/day, *M* ± *SD*	*n*	Dose CPZeq, mg/day, *M* ± *SD*	
Risperidone	14	289.3 ± 78.9	17	291.2 ± 100.4	0.386
Quetiapine	12	709.4 ± 517.7	8	432.5 ± 298.4	0.154
Aripiprazole	5	146.6 ± 50.6	6	133.3 ± 81.6	0.374
Olanzapine	8	262.5 ± 178.8	5	280 ± 148.3	0.754
Clozapine	12	175.8 ± 86.2	7	141.9 ± 68.3	0.588
All	51	343.2 ± 233.93	43	295.4 ± 176.5	0.00046*

DISCUSSION

In the present study, the EEG data of 94 patients with schizophrenia who received clozapine, olanzapine, quetiapine, aripiprazole or risperidone as monotherapy were studied. The largest percentage of EEG modifications (class >1A) was found in the group of patients taking clozapine (73.7%), which is slightly higher than in other studies [13, 15, 18]. However, severe modifications (class 4C and 4D) were not detected in any of the patient groups.

The frequency of modifications associated with the presence of epileptiform patterns when taking the above antipsychotics is consistent with research data [13, 15, 16]. However, in contrast to the results of the study conducted by F. Centorrino et al. [15], the frequency of paroxysmal activity for clozapine was significantly lower (10.5%,) whereas for olanzapine it was higher (30.7%).

It is known that the risk of seizures caused by antipsychotics is higher for patients taking olanzapine and clozapine than for those taking risperidone and aripiprazole [20]. In this regard, EEG monitoring is recommended when the average daily dose is 20 mg for olanzapine and 400 mg for clozapine [21, 22]. Like clozapine, olanzapine can cause EEG changes, such as the appearance of slow waves, sharp waves, and paroxysmal slow-wave discharges, but the risk of seizures is considered low [22].

We found no differences in the frequency of paroxysmal activity depending on the average daily doses of any antipsychotic. Thus, it can be assumed that there is no dose-dependent effect of antipsychotics on convulsive activity. However, the number of patients with epileptiform patterns in our study was small. Studies on larger samples could confirm or refute this assumption.

EEG slowing was observed in the majority of the studied patients – 51 (54.3%), which is also consistent with the literature data [15–18]. The most common EEG modification in patients taking antipsychotics was diffuse slowing of bioelectrical activity (73.9%). Diffuse EEG slowing is often associated with the effect of psychotropic drugs and compared with the effect of electroconvulsive therapy [23]. There is an assumption that diffuse or paroxysmal EEG slowing during antipsychotic therapy may indicate a favorable outcome of the therapy [14]. However, some researchers [12, 13] found that patients with a long duration of therapy had EEG slowing and explained this phenomenon by an increase in the severity of the disease [13].

In our opinion, it is impossible to exclude the influence of the disease duration on these parameters, since schizophrenia is a pathology requiring specific

treatment [24, 25]. In our study, we found no differences in the frequency of EEG slowing depending on the average daily doses of any atypical antipsychotic. However, taking into account the average doses of all antipsychotics, it was found that the dose of the chlorpromazine equivalent was significantly higher in the group of patients with EEG slowing. Thus, we assume that with an increase in the therapeutic dose of antipsychotics, we can expect an increase in slow-wave activity in the EEG and, as a consequence, generalized slowing in the bioelectrical activity of the brain. Another important result of the study was the fact that the effect of antipsychotics on the EEG was found to correspond to the spectrum of their atypia described by M. Carli et al. [26].

CONCLUSION

The study revealed several interesting results. Firstly, the most frequent EEG changes were observed in patients taking clozapine compared to other atypical antipsychotics. These changes were more related to EEG slowing. Secondly, epileptiform patterns were most often detected in the group of patients taking olanzapine compared to other antipsychotics, although olanzapine also caused EEG slowing. Thirdly, we found a dose-dependent effect of atypical antipsychotics in relation to EEG slowing. A higher percentage of EEG slowing episodes appears to be associated with higher doses of the chlorpromazine equivalent. Thus, the data obtained indicate the need for the use of electroencephalography in monitoring antipsychotic therapy.

REFERENCES

1. Galderisi S., Sannita W.G. Pharmaco-EEG: A history of progress and a missed opportunity. *Clin. EEG Neurosci*. 2006;37(2):61–65. DOI: 10.1177/155005940603700204.
2. Dasberg H., Robinson S. The influence of anti-psychotic drugs on the EEG of mental patients. *Electroencephalogr. Clin. Neurophysiol*. 1970; 8(6):643.
3. Dasberg H., Robinson S. Electroencephalographic variations following anti-psychotic drug treatment. (Diagnostic and prognostic significance). *Dis. Nerv. Syst*. 1971;32(7):472–478.
4. Galkin S.A., Roshchina O.V., Kisel N.I., Ivanova S.A., Bokhan N.A. Clinical and neurophysiological characteristics of alcohol dependence and its comorbidity with affective disorders. *Neuroscience and Behavioral Physiology*. 2021;51(6):720–723. DOI: 10.1007/s11055–021–01127–w.
5. Iznak E.V., Damyanovich E.V., Levchenko N.S., Oleychik I.V., Iznak A.F. EEG Asymmetries in Depressive Female Adolescents with Different Kinds of Auto-Aggressive Behavior. *Psychiatry*. 2020;18(3):14–21 (in Russ.). DOI: 10.30629/2618–6667–2020–18–3–14–21.
6. Arzumanov Y.L., Lapin I.A., Meshcheryakov A.F., Brodyansky V.M., Abakumova A.A., Vinnikova M.A., et al. Electrophysiological correlates of the genetic risk of alcohol addiction. *Journal of Addiction Problems*. 2016;(2):5–23 (in Russ.).
7. Galkin S.A., Peshkovskaya A.G., Roshchina O.V., Kisel N.I., Ivanova S.A., Bohan N.A. Features of brain activity in alcohol dependence in the task of inhibitory control. *Bulletin of Siberian Medicine*. 2020;19(4):38–45 (in Russ.). DOI: 10.20538/1682–0363–2020–4–38–45.
8. Kutepov I.E., Krysko A.V., Dobriyan V.V., Yakovleva T.V., Krylova E.Yu., Krysko V.A. Visualization of eeg signal entropy in schizophrenia. *Scientific Visualization*. 2020;12(1):1–9. DOI: 10.26583/sv.12.1.01.
9. Boutros N.N. Psychotic and Affective Disorders. In: Standard EEG: A Research Roadmap for Neuropsychiatry. *Springer, Cham*. 2013. DOI: 10.1007/978–3–319–04444–6_11.
10. O'Sullivan S.S., Mullins G.M., Cassidy E.M., McNamara B. The role of the standard EEG in clinical psychiatry. *Hum. Psychopharmacol*. 2006;21(4):265–271. DOI: 10.1002/hup.767.
11. Itil T.M. The use of electroencephalography in the practice of psychiatry. *Psychosomatics*. 1982;23(8):799–803. DOI: 10.1016/S0033–3182(82)73079–8.
12. Aiyer R., Novakovic V., Barkin R.L. A systematic review on the impact of psychotropic drugs on electroencephalogram waveforms in psychiatry. *Postgrad. Med*. 2016;128(7):656–664. DOI: 10.1080/00325481.2016.1218261.
13. Dias Alves M., Micoulaud-Franchi J.A., Simon N., Vion-Dury J. Electroencephalogram modifications associated with atypical strict antipsychotic monotherapies. *J. Clin. Psychopharmacol.* 2018;38(6):555–562. DOI: 10.1097/JCP.0000000000000953.
14. Kikuchi Y.S., Sato W., Ataka K., Yagisawa K., Omori Y., Kanbayashi T., Shimizu T. Clozapine–induced seizures, electroencephalography abnormalities, and clinical responses in Japanese patients with schizophrenia. *Neuropsychiatr. Dis. Treat*. 2014;10:1973–1978. DOI: 10.2147/NDT.S69784.
15. Centorrino F., Price B.H., Tuttle M., Bahk W.M., Hennen J., Albert M.J. et al. EEG abnormalities during treatment with typical and atypical antipsychotics. *Am. J. Psychiatry*. 2002;159(1):109–115. DOI: 10.1176/appi.ajp.159.1.109.
16. Pillmann F., Schlote K., Broich K., Marneros A. Electroencephalogram alterations during treatment with olanzapine. *Psychopharmacology (Berl.).* 2000;150(2):216–219. DOI: 10.1007/s002130000426.
17. Wichniak A., Szafranski T., Wierzbicka A., Waliniowska E., Jernajczyk W. Electroencephalogram slowing, sleepiness and treatment response in patients with schizophrenia during olanzapine treatment. *J. Psychopharmacol*. 2006;20(1):80–85. DOI: 10.1177/0269881105056657.
18. Amann B.L., Pogarell O., Mergl R., Juckel G., Grunze H., Mulert C., Hegerl U. EEG abnormalities associated with antipsychotics: a comparison of quetiapine, olanzapine, haloperidol and healthy subjects. *Hum. Psychopharmacol*. 2003;18(8):641–646. DOI: 10.1002/hup.537.
19. Micoulaud-Franchi J.A., Balzani C., Faugere M. Neurophysiologie clinique en psychiatrie : 1 – Techniques, vocabulaires et indications de l'électroencéphalographie conventionnelle. *Annales Médico-psychologiques, Revue Psychiatrique.* 2013;171(5):334–341. DOI: 10.1016/j.amp.2013.04.005.

20. Wu C.S., Wang S.C., Yeh I.J., Liu S.K. Comparative risk of seizure with use of first- and second-generation antipsychotics in patients with schizophrenia and mood disorders. *J. Clin. Psychiatry.* 2016;77(5):e573–579. DOI: 10.4088/JCP.15m09898.
21. Varma S., Bishara D., Besag F.M., Taylor D. Clozapine-related EEG changes and seizures: dose and plasma-level relationships. *Ther. Adv. Psychopharmacol*. 2011;1(2):47–66. DOI: 10.1177/2045125311405566.
22. Degner D., Nitsche M.A., Bias F., Rüther E., Reulbach U. EEG alterations during treatment with olanzapine. *Eur. Arch. Psychiatry Clin. Neurosci*. 2011;261(7):483–488. DOI: 10.1007/s00406–011–0208–4.
23. Matsuura M., Yoshino M., Ohta K., Onda H., Nakajima K., Kojima T. Clinical significance of diffuse delta EEG activity in chronic schizophrenia. *Clin. Electroencephalogr*. 1994;25(3):115–121. DOI: 10.1177/155005949402500309.
24. Marusin A.V., Kornetov A.N., Swarovskaya M.G., Vagaytseva K.V., Pavlenyuk E.S., Stepanov V.A. Genetic predisposition to alcoholism, schizophrenia and Alzheimer's disease with psychodiagnostic characteristics in the Russian population. *Bulletin of Siberian Medicine*. 2016;15(5):83–96 (in Russ.). DOI: 10.20538/1682–0363–2016–5–83–96.
25. Kornetov A. Old age psychiatry: training in Siberia. *Mental Health Reforms*. 2002;7(2):7–8.
26. Carli M., Kolachalam S., Longoni B., Pintaudi A., Baldini M., Aringhieri S. et al. Atypical antipsychotics and metabolic syndrome: from molecular mechanisms to clinical differences. *Pharmaceuticals (Basel)*. 2021;14(3):238. DOI: 10.3390/ph14030238.

Authors' contribution

Galkin S.A. – neurophysiological examination of patients, analysis and interpretation of the data, drafting of the manuscript. Kornetova E.G. – conception and design, clinical, psychopathological, and psychometric examination of the sample, critical revision of the manuscript for important intellectual content. Ivanova S.A. – final approval of the manuscript for publication.

Authors' information

Galkin Stanislav A. – Cand. Sci. (Med.), Researcher, Mental Health Research Institute, Tomsk NRMC, Tomsk, s01091994@yandex.ru, http://orcid.org/0000-0002-7709-3917

Kornetova Elena G. – Dr. Sci. (Med.), Head of the Endogenous Disorders Department, Mental Health Research Institute, Tomsk NRMC, Tomsk, http://orcid.org/0000-0002-5179-9727

Ivanova Svetlana A. – Dr. Sci. (Med.), Professor, Deputy Director for Science, Head of the Laboratory for Molecular Genetics and Biochemistry, Mental Health Research Institute, Tomsk NRMC, Tomsk, http://orcid.org/0000-0001-7078-323X

(✉) **Galkin Stanislav A.,** e-mail: s01091994@yandex.ru

Received 08.06.2023;
approved after peer review 22.06.2023;
accepted 14.09.2023

УДК 616.24-006.6:616.15-033.2:577.17
https://doi.org/10.20538/1682-0363-2024-1-23-29

Metastasis suppressor kisspeptin (KISS1) in the blood serum of lung cancer patients

Gershtein E.S.[1, 2], Kovaleva O.V.[1], Kuzmin Yu.B.[1, 2], Alferov A.A.[1, 2], Rogozhin D.V.[1], Yanushevich O.O.[2], Stilidi I.S.[1], Kushlinskii N.E.[1, 2]

[1] *N.N. Blokhin National Medical Research Center of Oncology*
24, Kashirskoe Highway, Moscow, 115522, Russian Federation

[2] *A.I. Evdokimov Moscow State University of Medicine and Dentistry*
20/1, Delegatskaya Str., Moscow, 127473, Russian Federation

ABSTRACT

Aim. To conduct a comparative assessment of the content of kisspeptin (KISS1) metastasis suppressor in the blood serum of apparently healthy individuals and patients with lung cancer (LC) and to analyze the associations between the KISS1 level and clinical and pathological characteristics of the disease.

Materials and methods. The study included 74 LC patients and 46 apparently healthy individuals. Stage I LC was diagnosed in 8 patients, stage II LC – in 7 patients, stage III LC – in 28 patients, and stage IV LC – in 31 patients. According to the histologic pattern, 32 tumors were characterized as adenocarcinoma, 29 – as squamous-cell carcinoma, 11 – as small-cell LC (SCLC), and 2 – as large-cell lung carcinoma. The pre-treatment KISS1 level in the blood serum was determined using the enzyme-linked immunosorbent assay kit (KISS1, Cloud-Clone Corp., USA).

Results. The median serum KISS1 level in LC patients was 213 (range 7.8–716) pg / ml and was significantly higher than in the control group – 83.4 (0–180) pg / ml ($p < 0.0001$). The ROC analysis of the diagnostic value of serum KISS1 level demonstrated that the sensitivity of the test in relation to the healthy controls was 70% at a cut-off value of 152 pg / ml, and the specificity was 85% (AUC – 0.817; $p < 0.0001$). In stage I–II LC, the sensitivity did not exceed 50%. The level of KISS1 in the blood serum did not depend on the histologic type of the tumor. No significant differences in the serum KISS1 levels were observed both between non-small cell lung cancer (NSCLC) on the whole and neuroendocrine SCLC and between the main histologic types of NSCLC. The level of KISS1 increased with the disease stage ($p < 0.05$). However, none of the TNM staging system indices significantly influenced the level of the marker. No differences were found between serum KISS1 levels in patients with central or peripheral localization of the tumor.

Conclusion. The KISS1 level was elevated in LC patients compared to healthy controls and was a stage-dependent marker. It has high diagnostic specificity but insufficient sensitivity, especially at early stages of the disease. Based on the results of this study and literature data on the role of KISS1in NSCLC, we conclude that clinical implications of KISS1 in this disease require further research.

Keywords: lung cancer, KISS1, blood serum

Conflict of interest. The authors declare the absence of obvious or potential conflicts of interest related to the publication of this article.

Source of financing. The authors state that they received no funding for the study.

Conformity with the principles of ethics. All patients signed an informed consent to participate in the study. The study was approved by the local Ethics Committee at N.N. Blokhin National Medical Research Center of Oncology (Protocol No. 6 of 06.06.2023).

For citation: Gershtein E.S., Kovaleva O.V., Kuzmin Yu.B., Alferov A.A., Rogozhin D.V., Yanushevich O.O., Stilidi I.S., Kushlinskii N.E. Metastasis suppressor kisspeptin (KISS1) in the blood serum of lung cancer patients. *Bulletin of Siberian Medicine.* 2024;23(1):23–29. https://doi.org/10.20538/1682-0363-2024-1-23-29.

✉ *Gershtein Elena S.,* esgershtein@gmail.com

Супрессор метастазирования кисспептин (KISS1) в сыворотке крови больных раком легкого

Герштейн Е.С.[1, 2], Ковалева О.В.[1], Кузьмин Ю.Б.[1, 2], Алферов А.А.[1, 2], Рогожин Д.В.[1], Янушевич О.О.[2], Стилиди И.С.[1], Кушлинский Н.Е.[1, 2]

[1] Национальный медицинский исследовательский центр (НМИЦ) онкологии им. Н.Н. Блохина Россия, 115522, г. Москва, Каширское шоссе, 24

[2] Московский государственный медико-стоматологический университет (МГМСУ) им. А.И. Евдокимова Россия, 127473, г. Москва, ул. Делегатская, 20/1

РЕЗЮМЕ

Цель – сравнительная оценка содержания супрессора метастазирования кисспептина (KISS1) в сыворотке крови практически здоровых людей и больных раком легкого (РЛ), анализ взаимосвязи уровня KISS1 с основными клинико-морфологическими особенностями заболевания.

Материалы и методы. Обследованы 74 больных РЛ и 46 здоровых доноров. У 8 пациентов диагностирована I стадия, у 7 – II, у 28 – III, у 31 – IV стадия. По гистологическому строению 32 опухоли представляли собой аденокарциному, 29 – плоскоклеточный, 11 – мелкоклеточный и две – крупноклеточный рак. Содержание KISS1 в сыворотке крови определяли до лечения наборами реактивов для иммуноферментного анализа (Kisspeptin 1 – KISS1, Cloud-Clone Corp., США).

Результаты. Медиана содержания KISS1 в крови больных РЛ составила 213 (пределы колебаний 7,8–716) пг/мл и была значимо выше, чем в контрольной группе: 83,4 (0–180) пг/мл ($p < 0,0001$). ROC-анализ диагностической значимости сывороточного уровня KISS1 показал, что чувствительность данного теста относительно здорового контроля при пороговом уровне 152 пг/мл составляет 70%, специфичность – 85% (AUC – 0,817; $p < 0,0001$). При I–II стадии заболевания чувствительность не превышает 50%. Содержание KISS1 в сыворотке крови не зависит от гистологического типа опухоли. Значимых различий уровней KISS1 как между НМРЛ в целом и нейроэндокринным МРЛ, так и между основными гистологическими типами НМРЛ не наблюдается. Уровень KISS1 возрастает с увеличением стадии заболевания ($p < 0,05$), однако ни один из индексов системы TNM значимо не влияет на уровень маркера. Не обнаружено различий между сывороточными уровнями KISS1 у пациентов с центральной или периферической локализацией опухоли.

Заключение. Уровень KISS1 в сыворотке крови больных РЛ повышен по сравнению с контролем и является стадия-зависимым маркером. Он обладает высокой диагностической специфичностью, но недостаточной чувствительностью, в особенности на ранних стадиях заболевания. Основываясь на собственных результатах и данных литературы о роли KISS1 при НМРЛ, полагаем, что клиническое значение кисспептина при данном заболевании заслуживает дальнейшего более углубленного изучения.

Ключевые слова: рак легкого, KISS1, сыворотка крови

Конфликт интересов. Авторы декларируют отсутствие явных и потенциальных конфликтов интересов, связанных с публикацией настоящей статьи.

Источник финансирования. Авторы заявляют об отсутствии финансирования при проведении исследования.

Соответствие принципам этики. Все пациенты подписали информированное согласие на участие в исследовании. Исследование одобрено локальным этическим комитетом НМИЦ онкологии им. Н.Н. Блохина (протокол № 6 от 06.06.2023).

Для цитирования: Герштейн Е.С., Ковалева О.В., Кузьмин Ю.Б., Алферов А.А., Рогожин Д.В., Янушевич О.О., Стилиди И.С., Кушлинский Н.Е. Супрессор метастазирования кисспептин (KISS1) в сыворотке крови больных раком легкого. *Бюллетень сибирской медицины.* 2024;23(1):23–29. https://doi.org/10.20538/1682-0363-2024-1-23-29.

INTRODUCTION

Kisspeptin, or metastatin, a product of the *KISS1* gene, is now considered to be a metastasis suppressor for different tumors. The *KISS1* gene, which encodes a protein composed of 145 amino acid residues (kisspeptin-145) that subsequently cleaves into minor functionally active proteins, was discovered in 1996 as a melanoma metastasis suppressor gene [1, 2]. Metastasis suppression after the restoration of KISS1 expression was also demonstrated in several other cell lines characterized by high metastatic potential [3–5]. Under normal conditions, the physiological role of kisspeptin includes the invasion of placental trophoblasts as well as the regulation of gonadotropin secretion [6]. The mechanisms mediating the ability of this protein to suppress metastasis formation are still insufficiently explored. However, it is known that it exerts its effects through the GPR54 receptor associated with G-proteins from the Gq/11 subfamily [7, 8].

The largest expression of the *KISS1* and *GPR54* genes is observed in the placenta and various brain structures, including the hypothalamus and basal nucleus [9], while low expression is found in the pancreas, kidneys, lungs, prostate, and small intestine [7]. The expression level of *KISS1* has ambiguous prognostic value in different malignant tumors. Particularly, it correlates with the invasiveness of some human tumors, including renal cell cancer, melanoma, esophageal cancer, bladder cancer, breast cancer, ovarian cancer, and prostate cancer [10]. The study of metastasis suppressor genes and their products not only increases the understanding of the mechanisms of tumor progression, but also has practical value for the diagnosis, prognosis, and the establishment of new molecular targets for antitumor therapy [11]. In terms of noninvasive and possibly early diagnosis of tumors, the most interesting approach consists not in the study of gene and protein expression in tumor tissue, but rather in the identification of their soluble forms circulating in the peripheral blood. Quite a few works devoted to the study of circulating kisspeptin in patients with pancreatic [12], colorectal [13], and gastric cancer [14] have been published. The data on the role of the *KISS1* gene and its product, kisspeptin, in lung cancer (LC) are scarce and rather ambiguous [15–18].

The aim of this study was to conduct a comparative assessment of KISS1 content in the blood serum of apparently healthy persons and patients with lung cancer and to analyze the associations between the marker level and the clinical and pathologic characteristics of the disease.

MATERIALS AND METHODS

The study included 74 LC patients (54 males and 20 females) aged 31–85 years (median – 74 years) undergoing examination and treatment at the N.N. Blokhin National Medical Research Center of Oncology, and 46 apparently healthy persons (22 males and 24 females) aged 29–76 years (median – 45 years). The clinical diagnosis was confirmed in all patients by the results of the morphologic assessment of the tumor according to the 2021 WHO Classification of Lung Tumors (WHO, 2021). Stage I LC was diagnosed in 8 patients, stage II – in 7 patients, stage III – in 28 individuals, and stage IV – in 31 patients. By the histologic pattern, 32 tumors were characterized as adenocarcinoma (AC), 29 – as squamous-cell carcinoma, 11 – as small-cell LC (SCLC), and 2 – as large-cell lung carcinoma.

All procedures performed in the study involving patients and healthy controls comply with the standards of the Ethics Committee of the Research Center and the Declaration of Helsinki (1964) and its further amendments, or equivalent ethical norms. All participants included in the study signed an informed voluntary consent. The study was approved by the local Ethics Committee at N.N. Blokhin National Medical Research Center of Oncology (Protocol No. 6 of 06.06.2023).

KISS1 content in the blood serum obtained by a standard procedure before the initiation of a specific treatment was measured with the help of the reagent kit for direct enzyme-linked immunosorbent assay Kisspeptin 1 – KISS1 (Cloud-Clone Corp., USA) according to the manufacturer's instructions. The registration of the results was performed using the automatic immune enzymatic analyzer BEP 2000 Advance (Siemens Healthcare Diagnostics, Germany). The content of the marker was expressed in picograms (pg) per 1 ml of blood serum.

The data obtained were processed using the GraphPad Prism 9.0 program package. The nonparametric Mann – Whitney and Kruskal – Wallis tests, the median test (*Me (25–75%)),* and the Spearman's rank correlation coefficient were used to compare the parameters and analyze their relationships. The analysis of the diagnostic value of the test based on the assessment of its sensitivity and specificity was performed by constructing ROC curves and calculating the area under the curve (AUC). Differences and correlations were considered statistically significant at $p < 0.05$.

RESULTS

At the first stage of the research, KISS1 content in the blood serum of LC patients was compared to that of healthy controls to evaluate the possible diagnostic value of this marker. Median serum KISS1 concentration in LC patients was 213 (range 7.8–716) pg / ml and was significantly higher than in the control group – 83.4 (range 0–180) pg / ml (Fig. 1, *a*; $p < 0.0001$).

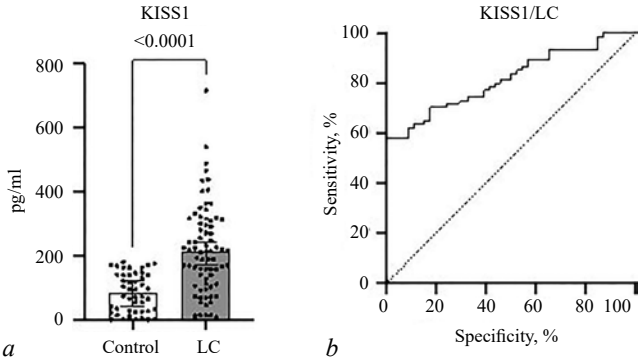

Fig. 1. Comparative analysis of KISS1 content in the blood serum of LC patients and the control group (a), ROC analysis of KISS1 in LC patients (b): area under the curve (AUC) is 0.829 ($p < 0.0001$)

The ROC analysis of the diagnostic value of the KISS1 level in the serum of LC patients demonstrated (Fig. 1, *b*) that the sensitivity of this test in relation to healthy controls was 70% at an optimal cut-off value of 152 pg / ml, and the specificity was 85% (AUC was 0.817 with a 95% confidence interval (CI) of 0.759–0.899; $p < 0.0001$). The analysis of the marker level depending on the disease stage (Table 1) indicates that at early (I–II) clinical stages, the sensitivity did not exceed 50%.

The serum KISS1 level in male patients was significantly higher than in female patients (*Me* 221 and 162 pg / ml, respectively; $p < 0.05$). Similar significant differences were also observed in the control group. A weak but statistically significant positive correlation was found between serum KISS1 level and the age of LC patients ($r_s = 0.31$; $p = 0.007$). Meanwhile, in the control group, the KISS1 – age correlation was negative: $r_s = -0.29$; $p = 0.048$.

Next, we assessed serum KISS1 content in relation to the histologic type of LC. The comparison was made both between the groups of SCLC and non-SCLC (NSCLC) as a whole and between various types of NSCLC (Figure 2).

It was established that serum KISS1 content did not depend on the histologic type of the tumor, since no significant differences were found either between the combined NSCLC and neuroendocrine SCLC patient groups or between patients with various NSCLC variants. However, in all histologic types of LC, the KISS1 level was significantly higher than in the control group.

Based on the observation above, further analysis of associations of serum KISS1 levels with the indices of tumor advancement and localization was performed for the LC group as a whole, without considering the histologic pattern of the tumor (Table).

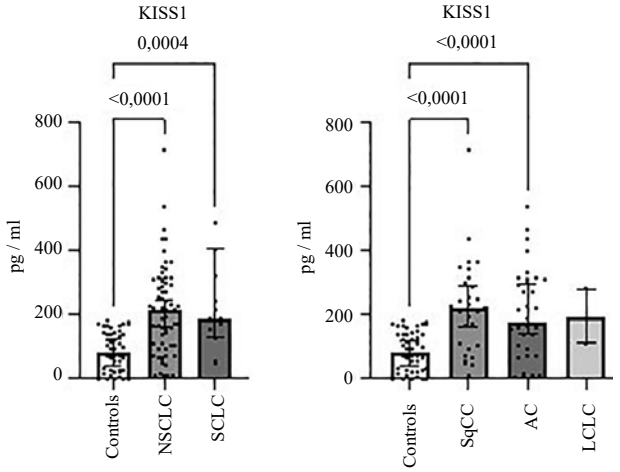

Fig. 2. KISS1 content in the blood serum of LC patients depending on the histologic type of the tumor

Table

KISS1 content in the blood serum of LC patients in relation to clinical and pathological characteristics

Parameter	KISS1, pg / ml		
	Me	25–75%	*p*
Gender			
– male ($n = 54$);	221	149.8–316	0.042
– female ($n = 20$)	162	77.7–230	
Stage:			
I ($n = 8$);	188	69.9–275	
II ($n = 7$);	148	45.1–193	0.042
III ($n = 28$);	241	157–351	
IV ($n = 31$)	216	139–296	
Tumor size (T):			
– T1–T2;	187.6	111.0–271.0	0.179
– T3–T4	224.8	128.0–317.1	
Nodal status (N):			
– N0;	210.4	88.8–293.9	0.569
– N+	215.8	119.5–314.2	
Distant metastasis (M):			
– M0;	201.6	88.4–303.5	0.405
– M+	218.5	159.1–311.8	
Localization:			
– central;	224.8	106.9–316.6	0.248
– peripheral	178.1	109.9-255.2	

A statistically significant increase in the serum KISS1 concentration was observed along with progression of the disease stage ($p < 0.05$ according to the median test), but none of the TNM system criteria (the size of the primary tumor T, the presence of both regional N and distant metastases M) significantly affected the level of the marker. No differences were found between serum KISS1 levels in patients with central or peripheral localization of LC.

DISCUSSION

We found that the level of KISS1 protein, the product of corresponding metastasis suppressor gene, in the blood serum of LC patients is significantly elevated compared to healthy controls and increases with progression of the disease. The study group included both patients with classical NSCLC, and those with neuroendocrine SCLC. However, no fundamental differences in serum KISS1 levels were found between these two LC types. No differences were found in different histologic variants of NSCLC. The analysis of the diagnostic value of serum KISS1 in LC demonstrated rather high (85%) specificity of this test in relation to healthy controls, but its sensitivity was only 70% for all participants and did not exceed 50% at early stages of LC.

The increase in the level of the soluble form of the metastasis suppressor KISS1 in the blood serum of LC patients as a whole, and particularly at advanced stages of the disease, is somewhat paradoxical from a fundamental point of view, but is consistent with the data of some publications devoted to the study of circulating KISS1 (in the blood serum or plasma) [12–14; 16]. All these studies demonstrated an increase in the level of this protein in patients with various tumors (pancreatic, colorectal, and gastric cancer) compared to healthy controls. Though in the most detailed of these publications [12], neither significant associations between KISS1 levels and the clinical and pathological characteristics of pancreatic cancer nor any effects of this marker on the overall and relapse-free survival of patients were found.

The study by S. Zheng et al. [19] demonstrated that *KISS1* expression at the mRNA level in NSCLC patients was significantly lower at advanced disease stages and was inversely correlated with regional metastasis. The authors also found that *KISS1* expression was higher in primary tumors than in the secondary metastatic focus, which indirectly confirms the functional role of KISS1 as a metastasis suppressor. Similar results were obtained by Y.B. Sun et al. [15]; according to their data, not only was KISS1 and KISS1R expression lower at stage IV NSCLC compared to stage IIIB LC, but also soluble KISS1 levels in the blood serum at the advanced stage were decreased. At the same time, the survival of patients with high tumor KISS1 and KISS1R expression was better than that of patients with tumors not expressing these proteins. At the same time, E.M. Karapanagiotou et al. [17] did not find any differences in plasma KISS1 levels between NSCLC patients and healthy controls, as well as between patients with locally advanced and metastatic cancer.

The results of our study, which indicate that KISS1 content in the blood serum increases with the progression of lung tumors, are consistent with the results of L. Gatti et al. [16], who demonstrated elevation of its level in NSCLC patients as compared to controls and a decrease in its level after surgery or chemotherapy.

CONCLUSION

Currently, studying possible clinical implications of genes and proteins that function as metastasis suppressors in various cancers is becoming of particular interest. They are considered primarily as potential targets of new types of molecular-targeted therapy and as possible prognostic or diagnostic markers.

The present study demonstrates that the level of one of such proteins, KISS1 or kisspeptin, significantly increases in the blood serum of LC patients as compared to healthy controls regardless of the histologic type of the tumor and is a stage-dependent marker in this disease. It has sufficiently high diagnostic specificity (85%), but is not sensitive enough, especially at early stages of the disease. Based on our results and rather controversial literature data on the role of KISS1 in NSCLC, we conclude that the clinical significance of kisspeptin in LC deserves further in-depth study.

REFERENCES

1. Ly T., Harihar S., Welch D.R. KISS1 in metastatic cancer research and treatment: potential and paradoxes. *Cancer Metastasis Rev.* 2020;39(3):739–754. DOI: 10.1007/s10555-020-09868-9.
2. Harihar S., Welch D.R. KISS1 metastasis suppressor in tumor dormancy: a potential therapeutic target for metastatic cancers? *Cancer Metastasis. Rev.* 2023;42(1):183–196. DOI: 10.1007/s10555-023-10090-6.
3. Wang C.H., Qiao C., Wang R.C., Zhou W.P. KiSS-1-mediated suppression of the invasive ability of human pancreatic carcinoma cells is not dependent on the level of KiSS-1 receptor GPR54. *Mol. Med. Rep.* 2016;13(1):123–129. DOI: 10.3892/mmr.2015.4535.
4. Wang W., Yang Z.L., Liu J.Q., Yang L.P., Yang X.J., Fu X. Overexpression of MTA1 and loss of KAI-1 and KiSS-1

expressions are associated with invasion, metastasis, and poor-prognosis of gallbladder adenocarcinoma. *Tumori.* 2014;100(6):667–674. DOI: 10.1700/1778.19276.
5. Teng Y., Mei Y., Hawthorn L., Cowell J.K. WASF3 regulates miR-200 inactivation by ZEB1 through suppression of KISS1 leading to increased invasiveness in breast cancer cells. *Oncogene.* 2014;33(2):203–211. DOI: 10.1038/onc.2012.565.
6. Hu K.L., Chang H.M., Zhao H.C., Yu Y., Li R., Qiao J. Potential roles for the kisspeptin/kisspeptin receptor system in implantation and placentation. *Hum. Reprod. Update.* 2019;25(3):326–343. DOI: 10.1093/humupd/dmy046.
7. Zhu N., Zhao M., Song Y., Ding L., Ni Y. The KiSS-1/GPR54 system: Essential roles in physiological homeostasis and cancer biology. *Genes. Dis.* 2022;9(1):28–40. DOI: 10.1016/j.gendis.2020.07.008/
8. Ohtaki T., Shintani Y., Honda S., Matsumoto H., Hori A., Kanehashi K. et al. Metastasis suppressor gene KiSS-1 encodes peptide ligand of a G-protein-coupled receptor. *Nature.* 2001;411(6837):613–617. DOI: 10.1038/35079135.
9. Kuohung W., Kaiser U.B. GPR54 and KiSS-1: role in the regulation of puberty and reproduction. *Rev. Endocr. Metab. Disor.* 2006;7(4):257–263. DOI: 10.1007/s11154-006-9020-2.
10. Ciaramella V., Della Corte C.M., Ciardiello F., Morgillo F. Kisspeptin and cancer: molecular interaction, biological functions, and future perspectives. *Front. Endocrinol. (Lausanne).* 2018;9:115. DOI: 10.3389/fendo.2018.00115.
11. Steeg P.S., Ouatas T., Halverson D., Palmieri D., Salerno M. Metastasis suppressor genes: basic biology and potential clinical use. *Clin. Breast Cancer.* 2003;4(1):51–62. DOI: 10.3816/cbc.2003.n.012.
12. Loosen S.H., Luedde M., Lurje G., Spehlmann M., Paffenholz P., Ulmer T.F. et al. Serum levels of kisspeptin are elevated in patients with pancreatic cancer. *Dis. Markers.* 2019;2019:5603474. DOI: 10.1155/2019/5603474.
13. Canbay E., Ergen A., Bugra D., Yamaner S., Eraltan I.Y., Buyukuncu Y. et al. Kisspeptin-54 levels are increased in patients with colorectal cancer. *World J. Surg.* 2012;36(9):2218–2224. DOI: 10.1007/s00268-012-1636-7.
14. Ergen A., Canbay E., Bugra D., Zeybek U., Yamaner S., Bulut T. Plasma Kisspeptin-54 levels in gastric cancer patients. *Int. J. Surg.* 2012;10(9):551–554. DOI: 10.1016/j.ijsu.2012.08.014.
15. Sun Y.B., Xu S. Expression of KISS1 and KISS1R (GPR54) may be used as favorable prognostic markers for patients with non-small cell lung cancer. *Int. J. Oncol.* 2013;43(2):521–530. DOI: 10.3892/ijo.2013.1967.
16. Gatti L., Rolli L., Corno C., Carenini N., Corna E., Ciusani E. et al. Increased serum levels of KiSS1-derived peptides in non-small cell lung cancer patient liquid biopsies and biological relevance. *Transl. Lung Cancer Res.* 2022;11(7):1315–1326. DOI: 10.21037/tlcr-22-52.
17. Karapanagiotou E.M., Dilana K.D., Gkiozos I., Gratsias I., Tsimpoukis S., Polyzos A. et al. Metastin is not involved in metastatic potential of non-small cell lung cancer. *Med. Oncol.* 2011;28(2):559–564. DOI: 10.1007/s12032-010-9466-7.
18. Wang G., Wang Z., Li C., Wang P., Chai D., Cheng Z. Relationship among the expression of lymphatic vessel density, microvessel density, carcinoembryonic antigenic mRNA, KAI1, and Kiss-1, and prognosis in patients with non-small cell lung cancer. *Zhongguo Fei Ai Za Zhi.* 2012;15(6):348–354. DOI: 10.3779/j.issn.1009-3419.2012.06.05.
19. Zheng S., Chang Y., Hodges K.B., Sun Y., MaX., Xue Y. et al. Expression of KISS1 and MMP-9 in non-small cell lung cancer and their relations to metastasis and survival. *Anticancer Res.* 2010;30(3):713–718.

Authors' contribution

Gershtein E.S. – analysis of literature data, drafting of the manuscript. Kovaleva O.V. – analysis of literature data, statistical processing of research results. Kuzmin Yu.B., Alferov A.A. – acquisition of experimental data. Rogozhin D.V. – morphological examination of tumors. Stilidi I.S., Yanushevich O.O. – academic editing of the manuscript. Kushlinskii N.E. – conception and design, general management, academic editing of the manuscript. All authors have read and approved the final version of the manuscript before publication, agree to be responsible for all aspects of the work and ensure that they have properly considered and resolved issues related to the accuracy and integrity of all parts of the work.

Authors' information

Gershtein Elena S. – Dr. Sci. (Biology), Professor, Senior Researcher, Clinical Diagnostic Laboratory of the Centralized Scientific and Clinical Laboratory Department, Consultative and Diagnostic Center, N.N. Blokhin National Research Medical Center of Oncology; Professor, Department of Clinical Biochemistry and Laboratory Diagnostics, A.I. Evdokimov Moscow State University of Medicine and Dentistry, Moscow, esgershtein@gmail.com, https://orcid.org/0000-0002-3321-801X

Kovaleva Olga V. – Cand. Sci. (Biology), Senior Researcher, Laboratory of Regulation of Cellular and Viral Oncogenes, Research Institute of Carcinogenesis, N.N. Blokhin National Research Institute of Oncology, Moscow, ovkovleva@gmail.com, https://orcid.org/0000-0001-6132-9924

Alferov Alexander A. – Cand. Sci. (Med.), Doctor of Clinical Laboratory Diagnostics, Clinical Diagnostic laboratory of the Centralized Scientific and Clinical Laboratory Department, Consultative and Diagnostic Center, N.N. Blokhin National Research Medical Center of

Oncology; Assistant, Department of Clinical Biochemistry and Laboratory Diagnostics, A.I. Evdokimov Moscow State University of Medicine and Dentistry, Moscow, aleksandr.alferov@yahoo.com, https://orcid.org/0000-0003-3585-569

Kuzmin Yuri B. – Cand. Sci. (Biology), Senior Laboratory Assistant, Clinical Diagnostic Laboratory of the Centralized Scientific and Clinical Laboratory Department, Consultative and Diagnostic Center, N.N. Blokhin National Research Medical Center of Oncology; Department of Clinical Biochemistry and Laboratory Diagnostics, A.I. Evdokimov Moscow State University of Medicine and Dentistry, Moscow, biochimia@yandex.ru, https://orcid.org/0000-0003-0430-2754

Rogozhin Dmitry V. – Dr. Sci. (Med.), Head of the Department of Morphological and Molecular Genetic Diagnostics of Tumors, Research Institute of Clinical Oncology named after Academician of the Russian Academy of Medical Sciences and RAS N.N. Trapeznikov, N.N. Blokhin National Research Medical Center of Oncology, Moscow, pathol.777@mail.ru, https://orcid.org/0000-0003-0777-9152

Yanushevich Oleg O. – Dr. Sci. (Med.), Professor, Academician of the Russian Academy of Sciences, Rector of A.I. Evdokimov Moscow State University of Medicine and Dentistry, Moscow, mail@msmsu.ru, https://orcid.org/0000-0003-0059-4980

Stilidi Ivan S. – Dr. Sci. (Med.), Professor, Academician of the Russian Academy of Sciences, Director of N.N. Blokhin National Research Institute of Oncology, Moscow, ronc@list.ru, https://orcid.org/0000-0002-0493-1166

Kushlinskii Nikolay E. – Dr. Sci. (Med.), Professor, Academician of the Russian Academy of Sciences, Academic Director of the Laboratory of Clinical and Diagnostic of the Centralized Scientific and Clinical Laboratory Department, Consultative and Diagnostic Center, N.N. Blokhin National Research Medical Center of Oncology; Head of the Department of Clinical Biochemistry and Laboratory Diagnostics, A.I. Evdokimov Moscow State University of Medicine and Dentistry, Moscow, biochimia@yandex.ru, https://orcid.org/0000-0002-3898-4127

(✉) **Gershtein Elena S.,** esgershtein@gmail.com

Received 22.11.2023;
approved after peer review 15.11.2023;
accepted 21.12.2023

УДК 616.61-02:616.379-008.64]-092.9
https://doi.org/10.20538/1682-0363-2024-1-30-36

Transcriptional regulation of lactate dehydrogenase activity in rat kidney cells in diabetic nephropathy

Eprintsev A.T., Presnyakov E.S., Selivanova N.V.

Voronezh State University
1, Universitetskaya Square, Voronezh, 394063, Russian Federation

ABSTRACT

Aim. To study the features of transcriptional regulation of the activity and isoenzyme composition of lactate dehydrogenase in the kidneys of *Rattus norvegicus* L. in diabetic nephropathy.

Materials and methods. The study included 20 male laboratory rats (*Rattus norvegicus* L.) divided into two equal groups: "Norm" – intact rats injected with 0.9% NaCl intraperitoneally and "Diabetes" – animals with alloxan-induced diabetes (DM1 model). The activity, subcellular localization, and mobility of lactate dehydrogenase (LDH, EC 1.1.1.27) isoenzymes were studied using spectrophotometry and electrophoresis. *LDHA* and *LDHB* gene transcripts were analyzed by the polymerase chain reaction.

Results. Analysis of the LDH activity showed that this parameter increased by more than 6 times in the animals with diabetic nephropathy compared to the control group. Moreover, the increase in the rate of the LDH activity was a consequence of the enzyme activation in all the studied compartments of the cell and is consistent with the parameter in the homogenate. The increase in the LDH activity in diabetic nephropathy may result from redistribution of the activity rate between the available isoforms and may be associated with an increase in the transcription rate of genes encoding subunits A and B of this enzyme.

Conclusion. The increase in the LDH activity is likely associated with the activation of renal gluconeogenesis, the main substrate for which is lactic acid reabsorbed in the renal glomeruli. The revealed increase in the LDH activity in the kidneys of rats with diabetic nephropathy may be associated with adaptation of their metabolism to the pathological state.

Keywords: lactate dehydrogenase, diabetic nephropathy, isoenzyme, regulation, transcription

Conflict of interest. The authors declare the absence of obvious or potential conflicts of interest related to the publication of this article.

Source of financing. The study was supported by the RFBR (project No. 20-04-00296).

Conformity with the principles of ethics. The study was approved by the Ethics Committee for Biomedical Research at Voronezh State University (Protocol No. 42-04 of 05.09.2022).

For citation: Eprintsev A.T., Presnyakov E.S., Selivanova N.V. Transcriptional regulation of lactate dehydrogenase activity in rat kidney cells in diabetic nephropathy. *Bulletin of Siberian Medicine.* 2024;23(1):30–36. https://doi.org/10.20538/1682-0363-2024-1-30-36.

✉ *Selivanova Natalia V.,* kir2202@yandex.ru

Транскрипционная регуляция функционирования лактатдегидрогеназы в клетках почек крыс при диабетической нефропатии

Епринцев А.Т., Пресняков Е.С., Селиванова Н.В.

Воронежский государственный университет (ВГУ)
Россия, 394063, г. Воронеж, Университетская пл., 1

РЕЗЮМЕ

Целью данной работы являлось изучение особенностей транскрипционной регуляции активности и изоферментного состава лактатдегидрогеназы в почках *Rattus norvegicus* L. при диабетической нефропатии.

Материалы и методы. Проведено исследование 20 самцов лабораторных крыс *Rattus norvegicus* L., разделенных на две равные группы: «Норма» – интактные крысы, которым внутрибрюшинно вводили 0,9%-й NaCl, и «Диабет» – животные с аллоксановым диабетом. Исследовалась активность, субклеточная локализация и подвижность изоферментов лактатдегидрогеназы (ЛДГ, КФ 1.1.1.27) с использованием спектрофотометрических, электрофоретических методов, а также использовалась полимеразная цепная реакция в реальном времени для анализа транскриптов генов *LDHA* и *LDHB*.

Результаты. Анализ активности ЛДГ показал, что данный параметр вырос более чем в 6 раз у животных с диабетической нефропатией по сравнению с контрольной группой. Возрастание скорости функционирования ЛДГ является следствием активизации фермента во всех исследуемых компартментах клетки и согласуется с показателем в гомогенате. Вероятно, увеличение активности ЛДГ при диабетической нефропатии является следствием перераспределения скорости функционирования между имеющимися изоформами и связано с усилением скорости транскрипции генов, кодирующих субъединицы А и В данного фермента.

Заключение. Усиление работы ЛДГ, вероятно, является следствием активизации почечного глюконеогенеза, основным субстратом для которого является именно молочная кислота, реадсорбируемая в почечных клубочках. Выявленное увеличение активности ЛДГ в почках крыс при диабетической нефропатии может быть связано с адаптацией их биохимического метаболизма к патологическому состоянию.

Ключевые слова: лактатдегидрогеназа, диабетическая нефропатия, изофермент, регуляция, транскрипция

Конфликт интересов. Авторы декларируют отсутствие явных и потенциальных конфликтов интересов, связанных с публикацией настоящей статьи.

Источник финансирования. Исследование выполнено при финансовой поддержке РФФИ (проект № 20-04-00296).

Соответствие принципам этики. Исследование одобрено этическим комитетом по экспертизе биомедицинских исследований ВГУ (протокол № 42-04 от 05.09.2022).

Для цитирования: Епринцев А.Т., Пресняков Е.С., Селиванова Н.В. Транскрипционная регуляция функционирования лактатдегидрогеназы в клетках почек крыс при диабетической нефропатии. *Бюллетень сибирской медицины.* 2024;23(1):30–36. https://doi.org/10.20538/1682-0363-2024-1-30-36.

INTRODUCTION

Diabetes mellitus is one of the most important medical, social, and economic problems worldwide [1]. The main danger of this pathology is associated with the development of various complications, which include diabetic nephropathy (DN). Every year the number of people with diabetes mellitus grows, therefore, the risk of developing this disease increases for each person [2]. The mechanism of DN is based on the development of sclerotic changes in the renal glomeruli, which lead to impaired kidney function and chronic renal failure. The main problem of this pathology is that there are no pronounced symptoms at initial stages of diabetes mellitus. By the time the symptoms manifest and a diagnosis of DN is made, the disease is already progressing very actively and becomes practically incurable [3].

The kidneys maintain high resting metabolic rate in the human body [4] and occupy the second place in terms of oxygen consumption and mitochondrial content, after

the heart [5]. Such an active mechanism of energy production is crucial for maintaining normal kidney function, which requires active transport and reabsorption of dissolved substances, including amino acids, sugars and other essential elements, back into the blood. However, in DN caused by diabetes mellitus, damage to the kidney tissues is observed, which can cause metabolic changes in them, including activation of glycolysis and fatty acid metabolism, as well as mitochondrial dysfunction and impaired ATP production [6].

The kidneys contain lactate dehydrogenase (LDH, EC 1.1.1.27), which is involved in the final stage of anaerobic glycolysis and performs reversible conversion of pyruvate into lactate [7]. But there is very little information about the activity of this enzyme in DN, which is a relevant and interesting topic to study.

MATERIALS AND METHODS

The study included male laboratory rats (*Rattus norvegicus L)* weighing about 150–200 g (Stezar breeding station, Russia). The study was approved by the Ethics Committee for Biomedical Research at Voronezh State University (Protocol No. 42-04 of 05.09.2022). The study was performed in accordance with the principles of humanity set out in the European Council directives (86 / 609 / EEC) and the Declaration of Helsinki.

The DN model in type 1 diabetes mellitus was created by a single intraperitoneal injection of a 5% solution of alloxan diluted in 0.9% sodium citrate at a dose of 150 mg / kg of live weight [8]. The animals (n = 20) were randomly divided into 2 equal experimental groups: “Norm” – intact rats injected with 0.9% NaCl intraperitoneally, and “Diabetes” – animals with alloxan-induced diabetes. To control the incidence of diabetes mellitus in the experimental group of rats, the blood glucose level was determined using the glucose meter Sattelit Plus PKG-02.4. Blood sampling was performed from the caudal vein in the morning on an empty stomach. Creatinine clearance was assessed by the concentration of creatinine in the blood serum and urine using the Jaffe’s method using the Creatinine Vital kit (Vital Development Corporation LLC, Russia). The calculation was carried out according to the formula:

$$\text{Creatinine clearance}((\text{ml/min})/\text{kg}) = \frac{\text{urine volume in 24 h (ml)} \times \text{urine creatinine (mmol/l)}}{\frac{\text{serum creatinine (mmol/l)} \times 0.001}{\text{rat weight (kg)}}}$$

The anesthetized animals were decapitated 3 months after the administration of alloxan, and the kidneys were extracted. Kidney tissue was homogenized in a 10-fold volume of the isolation medium containing 1 mM EDTA; 2 mM KCl; 3 mM DTT; 0.35 M sucrose; and 50 mM Tris-HCl buffer (pH = 7.8). Centrifugation was carried out for 5 minutes at 3,000 g and a temperature of 4 °C. A supernatant (homogenate) was selected, which was later used to measure the activity of the enzyme. Cytoplasm and mitochondria were separated by differential centrifugation [9].

The cross-contamination assay was used to assess the purity of the studied fractions, measuring the activity of succinate dehydrogenase [10] and alcohol dehydrogenase [11].

LDH activity was measured by spectrophotometry at a wavelength of 340 nm. A decrease in the optical density of the solution associated with the utilization of NADH during the conversion of pyruvate to lactate in the spectrophotometry medium of the following composition was evaluated: 5 mM MgCl; 10 mM KCl; 1.25 mM NADH; 3 mM pyruvate; 10 mM potassium phosphate buffer, pH = 7.8.

Separation of LDH isoenzymes was performed by polyacrylamide gel electrophoresis at a temperature of 4 °C. For the gel to be seen, a tetrazolium salt-based method was used, which is based on the emergence of a blue-colored compound formazan, that is a product of HCT reduction [12].

The nucleotide sequences of the rat *LDHA* and *LDHB* mRNA genes were obtained from the international GenBank sequence database (https://www.ncbi.nlm.nih.gov/gene /?term=lactate+dehdrogenase+rat). Identification of gene homology and comparative analysis of their composition were carried out using the BLAST software (https://blast.ncbi.nlm.nih.gov /). The Primer- BLAST program located on the NCBI website was used for the selection of primers. The obtained sequences were tested for specificity to the desired genes in the Primer- BLAST and for the formation of crosslinking and other secondary structures in the ClustalOmega program. Specific primers for *LDHA* and *LDHB* rat LDH genes (*LDHA*: forward 5’-ctcagcgtcccatgtatcct-3’; reverse 5’-tgagatttcccccagaccac-3’; *LDHB*: forward 5’- ctggattctgctcggtttcg-3’; reverse 5’- tgaggtcagccacacttagg-3’) were selected based on the analyzed sequences.

RNA was isolated by phenol chloroform extraction [13], followed by visualization by agarose gel electrophoresis (1%) [14]. Reverse transcription was carried out in order to obtain cDNA using the M-MuLV reverse transcriptase enzyme and oligo(dT) primers (SibFerment, Russia) for the synthesis of the first cDNA chain according

to the manufacturer's instructions. The real-time polymerase chain reaction was carried out on the LightCycler 96 PCR analyzer (Roche, Switzerland). The Extra-mix for PCR HS-Taq PCR kits (DiaM, Russia) were used as reagents. SYBR Green I was taken as a dye. Amplification parameters: preliminary denaturation at 95 °C for 5 min, then a cycle: 95 °C – 20 s, 59 °C – 30 s, 72 °C – 40 s (detection), final elongation – 72 °C – 10 min.

To verify the reliability of the data obtained, all experiments and measurements were carried out using 8x biological and 5x analytical replicates. Calculations were carried out in the Microsoft Office Excel 2007 program, and their further analysis was performed in the Stattech program (StatTech v. 1.2.0; Stattech LLC, Russia). Quantitative variables were checked for normality of distribution using the Shapiro – Wilk test. The figures present the data as the mean and the standard error of the mean ($M \pm SE$). The results of the experiment were analyzed using the Student's t-test with the calculation of the mean and the standard deviation. The correlation analysis using the Pearson's correlation coefficient was performed to identify the relationships between the parameters. All the data presented in this paper are statistically significant, $p < 0.05$.

RESULTS

The data obtained when measuring the concentration of glucose in the blood of the rats are shown in Fig. 1. It demonstrates that in the rats included in the "Norm" group, the concentration of glucose in the blood fluctuated within 4.1 ± 1.3 mmol / l throughout the entire experiment, whereas in the animals exposed to prolonged alloxan intoxication, this parameter significantly exceeded normal values and was approximately 15.5 ± 2.7 mmol / l.

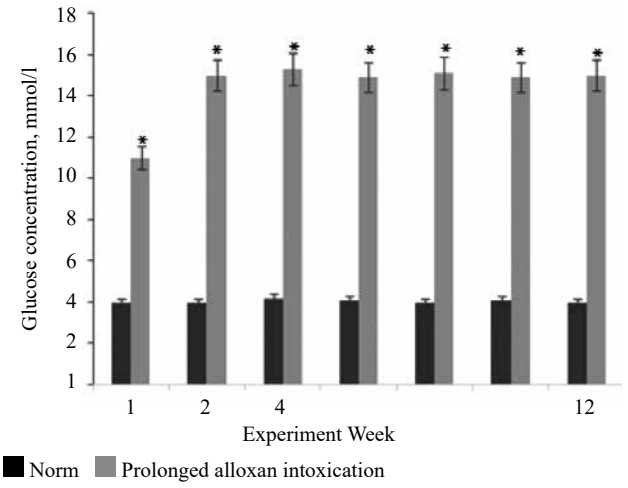

Fig. 1. Glucose concentration in the blood of experimental animals. Norm – healthy rats; Prolonged alloxan intoxication – animals with alloxan-induced diabetes. * $p < 0.01$. Here and in Fig. 2–4, 6, the method used is Student's *t*-test

A significant increase in blood glucose levels is the evidence of diabetes mellitus initiation.

We determined creatinine clearance in the blood serum of the experimental animals to assess glomerular filtration rate. The results presented in Fig.2 show that creatinine clearance increased by 1.64 times (3.05 and 1.83 ml / min / kg; $p < 0.05$) compared with the control group, which may indicate the development of an early stage of DN.

It was revealed that the level of protein excretion in the urine increased by 3.6 times by the second month of the experiment (from 8.1 to 28.9 mg / day; $p < 0.03$) (Fig. 3). At week 12 of the experiment, the value of the studied parameter decreased slightly and was 25.9 ± 0.1 mg / day. In the control group (rats injected with saline), the protein concentration in the urine fluctuated at the level of 7.89–8.01 mg / day, which corresponds to physiological values.

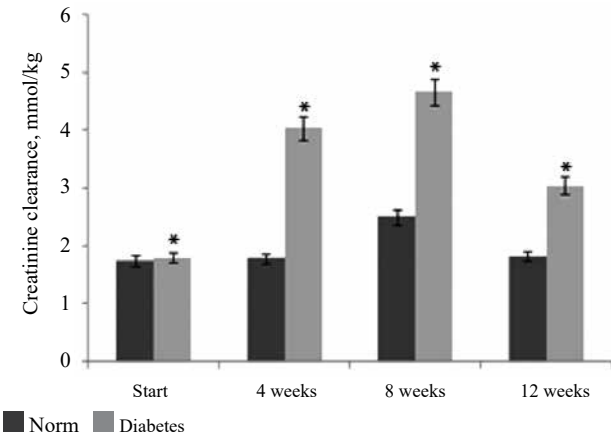

Fig.2. Determination of creatinine clearance in the blood serum of the animals with prolonged alloxan intoxication. Start – the beginning of the experiment; Norm – healthy rats; Diabetes – animals with alloxan-induced diabetes; * $p < 0.05$

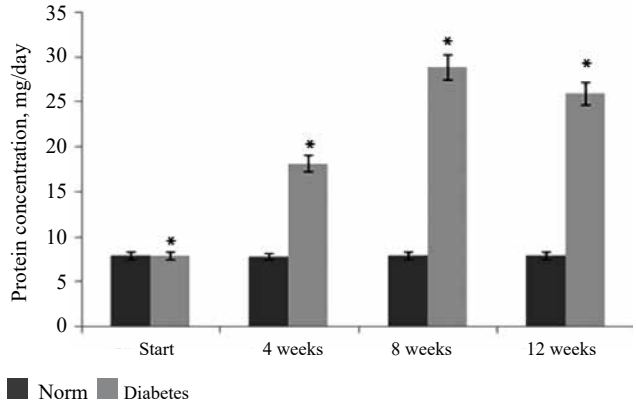

Fig. 3. Determination of protein concentration in the urine in the animals. Norm – healthy rats; Diabetes – animals with prolonged alloxan intoxication; * $p < 0.05$.

The analysis of the rate of LDH activity showed that this parameter increased by more than 6 times in the kidneys of the animals with DN compared with the control group (2.3 and 14.5 U / gram of wet mass; $p < 0.01$) (Fig. 4, *a*).

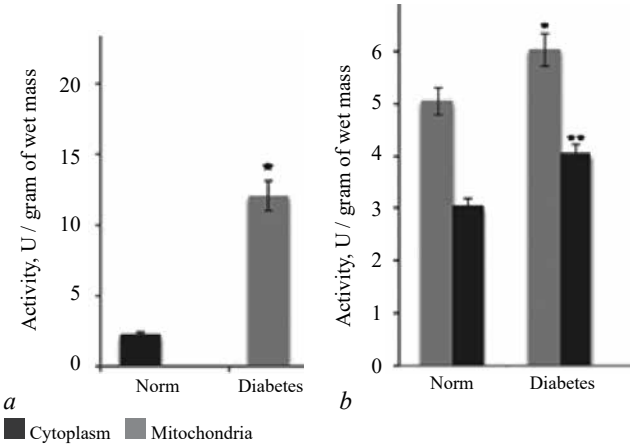

Fig. 4. Lactate dehydrogenase activity in the homogenate (*a*), cytoplasm and mitochondria (*b*) of rat kidneys. * $p < 0.01$; ** $p \leq 0.03$

LDH activity is observed both in the cytoplasm and mitochondria (Fig. 4, *b*), which is confirmed by the literature data on the subcellular localization of the enzyme under study.

Polyacrylamide gel electrophoresis conducted with subsequent manifestation of LDH activity showed the presence of 4 forms of the enzyme in the kidney cells of both groups of animals with R_f 0.04; 0.18; 0.26, and 0.32 (Fig. 5).

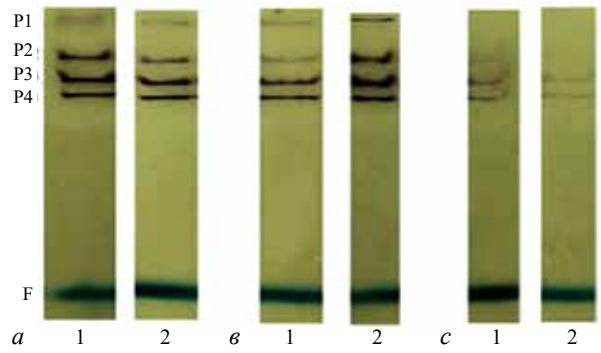

Fig. 5. Isoenzyme composition of lactate dehydrogenase in kidney cells of intact rats (1) and animals exposed to prolonged alloxan intoxication (2): *a* – homogenate; *b* – cytoplasmic fraction; *c* – mitochondria; P1–4 – protein bands; F – front line

A real-time polymerase chain reaction was performed to assess the expression level of genes encoding lactate dehydrogenase A and B subunits. As the analysis of the data obtained shows (Fig. 6), both genes are actively transcribed in the kidneys of rats with DN, but are less active in the kidneys of healthy animals. Moreover, with the development of this pathology, the expression of the *LDHA* gene increased by almost 3 times, and the expression of the *LDHB* gene – by more than 4 times.

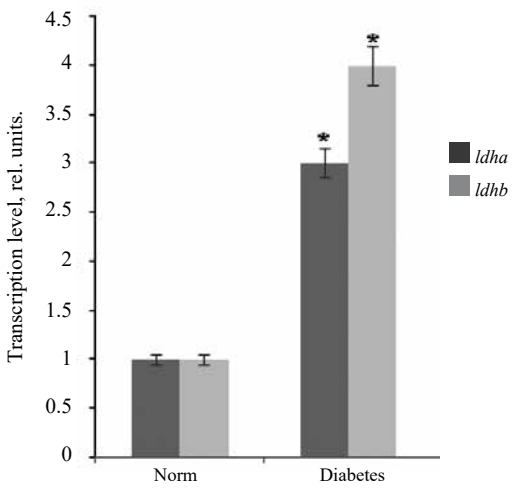

Fig. 6. Relative transcription level of *LDHA* and *LDHB* genes in the kidneys of healthy rats (Norm) and animals with diabetic nephropathy (Diabetes). * $p < 0.01$

DISCUSSION

The analysis of the results of blood and urine biochemistry in healthy rats and animals with prolonged alloxan intoxication showed that the latter have impaired kidney function against the background of diabetes mellitus. Thus, the data obtained confirm DN development in the experimental group of rats.

An increase in the LDH activity in the kidneys of the rats with DN may be associated with a need to utilize lactate entering the kidneys from the blood. It is known that in type 1 diabetes mellitus, there is a significant increase in renal gluconeogenesis, the main substrate for which is lactic acid reabsorbed in the renal glomeruli. This fact also explains the reason for the accumulation of glycogen in diabetic kidneys [15]. The LDH activity is observed both in the cytoplasm and in mitochondria, which is in line with the literature data on the subcellular localization of the enzyme under study [16].

A slight increase in the LDH activity in the mitochondria of the rats with alloxan-induced diabetes may be associated with the cell's need for additional energy to adapt the body to oxidative stress caused by alloxan administration. In addition, it is known that acceleration of mitochondrial oxidation of lactic acid is observed with intensive development of the nervous system, food deprivation, and physical overstrain [17]. The reliability of the data obtained was confirmed by the determination of cross-contamination with succinate dehydroge-

nase (mitochondrial enzyme) and alcohol dehydrogenase (cytoplasmic marker), which was approximately 11–14%. This fact testifies to the successful separation of factions.

Four isoforms of the enzyme were found in the kidney cells of both groups of animals when studying the isoenzyme composition of LDH. The increase in the LDH activity in DN may not be associated with the synthesis of additional forms of the enzyme, but is a consequence of the redistribution of the activity rate between the existing isoforms. Interestingly, in the cytoplasmic fraction of both intact (healthy) rats and animals with prolonged alloxan intoxication, the presence of four forms of the enzyme is also observed. At the same time, only two isoforms were found in the mitochondria.

The analysis of the level of gene expression revealed the relationship of this parameter ($r_s = 1$) with the LDH activity in rat kidney cells under normal and pathological conditions. The increase in the rate of LDH activity in the kidneys of the rats with prolonged alloxan intoxication is likely associated with the increase in the transcription rate of genes encoding subunits A and B of this enzyme.

CONCLUSION

Induction of prolonged alloxan intoxication allowed to determine a number of biochemical disorders (the level of protein excretion in the urine increased by 3.6 times (from 8.01 to 28.94 mg / day; $p < 0.03$), creatinine clearance – by 1.64 times (3.05 and 1.83 ml / min / kg; $p < 0.05$) compared with the control group of animals) associated with the development of DN against the background of high blood glucose. The analysis of the LDH activity showed that this parameter increased by more than 6 times in the kidneys of the animals with DN compared with the healthy animals.

It may be due to the increase in the concentration of transcripts of genes encoding subunits A and B of this enzyme. At the same time, no changes in the isoenzyme composition of LDH were detected. Increasing LDH activity may be necessary to activate renal gluconeogenesis, the main substrate for which is lactic acid reabsorbed in the renal glomeruli [17]. Thus, during the study, we revealed the increase in the rate of LDH activity in the kidneys of the rats with DN, which may be associated with the adaptation of their metabolism to the pathological condition.

REFERENCES

1. Schmidt A.M. Highlighting diabetes mellitus: the epidemic continues. *Arterioscler. Thromb. Vasc. Biol*. 2018;38(1):e1–e8 DOI: 10.1161/ATVBAHA.117.310221.
2. Shen Z., Fang Y., Xing T., Wang F. Diabetic nephropathy: from pathophysiology to treatment. *J. Diabetes Res*. 2017:2379432. DOI: 10.1155/2017/2379432.
3. Nagib A.M., Matter Y.E., Gheith O.A., Refaie A.F., Othman N.F., Al-Otaibi T. Diabetic nephropathy following posttransplant diabetes mellitus. *Exp. Clin. Transplant*. 2019;17(2):138–146. DOI: 10.6002/ect.2018.0157.
4. Silva P.H.I., Mohebbi N. Kidney metabolism and acid-base control: back to the basics. *Pflugers Arch*. 2022;474(8):919–934. DOI: 10.1007/s00424-022-02696-6.
5. Clark A.J., Parikh S.M. Mitochondrial metabolism in acute kidney injury. *Semin. Nephrol.* 2020;40(2):101–113. DOI: 10.1016/j.semnephrol.2020.01.002.
6. Samsu N. Diabetic nephropathy: challenges in pathogenesis, diagnosis, and treatment. *Biomed. Res. Int*. 2021;1497449. DOI: 10.1155/2021/1497449.
7. Osis G., Traylor A.M., Black L.M., Spangler D., George J.F., Zarjou A. et al. Agarwal expression of lactate dehydrogenase A and B isoforms in the mouse kidney. *Am. J. Physiol. Renal. Physiol.* 2021;320(5):F706–F718. DOI: 10.1152/ajprenal.00628.2020.
8. Ighodaro O.M., Adeosun A.M., Akinloye O.A. Alloxan-induced diabetes, a common model for evaluating the glycemic-control potential of therapeutic compounds and plants extracts in experimental studies. *Medicina (Kaunas)*. 2017;53(6):365–374. DOI: 10.1016/j.medici.2018.02.001.
9. Djafarzadeh S., Jakob S.M. Isolation of intact mitochondria from skeletal muscle by differential centrifugation for high-resolution respirometry measurements. *J. Vis. Exp*. 2017;121:55251. DOI: 10.3791/55251.
10. Eprintsev A.T., Fedorin D.N., Selivanova N.V. Molecular aspects of the formation of the oligomeric structure in succinate dehydrogenase. Voronezh: Publishing House of the Central – Chernozem Region, 2016:263 (in Russ.).
11. Piechota J., Jelski W., Orywal K., Mroczko B. The comparison of total bile acid concentration and alcohol dehydrogenase activity as markers of intrahepatic cholestasis of pregnancy. *Acta Biochim. Pol.* 2021;69(1):173–176. DOI: 10.18388/abp.2020_5841.
12. Eprintsev A. T., Bondareva I. R., Selivanova N.V. Expression levels and activity of rat liver lactate dehydrogenase isoenzymes in alloxan-induced diabetes. *Biomedical Chemistry*. 2022;68(1):33–38 (in Russ.). DOI: 10.18097/PBMC20226801032.
13. Toni L.S., Garcia A.M., Jeffrey D.A., Jiang X., Stauffer B.L., Miyamoto Sh.D. et al. Optimization of phenol-chloroform RNA extraction. *MethodsX*. 2018;5:599–608. DOI: 10.1016/j.mex.2018.05.011.
14. Wittmeier P., Hummel S. Agarose gel electrophoresis to assess PCR product yield: comparison with spectrophotometry, fluorometry and qPCR. *Biotechniques*. 2022;72(4):155–158. DOI: 10.2144/btn-2021-0094.
15. Kume S., Araki S.I., Ugi S., Morino K., Koya D., Nishio Y. et al. Secular changes in clinical manifestations of kidney disease among Japanese adults with type 2 diabetes from 1996 to 2014. *Journal of Diabetes Investigation*. 2019;10(4):1032–1040. DOI: 10.1111/jdi.12977
16. Young A., Oldford C., Mailloux R. J. Lactate dehydrogenase supports lactate oxidation in mitochondria isolated from different mouse tissues. *Redox Biol*. 2020;28:101339. DOI: 10.1016/j.redox.2019.101339.

17. Glancy B., Kane D.A., Kavazis A.N., Goodwin M.L., Willis W.T., Gladden L.B. Mitochondrial lactate metabolism: history and implications for exercise and disease. *J. Physiol.* 202;599(3):863–888. DOI: 10.1113/JP278930.

Authors' information

Eprintsev Alexander T. – Dr. Sci. (Biology), Professor, Head of the Department of Biochemistry and Cell Physiology, Voronezh State University, Voronezh, bc366@bio.vsu.ru, http://orcid.org/0009-0007-7339-7773

Presnyakov Evgeny S. – 6th-year Student, Department of Medicine and Biology, Voronezh State University, Voronezh, bc366@bio.vsu.ru

Selivanova Natalia V. – Cand. Sci. (Biology), Associate Professor, Department of Biochemistry and Cell Physiology, Voronezh State University, Voronezh, kir2202@yandex.ru, http://orcid.org/0000-0001-7148-3415

(✉) **Selivanova Natalia V.,** kir2202@yandex.ru

Received 01.02.2023;
approved after peer review 17.05.2023;
accepted 14.09.2023

УДК 617.51/.53-006.61:615.849.12
https://doi.org/10.20538/1682-0363-2024-1-37-47

Study of head and neck squamous cell carcinoma transcriptome after proton therapy

Jumaniyazova E.D.[1], Vishnyakova P.A.[1,2], Chirkova M.V.[3], Karpulevich E.A.[3], Eremina I.Z.[1], Gordon K.B.[1,4], Kaprin A.D.[1,5], Fatkhudinov T.H.[1,6]

[1] Research Institute of Molecular and Cellular Medicine of the Peoples' Friendship University of Russia (RUDN Research Institute of MCM)
6, Miklukho-Maklaya Str., Moscow, 117198, Russian Federation

[2] National Medical Research Center of Obstetrics, Gynecology and Perinatology named after Academician V.I. Kulakov
4, Akademika Oparina Str., Moscow, 117997, Russian Federation

[3] Ivannikov Institute for System Programming of the Russian Academy of Sciences (ISP RAS)
25, Aleksandra Solzhenitsyna Str., Moscow, 109004, Russian Federation

[4] A. Tsyb Medical Radiological Research Center – branch of FGBU National Medical Research Center of Radiology (a branch of FGBU National Medical Research Center of Radiology)
10, Marshala Zhukova Str., Obninsk, 249036, Russian Federation

[5] National Medical Research Center of Radiology (NMC Radiology of the Ministry)
4, Koroleva Str., Obninsk, 249036, Russian Federation

[6] Avtsyn Research Institute of Human Morphology
3, Tsyurupy Str., Moscow, 117418, Russian Federation

ABSTRACT

Aim. To evaluate changes in the transcriptome of head and neck squamous cell carcinoma (HNSCC) tissue cells in patients after proton therapy.

Materials and methods. Biopsy material obtained from 3 HNSCC patients before and after proton therapy at a total dose of 10 isoGy was homogenized, purified, and concentrated. Then total RNA was isolated with further purification and concentration with the RNA Clean & Concentrator kit (Zymo Research). Library quantitation was assessed using the Qubit 2.0 instrument (Invitrogen, Life Technologies). After isolation of 1 μg total RNA for sequencing, libraries were prepared on the Illumina platform using the TruSeq RNA Sample Prep Kit v2 with a 10-cycle enrichment step according to the manufacturer's recommendations. The quality of RNA and the resulting libraries was checked using the Agilent 2100 Bioanalyzer system (Agilent Tec. Inc., USA). The RIN parameter for RNA was at least 7. The library concentration was assessed by real-time PCR on the CFX96 Touch Real-Time PCR Detection System (Bio-Rad, USA). Final libraries were pooled in equimolar ratios before sequencing on the Illumina HiSeq 2500 platform using 50 base-pair paired-end reads. The Q20 parameter for all samples was > 97%, and the number of reads averaged 60.2 million per sample. Raw reads were processed using the RTA 1.17.21.3 and Casava 1.8.2 (Illumina). The enrichment analysis was performed using the PANTHER 17.0 software.

Results. The transcriptome analysis of HNSCC after proton radiation therapy (5 x 2 isoGy) at a total dose of 10 isoGy revealed 1,414 significantly differentially expressed genes. The 10 most and least expressed genes and their associated signaling pathways were identified. A number of signaling pathways associated with the underexpressed genes were detected in HNSCC after proton therapy, such as: STAT5; PD-1 signaling pathway; marked MET-mediated activation of PTK2 signaling pathway, PDGF signaling; CD22-mediated regulation of

✉ *Jumaniyazova Enar D.,* enar2017@yandex.ru

BCR; and FCERI-mediated MAPK activation. In addition to the above signaling pathways, activation of collagen degradation, FCGR3A-mediated phagocytosis, and FCGR3A-mediated interleukin (IL)-10 synthesis are of interest. In the enrichment analysis among highly expressed genes, keratinization and biological oxidation processes were activated in HNSCC tissues after proton therapy.

Conclusion. Proton therapy in HNSCC leads to overexpression of genes involved in the regulation of keratinization and biological oxidation processes as well as to underexpression of genes associated with suppression of signaling pathways: STAT5, PD-1, MET-mediated activation of PTK2 signaling pathway, PDGF signaling; CD22-mediated regulation of BCR; FCERI-mediated MAPK activation, collagen degradation, FCGR3A-mediated phagocytosis activation, and FCGR3A-mediated IL-10 synthesis. All signaling pathways of underexpressed genes function in HNSCC cells if there is no negative influence on the tumor from outside (irradiation or delivery of antitumor drugs). The predominance of suppressed signaling pathways over activated ones most likely indicates a decrease in the functional potential of cells after proton therapy. The dose-dependence of proton therapy effects requires further study of changes in cellular and molecular-genetic signatures of HNSCC after proton therapy at different doses.

Keywords: head and neck squamous cell carcinoma, transcriptome, proton therapy, signaling pathways

Conflict of interest. The authors declare the absence of obvious or potential conflicts of interest related to the publication of this article.

Source of financing. The study was supported by the Ministry of Science and Higher Education of the Russian Federation (agreement No. 075-15-2022-294 dated April 15, 2022) and the Ministry of Science and Higher Education of the Russian Federation, agreement No. 075-15-2021-1356 dated October 7, 2021 (identifier RF 0951.61321X0012, No. 15.SIN.21.0011).

Conformity with the principles of ethics. All patients signed an informed consent to participate in the study. Before enrollment in the study, the study protocol and patient information and informed consent forms were approved by an independent Ethics Committee (Protocol No. 634 of 17.11.2021, Protocol No. 684 of 02.03.2022).

For citation: Jumaniyazova E.D., Vishnyakova P.A., Chirkova M.V., Karpulevich E.A., Eremina I.Z., Gordon K.B., Kaprin A.D., Fatkhudinov T.H. Study of head and neck squamous cell carcinoma transcriptome after proton therapy. *Bulletin of Siberian Medicine.* 2024;23(1):37–47. https://doi.org/10.20538/1682-0363-2024-1-37-47.

Исследование транскриптома плоскоклеточного рака головы и шеи после протонного облучения

Джуманиязова Э.Д.[1], Вишнякова П.А.[1, 2], Чиркова М.В.[3], Карпулевич Е.А.[3], Еремина И.З.[1], Гордон К.Б.[1, 4], Каприн А.Д.[1, 5], Фатхудинов Т.Х.[1, 6]

[1] Научно-исследовательский институт молекулярной и клеточной медицины Российского университета дружбы народов (НИИ МКМ РУДН)
Россия, 117198, г. Москва, ул. Миклухо-Маклая, 6

[2] Национальный медицинский исследовательский центр акушерства, гинекологии и перинатологии (НМИЦ АПГ) им. акад. В.И. Кулакова
Россия, 117997, г. Москва, ул. Академика Опарина, 4

[3] Институт системного программирования им. В.П. Иванникова Российской академии наук (ИСП РАН)
Россия, 109004, г. Москва, ул. Александра Солженицына, 25

[4] Медицинский радиологический научный центр (МРНЦ) им. А. Цыба – филиал Национального медицинского исследовательского центра радиологии (филиал «НМИЦ радиологии»)
Россия, 249036, г. Обнинск, ул. Маршала Жукова, 10

[5] Национальный медицинский исследовательский центр (НМИЦ) радиологии
Россия, 249036, г. Обнинск, ул. Королева, 4

[6] Научно-исследовательский институт морфологии человека (НИИМЧ) им. акад. А.П. Авцына
Россия, 117418, г. Москва, ул. Цюрупы, 3

РЕЗЮМЕ

Цель – оценить изменения транскриптома клеток ткани плоскоклеточного рака головы и шеи (ПРГШ) у пациентов после протонного облучения.

Материалы и методы. Биопсийный материал, полученный от трех пациентов ПРГШ до и после протонного облучения в суммарной дозе 10 изоГр, был подвергнут гомогенизации, очистке и концентрации. После чего была выделена тотальная РНК с последующей очисткой и концентрацией набором RNA Clean & Concentrator (Zymo Research), количество оценивали с помощью прибора Qubit 2.0 (Invitrogen, Life Technologies). После выделения тотальной РНК из 1 мкг для секвенирования на платформе Illumina были приготовлены библиотеки с использованием набора TruSeq RNA Sample Prep Kit v2 с этапом обогащения в 10 циклов в соответствии с рекомендациями производителя. Качество РНК и полученных библиотек проверялось с помощью системы капиллярного электрофореза Agilent 2100 Bioanalyzer (Agilent Tec. Inc., США). Параметр RIN для РНК составлял не менее 7. Концентрацию библиотек оценивали с помощью полимеразной цепной реакции в реальном времени на приборе CFX96 Touch Real-Time PCR Detection System (Bio-Rad, США). Окончательные библиотеки объединяли в эквимолярных пропорциях перед секвенированием на платформе Illumina HiSeq 2500 с использованием парно-концевых прочтений по 50 оснований. Параметр Q20 для всех образцов составил более 97%, а количество прочтений в среднем равнялось 60,2 млн на образец. Сырые прочтения были обработаны с использованием RTA 1.17.21.3 и Casava 1.8.2 (Illumina). Анализ обогащения был выполнен с помощью программного обеспечения PANTHER 17.0.

Результаты. В ходе транскриптомного анализа ПРГШ после пятикратного облучения пациентов протонами (2 изоГр) в суммарной дозе 10 изоГр было обнаружено 1 414 значимо дифференциально экспрессированных генов. Выделены 10 наиболее и наименее экспрессируемых генов и ассоциированные с ними сигнальные пути. В ПРГШ после облучения протонами обнаружен ряд сигнальных путей, связанных с низкоэкспрессированными генами, таких как STAT5; сигнальный путь PD-1; отмечена MET-опосредованная активация сигнального пути PTK2, передача сигналов PDGF; CD22-опосредованная регуляция BCR; активация MAPK, опосредованная FCERI. Кроме вышеназванных сигнальных путей обращает на себя внимание активация процесса распада коллагена, FCGR3A-опосредованного фагоцитоза и FCGR3A-опосредованного синтеза интерлейкина-10 (IL10). При анализе обогащения среди высокоэкспрессируемых генов в ткани ПРГШ после протонного облучения были активированы процессы ороговения и биологического окисления.

Заключение. Облучение протонами при ПРГШ приводит к гиперэкспрессии генов, вовлеченных в регуляцию процессов ороговения и биологического окисления; гипоэкспрессии генов, связанных с подавлением сигнальных путей: STAT5, PD-1, MET-опосредованной активации сигнального пути PTK2, передачи сигналов PDGF; CD22-опосредованной регуляции BCR; активации MAPK, опосредованной FCERI, процесса распада коллагена, активации FCGR3A-опосредованного фагоцитоза и FCGR3A-опосредованного синтеза IL10. Все сигнальные пути гипоэкспрессированных генов функционируют в клетках ПРГШ, если негативного влияния на опухоль не оказывается извне (облучение или поступление противоопухолевых препаратов). Преобладание подавленных сигнальных путей над активированными, вероятнее всего, свидетельствует о снижении функционального потенциала клеток после облучения протонами. Дозозависимость эффектов ПТ обусловливает необходимость дальнейшего изучения изменений клеточных и молекулярно-генетических сигнатур ПРГШ после протонного облучения разными дозами.

Ключевые слова: плоскоклеточный рак головы и шеи, транскриптом, протонное облучение, сигнальные пути

Конфликт интересов. Авторы декларируют отсутствие явных и потенциальных конфликтов интересов, связанных с публикацией настоящей статьи.

Источник финансирования. Работа выполнена при финансовой поддержке Министерства науки и высшего образования Российской Федерации (соглашение № 075-15-2021-1356 от 7.10.2021 (идентификатор РФ 0951.61321X0012, № 15.СИН.21.0011)). Обсчеты выполнены при финансовой поддержке Министерства науки и высшего образования Российской Федерации (соглашение № 075-15-2022-294 от 15.04.2022).

Соответствие принципам этики. Все пациенты подписали информированное согласие на участие в исследовании. Исследование одобрено независимым комитетом по этике (протокол № 634 от 17.11.2021, протокол № 684 от 02.03.2022).

Для цитирования: Джуманиязова Э.Д., Вишнякова П.А., Чиркова М.В., Карпулевич Е.А., Еремина И.З., Гордон К.Б., Каприн А.Д., Фатхудинов Т.Х. Исследование транскриптома плоскоклеточного рака головы и шеи после протонного облучения. *Бюллетень сибирской медицины.* 2024;23(1):37–47. https://doi.org/10.20538/1682-0363-2024-1-37-47.

INTRODUCTION

Head and neck squamous cell cancer (HNSCC) ranks 7th in the overall incidence of malignant neoplasms with 0.7 million new cases per year [1, 2]. Characteristic features of HNSCC are frequent recurrences and low 5-year survival rates for both localized and advanced stages of the disease (69 and 34%, respectively) [1]. Low patient survival is associated with late diagnosis, poor response to various treatments, and high recurrence rates [2–4]. In most cases, HNSCC is diagnosed at a locally advanced stage, for which radiation therapy (RT) with or without concomitant radiosensitizing chemotherapy is one of the main treatment approaches used in 80% of cases [5].

Proton therapy (PT) is one of the most promising types of corpuscular radiation. Its implementation into clinical practice allows to minimize the occurrence of radiation-related adverse events. The therapeutic effect of PT consists in persistent damage to the genetic material of tumor cells, leading to their death [6]. At the same time, the cytotoxic effect of protons is caused both by direct damage to the DNA chain of tumor cells and by indirect induction of reactive oxygen species (ROS) formation [7] and stimulation of apoptosis (due to caspase-3 activation by protons) [8].

In our previous review [9], we described the biological effects of PT. Nasopharyngeal squamous cell cancer is considered to be one of the main indications for PT due to its complex anatomy and proximity to critical anatomical structures and organs, such as optic chiasm, temporal lobes and brain stem, pharyngeal constrictor muscles, and salivary glands [10]. Several studies demonstrated a significant reduction in the incidence of acute post-radiation complications in patients with nasopharyngeal squamous cell carcinoma receiving PT compared to patients receiving classical RT [11].

The accumulating clinical experience in applying proton radiation therapy significantly outpaces basic radiobiological research and contributes to the increasing number of proton centers in different countries of the world [12]. However, limited knowledge about the molecular and genetic changes induced by PT in tumor cells hinders the development of new therapeutic and combination strategies. This study is devoted to the description of transcriptional changes in HNSCC cells after PT.

The aim of the study was to evaluate changes in the transcriptome of HNSCC tissue cells in patients after PT.

MATERIALS AND METHODS

Biopsy material of tumor tissue was obtained from 3 patients with HNSCC before and after PT at the total irradiation dose of 10 isoGy (relative biological effectiveness (RBE) coefficient 1.1). All patients signed an informed consent to participate in the study. The study was approved by the independent Ethics Committee (Protocol No. 634 of 17.11.2021, Protocol No. 684 of 02.03.2022). The study was carried out in compliance with the ethical principles set out in the WMA Declaration of Helsinki "Ethical principles for medical research involving human subjects" amended in 2000 and Rules of Good Clinical Practice in the Russian Federation adopted by the order of the Ministry of Health of Russia No. 266 of 19.06.2003. The study participants were identified only by the patient number.

The patients were irradiated with protons using a fixed horizontal proton beam in the sitting position on the PT complex Prometheus (Protom, Russia). All patients underwent daily verification of the position using integrated cone beam computed tomography. The thickness of the slices was 1 mm. Patient fixation was performed using a reinforced thermoplastic mask and head restraints.

Biomaterial processing was performed using aseptic techniques and sterile materials. Total RNA was isolated from the tissue after homogenization with Teflon beads in QIAzol (Qiagen), followed by purification and concentration with the RNA Clean & Concentrator kit (Zymo Research). Quantitation was assessed using the Qubit 2.0 instrument (Invitrogen, Life Technologies). After isolation of 1 μg total RNA for sequencing, libraries were prepared on the Illumina platform using the TruSeq RNA Sample Prep Kit v2 with a 10-cycle enrichment step according to the manufacturer's recommendations.

The quality of RNA and the resulting libraries was checked using the Agilent 2100 Bioanalyzer system (Agilent Tec. Inc., USA). The RIN parameter for RNA was at least 7. The concentration of libraries was assessed by real-time PCR on the CFX96 Touch Real-Time PCR Detection System (Bio-Rad, USA). Final libraries were pooled in equimolar ratios before sequencing on the Illumina HiSeq 2500 platform using 50 base-pair paired-end reads. The Q20 parameter for all samples was > 97%, and the number of reads averaged 60.2 million per sample. Raw reads were processed using the RTA 1.17.21.3 and Casava 1.8.2 (Illumina).

The nf-core/rnaseq pipeline version 3.0 was used to obtain expression matrices from FASTQ files. The pipeline was run with the GRCh38 reference genome, alignment was performed using the STAR tool, and quantification was performed using the Salmon tool. The differential gene expression analysis was performed between tumor samples before and after PT. It was performed independently using several tools, such as DESeq2, EBSeq, limma-voom, NOISeq, and edgeR. For each tool, tables with differential gene expression scores were generated. The results obtained were compared using the Hobotnica metric [13].

Hobotnica is a tool for assessing the quality of differential expression tools. The tool is based on the quality quantification approach based on the ability to separate data from different experiments based on distance matrices. Cut-off values for differential gene expression were |log2FC| > 1, $p < 0.05$ for DESeq2, limma-voom and edgeR, $q > 0.9$ for NOISeq, and |log2FC| > 1, PPDE > 0.95 for EBSeq. For multiple comparisons, the Bonferroni correction and the Wald maximin criterion (extreme pessimism criterion) were used to calculate the *p* value. Based on the comparison results, DESeq2 performed better when comparing tumor samples before and after PT. The enrichment analysis was performed using the PANTHER 17.0 software. The threshold for statistical significance for including a signaling pathway in the list of enriched pathways was $p < 0.05$ (Table 1).

Table 1

The assessment of the differential gene expression tool quality using the Hobotnica tool

Tool	Hobotnica score
DESeq2	1
EBSeq	0.96
edgeR	0.5
limma-voom	0.5
NOISeq	0.67

To establish significance, the data were analyzed by the paired Student's *t*-test using the GraphPad Prism 8 statistical software package (GraphPad Software). The significance level was set at $p \leq 0.05$. For multiple comparisons, the Bonferroni correction and the Wald maximin criterion (the criterion of extreme pessimism) were used, which are generally considered as the most cautious ones.

RESULTS

The transcriptome analysis of HNSCC tumor tissue after proton radiation therapy (5 x 2 isoGy) at a total dose of 10 isoGy revealed 1,414 significantly differentially expressed genes. We identified 10 genes based on the minimum (with the most reduced expression) and maximum (with the most increased expression) LOG2FC values. The lowest expression after PT was observed in the following genes: *CLEC4E, IGHV2-70, P2RX1, SLC5A3, MYBPC1, RP11-551L14,1, FCRLA, FAM30A, IGHV2-26, IGHV2-5* (Table 2).

Table 2

The most underexpressed genes in HNSCC biopsy samples after proton therapy

Genes	*p*-value	LOG2FC	Deciphering the name	Functions
CLEC4E	1.89E-06	-5.0	C-Type Lectin Domain Family 4 Member E	Encodes a member of the C-type lectin / C-type lectin-like domain (CTL/CTLD) superfamily involved in cell adhesion, cell-to-cell signaling, glycoprotein metabolism, inflammation, and immune response
IGHV2-70	8.57E-06	-5.1	Immunoglobulin Heavy Variable 2-70	Provides antigen-binding activity and immunoglobulin receptor-binding activity; participates in the activation of the immune response, defense against another organism and phagocytosis
P2RX1	3.99E-05	-5.2	Purinergic Receptor P2X 1	The protein encoded by this gene belongs to the P2X family of G-protein-coupled receptors. It functions as an ATP-controlled ion channel and provides fast and selective permeability for cations
SLC5A3	2.37E-05	-5.2	Solute Carrier Family 5 Member 3	Involved in inositol metabolism; transmembrane transport of monosaccharides; import of myo-inositol across the plasma membrane
MYBPC1	0.000185	-5.2	Myosin Binding Protein C1	Involved in the contraction of transverse striated muscles
RP11-551L14,1	0.011218	-5.3	No data	No data
FCRLA	0.000857	-5.3	Fc Receptor Like Protein A	Involved in humoral immunity: antibody-induced destruction of IgG-coated antigens and cells
FAM30A	0.000853	-5.3	Family With Sequence Similarity 30 Member A	Its exact function is unclear, but its activation has been linked to cancer

Table 2 (continued)

Genes	*p*-value	LOG2FC	Deciphering the name	Functions
IGHV2-26	0.002372	-5.4	Immunoglobulin Heavy Variable 2-26	Involved in activation of the immune response; defense against another organism; phagocytosis.
IGHV2-5	0.018504	-5.4	Immunoglobulin Heavy Variable 2-5	Provides antigen-binding activity and immunoglobulin receptor-binding activity. Activates immune response; defense against another organism; phagocytosis.

The highest gene expression in HNSCC biopsy samples after PT was observed in the following genes: *PIK3R2; CTD-3074O7,11; GOLGA6L9; GP1BB; NPIPA2; RP11-96O20,4; AC008132,13; SNX31; RP1-127D3,4; RPL21P119* (Table 3).

In order to determine whether significantly highly expressed and low-expression genes belong to different signaling pathways, we performed the enrichment analysis for each of these groups of genes separately. In tumor tissue samples after PT, compared to tumor tissue before it, among low-expression genes, the signaling pathways presented in Table 4 were detected more than others. A number of signaling pathways related to low-expression genes were detected in HNSCC after PT, such as: STAT5; PD-1 signaling pathway; marked MET-mediated activation of PTK2 signaling pathway, PDGF signaling; CD22-mediated regulation of BCR; FCERI-mediated MAPK activation. In addition to the above signaling pathways, collagen degradation, FCGR3A-mediated phagocytosis activation, and FCGR3A-mediated interleukin (IL)-10 synthesis attract attention (Table 4).

In the enrichment analysis among highly expressed genes, the processes of keratinization and biological oxidation were activated in HNSCC tissue after PT (Table 5).

Table 3

The most highly expressed genes in the samples of HNSCC biopsies after proton therapy

Genes	*p*-value	LOG2FC	Deciphering the name	Functions
PIK3R2	0.001165114	4.9	Phosphoinositide-3-Kinase Regulatory Subunit 2	Phosphorylates phosphatidylinositol and similar compounds, creating secondary messengers important in growth factor signaling pathways
CTD-3074O7,11	2.72E-06	4.6	No data	Involved in the development of the eyes, limbs, heart, and reproductive system
GOLGA6L9	1.59E-07	4.5	Golgin A6 Family Like 9	No data
GP1BB	4.01E-10	4.3	Glycoprotein Ib Platelet Subunit Beta	Promotes platelet adhesion.
NPIPA2	8.65E-10	4.0	Nuclear Pore Complex Interacting Protein Family Member A2	Involved in mRNA transport and protein transport
RP11-96O20,4	3.93E-11	3.8	No data	No data
AC008132,13	1.07E-11	3.6	No data	No data
SNX31	7.48E-13	3.4	Sorting Nexin 31	Involved in intracellular protein transport
RP1-127D3,4	7.48E-13	3.4	No data	No data
RPL21P119	4.15E-12	3.4	Ribosomal Protein L21 Pseudogene 119	Pseudogene

Table 4

Signaling pathways of HNSCC associated with low-expression genes after proton therapy

Reactome pathways	Number of genes from the reference list of the database in a normal human population	Number of genes related to this signaling pathway in the submitted samples	Fold enrichment	*p* value	FDR Probability of false positives
Activation of STAT5 R-HSA9702518.2	10	4	15.63	3.15E-04	1.60E-02

Table 4 (continued)

Reactome pathways	Number of genes from the reference list of the database in a normal human population	Number of genes related to this signaling pathway in the submitted samples	Fold enrichment	*p* value	FDR Probability of false positives
PD-1 signaling pathway R-HSA-389948.3	29	7	9.43	2.58E-05	2.22E-03
Collagen degradation R-HSA-1442490.4	64	14	8.55	7.25E-09	6.03E-06
MET -mediated activation of signaling pathway PTK2 R-HSA-8874081.2	30	6	7.81	2.42E-04	1.31E-02
PDGF signaling R-HSA-186797.5	54	8	5.79	1.48E-04	9.44E-03
AKT1 E17K signaling pathway in cancer R-HAS-5674400.2	26	5	7.51	9.44E-04	4.13E-02
CD22-mediated BCR regulation R-HSA-5690714.3	67	9	5.25	1.13E-04	7.43E-03
Interferon-gamma signaling R-HSA-877300.6	91	12	5.15	1.00E-05	1.09E-03
FCERI-mediated MAPK activation R-HSA-2871796.3	89	11	4.83	4.03E-05	3.14E-03
FCGR3A-mediated synthesis of IL-10 R-HSA-9664323.2	100	12	4.69	2.37E-05	2.11E-03

Here and in Table 5: 1 Fold enrichment is defined as the percentage of genes in the submitted samples belonging to the indicated pathway compared to the background set of genes. 2 +/-. A positive sign indicates overrepresentation of this category of genes in the experiment (more genes than expected). Conversely, a negative sign indicates underrepresentation. All signaling pathways showed overrepresentation.

Table 5

Activated signaling pathways of HNSCC associated with highly expressed genes after proton therapy

Reactome pathways	Number of genes from the reference list of the database in a normal human population	Number of genes related to this signaling pathway in the submitted samples	Fold enrichment	*p* value	FDR Probability of false positives
Formation of the keratinizing membrane R-HSA-6809371.5	129	14	6.96	4.57E-08	1.14E-04
Biological oxidation R-HSA-211859.3	220	15	4.37	3.83E-06	4.77E-03

The data obtained in the course of this research work are unique in their kind, as there is limited information on PT-induced changes at the transcriptome level in the literature. This is due, firstly, to the difficulty of collecting biopsies from patients, since for such analysis it is necessary to collect material before PT and after irradiation in order to identify significantly altered signatures. Secondly, not all centers have the necessary expensive equipment for PT, and often clinicians limit themselves to prescribing classical photon radiation therapy. Thirdly, transcriptional analysis and bioinformatic data processing are rather complicated and require highly qualified specialists.

DISCUSSION

The transcriptome is a dynamically changing system influenced by various factors. As a precision oncology assay, the transcriptional analysis has only recently begun to be used [14, 15]. There are no data in the literature describing changes at the level of the HNSCC transcriptome induced by PT. Understanding the transcriptional heterogeneity of HNSCC contributes to the development of diagnostic and prognostic

biomarkers that will enable to select personalized therapy, leading to increased positive responses to antitumor therapy and improved outcomes / increased number of positive responses to treatment.

The key role for the activation of signal transducers and activators of transcription 5 (STAT5) has been found in many malignancies. In most cases, STAT5 enhances squamous epithelial cell growth, increases migration and invasion of cells in squamous cell cancer, and induces phenotypic and molecular changes associated with epithelial – mesenchymal transition [16]. In HNSCC, STAT5 activation correlates with enhanced tumor growth, invasion, and epithelial – mesenchymal transition [17]. Suppression of STAT5 was observed after PT in HNSCC.

Non-receptor protein – tyrosine kinase 2 (PTK2), also known as focal adhesion kinase (FAK), is a multifunctional regulator of cell signaling between tumor cells and the tumor microenvironment. Activated PTK2 is involved in the regulation of several cellular functions: adhesion, proliferation, and migration [18, 19]. Proteomic analysis showed that PTK2 / FAK overexpression is a biomarker of radioresistance of HNSCC. Combinations of PTK2 / FAK inhibition with radiation therapy are currently being investigated as a therapeutic strategy to improve local control in HPV-negative PRGS [20].

Activation of the PD-1 / PD-L1 signaling pathway is associated with the induction and maintenance of immune tolerance in tumor tissue by suppressing effector T cell functions [21]. PD-L1 expression levels in HNSCC correlate significantly with marked clinical progression and poor patient survival [22]. The activity of PD-1 and its ligands PD-L1 or PD-L2 is responsible for the activation, proliferation, and cytotoxic secretion of T lymphocytes [23]. Our transcriptome analysis revealed suppression of this signaling pathway.

IL-10 synthesis in HNSCC tumor tissue was also reduced after PT. In the process of carcinogenesis, IL-10 functions both as a pro-oncogenic cytokine, inhibiting antitumor immunity, and as an antitumor cytokine, performing an antianginal role [24]. Importantly, it is involved in the control of tumor cell proliferation and invasion via the JAK / STAT signaling pathway [25,26].

The PDGF / PDGFR signaling pathway plays a key role in tumor progression [27]. PDGF overexpression promotes tumor cell growth [28] and induces angiogenesis [29] by affecting cells in the tumor microenvironment, thereby inducing tumor progression. In addition, there is evidence that increased PDGF activity in the tumor is associated with drug treatment resistance caused by impaired capillary blood flow in the tumor due to increased interstitial fluid pressure [30]. In the present study, PT caused suppression of the PDGF signaling pathway in HNSCC.

The mitogen-activated protein kinase (MAPK) signaling pathway is a key mediator that integrates extracellular signals to control cell proliferation, survival, differentiation, senescence, and drug resistance [31]. HNSCC patients with high intratumoral expression of p-MAPK1/3 (p-ERK1/2) are characterized by worse survival [32]. It is believed that the altered kinase signaling network including EGFR, PDGFR, PAK1, PTK2 (FAK), and MAP2K2 seems to regulate aberrant changes in tumor tissue accompanying relapse [33].

In addition to the above, detection of changes in HNSCC after PT at the transcriptomic level will allow to divide patients into groups with a different prognosis and response to treatment. For example, the survival of patients with HNSCC can be stratified by the intensity of the keratinization process, especially in patients with non-HPV-associated HNSCC. Activation of the keratinization process in HNSCC is associated with a poor prognosis and shorter overall survival of patients [34].

CONCLUSION

PT in HNSCC leads to overexpression of genes involved in the regulation of keratinization and biological oxidation processes as well as to underexpression of genes associated with suppression of signaling pathways: STAT5, PD-1, MET-mediated activation of PTK2 signaling pathway, PDGF signaling; CD22-mediated regulation of BCR; FCERI-mediated MAPK activation, collagen degradation, FCGR3A-mediated phagocytosis activation, and FCGR3A-mediated IL10 synthesis.

Summarizing the results obtained during the transcriptome study of HNSCC after PT at a total dose of 10 isoGy, the predominant number of suppressed signaling pathways over the activated ones is of great interest. At the same time, some of the detected signaling pathways correspond to the data described in the literature, while some of the pathways altered during the study differ from the available data. All signaling pathways of underexpressed genes function in HNSCC cells if there is no negative influence on the tumor from outside (irradiation or delivery of antitumor drugs). The predominance of suppressed

signaling pathways over activated ones most likely indicates a decrease in the functional potential of cells after proton therapy. The dose-dependence of proton therapy effects requires further study of changes in cellular and molecular-genetic signatures of HNSCC after proton therapy at different doses.

REFERENCES

1. Sung H., Ferlay J., Siegel R.L., Laversanne M., Soerjomataram I., Jemal A., Bray F. Global cancer statistics 2020: GLOBOCAN estimates of incidence and mortality worldwide for 36 cancers in 185 countries. *CA: a Cancer Journal for Clinicians*. 2021;71(3):209–249. DOI: 10.3322/caac.21660.
2. Bhat G.R., Hyole R.G., Li J. Head and neck cancer: Current challenges and future perspectives. *In Advances in Cancer Research.* 2021;152(1):67–102. DOI: 10.1016/bs.acr.2021.05.002.
3. Johnson D.E., Burtness B., Leemans C.R., Lui W.Y., Bauman J.E., Grandis J.R. Head and neck squamous cell carcinoma. *Nature Reviews Disease Primers.* 2020;6(1):92–112. DOI: 10.1038/s41572-020-00224-3.
4. Lozano R., Naghavi M., Foreman K., Lim S., Shibuya K., Aboyans V. et al. Global and regional mortality from 235 causes of death for 20 age groups in 1990 and 2010: a systematic analysis for the Global Burden of Disease Study 2010. *Lancet.* 2012;380(9859):2095–2128. DOI: 10.1016/S0140-6736(12)61728-0.
5. Borras J.M., Barton M., Grau C., Corral J., Verhoeven R., Lemmens V. et al. The impact of cancer incidence and stage on optimal utilization of radiotherapy: Methodology of a population based analysis by the ESTRO-HERO project. *Radiotherapy and Oncology*. 2015;116(1):45–50. DOI: 10.1016/j.radonc.2015.04.021.
6. Vitti E.T., Parsons J.L. The radiobiological effects of proton beam therapy: Impact on DNA damage and repair. *Cancers*. 2019;11(7):1–15. DOI: 10.3390/cancers11070946.
7. Răileanu M., Straticiuc M., Iancu D.A., Andrei R.F. Proton irradiation induced reactive oxygen species promote morphological and functional changes in HepG2 cells. *Journal of Structural Biology.* 2022;214(4):1–11. DOI: 10.1016/j.jsb.2022.107919.
8. Alan Mitteer R., Wang Y., Shah J., Gordon S., Fager M., Butter P.P. et al. Proton beam radiation induces DNA damage and cell apoptosis in glioma stem cells through reactive oxygen species. *Scientific Reports*. 2015;5(1):1–12. DOI: 10.1038/srep13961.
9. Jumaniyazova E.D., Smyk D.I., Vishnyakova P.A., Fatkhudinov T.Kh., Gordon K.B. Photon-and proton-mediated biological effects: what has been learned? *Life.* 2022;3(1):30–46. DOI: 10.3390/life13010030.
10. Nuyts S., Bollen H., Ng S.P., Corry J., Eisbruch A., Mendenhall W.M. et al. Proton therapy for squamous cell carcinoma of the head and neck: early clinical experience and current challenges. *Cancers*. 2022;14(11):1–18. DOI: 10.3390/cancers14112587.
11. Holliday E.B., Garden A.S., Rosenthal D.I., Fuller C.D., Morrison W.H., Gunn G.B. et al. Proton therapy reduces treatment-related toxicities for patients with nasopharyngeal cancer: a case-match control study of intensity-modulated proton therapy and intensity-modulated photon therapy. *International Journal of Particle Therapy.* 2015;2(1):19–28. DOI: 10.14338/IJPT-15-00011.1.
12. Tian X., Liu K., Hou Y., Cheng J., Zhang J. The evolution of proton beam therapy: Current and future status. *Molecular and Clinical Oncology*. 2018;8(1):15–21. DOI: 10.3892/mco.2017.1499.
13. Stupnikov A., Sizykh A., Budkina A., Sizykh A., Budkina A., Favorov A. et al. Hobotnica: exploring molecular signature quality [version 2; peer review: 2 approved]. *F1000Research*. 2022:10:1260. DOI: 10.12688/f1000research.74846.2.
14. Rodon J., Soria J.C., Berger R., Miller W.H., Rubin E., Kugel A. et al. Genomic and transcriptomic profiling expands precision cancer medicine: the WINTHER trial. *Nature Medicine.* 2019;25(5):751–758. DOI: 10.1038/s41591-019-0424-4.
15. Worst B.C., van Tilburg C.M., Balasubramanian G.P., Fiesel P., Witt R., Freitag A. et al. S. Next-generation personalised medicine for high-risk paediatric cancer patients–The INFORM pilot study. *European Journal of Cancer.* 2016;65(1):91–101. DOI: 10.1016/j.ejca.2016.06.009.
16. Choi S., Myers J.N. Molecular pathogenesis of oral squamous cell carcinoma: implications for therapy. *Journal of Dental Research.* 2008;87(1):14–32. DOI: 10.1177/154405910808700104.
17. Koppikar P., Lui V.W.Y., Man D., Xi S., Chai R.L., Nelson E. et al. Constitutive activation of STAT5 contributes to tumor growth, epithelial-mesenchymal transition, and resistance to EGFR targeting. *Clinical Cancer Research.* 2008;14(23):7682–7690. DOI: 10.1158/1078-0432.CCR-08-1328.
18. Zhou J., Yi Q., Tang, L. The roles of nuclear focal adhesion kinase (FAK) on Cancer: a focused review. *Journal of Experimental & Clinical Cancer Research*. 2019;38(1):1–11. DOI: 10.1186/s13046-019-1265-1.
19. Zhang Z., Li J., Jiao S., Han G., Zhu J., Liu T. Functional and clinical characteristics of focal adhesion kinases in cancer progression. *Frontiers in Cell and Developmental Biology*. 2022;10(1):1040311–1040335. DOI: 10.3389/fcell.2022.1040311.
20. Skinner H.D., Giri U., Yang L., Woo S.H., Story M.D., Pickering C.R. et al. Proteomic profiling identifies PTK2/FAK as a driver of radioresistance in HPV-negative head and neck cancer. *Clinical Cancer Research*. 2016;22(18):4643–4650. DOI: 10.1158/1078-0432.CCR-15-2785.
21. Chen L., Han X. Anti–PD-1/PD-L1 therapy of human cancer: past, present, and future. *The Journal of Clinical Investigation.* 2015;125(9):3384–3391. DOI: 10.1172/JCI80011.

22. Cui P., Jing P., Liu X., Xu W. Prognostic significance of PD-L1 expression and its tumor-intrinsic functions in hypopharyngeal squamous cell carcinoma. *Cancer Management and Research.* 2020;1:5893–5902. DOI: 10.2147/CMAR.S257299.
23. Han Y., Liu D., Li L. PD-1/PD-L1 pathway: current researches in cancer. *American Journal of Cancer Research*. 2020;10(3):727–742.
24. Howell W.M., Rose-Zerilli M.J. Cytokine gene polymorphisms, cancer susceptibility, and prognosis. *The Journal of Nutrition*. 2007;137(1):194S–199S. DOI: 10.1093/jn/137.1.194S.
25. Béguelin W., Sawh S., Chambwe N., Chan F.C., Jiang Y. IL10 receptor is a novel therapeutic target in DLBCLs. *Leukemia.* 2015;29(8):1684–1694. DOI: 10.1038/leu.2015.57.
26. Han Y., Ding Z., Chen B., Liu Y., Liu Y. A novel inflammatory response–related gene signature improves high-risk survival prediction in patients with head and neck squamous cell carcinoma. *Frontiers in Genetics.* 2022;13(1):1–15. DOI: 10.3389/fgene.2022.767166.
27. Heldin C.H. Targeting the PDGF signaling pathway in tumor treatment. *Cell Communication and Signaling.* 2013;11:1–18. DOI: 10.1186/1478-811X-11-97.
28. Pietras K., Sjöblom T., Rubin K., Heldin C.H., Östman A. PDGF receptors as cancer drug targets. *Cancer Cell*. 2003;3(5):439–443. DOI: 10.1016/s1535-6108(03)00089-8.
29. Lindahl P., Johansson B.R., Leveen P., Betsholtz C. Pericyte loss and microaneurysm formation in PDGF-B-deficient mice. *Science.* 1997;277(5323):242–245. DOI: 10.1126/science.277.5323.242.
30. Heldin C.H., Rubin K., Pietras K., Östman A. High interstitial fluid pressure—an obstacle in cancer therapy. *Nature Reviews Cancer.* 2004;4(10):806–813. DOI: 10.1038/nrc1456.
31. Braicu C., Buse M., Busuioc C., Drula R., Gulei D., Raduly L. et al. A comprehensive review on MAPK: a promising therapeutic target in cancer. *Cancers.* 2019;11(10):1–25. DOI: 10.3390/cancers11101618.
32. Theocharis S., Kotta-Loizou I., Klijanienko J., Giaginis C., Alexandrou P., Rodriguez J. et al. Extracellular signal-regulated kinase (ERK) expression and activation in mobile tongue squamous cell carcinoma: associations with clinicopathological parameters and patients survival. *Tumor Biology*. 2014;35:6455–6465. DOI: 10.1007/s13277-014-1853-9.
33. Kaneko T., Zeng P.Y., Liu X., Abdo R., Barrett J.W., Zhang Q. et al. Proteome and phosphoproteome signatures of recurrence for HPV+ head and neck squamous cell carcinoma. *Communications Medicine.* 2022;2(1):95–110. DOI: 10.1038/s43856-022-00159-8.
34. Cooper T., Biron V.L., Adam B., Klimowicz A.C., Puttagunta L., Seikaly H. Association of keratinization with 5-year disease-specific survival in oropharyngeal squamous cell carcinoma. *JAMA Otolaryngol Head Neck Surg.* 2015;141(3):250–256. DOI: 10.1001/jamaoto.2014.3335.

Authors' contribution

Jumaniyazova E.D. – analysis and interpretation of the data, drafting of the manuscript. Vishnyakova P.A. – conception and design, critical revision of the manuscript for important intellectual content. Chirkova M.V., Karpulevich E.A. – bioinformatics analysis of the results obtained. Eremina I.Z., Kaprin A.D. – final approval of the manuscript for publication. Gordon K.B. – delivery of the biological material, critical revision of the manuscript for important intellectual content. Fatkhudinov T.H. – conception and design, critical revision of the manuscript for important intellectual content, final approval of the manuscript for publication.

Authors' information

Jumaniyazova Enar D. – Post-Graduate Student, Teaching Assistant, Department of Histology, Cytology and Embryology, RUDN Medical Institute; Research Intern, Laboratory for Molecular Pathophysiology of the Cell, RUDN Research Institute of MCM, Moscow, enar2017@yandex.ru, http://orcid.org/0000-0002-8226-0433

Vishnyakova Polina A. – Cand. Sci. (Biology), Associate Professor, Department of Histology, Cytology and Embryology, RUDN Medical Institute; Head of the Laboratory for Regenerative Medicine, V.I. Kulakov National Medical Research Center of Obstetrics, Gynecology and Perinatology; Head of the Laboratory for Molecular Pathophysiology of the Cell, RUDN Research Institute of MCM, Moscow, p_vishnyakova@oparina4.ru, http://orcid.org/0000-0001-8650-8240

Chirkova Miroslava V. – Laboratory Assistant, ISP RAS, Moscow, mirachirkova@ispras.ru , http://orcid.org/0009-0008-3659-0360

Karpulevich Evgeny A. – Researcher, ISP RAS, Moscow, karpulevich@ispras.ru, http://orcid.org/0000-0002-6771-2163

Eremina Irina Z. – Cand. Sci. (Biology), Associate Professor, Department of Histology, Cytology and Embryology, RUDN Medical Institute, Moscow, eremina_iz@rudn.university, http://orcid.org/0000-0002-5093-6232

Gordon Konstantin B. – Cand. Sci. (Med.), Associate Professor, Department of Histology, Cytology and Embryology, RUDN Medical Institute, Radiotherapist, Researcher, Department of Proton and Photon Radiation Therapy, Tsyb Medical Radiological Research Center, Moscow, drgordonkb@gmail.com,: http://orcid.org/0000-0002-2759-297X

Kaprin Andrey D. – Dr. Sci. (Med.), Academician of the Russian Academy of Sciences, Head of the Department of Oncology and Radiology named after Academician Kharchenko, RUDN Medical Institute; Director General, NMRC Radiology; Moscow, kaprin-ad@rudn.ru, http://orcid.org/0000-0001-8784-8415

Fatkhudinov Timur H. – Dr. Sci. (Med.), Professor, Head of the Department of Histology, Cytology and Embryology, RUDN Medical Institute, Deputy Director for Research, RUDN Medical Institute; Deputy Director, A.P. Avtsyn Research Institute of Human Morphology; Director, RUDN Research Institute of MCM, Moscow, tfat@yandex.ru, http://orcid.org/0000-0002-6498-5764

(✉) **Jumaniyazova Enar D.,** enar2017@yandex.ru

Received 03.09.2023;
approved after peer review 27.10.2023;
accepted 16.11.2023

УДК 616.379-008.64:613.65:577.125]-092.9
https://doi.org/10.20538/1682-0363-2024-1-48-55

Oxidative phosphorylation in brown adipose tissue in a type II diabetes mellitus mouse model after forced treadmill running

Zakharova A.N.[1], Milovanova K.G.[1], Orlova A.A.[1], Kollantay O.V.[1], Shuvalov I.Yu.[1], Kapilevich L.V.[1, 2]

[1] *National Research Tomsk State University*
36, Lenina Av., Tomsk, 634050, Russian Federation

[2] *Siberian State Medical University*
2, Moscow Trakt, Tomsk, 634050, Russian Federation

ABSTRACT

Aim. To study the effect of forced exercises on the content and parameters of oxidative phosphorylation in brown adipose tissue of mice with type II diabetes mellitus.

Materials and methods. To model the disease, we used a high-fat diet and physical exercises in the form of forced treadmill running for 4 weeks. The content of oxidative phosphorylation enzymes in brown adipose tissue was determined by Western blotting.

Results. Modeling diabetes in experimental animals was accompanied by expansion of adipose tissue. However, in brown adipose tissue, the content of all oxidative phosphorylation components decreases. Apparently, during type II diabetes mellitus modeling in mice, there is a decrease in the "energy efficiency" in brown adipose tissue, which is partially offset by an increase in its content in the body.

Regular physical activity in mice with type II diabetes mellitus, in contrast to healthy animals, contributes to a decrease in the content of brown adipose tissue. At the same time, the content of most oxidative phosphorylation components in brown adipose tissue increases, in some casesб it even exceeds the baseline values. The latter is typical of a variable load mode – when the execution time of exercises periodically changes.

Conclusion. The obtained results suggest that metabolic rearrangements in brown adipose tissue may serve as some of the mechanisms of preventive and projective effects of physical activity in type 2 diabetes mellitus.

Keywords: brown fat, running load, diabetes, obesity

Conflict of interest. The authors declare the absence of obvious or potential conflicts of interest related to the publication of this article.

Source of financing. The study was supported by the Russian Science Foundation grant (No. 19-15-00118, https://rscf.ru/project/19-15-00118-p).

Conformity with the principles of ethics. The study was approved by the Bioethics Committee at the Biology Institute of National Research Tomsk State University (Protocol No. 32 of 02.12.2019).

For citation: Zakharova A.N., Milovanova K.G., Orlova A.A., Kollantay O.V., Shuvalov I.Yu., Kapilevich L.V. Oxidative phosphorylation in brown adipose tissue in a type II diabetes mellitus mouse model after forced treadmill running. *Bulletin of Siberian Medicine.* 2024;23(1):48–55. https://doi.org/10.20538/1682-0363-2024-1-48-55.

✉ *Kapilevich Leonid V.,* kapil@yandex.ru

Окислительное фосфорилирование в ткани бурого жира у мышей с моделью сахарного диабета II типа после принудительных беговых нагрузок

Захарова А.Н.[1], Милованова К.Г.[1], Орлова А.А.[1], Коллантай О.В.[1], Шувалов И.Ю.[1], Капилевич Л.В.[1, 2]

[1] *Национальный исследовательский Томский государственный университет (НИ ТГУ)*
Россия, 634050, г. Томск, пр. Ленина, 36

[2] *Сибирский государственный медицинский университет (СибГМУ)*
Россия, 634050, г. Томск, Московский тракт, 2

РЕЗЮМЕ

Цель: изучить влияние принудительных физических нагрузок на содержание и показатели окислительного фосфорилирования в ткани бурого жира у мышей с моделью сахарного диабета (СД) II типа.

Материалы и методы. Для формирования модели заболевания использовалась высокожировая диета, физические нагрузки в виде принудительного бега проводились в течение 4 нед. Содержание ферментов окислительного фосфорилирования в бурой жировой ткани определялось методом вестерн-блоттинга.

Результаты. Формирование диабетических расстройств у экспериментальных животных сопровождается возрастанием количества как белой, так и бурой жировой ткани. Однако в бурой жировой ткани при этом снижается содержание всех компонентов системы окислительного фосфорилирования. По-видимому, при формировании модели СД II типа у мышей происходит снижение «энергетической эффективности» бурой жировой ткани, что частично компенсируется увеличением ее содержания в организме.

Регулярные физические нагрузки у мышей с моделью СД II типа, в отличие от здоровых животных, способствуют снижению содержания бурой жировой ткани. В то же время при этом в буром жире возрастает содержание большинства компонентов системы окислительного фосфорилирования, в некоторых случаях – даже выше исходных значений. Последнее характерно для нагрузок, применяемым в переменном режиме – когда время выполнения нагрузок периодически изменяется.

Заключение. Полученные результаты позволяют предположить, что метаболические перестройки бурой жировой ткани могут служит одним из механизмов профилактических и проекторных эффектов физических нагрузок при сахарном диабете второго типа.

Ключевые слова: бурый жир, беговая нагрузка, сахарный диабет, ожирение

Конфликт интересов. Авторы декларируют отсутствие явных и потенциальных конфликтов интересов, связанных с публикацией настоящей статьи.

Источник финансирования. Исследование выполнено за счет гранта Российского научного фонда (№ 19-15-00118, https://rscf.ru/project/19-15-00118-р).

Соответствие принципам этики. Исследование одобрено комитетом по биоэтике Биологического института Национального исследовательского Томского государственного университета (протокол № 32 от 02.12.2019).

Для цитирования: Захарова А.Н., Милованова К.Г., Орлова А.А., Коллантай О.В., Шувалов И.Ю., Капилевич Л.В. Окислительное фосфорилирование в ткани бурого жира у мышей с моделью сахарного диабета II типа после принудительных беговых нагрузок. *Бюллетень сибирской медицины.* 2024;23(1):48–55. https://doi.org/10.20538/1682-0363-2024-1-48-55.

INTRODUCTION

Brown fat (also known as thermogenic fat) is a type of adipose tissue whose main function is thermogenesis [1, 2]. Brown adipose tissue is capable of expending energy, unlike white fat, which stores it. As a result, brown adipose tissue has a regulatory effect on metabolism and may be involved in the control of blood glucose levels [3].

Patients with type II diabetes may have a lack of brown fat, which can lead to poor glucose management and an increased risk of complications. Some

studies suggest that stimulating brown fat storage may improve glucose management and reduce the risk of diabetic complications [4]. Ways to stimulate the growth of brown adipose tissue may include physical activity, consumption of certain foods, and the use of medications [5].

Physical activity of varying intensity launches a large number of biochemical, molecular, genetic, and epigenetic mechanisms that underlie the body's adaptive response to physiological stress [6, 7]. In particular, physical activity has been shown to have a positive effect on metabolic disorders [7, 8]. Animal experiments have shown that exercise increases insulin sensitivity and improves high-fat diet-induced glucose tolerance not only in the animals themselves, but also in their offspring [9]. Circadian rhythms have also been shown to influence the effects of exercise. Glucose uptake by muscles and insulin tolerance also have a circadian nature, and physical training does not affect the circadian rhythm of these parameters [10].

In connection with the above, the aim of the research was to study the effect of forced exercises on the content and parameters of oxidative phosphorylation in brown adipose tissue in a mouse model of type II diabetes mellitus.

MATERIALS AND METHODS

Male mice of the C 57bl/6 line were used as the object of the study. The mice were obtained from the vivarium of the Tomsk National Research Medical Center of the Russian Academy of Sciences, Goldberg Research Institute of Pharmacology and Regenerative Medicine. The age of the mice at the beginning of the experiment was 32 weeks. Animal keeping regime: 12 h / 12 h light / dark cycle, light cycle starts at 6 a.m., free access to food and water, room temperature 24 °C.

The study was conducted in accordance with the principles of the Basel Declaration and approved by the Bioethics Committee at the Biology Institute of Tomsk State University (Protocol No. 32 of 2.12.2019). The study was carried out in accordance with the principles of humanity set out in the European Council Directives (86/609/EEC) and the Declaration of Helsinki.

The experiment lasted 16 weeks. Until week 12, the mice were divided into 2 subgroups:

– animals receiving a high-fat diet – 28 mice.

– animals receiving a standard diet – 28 mice.

Type II diabetes mellitus (T2DM) and a high-fat diet for 12 weeks, developed specifically for this experiment, were used to model T2DM. The composition and energy value of the feed are described in detail in our previous work [11].

Starting from week 12 of the experiment, each group of animals was divided into two subgroups – those exposed (main group, n = 21) and those not exposed (control group, n = 7) to forced treadmill running.

Subgroups of mice from the main group were exposed to forced running exercise at different times of the day:

Group A – mice exposed to forced treadmill running during the light cycle (from 8:00 to 10:00), 7 animals;

Group B – mice exposed to forced treadmill running during the dark cycle (from 19:00 to 21:00), 7 animals;

Group C – the time of forced treadmill running alternated (alternating light / dark cycle): weeks 1 and 3 – in the dark cycle (from 19:00 to 21:00), weeks 2 and 4 – in the light cycle (from 8:00 to 10:00), 7 animals.

To normalize physical activity, the BMELAB SID – TM 10 treadmill for mice was used [12].

The animals had been exposed to forced treadmill running 6 times a week for 4 weeks. The duration of the exercise was gradually increased from 10 to 60 minutes during the first 6 days (an increase of 10 minutes per day) and did not change over the next 3 weeks. Every week, the elevation angle of the treadmill (from 0 to 10°) and its rotation speed (from 15 to 18 m / min) were changed. Once a week exercise was not performed (on the 7th day).

Body weight was measured using laboratory scales. Body weight of each animal was measured separately. Measurements were taken 11 times over 16 weeks.

The experimental animals were decapitated 24 hours after the last exercise. White and brown adipose tissue was extracted. The collected samples were weighed, then frozen in liquid nitrogen and stored in the freezer at –80 °C.

To homogenize the adipose tissue, 500 µl buffer per 50 mg of tissue was applied using the Vortex – Genie 2 laboratory mixer for 15 minutes at 4 °C with metal balls. Then the tissue was placed in the refrigerated mini rotary shaker for 1 hour, then left in the shaker rack in the cold for 15 minutes, and then again placed in the Vortex – Genie 2 laboratory mixer for 15 minutes at 4 °C.

After this, the tubes were transferred to a centrifuge at 4 °C and spun for 5 minutes at 8,000 rpm.

Then the lipid layer was carefully removed, placed again in the centrifuge for 15 minutes, after which clear supernatant under the remaining lipid layer was collected. Total protein in the sample was determined by the Bradford method.

Polyacrylamide gel electrophoresis was carried out under denaturing conditions according to the method described by Laemmil, with 5% stacking and 10% separating gels using the electrophoresis system (electrophoresis cell (Mini – PROTEAN Tetra Cell, USA), current source (PowerPacBasic, USA)). The amount of total protein applied to each well was 10 μg. Using the transfer system (Trans – Blot Turbo, USA), proteins were transferred from the gel to a PVDF membrane (Bio-Rad, USA) with further blocking with 5% skim milk (Bio-Rad, USA) in TBSt 1X (TBS supplemented with 0.1% Tween 20) for 1 h at room temperature.

Target proteins were determined by overnight incubation at 4 °C in 5% dry milk in TBSt with a 1:1000 dilution with rabbit polyclonal antibodies against citrate synthetase (cat. no. ab96600, abcam, UK), with rabbit polyclonal antibodies against hexokinase (cat. no. ab227198, abcam, UK), and a cocktail with antibodies Total OXPHOS Rodent WB (cat. no. ab110413, abcam, UK), containing 5 mouse antibodies, each against the subunits NDUFB8, SDHB, UQCRC2, MTCO1, and ATP5A. The sample was then incubated with secondary antibodies conjugated with horseradish peroxidase (anti-mouse, cat. no. 1706516, anti-rabbit, cat. no. 1706515, Bio-Rad, USA) for 1 h at room temperature in 5% dry milk in TBSt.

Antigen – antibody complexes were visualized using the ECL kit (SuperSigna West Dura, Thermo Scientific, USA) and gel documentation systems (ChemiDoc - It 2, UVP, UK). The densitometric analysis was performed using the ImageJ software. The Western blotting data were presented in relative units compared to the standard sample (the same sample was present on all blots). The values of the standard sample were taken as 100%.

The data were presented as the mean and the error of the mean ($M \pm m$). After checking the normality of data distribution using the Kolmogorov – Smirnov test, the results were analyzed using the two-way Kruskal – Wallis analysis of variance. Statistical processing of the results was carried out using the GraphPad Prism application package.

RESULTS

Figure 1 shows the dynamics of the body weight in the mice during the experiment. Already starting from week 4, a statistically significant increase in the body weight was observed in the mice receiving a high-fat diet ($p < 0.05$). The average body weight of the animals receiving a high-fat diet was 35.2 ± 2.0 g, and the average body weight of the animals receiving a standard diet was 32.7 ± 1.3 g. At week 12, the differences between the high-fat diet group (body weight 44.3 ± 2.6 g) and the standard diet group (32.2 ± 1.2 g) increased.

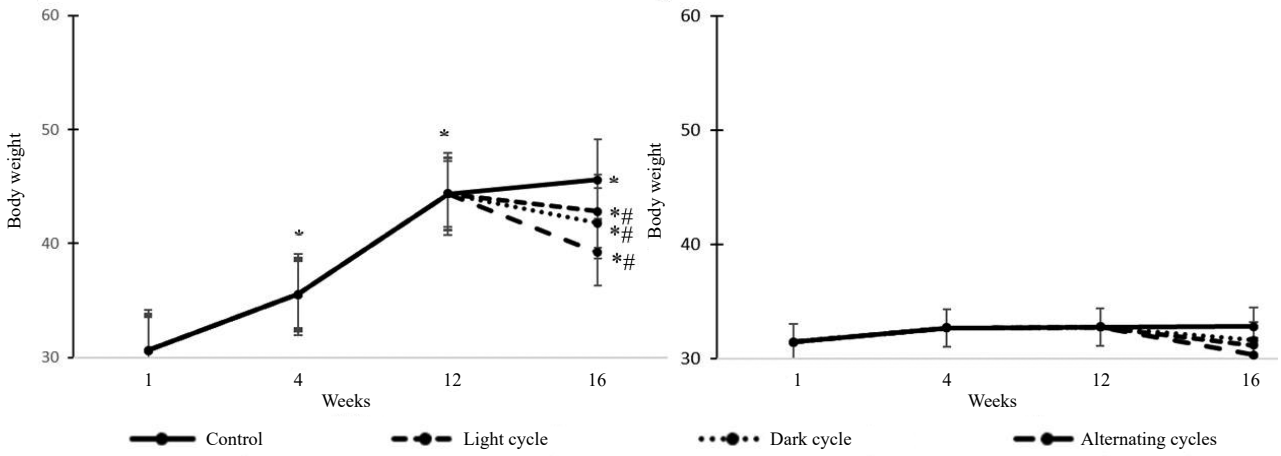

Fig. 1. Changes in the body weight of mice during the experiment: *a* – high-fat diet group; *b* – standard diet group. Here and in Fig. 2, 3, $M \pm m$, $n = 6$. * – statistically significant differences with the values at week 1 ($p < 0.05$), # – statistically significant differences with the group without physical exercises ($p < 0.05$)

Starting from week 12, both groups were divided into 4 subgroups, in which the animals were exposed to physical activity at different times of the day (light cycle, dark cycle, alternating cycles). At week 16 (final) of the experiment, we observed that in the high-fat diet group (45.6 ± 4.5 g) and standard diet group (32.8 ± 2.4 g), the difference in the body weight remained statistically significant ($p < 0.05$).

In the group receiving a fat diet, statistically significant differences ($p < 0.05$) in the body weight compared to the control group were observed in all 3 subgroups exposed to physical activity. The most effective was alternating exposure to physical activity (39.2 ± 4.4 g). In this group, the body weight was 1.2 times lower than in the control group.

Figure 2 shows the amount of abdominal white adipose tissue and brown adipose tissue in the mice after completion of the experiment. The increase in the body weight in the mice was largely due to an increase in the amount of white adipose tissue, but the content of brown adipose tissue in the body also increased significantly. It is important to note that forced physical exercise, while causing a decrease in the amount of white adipose tissue in all subgroups, had a much weaker effect on the content of brown adipose tissue. Only physical activity performed with a phase shift in the circadian rhythm helped reduce the amount of brown fat by half.

Figure 3 shows the results of determining the content of citrate synthase and OXFOS proteins in brown adipose tissue of the mice. The results are presented as a percentage of the control sample. As can be seen from the presented results, the content of citrate synthase in brown adipose tissue did not depend on the type of nutrition and increased slightly only when forced treadmill running was used during a phase shift in the circadian rhythm (Fig. 3, *a*).

ATP5A concentrations (Fig. 3, *b*) were reduced in the high-fat diet group compared to the standard diet group. Physical exercise in the high-fat diet group helped increase the content of this protein; the effect of evening exercise and training in the alternating regimen was more pronounced. In the standard diet group, on the contrary, physical exercise led to a decrease in the content of this protein.

MTCO1 concentration (Fig. 3, *c*) was significantly reduced in the mice fed with a high-fat diet compared to the standard diet group. Physical exercise in the standard diet group increased the content of this protein if applied in the alternating regimen.

The concentration of SD HB (Fig. 3, *d*) in the high-fat diet group decreased slightly compared to the standard diet group. Physical activity in the high-fat diet group increased the content of this protein. The effect of exercise was more pronounced during the dark cycle and alternating cycles. In the mice fed with a standard diet, on the contrary, physical exercise led to a decrease in the content of this protein.

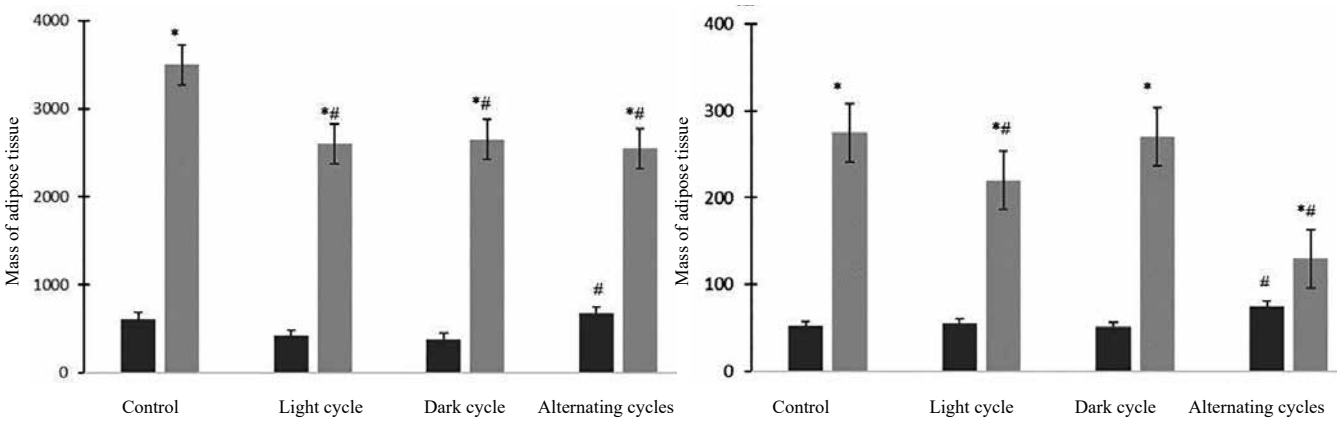

Fig. 2. Mass of white and brown adipose tissue in mice at 16 weeks of the experiment: light columns – high-fat diet group; dark columns – standard diet group. Here and in Fig. 3: * – statistically significant differences with the standard diet group ($p < 0.05$), # – statistically significant differences with the control group ($p < 0.05$).

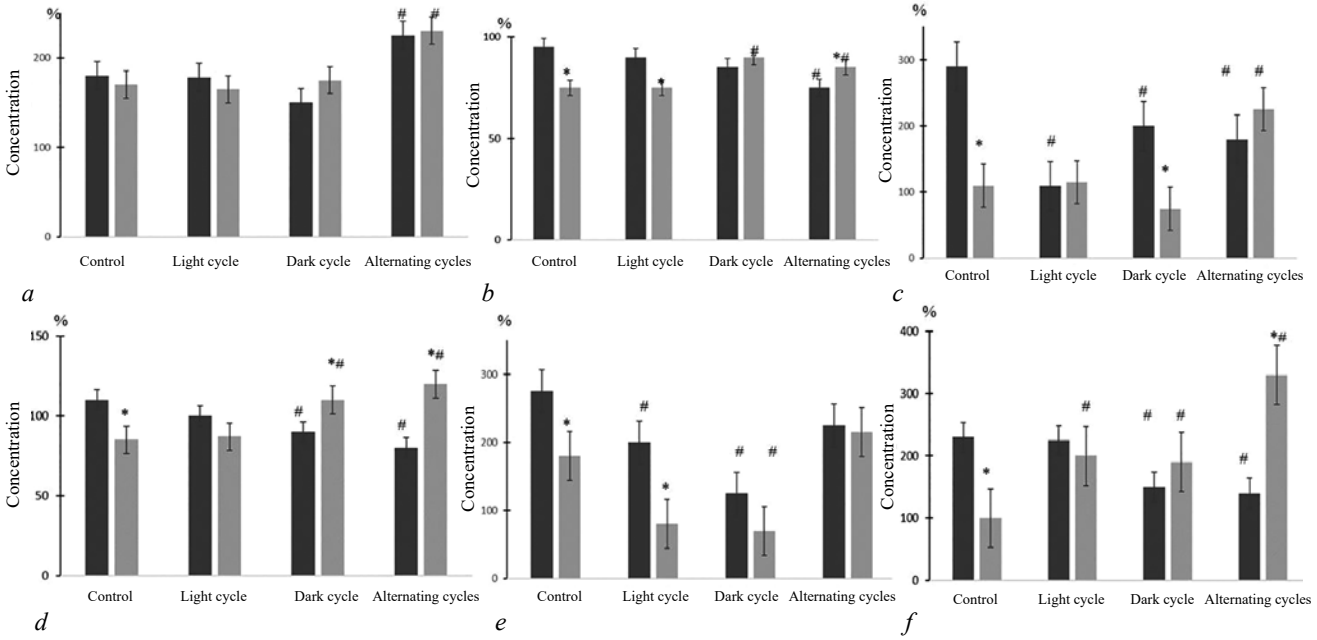

Fig. 3. Content of citrate synthase and OXFOS proteins in brown adipose tissue of mice: light columns – high-fat diet group, dark columns – standard diet group. Citrate synthase (*a*), ATP5A (*b*), MTCO1 (*c*), SD HB (*d*), UQCRC2 (*e*), NDUFB8 (*f*)

The concentration of UQCRC2 (Fig. 3, *e*) was reduced in the high-fat diet group compared to the standard diet group. Exercise in the high-fat diet group resulted in a significant a decrease when applied during the light or dark cycle, and in an increase when applied during the alternating cycles. In the mice fed with a standard diet, physical exercise led to similar, but less pronounced changes.

The concentration of NDUFB8 (Fig. 3, *f*) was reduced in the high-fat diet group compared to the standard diet group. Physical exercise in the high-fat diet group increased the content of this protein, especially if used in the alternating regimen. In the mice fed with a standard diet, on the contrary, physical exercise led to a decrease in the content of this protein.

DISCUSSION

The results obtained indicate that the use of a high-fat diet in mice leads to the increase in body weight and development of obesity (body weight was more than 25% greater than in the control group). Forced physical exercise in the form of daily treadmill running has a pronounced effect on metabolism in mice with a model of type II diabetes mellitus. First of all, this manifested itself by a decrease in the body weight of the animals and depended on the time of the day when the exercise was performed. Both gain and loss of body weight mainly occurred due to changes in the amount of white abdominal fat; the content of brown fat changed to a lesser extent.

At the same time, significant metabolic changes were observed in brown adipose tissue. Modeling type II diabetes mellitus was accompanied by a decrease in the content of all oxidative phosphorylation system (OXPHOS) components. The content of MTCO1 and NDUFB8 decreased to the greatest extent. Apparently, during the formation of a model of type II diabetes mellitus in mice, there was a decrease in the metabolic efficiency of brown adipose tissue, which was partially compensated by an increase in its content in the body.

The effects of exercise on brown fat levels have been somewhat controversial. According to the literature, regular physical activity helps increase the amount of brown fat in the body [13]. Thus, healthy young men who exercised daily for 12 weeks had more active brown fat than those who did not exercise [14]. We observed similar results in the mice without metabolic disorders fed with a standard diet – they showed an increase in the brown fat content after regular forced physical activity. However, in the mice with a model of type II diabetes mellitus, we observed the opposite effect – the content of brown fat in the body decreased with regular physical activity. This may be due to the fact that in these animals, during the development of pathology, the content of brown fat increased fivefold.

However, a decrease in the content of brown fat after exercise in the mice with a model of type II diabetes mellitus was accompanied by an increase in the content of most OXPHOS components; in some cases, their values even exceeded the baseline ones. The latter is typical of exercise applied in the alternating regimen – when the time of exercise performance periodically changes. Similar changes were observed for citrate synthase. Apparently, in metabolic disorders, the effects of physical activity can be realized not by increasing the amount of brown adipose tissue, but by improving its metabolic efficiency.

As mentioned above, promoting brown fat storage may improve glucose management and reduce the risk of diabetic complications [15]. Apparently, metabolic changes in brown adipose tissue may serve as some of the mechanisms for preventive and predictive effects of physical activity in T2DM.

CONCLUSION

The results obtained allow to draw several important conclusions.

Firstly, the development of diabetic disorders in experimental animals is accompanied by an increase in the amount of both white and brown adipose tissue. However, in brown adipose tissue, the content of all oxidative phosphorylation system components decreases. The content of MTCO1 and NDUFB8 decreases to the greatest extent. Apparently, during the formation of a model of type II diabetes mellitus in mice, there is a decrease in the metabolic efficiency of brown adipose tissue, which is partially compensated by an increase in its content in the body.

Secondly, regular physical exercise in mice with a model of type II diabetes mellitus, in contrast to healthy animals, helps reduce the content of brown adipose tissue. At the same time, the content of most OXPHOS components in brown fat increases, in some cases even above the baseline values. The latter is typical of exercise performed in the alternating regimen, when the time of exercise performance periodically changes. Similar changes are observed for citrate synthase.

The results obtained suggest that metabolic changes in brown adipose tissue may serve as some of the mechanisms for the preventive and predictive effects of physical activity in type II diabetes mellitus.

REFERENCES

1. Betz M.J., Enerbäck S. Targeting thermogenesis in brown fat and muscle to treat obesity and metabolic disease. *Nat. Rev. Endocrinol.* 2018;14(2):77–87. DOI: 10.1038/nrendo.2017.132.
2. Jung S.M., Sanchez-Gurmaches J., Guertin D.A. Brown adipose tissue development and metabolism. *Handb. Exp. Pharmacol.* 2019;251:3–36. DOI: 10.1007/164_2018_168.
3. Koksharova E.O., Mayorov A.Yu., Shestakova M.V., Dedov I.I. Metabolic features and therapeutic potential of brown and beige adipose tissue. *Diabetes.* 2014;17(4):5–15 (in Russ.). DOI: 10.14 341/DM201445-15.
4. Cheng L., Wang J., Dai H., Duan Y., An Y., Shi L. et al. Brown and beige adipose tissue: a novel therapeutic strategy for obesity and type 2 diabetes mellitus. *Adipocyte.* 2021;10(1):48–65. DOI: 10.1080/21623945.2020.1870060.
5. Kaisanlahti A., Glumoff T. Browning of white fat: agents and implications for beige adipose tissue to type 2 diabetes. *J. Physiol. Biochem.* 2019;75(1):1–10. DOI: 10.1007/s13105-018-0658-5.
6. Coffey V.G., Hawley J.A. The molecular bases of training adaptation. *Sports Med.* 2007;37(9):737–763. DOI: 10.2165/00007256-200737090-00001.
7. Karstoft K., Pedersen B.K. Exercise and type 2 diabetes: focus on metabolism and inflammation. *Immunol. Cell Biol*. 2016;94(2):146–150. DOI: 10.1038/icb.2015.101.
8. Pedersen B.K., Saltin B. Exercise as medicine – evodence for prescribing exercise as therapy in 26 different chronic diseases. *Scand. J. Med. Sci. Sports*. 2015;25:1–72. DOI: 10.1111/sms.12581.
9. Stanford K.I., Rasmussen M., Baer L.A., Lehnig A.C., Rowland L.A., White J.D. et al. Paternal Exercise improves glucose metabolism in adult offspring. *Diabetes*. 2018;67(12):2530–2540. DOI: 10.2337/db18-0667.
10. Basse A.L., Dalbram E., Larsson L., Gerhart-Hines Z., Zierath J.R., Treebak J.T. Skeletal muscle insulin sensitivity show circadian rhythmicity which is independent of exercise training status. *Front Physiol.* 2018;9:1198. DOI: 10.3389/fphys.2018.01198.
11. Kapilevich L.V., Zakharova A.N., Dyakova E.Yu., Kalinnikova J.G., Chibalin A.V. Mice experimental model of diabetes mellitus type ii based on high fat diet. *Bull. Siberian Med.* 2019;18(3):53–61. DOI: 10.20538/1682-0363-2019-3-53-61.
12. Zakharova A.N., Kalinnikova Y., Negodenko E.S., Orlova A.A., Kapilevich L.V. Experimental simulation of cyclic training loads. *Teor. Prakt. Fizich. Kult.* 2020;10:26–27.
13. Lehnig A.C., Stanford K.I. Exercise-induced adaptations to white and brown adipose tissue. *J. Exp. Biol.* 2018;221(Pt. Suppl.):jeb161570. DOI: 10.1242/jeb.161570.
14. Aldiss P., Betts J., Sale C., Pope M., Budge H., Symonds M.E. Exercise-induced 'browning' of adipose tissues. *Metabolism.* 2018;81:63–70. DOI: 10.1016/j.metabol.2017.11.009.
15. Mu W.J., Zhu J.Y., Chen M., Guo L. Exercise-mediated browning of white adipose tissue: its significance, mechanism and effectiveness. *Int. J. Mol. Sci.* 2021;22(21):11512. DOI: 10.3390/ijms222111512.

Authors' contribution

Kapilevich L.V. – research supervision, conception of the study, editing of the manuscript, final approval of the manuscript for publication. Zakharova A.N. – conception and design, analysis and interpretation of the data, drafting of the manuscript. Milovanova K.G., Kollantay O.V., Orlova A.A., Shuvalov I.Yu. – collection and analysis of the data, processing and interpretation of the results.

Authors' information

Zakharova Anna N. – Cand. Sci. (Biology), Associate Professor, Division of Sports and Health Tourism, Sports Physiology and Medicine, Department of Physical Education, National Research Tomsk State University, Tomsk, azakharova91@gmail.com, https://orcid.org/0000-0003-1102-2830

Milovanova Ksenia G. – Cand. Sci. (Biology), Associate Professor, Division of Sports and Health Tourism, Sports Physiology and Medicine, Department of Physical Education, National Research Tomsk State University, Tomsk, naffys@mail.ru, https://orcid.org/0000-0002-3038-3298

Orlova Anna A. – Post-Graduate Student, Division of Sports and Health Tourism, Sports Physiology and Medicine, Department of Physical Education, National Research Tomsk State University, Tomsk, anna.orlova.96@mail.ru, https://orcid.org/0000-0002-9886-9454

Kollantay Olesya V. – Post-Graduate Student, Division of Sports and Health Tourism, Sports Physiology and Medicine, Department of Physical Education, National Research Tomsk State University, Tomsk, olesya.tay@mail.ru, https://orcid.org/0009-0001-2445-0124

Shuvalov Igor Yu. – Post-Graduate Student, Division of Sports and Health Tourism, Sports Physiology and Medicine, Department of Physical Education, National Research Tomsk State University, Tomsk, oleg-100500-lol@mail.ru, https://orcid.org/0000-0002-1096-807X

Kapilevich Leonid V. – Dr. Sci. (Med.), Professor, Head of the Division of Sports and Health Tourism, Sports Physiology and Medicine, Department of Physical Education, National Research Tomsk State University; Siberian State Medical University, Tomsk, kapil@yandex.ru, http://orcid.org/0000-0002-2316-576X

(✉) **Kapilevich Leonid V.,** kapil@yandex.ru

Received 11.04.2023;
approved after peer review 28.04.2023;
accepted 14.09.2023

УДК 612.017.1:612.112.91
https://doi.org/10.20538/1682-0363-2024-1-56-63

Neutrophil extracellular traps in the anti-infectious defense of human organism

Kazimirskii A.N., Salmasi J.M., Poryadin G.V., Panina M.I., Stupin V.A., Kim A.E., Titova E.G., Rogozhina L.S.

Pirogov Russian National Research Medical University
1, Ostrovityanova Str., Moscow, 117997, Russian Federation

ABSTRACT

Background. Neutrophil extracellular traps (NETs) are net-like structures that have been investigated in inflammatory diseases. However, the presence of NETs in infected persons without clinical symptoms has not been yet studied.

Aim. To reveal NETs in healthy persons during and after the H1N1 influenza pandemic as well as to study the functional activity of NETs.

Materials and methods. The study included two groups of volunteers (n = 10 in each group) aged 20–25 years. The first group of volunteers was examined in the absence of acute diseases during one month before the study and in the absence of chronic diseases in the medical history. Volunteers of the second group were in contact with patients with influenza, but did not get sick. The comparative study also included patients with acute inflammation in the abdominal cavity (appendicitis, cholecystitis, abscess; 12 patients) and 9 patients with non-specific ulcerative colitis. Neutrophils were isolated from the blood by the traditional method of Ficoll density centrifugation. The number, morphology, and functional activity of NETs were determined (by capture of *Klebsiella pneumoniae*). SYBR Green I-based fluorescence microscopy was used to visualize and quantify NETs.

Results. In healthy volunteers who were not in contact with infected patients, spontaneous NETs formation did not occur. Neutrophils of persons who were in contact with infected patients spontaneously formed NETs. In this case the number of NETs reached 8.58 ± 0.51%, and the size of NETs amounted to 39.68 ± 3.52 μm. NETs effectively captured cells of the tested microorganism, which was accompanied by retraction of network fibers and transformation of the network structure into a cloud-like one, which retained 89.38 ± 5.86 microbial cells. For comparison, the NETs in patients with acute inflammation in the abdominal cavity captured and bound 20.2 ± 1 .67 microbial cells and with non-specific ulcerative colitis – 5.53 ± 0.34 cells.

Conclusion. High binding capacity of NETs is a factor contributing to effective defense of the body against the development of an infectious disease with manifested clinical symptoms.

Keywords: functional activity of NETs, neutrophil extracellular traps, cloud-like appearance, healthy volunteers, H1N1 influenza, *Klebsiella pneumoniae*, inflammatory diseases

Conflict of interest. The authors declare the absence of obvious or potential conflicts of interest related to the publication of this article.

Source of financing. The authors state that they received no funding for the study.

Conformity with the principles of ethics. All patients signed an informed consent to participate in the study. The study was approved by the Ethics Committee at Pirogov Russian National Research Medical University (Protocol No. 203 of 21.12.2021).

For citation: Kazimirskii A.N., Salmasi J.M., Poryadin G.V., Panina M.I., Stupin V.A., Kim A.E., Titova E.G., Rogozhina L.S. Neutrophil extracellular traps in the anti-infectious defense of human organism. *Bulletin of Siberian Medicine.* 2024;23(1):56–63. https://doi.org/10.20538/1682-0363-2024-1-56-63.

✉ *Kazimirskii Alexander N.,* alnica10@mail.ru

Противоинфекционная защита организма человека с участием нейтрофильных сетей

Казимирский А.Н., Салмаси Ж.М., Порядин Г.В., Панина М.И., Ступин В.А., Ким А.Э., Титова Е.Г., Рогожина Л.С.

Российский национальный исследовательский медицинский университет (РНИМУ) им. Н.И. Пирогова Россия, 117997, г. Москва, ул. Островитянова, 1

РЕЗЮМЕ

Введение. Нейтрофильные экстраклеточные ловушки (НЭЛ) в форме сетей исследованы при воспалительных заболеваниях. Присутствие нейтрофильных сетей у инфицированных людей без клинических симптомов не изучено.

Цель. Выявление НЭЛ у неболеющих людей в период пандемии гриппа H1N1 и вне этого периода, а также исследование функциональной активности НЭЛ.

Пациенты и методы. Две группы волонтеров (по 10 человек) в возрасте 20–25 лет. Первая группа добровольцев обследована в спокойный эпидемиологический период, при отсутствии острых заболеваний в течение 1 мес до исследования и хронических заболеваний в анамнезе. Волонтеры 2-й группы контактировали с больными гриппом, но при этом не заболевали. В исследование также были включены больные (12 человек) с острым воспалением в брюшной полости (аппендицит, холецистит, абсцесс) и 9 – с неспецифическим язвенным колитом. Нейтрофилы выделяли из крови традиционным методом на градиенте фиколла. Определяли количество, морфологию и функциональную активность НЭЛ (по захвату *Klebsiella pneumoniae*). Для визуализации и подсчета НЭЛ использовали флуоресцентную микроскопию с красителем SYBR Green.

Результаты. У здоровых волонтеров, не контактировавших с больными, спонтанного формирования НЭЛ не возникало. Нейтрофилы же добровольцев, контактировавших с больными, спонтанно формировали нейтрофильные сети. Количество НЭЛ у них достигало 8,58 ± 0,51%, а размеры НЭЛ – 39,68 ± 3,52 мкм. НЭЛ эффективно захватывали клетки тестового микроорганизма, что сопровождалось ретракцией волокон сети и преобразованием сетевидной структуры в вуалеобразную, которая удерживает 89,38 ± 5,86 микробных клеток. Для сравнения: нейтрофильная сеть больных с острым воспалением брюшной полости захватывает и связывает 20,2 ± 1,67 микробных клеток, при неспецифическом язвенном колите – 5,53 ± 0,34.

Заключение. Высокая связывающая способность нейтрофильных сетей является фактором эффективной защиты от развития инфекционного заболевания с манифестацией клинических симптомов.

Ключевые слова: функциональная активность нейтрофильных сетей, нейтрофильные экстраклеточные ловушки, вуалеобразная форма, не болеющие волонтеры, грипп H1N1, *Klebsiella pneumoniae*, воспалительные заболевания

Конфликт интересов. Авторы декларируют отсутствие явных и потенциальных конфликтов интересов, связанных с публикацией настоящей статьи.

Источник финансирования. Авторы заявляют об отсутствии финансирования при проведении исследования.

Соответствие принципам этики. Все участники исследования подписали добровольное информированное согласие. Исследование одобрено этическим комитетом РНИМУ им. Н.И. Пирогова (протокол № 203 от 21.12.2021).

Для цитирования: Казимирский А.Н., Салмаси Ж.М., Порядин Г.В., Панина М.И., Ступин В.А., Ким А.Э., Титова Е.Г., Рогожина Л.С. Противоинфекционная защита организма человека с участием нейтрофильных сетей. *Бюллетень сибирской медицины.* 2024;23(1):56–63. https://doi.org/10.20538/1682-0363-2024-1-56-63.

INTRODUCTION

Neutrophils form neutrophil extracellular traps (NETs) as a body defense mechanism against pathogens. In previous studies on responses of cells of innate immunity (neutrophils) to viral infections (hantaviruses, adenoviruses, human immunodeficiency virus, influenza viruses), data were obtained on the formation of NETs in patients with various acute viral diseases [1–3]. At the same time, researchers found that excessive formation of NETs is dangerous, as it can cause tissue damage and lead to complications of the underlying disease [3–6]. The role of neutrophils in viral infection has its own particular features, and

the threshold at which protective functions are surpassed by damage mechanisms, including immunopathological ones, is still quite unclear.

Recent studies have established that influenza viruses are capable of inducing the formation of NETs in the blood of healthy donors *in vitro* [7, 8]. At the same time, it was found that the formation of NETs in the form of net-like structures, as a response of innate immunity cells contributing to the fight against acute viral infection, is accompanied by a pronounced antiviral effect that helps control the virus at the systemic level [9]. It is generally accepted that NETs are absent in the blood of healthy people and are found only during inflammation. NETs have been described in detail, but their presence in the body of people without clinical manifestations of the disease is unknown. There is no exact data on the presence of NETs in the peripheral blood of people who are in contact with infected individuals but do not become ill. In addition, the mechanisms underlying the formation of NETs are still unclear.

Most researchers are not aware of various morphological forms of NETs; their functional activity has not been studied. One approach to elucidating these issues is to determine the content of NETs, their morphological structure, and functional activity in people who do not become ill during and after an influenza pandemic.

Th aim of the study was to reveal NETs in healthy persons during and after the H1N1 influenza pandemic as well as to study the functional activity of NETs.

MATERIALS AND METHODS

The study included two groups of volunteers (n = 10 in each group) aged 20–25 years. The inclusion criterion was the absence of acute diseases at the time of the study and chronic diseases in the medical history. The exclusion criterion was acute infectious diseases within a month before the day of the study.

Volunteers of the first group were examined in May – June 2022. During this period, the lowest morbidity rates for influenza and COVID-19 were recorded. Members of this group had no contact with people suffering from acute respiratory diseases.

Volunteers of the second group were examined in December 2022. During this period, the epidemic threshold for H1N1 influenza was exceeded in children and adults. Moreover, the volunteers of the second group during the month preceding the study were in constant contact with H1N1 influenza patients but did not get sick themselves.

The study also included patients treated in Moscow clinical hospital No. 51. Patients of the first group (n = 12) were hospitalized with acute inflammation in the abdominal cavity (acute appendicitis, acute cholecystitis, abscess). Patients of the second group (n = 9) were diagnosed with non-specific ulcerative colitis.

The blood test was carried out at the Department of Pathophysiology and Clinical Pathophysiology of Pirogov Russian National Research Medical University. All procedures were performed in accordance with the ethical standards of the WMA Declaration of Helsinki (as amended in 2004) and the patient's written informed consent. The study was approved by the Ethics Committee at Pirogov Russian National Research Medical University (Protocol No. 203 of 21.12.2021).

Determining NETs content. Obtaining cell fractions of neutrophils. The Vacutainer EDTA blood collection tubes were used to sample blood from volunteers to prevent clotting. Isolation of neutrophils from the EDTA-treated venous blood was performed by Ficoll density gradient centrifugation. To do this, the blood was diluted 4 times with sodium phosphate buffer solution, pH 7.4, and layered on the Ficoll – Hypaque density gradient. The top layer density was 1.077 g / cm^3, and the density of the bottom layer was 1.190 g / cm^3. After centrifugation (1,600 rpm, 30 min), neutrophils accumulated at the interface between the gradients (98−100% purity). Neutrophils were twice washed with sodium phosphate buffer (50 mM, pH 7.4) to remove Ficoll impurities. Sedimentation of blood cells was performed by centrifugation (1.200 rpm, 15 min). The isolated neutrophils in the RPMI-1640 medium were used for cell culture experiments. The viability of the isolated neutrophils was 95 % (test with 0.1% trypan blue solution).

Immunofluorescence detection of NETs. Fluorescence microscopy was used for detection and quantification of NETs [10]. The results were expressed as a percentage, as the ratio of the number of NETs to the total number of cells in the field of view. NETs were detected using the SYBR Green I fluorescent dye (Evrogen, Russia), which is able to bind specifically to double-stranded DNA. Microscopy, quantification, and photo registration of cells and extracellular structures were performed at ×1,000 magnification.

Capture of the test microorganism. The functional activity of NETs was determined using the test for capturing *Klebsiella pneumoniae* (ATCC 700603). To do this, the microbial culture of *Klebsiella pneumoniae* in the RPMI-1640 medium at a concentration of

10^3 / µl was added to neutrophils immobilized on the poly-L-lysine-coated glass slides. Net-like structures captured the test microorganism in accordance with the potential functional activity of NETs. After staining (SYBR Green, 15 min) and removing excess dye during microscopy, the number of *Klebsiella pneumoniae* cells associated with each NET was determined.

The STATISTICA 12.0 software package (StatSoft Ink., USA) was used for statistical data processing. The results were reported as the mean and the standard error of the mean ($M \pm m$). Comparison of quantitative variables was performed using the Mann – Whitney U-test and the Kruskal – Wallis test. The differences were considered statistically significant at $p < 0.05$.

RESULTS

Quantitative and qualitative characteristics of NETs were determined in *in vitro* research. We determined variants of their morphological structure, quantity, size, and functional activity (in the test with the capture of *Klebsiella pneumoniae*).

The results of the study in two groups of volunteers (those who had no contact with infected people (Group 1) and those who had contact with infected people, but did not have clinical signs of the disease (Group 2)), are shown in Table.

Table

Results of the study of NETs in healthy volunteers, $M \pm m$

Characteristics of the groups	Parameters of NETs		
	Morphological structure of NETs	Number of NETs, %	Size of NETs, µm
Volunteers who had no contact with infected patients, $n = 10$	–	0.00	0.00
Volunteers who contacted with infected patients and did not get sick, $n = 10$	net-like structure	8.58 ± 0.51*	39.68 ± 3.52*

* $p < 0.05$ compared to the controls

In healthy volunteers who had no contacts with infected people and were examined not during the pandemic (Group 1), spontaneous formation of net-like NETs did not occur. The neutrophils of the volunteers from Group 1 were presented as classic mature segmented granulocytes (Fig. 1).

In healthy volunteers who contacted with infected people (Group 2), the results were different. In this case, neutrophils spontaneously formed net-like traps (Fig. 2, 3). The number of neutrophil extracellular traps was 8.58 ± 0.51%, and the size of NETs amounted to 39.68 ± 3.52 µm. Neutrophils in this group spontaneously formed net-like structures without any additional stimulation. Consequently, volunteers who had contacts with infected patients were infected themselves, and their neutrophils were previously activated.

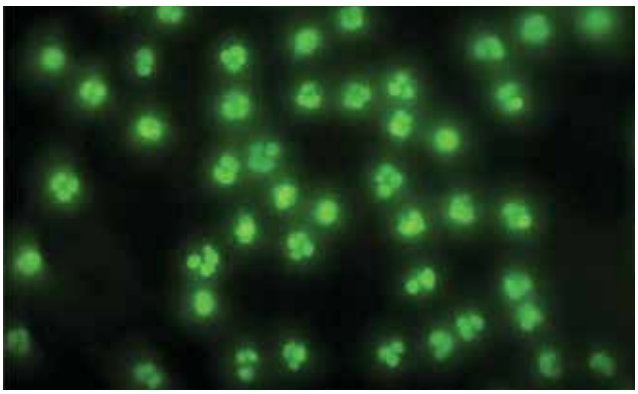

Fig. 1. Neutrophils of healthy people who had no contact with infected patients. Staining with CYBR Green I, x1,000.

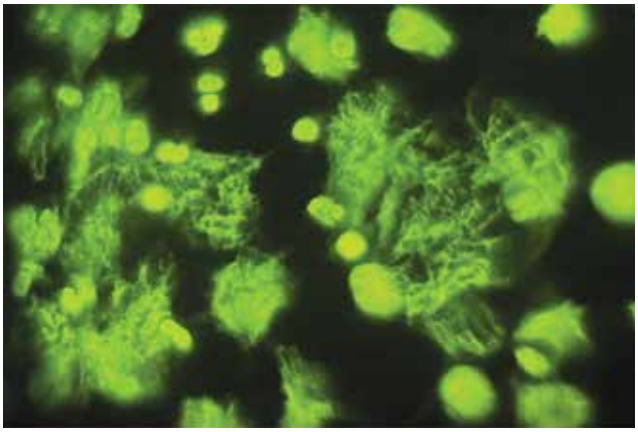

Fig. 2. NETs of people who had been in contact with infected patients but did not get sick: incubation time 1 hour. Staining with CYBR Green I, x1,000.

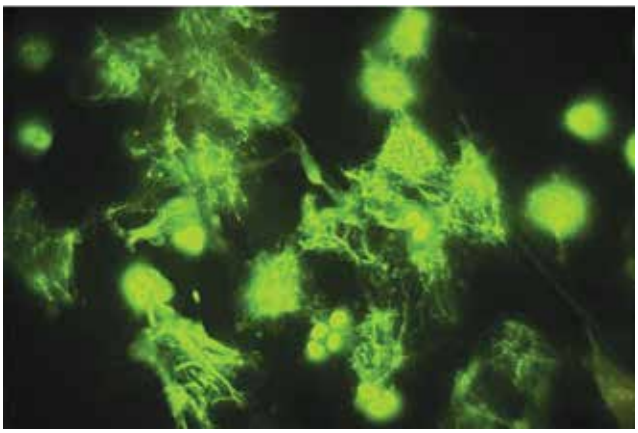

Fig. 3. NETs of people who had been in contact with infected patients but did not get sick: incubation time 1 hour. Staining with CYBR Green I, x1,000.

In the next series of experiments, the functional activity of the NETs found in the healthy volunteers who had contacts with infected patients (Group 2) was determined in the test with the capture of *Klebsiella pneumoniae* (ATCC 700603).

Neutrophils of the volunteers from Group 2 were added to the cells of the test microorganism *Klebsiella pneumoniae* placed on the glass slides (Fig. 4). The neutrophils of the disease-free volunteers who were examined during an unfavorable epidemiological period formed NETs (Fig. 2, 3) and captured the cells of the test microorganism. It was accompanied by retraction of network fibers and transformation of the net-like structure into a cloud-like one. Moreover, the size of the newly formed cloud-like traps, together with the captured cells of *Klebsiella pneumoniae*, became 2–3 times smaller than the size of the original net-like traps (Fig. 6). Our observations show that the capture of the test microorganism cells was very effective. An extensive array of *Klebsiella pneumoniae* cells was almost completely cleared of this pathogen, and all microorganisms were trapped inside the cloud-like structures (Fig. 4). Each cloud-like structure that originated from the net-like NET of the volunteers who were not ill but had contacts with infected people captured and retained 89.38 ± 5.86 cells of *Klebsiella pneumoniae* (Fig. 5).

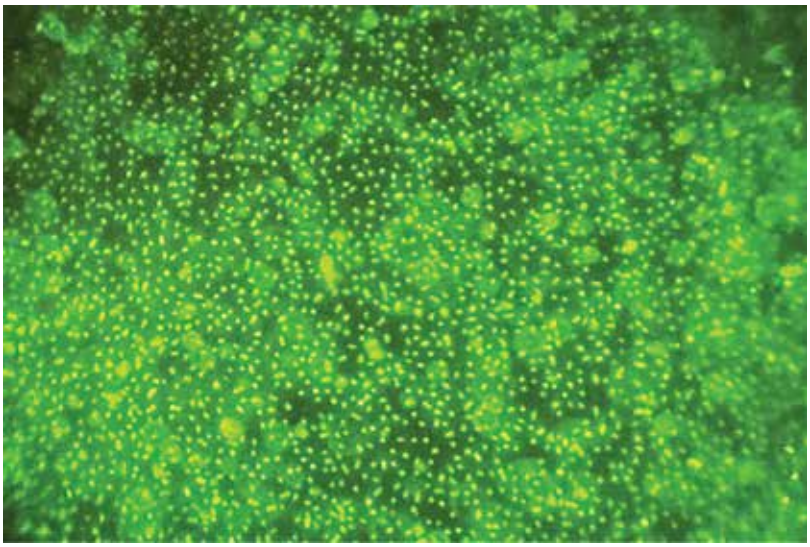

Fig. 4. Cells of *Klebsiella pneumoniae* (ATCC 700603) placed on glass slides. Staining with CYBR Green I, x1,000

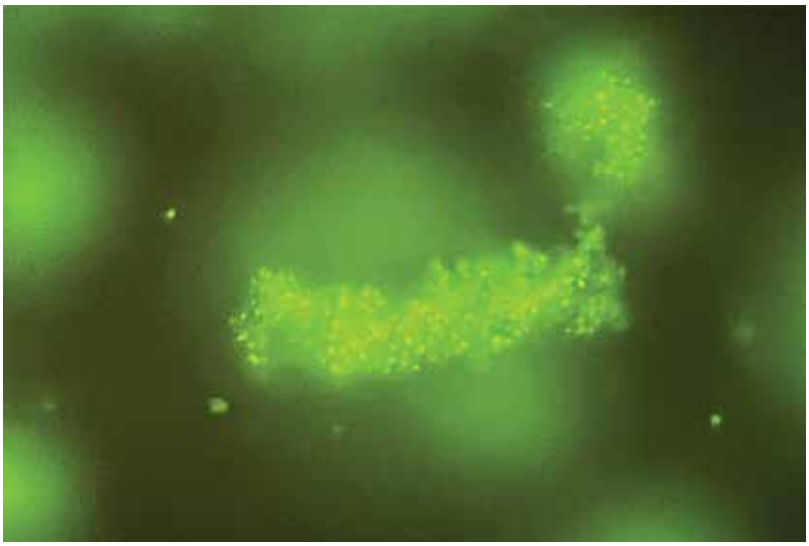

Fig. 5. Net-like NETs effectively capture and bind *Klebsiella pneumoniae* cells and turn into cloud-like structures. Incubation time of NETs with *Klebsiella pneumoniae* cells is 2 hours. Staining with CYBR Green I, x1,000

For comparison, the functional activity of neutrophils in the disease-free volunteers was compared with the results obtained in the test with the capture of *Klebsiella pneumoniae* in two other groups of patients. We studied the capture and binding of test microorganism cells by NETs in patients with acute infection and inflammation in the abdominal cavity (acute appendicitis, acute cholecystitis, abscess) and in patients with non-specific ulcerative colitis.

The functional activity of NETs in patients with acute infection and inflammation in the abdominal cavity was reduced. Each NET in such patients captured and bound 20.2 ± 1.67 microbial cells. The binding capacity decreased by more than 4 times compared to clinically healthy, disease-free volunteers (Fig. 6).

The study of the capturing and binding capacity of NETs the in patients with ulcerative colitis revealed a very weak functional activity of NETs in this group of patients. The number of Klebsiella pneumoniae microorganisms captured by NETs in patients with ulcerative colitis was only 5.53 ± 0.34 microbial bodies. Thus, the results of the comparative study of cell binding capacity in relation to the test microorganism (Fig. 7) showed that NETs in the healthy volunteers who had contacts with infected patients had the highest binding capacity. High binding capacity of NETs in such patients, apparently, was a factor in their effective protection from the development of the infection with manifestation of clinical symptoms.

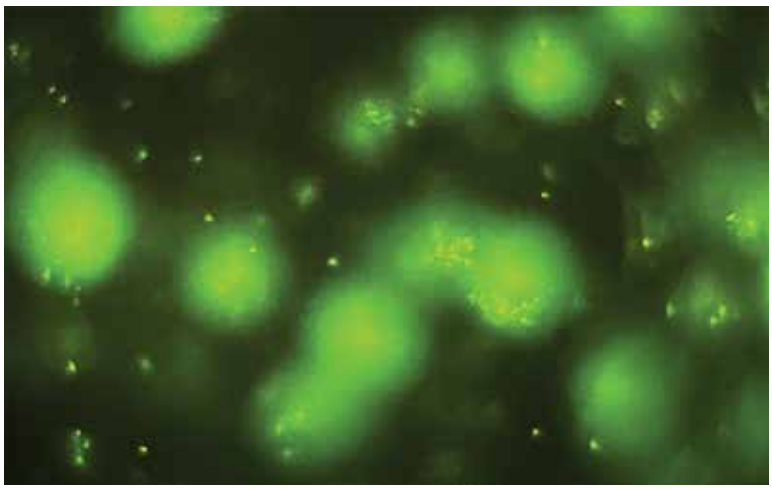

Fig. 6. Weakening of pathogen binding in patients with acute inflammation in the abdominal cavity. Net-like NETs of patients with inflammation in the abdominal cavity capture and bind *Klebsiella pneumoniae* cells and turn into cloud-like structures. Incubation time of NETs with *Klebsiella pneumoniae* cells is 2 hours. Staining with CYBR Green I, x1,000

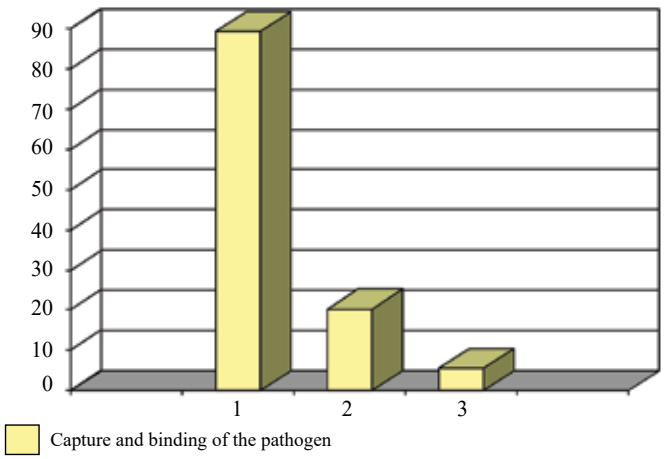

Fig. 7. Capture and binding of the *Klebsiella pneumoniae* pathogen by NETs in healthy people and in patients with various inflammatory diseases: on the vertical axis – the number of microbial bodies captured by one neutrophil structure, on the horizontal axis – healthy volunteers who had contact with infected patients (1); patients with acute inflammation in the abdominal cavity (2); patients with non-specific ulcerative colitis (3)

NETs in the patients with acute infection and inflammation in the abdominal cavity (appendicitis, cholecystitis, abscess) had a reduced capturing and binding capacity; however, it still remained at a fairly high level. The transformation of the net-like NETs into cloud-like structures in such patients was accompanied by weakening of their binding capacity in relation to the cells of the test microorganism.

NETs in the patients with ulcerative colitis had the lowest ability to bind pathogen cells. The weakening of the capturing and binding capacity of NETs in patients with this chronic autoimmune disease indicates reduced functional activity of NETs and, apparently, underlies comorbidity in patients with ulcerative colitis.

CONCLUSION

Obtaining detailed information about the morphological variants of NETs is based on the adequate method for their visualization, which we described earlier [10]. The results of the *in vitro* study demonstratев the structure of NETs and changes in their morphology during the response of neutrophils to the pathogen, which indicates the crucial role of these innate immunity cells in the body defense against infection.

The results obtained showed that the group of disease-free volunteers who were in contact with infected people were protected from infection due to the effective work of the neutrophil link of innate immunity. Their neutrophils were already pre-activated, as they were able to spontaneously form NETs. Net-like traps very effectively captured pathogen cells, developed fiber retraction, and turned into compact cloud-like structures. Then these structures naturally underwent phagocytosis; intracellular hydrolysis developed, and antigen presentation occurred. From this moment, the adaptive immunity response began.

In the patients with acute infection and inflammation in the abdominal cavity (appendicitis, cholecystitis, abscess), the experiment confirmed weakening of the capturing and binding capacity of NETs, which in the clinical setting can increase the risk of developing complications of the underlying disease.

The functional activity of NETs was drastically weakened in the patients with ulcerative colitis, which explains increased sensitivity to infection and high comorbidity in these patients.

The results of the study show that body defense against infection with the participation of innate immunity cells consists in the effective capture and binding of the pathogen. Weakening of the binding capacity of NETs carries a potential risk of complications.

The authors draw attention to the fact that this is the first study devoted to the study of the functional activity of NETs in the human body.

REFERENCES

1. Raftery M.J., Lalwani P., Krautkrämer E., Peters T., Scharffetter-Kochanek K., Krüger R.et al. β2 integrin mediates hantavirus-induced release of neutrophil extracellular traps. *J. Exp. Med*. 2014;211(7):1485–1497. DOI: 10.1084/jem.20131092.
2. Saitoh T., Komano J., Saitoh Y., Misawa T., Takahama M., Kozaki T.et al. Neutrophil extracellular traps mediate a host defense response to human immunodeficiency virus-1. *Cell. Host. Microb*. 2012;12(1):109–116. DOI: 10.1016/j.chom.2012.05.015.
3. Jenne C.N., Kubes P. Virus-induced NETs-critical component of host defense or pathogenic mediator? *PLoS Pathog*. 2015;11(1):e1004546. DOI: 10.1371/journal.ppat.1004546.
4. Veras F.P., Gomes G.F., Silva B.M.S., Caetité D.B., Almeida C.J.L.R., Silva C.M.S. et al. Targeting neutrophils extracellular traps (NETs) reduces multiple organ injury in a COVID-19 mouse model. *Respir. Res*. 2023;24(1):66. DOI: 10.1186/s12931-023-02336-2.
5. Narasaraju T., Yang E., Samy R.P., Ng H.H., Poh W.P., Liew A.A. et al. Excessive neutrophils and neutrophil extracellular traps contribute to acute lung injury of influenza pneumonitis. *Am. J. Pathol.* 2011;179(1):199–210. DOI: 10.1016/j.ajpath.2011.03.013.
6. Liuluan Z., Lu L., Yue Z., Lin P., Jingyuan L., Xingwang L. et al. High level of neutrophil extracellular traps correlates with poor prognosis of severe influenza a infection. *The Journal of Infectious Disease.* 2018;217(3):428–437. DOI: 10.1093/infdis/jix475.
7. Chan L.L.Y., Nicholls J.M., Peiris J.S.M., Lau Y.L., Chan M.C.W., Chan R.W.Y. Host DNA released by NETosis in neutrophils exposed to seasonal H1N1 and highly pathogenic H5N1 influenza viruses. *Respir. Res*. 2020;21(1):160. DOI: 10.1186/s12931-020-01425-w.
8. George S.T., Lai J., Ma J., Stacey H.D., Miller M.S., Mullarkey C.E. Neutrophils and influenza: a thin line between helpful and harmful. *Vaccines*. 2021;9(6):597. DOI: 10.3390/vaccines9060597.
9. Hiroki C.H., Toller-Kawahisa J.E., Fumagalli M.J., Colon D.F., Figueiredo L.T.M., Fonseca B.A.L.D. et al. Neutrophil extracellular traps effectively control acute chikungunya virus infection. *Front. Immunol*. 2020; 10:3108. DOI: 10.3389/fimmu.2019.03108.
10. Kazimirskii A.N., Salmasi J.M., Poryadin G.V., Panina M.I. New opportunities for diagnosis and investigation of the pathogenesis of various types of inflammation. *Pathological Physiology and Experimental Therapy*. 2022;66(2):34–42 (in Russ.). DOI: 10.25557/0031-2991.2022.02.34-42.

Authors' contribution

Kazimirskii A.N. – carrying out the experiment, drafting of figures and diagrams, drafting of the article. Salmasi J.M. – editing of the article. Poryadin G.V., Stupin V.A. – conception and design. Panina M.I. – editing of the article, statistical processing of the material. Kim A.E. – carrying out the experiment. Titova E.G. – carrying out the experiment, collection and processing of the material. Rogozhina L.S. – collection and processing of the material.

Authors' information

Kazimirskii Alexander N. – Dr. Sci. (Biology), Associate Professor, Leading Researcher, Division of Molecular Technologies, Pirogov Russian National Research Medical University, Moscow, alnica10@mail.ru, 0000-0002-3079-4089

Salmasi Jean M. – Dr. Sci. (Med.), Professor, Head of the Division of Pathophysiology and Clinical Pathophysiology, Department of Medicine, Pirogov Russian National Research Medical University, Moscow, profjms@yandex.ru, http://orcid.org/0000-0001-8524-0019

Poryadin Gennady V. – Dr. Sci. (Med.), Professor, Corresponding Member of RAS, Professor, Division of Pathophysiology and Clinical Pathophysiology, Faculty of Medicine, Pirogov Russian National Research Medical University, Moscow, poryadin_GV@rsmu.ru, http://orcid.org/0000-0003-2010-3296

Panina Marina I. – Dr. Sci. (Med.), Professor, Division of Pathophysiology and Clinical Pathophysiology, Department of Medicine, Pirogov Russian National Research Medical University, Moscow, pan-mar@list.ru, http://orcid.org/0000-0002-7651-0037

Stupin Viktor A. – Dr. Sci. (Med.), Professor, Head of the Division of Advanced Surgery No. 1 of the Department of Medicine, Pirogov Russian National Research Medical University, Moscow, stvictor@bk.ru, http://orcid.org/0000-0002-9522-8061

Kim Anna E. – Teaching Assistant, Division of Pathophysiology and Clinical Pathophysiology, Pirogov Russian National Research Medical University, Moscow, infoany@mail.ru, http://orcid.org/0000-0001-8119-772X

Titova Ekaterina G. – Senior Lecturer, Division of Pathophysiology and Clinical Pathophysiology, Pirogov Russian National Research Medical University, Moscow, Eka-gen@mail.ru, http://orcid.org/0000-0002-1655-322X

Rogozhina Lyudmila S. – Teaching Assistant, Division of Advanced Surgery No. 1, Pirogov Russian National Research Medical University, Moscow, lusy-090909@yandex.ru, http://orcid.org/0000-0002-3983-7890

(✉) **Kazimirskii Alexander N.,** alnica10@mail.ru

Received 14.06.2023;
approved after peer review 24.07.2023;
accepted 14.09.2023

ORIGINAL ARTICLES

УДК 616.36-06:616.37-002.2
https://doi.org/10.20538/1682-0363-2024-1-64-68

Association of polymorphic loci of the *GSS* gene with the risk of acute biliary pancreatitis

Samgina T.A.[1], Kochetova L.V.[2]

[1] *Kursk State Medical University*
3, Karla Marksa Str., Kursk, 305041, Russian Federation

[2] *Krasnoyarsk State Medical University*
1, Partizana Zheleznyaka Str., Krasnoyarsk, 660022, Russian Federation

ABSTRACT

Aim. To investigate the role of single nucleotide polymorphisms (SNPs) rs13041792, rs1801310, and rs6088660 in the *GSS* gene and environmental factors in the development of acute biliary pancreatitis (ABP) and its complications.

Materials and methods. The material for the study was blood samples obtained from 84 patients with ABP and 573 healthy individuals. Both groups were comparable in terms of gender and age. To diagnose ABP, we used the clinical guidelines recommended by the working group of the Russian Society of Surgeons. DNA was isolated by phenol / chloroform extraction. Multiplex genotyping of SNPs was performed by the iPLEX assay on the MALDI-TOF MassARRAY-4 genetic analyzer. Statistical data processing was performed using Statistica 10 and SNPStats software.

Results. We found that insufficient consumption of fresh vegetables and fruits increased the probability of ABP in carriers of genotypes G/A-A/A at rs1801310 in *GSS* ($p = 0.02$). The analysis revealed the association of the T allele at rs6088660 with the odds for developing acute pancreatitis ($p = 0.007$) and digestive fistulas ($p = 0.02$). A high probability of death was associated with rs1801310 (G/A genotype, $p = 0.002$) and rs6088660 (C/T genotype, $p = 0.01$) in the *GSS* gene.

Conclusion. SNPs rs6088660 and rs1801310 in the *GSS* gene can be used to predict the course of ABP.

Keywords: acute biliary pancreatitis, rs13041792, rs1801310, rs6088660 in the *GSS* gene

Conflict of interest. The authors declare the absence of obvious or potential conflicts of interest related to the publication of this article.

Source of financing. The authors state that they received no funding for the study.

Conformity with the principles of ethics. All individuals included in the study signed an informed consent to participate in the study. The study was approved by the regional Ethics Committee at Kursk State Medical university (Protocol No. 3 of 11.03.2013).

For citation: Samgina T.A., Kochetova L.V. Association of polymorphic loci of the *GSS* gene with the risk of acute biliary pancreatitis. *Bulletin of Siberian Medicine.* 2024;23(1):64–68. https://doi.org/10.20538/1682-0363-2024-1-64-68.

✉ *Samgina Tatiana A.,* tass@list.ru

Ассоциация вариантов нуклеотидной последовательности гена *GSS* с риском развития острого билиарного панкреатита

Самгина Т.А.[1], Кочетова Л.В.[2]

[1] *Курский государственный медицинский университет (КГМУ)*
Россия, 305041, Курск, ул. К. Маркса, 3

[2] *Красноярский государственный медицинский университет (КрасГМУ) им. проф. В.Ф. Войно-Ясенецкого*
Россия, 660022, Красноярск, ул. Партизана Железняка, 1

РЕЗЮМЕ

Цель: исследовать вклад вариантов нуклеотидной последовательности rs13041792, rs1801310 и rs6088660 гена *GSS* и некоторых средовых факторов в развитие острого билиарного панкреатита (ОБП) и его осложнений.

Материалы и методы. От 84 пациентов с ОБП и 573 здоровых индивидов были получены образцы крови для выделения геномной ДНК. Обе группы были сопоставимы по полу и возрасту. Диагностику заболевания проводили с использованием клинических рекомендаций, разработанных рабочей группой Российского общества хирургов. Геномную ДНК выделяли стандартным методом фенольно-хлороформной экстракции. Мультиплексное генотипирование SNPs проводили по технологии iPLEX на генетическом анализаторе MALDI-TOF MassARRAY-4. Статистическую обработку данных осуществляли с использованием программы Statistica 10, SNPStats.

Результаты. Установлено, что недостаточное употребление свежих овощей и фруктов повышает риск развития ОБП у носителей генотипов G/A-A/A rs1801310 *GSS* ($p = 0,02$). Проведенный анализ установил ассоциацию аллеля T rs6088660 с вероятностью развития гнойного парапанкреатита ($p = 0,007$) и дигестивных свищей ($p = 0,02$). Высокая вероятность смертельного исхода была связана с носительством SNPs rs1801310 (генотип G/A, $p = 0,002$) и rs6088660 (генотип C/T, $p = 0,01$) гена *GSS*.

Заключение. Варианты нуклеотидной последовательности rs6088660 и rs1801310 гена *GSS* можно использовать для прогнозирования течения ОБП.

Ключевые слова: острый билиарный панкреатит, rs13041792, rs1801310 и rs6088660 гена *GSS*

Конфликт интересов. Авторы декларируют отсутствие явных и потенциальных конфликтов интересов, связанных с публикацией настоящей статьи.

Источник финансирования. Авторы заявляют об отсутствии финансирования при проведении исследования.

Соответствие принципам этики. Все лица, участвующие в исследовании, подписали информированное согласие на участие в исследовании. Исследование одобрено региональным этическим комитетом при КГМУ (протокол № 3 от 11.03.2013).

Для цитирования: Самгина Т.А., Кочетова Л.В. Ассоциация вариантов нуклеотидной последовательности гена *GSS* с риском развития острого билиарного панкреатита. *Бюллетень сибирской медицины.* 2024;23(1):64–68. https://doi.org/10.20538/1682-0363-2024-1-64-68.

INTRODUCTION

Acute biliary pancreatitis (ABP) is a complication of cholelithiasis which occurs following an impairment of bile and pancreatic juice outflow. ABP is a multifactorial disease taking place due to the interaction of genetic and environmental factors. Most of the research in the world is devoted to studying the role of genes regulating the synthesis of pancreatic enzymes, the kallikrein – kinin system, and cytokines, that play the crucial the role in the pathogenesis of ABP [1–3]. Environmental risk factors include consumption of fatty, fried, spicy foods that stimulate the exocrine function of the pancreas, insufficient consumption of

fresh vegetables and fruits rich in vitamins and antioxidants, as well as alcohol abuse and smoking [4, 5].

Disturbances in redox homeostasis that develop in ABP due to premature intraductal activation of pancreatic enzymes and hypertension lead to an increase in the concentration of calcium ions in acinar cells. It is this mechanism that serves as a link between the activation of trypsinogen, nuclear factor kB (NF-kB), the development of mitochondrial dysfunction, and cell death [6].

The depletion of intracellular glutathione observed at the onset of acute pancreatitis [7, 8] prompted us to study the contribution of genes regulating glutathione metabolism to the pathogenesis of ABP. Only a few works on this issue are known in the literature [9].

The main enzyme for glutathione biosynthesis is glutathione synthetase, which is expressed in the liver and pancreas. No studies on its role in the development of ABP and its complications have been conducted in the world yet.

The aim of this study was to investigate the contribution of single nucleotide polymorphisms (SNPs) rs13041792, rs1801310. and rs6088660 in the *GSS* gene and environmental factors to the risk of ABP and its complications.

MATERIALS AND METHODS

We examined and treated 84 ethnically Russian (self-identification) patients with ABP (24 women and 60 men) who received inpatient treatment at the surgery departments of hospitals in Kursk (clinical sites of the Department of Surgical Diseases No. 2) in 2015–2021. The material of the study was blood samples obtained from 84 patients with ABP and 573 (161 women and 412 men) healthy individuals who were selected following regular health checkups carried out during the same period. The mean age of the patients was 48.9 ± 13.1 years, the mean age of healthy individuals was 47.8 ± 12.1 years. ABP was diagnosed using clinical guidelines recommended by the working group of the Russian Society of Surgeons [10]. All participants signed a voluntary informed consent to participate in the study. The study was approved by the regional Ethics Committee at Kursk State Medical University (Protocol No. 3 of 11.03.2013). All study participants answered the questions of the questionnaire which helped analyze the effect of environmental risk factors on the disease [11].

Genomic DNA was isolated by the standard phenol / chloroform extraction. Multiplex genotyping of SNPs was performed by the iPLEX assay on the MALDI-TOF MassARRAY-4 genetic analyzer (AgenaBioscience, USA).

To compare categorical variables between the groups, the c^2 test was used; to compare quantitative variables, the Student's *t*-test (for normally distributed variables) and the Mann – Whitney test (for non-normally distributed variables) were used. Since the distribution of the studied quantitative blood parameters was statistically significantly different from the normal one ($p < 0.05$, Kolmogorov – Smirnov test), these parameters were presented as the median and the interquartile range. To assess the influence of the studied SNPs on the normalized quantitative parameters, the linear regression analysis was used.

Associations of alleles and genotypes with the probability of developing the disease were assessed by the odds ratio (OR). The OR and 95% confidence interval (CI) were calculated by the logistic regression analysis with adjustment for sex and age using the SNPStats statistical package. To assess the associations of DNA markers with clinical characteristics (clinical forms, symptoms, nature of the course, severity of the disease, treatment efficacy), we also used the logistic regression analysis. Multiplicity adjustment of tests was performed by the permutation test (Pperm) using the PLINK program.

RESULTS

The genotype frequencies of the studied SNPs in the *GSS* gene met the Hardy – Weinberg principles in both study groups. We did not find associations of the studied SNPs with ABP.

The analysis of the role of environmental risk factors (alcohol abuse by frequency, volume, and duration; smoking; the content of proteins, fats and carbohydrates in the food consumed) in the risk of developing the disease found that insufficient consumption of fresh vegetables (less than 27 g / day) increased the risk of ABP in carriers of G/A-A/A at rs1801310 in the *GSS* gene (Table 1). Only statistically significant results are presented.

The analysis of the effect of SNPs on laboratory parameters, such as the level of amylase, oxidized glutathione, and blood leukocytes, established an association of rs1801310 in *GSS* with leukocytosis (Table 2).

The study also found that the frequency of the GG (rs1801310) *GSS* genotype was the lowest in patients with severe acute pancreatitis ($p = 0.01$) compared to mild and moderate forms of the disease.

Table 1

The influence of environmental factors on the development of acute biliary pancreatitis in carriers of the studied SNPs in the *GSS* gene (rs1801310)

Genotype	No risk factor			Presence of a risk factor		
	Healthy individuals	Patients with ABP	OR (95% CI)[1], *P*[2]	Healthy individuals	Patients with ABP	OR (95% CI)[1], *P*[2]
G/G	61 (35.5)	13 (40.6)	0.74 (0.33–1.62) 0.6	13 (59.1)	16 (30.8)	4.12 (1.38–12.28) 0.02
G/A-A/A	111 (64.5)	19 (59.4)		9 (40.9)	36 (69.2)	

[1] odds ratio and 95% confidence interval of associations of SNPs with the likelihood of developing the disease;
[2] significance levels for the most significant genetic models of associations of SNPs with the likelihood of developing the disease.

Table 2

Associations of SNPs with quantitative parameters of the blood in ABP patients

Parameter	*Me*	*Q1/Q3*	*p**
GSS G>A (rs1801310)	7.50	6.50/11.80	0.0005[D]
	9.10	6.75/15.00	
	7.90	6.60/11.20	

Note. D – dominant model.
* statistical significance of the association of SNP with normalized blood parameters (linear regression analysis).

The analysis of the associations of SNPs in the *GSS* gene with the likelihood of complications found that T allele at rs6088660 (OR=1.62, 95%CI 1.14–2.29, $p = 0.007$) was associated with the development of purulent acute pancreatitis and the formation of digestive fistulas (allele T, OR=4.54, 95%CI 1.19–17.33, $p = 0.02$).

A high probability of death was observed in carriers of the G/A genotype at rs1801310 (OR=6.76, 95%CI 1.51–30.38, $p = 0.002$) and C/T genotype at rs6088660 (OR=4.01,95%CI 1.24–13.04, $p = 0.01$) in the *GSS* gene.

DISCUSSION

Disturbances of redox homeostasis underlie many acute and chronic diseases; therefore, the study of the role of genes regulating glutathione metabolism enzymes is of great interest for researchers. When studying the effect of rs1801310 in the *GSS* gene on the risk of developing uterine fibroids, O.Yu. Bushueva et al. found no association of the locus with the disease [12]. However, associations of rs1801310 and rs6088660 in the *GSS* gene with the likelihood of ischemic stroke in men and women have been established [13].

Yu.E. Azarova et al. in the study on type 2 diabetes established an association of rs13041792 and rs6088660 in the *GSS* gene with changes in fasting blood glucose in men, an association of rs6088660 in *GSS* with a decrease in hydrogen peroxide in women, as well as an association of rs1801310 in *GSS* with a decrease in total glutathione in women [14]. W. Tang et al. established an association of rs13041792 in the *GSS* gene with the level of protein C in the blood plasma [15].

The logistic regression analysis established correlations between the expression of genes encoding glutathione metabolism enzymes with each other and with the genes encoding antioxidant enzymes (*GPX2, GSTP1*). Their co-expression with candidate genes for pancreatitis also attracts attention. *GSS* gene expression was positively associated with the level of *GGT6* gene mRNA ($r = 0.283$, $p = 0.0001$). SNPs rs1801310 and rs6088660 were associated with increased transcriptional activity of the *GSS* gene in the pancreas ($p = 0.01$) and liver ($p \leq 0.05$). Numerous eQTLs associated with the expression of molecular chaperones in the pancreas have been identified for SNPs of genes encoding glutathione metabolism enzymes.

Allele A at rs13041792 in the *GSS* gene was associated with increased expression of the *HSPE1* ($p = 0.0056$, $\beta = 0.11$), *HSPA1A* ($p = 0.0032$, $\beta = 0.16$), *HSPBP1* ($p = 0.0037$, $\beta = 0.15$), *HSPA4* ($p = 0.034$, $\beta = 0.095$), *HSPH1* ($p = 0.026$, $\beta = 0.12$), and *DNAJA1* ($p = 0.019$, $\beta = 0.12$) genes and decreased expression of *HSPA12A* ($p = 0.0019$, $\beta = –0.27$). Allele T at rs6088660 in *GSS* was associated with reduced expression of the chaperone genes *HSPE1* ($p = 0.030$, $\beta = –0.071$), *HSPA1A* ($p = 0.016$, $\beta = –0.11$), *HSPA1B* ($p = 0.0019$, $\beta = –0.13$), *HSPH1* ($p = 0.021$, $\beta = –0.10$), and *DNAJB1* ($p = 0.022$, $\beta = –0.11$). Allele G at rs1801310 in the *GSS* gene was associated with an increase in mRNA of the *HSPB1* gene ($p = 0.023$, $\beta = 0.083$). Allele G at rs1801310 was positively correlated with the expression level of the *CTSG* gene ($p = 0.048$, $\beta = 0.13$). Allele G at rs1801310 in the *GSS* gene was associated with increased expression of *AMY2A* ($p = 0.05$, $\beta = 0.075$), *CTRL* ($p = 0.011$, $\beta = 0.081$), *PRSS1* ($p = 0.043$, $\beta = 0.046$), and *SPINK1* ($p = 0.032$, $\beta = 0.096$) genes. Allele A at rs13041792 in *GSS* was associated with an increase in the transcriptional activity of the *SPINK1* gene ($p = 0.032$, $\beta = 0.096$). Allele T at rs6088660 in

the *GSS* gene was associated with an increased level of *CPA3* gene expression ($p = 0.035$, $\beta = –0.12$).

CONCLUSION

In the course of the study, we found that insufficient consumption of fresh vegetables and fruits increases the likelihood of developing ABP in carriers of the G/A-A/A genotypes at rs1801310 in the *GSS* gene ($p = 0.02$). The analysis of associations of SNPs of the *GSS* gene with an increased risk of complications established an association of the T allele at rs6088660 with the development of purulent acute pancreatitis ($p = 0.007$) and the formation of digestive fistulas ($p = 0.02$). A high risk of death was observed in carriers of the G/A genotype at rs1801310 ($p = 0.002$) and C/T genotype at rs6088660 ($p = 0.01$) in the *GSS* gene.

SNPs rs6088660 and rs1801310 of the *GSS* gene can be used to predict the course of ABP.

REFERENCES

1. Whitcomb D.C. Pancreatitis: TIGAR-O version 2 risk/etiology checklist with topic reviews, updates, and use primers. *Clinical and Translational Gastroenterology*. 2019;10(6):27–41. DOI: 10.14309/ctg.0000000000000027.
2. Mayerle J., Sendler M., Hegyi E., Beyer G., Lerch M.M., Sahin-Tóth M. Genetics, cell biology, and pathophysiology of pancreatitis. *Gastroenterology*. 2019;156(7):1951–1968. DOI: 10.1053/j.gastro.2018.11.081.
3. Dunayevskaya S.S., Sergeeva E.Yu., Deulina V.V., Domoratskaya E.A., Zambrzhitskaya M.K. Role of polymorphisms rs16944 (-511C/T) of the *IL1B* gene and rs1143634 (+ 3954 C/T) of the *IL1B* gene as genetic predictors of acute pancreatitis. *Experimental and Clinical Gastroenterology*. 2022;(8):28–34 (in Russ.). DOI: 10.31146/1682-8658-ecg-204-8-28-34.
4. Kodencova V.M., Vrzhesinskaya O.A., Risnik D.V., Nikityuk D.B., Tutel'yan V.A. Provision of the population of Russia with micronutrients and the possibility of its correction. State of the problem. *Voprosy Pitaniia.* 2017;86(4):113–124 (in Russ.). DOI: 10.24411/0042-8833-2017-00067.
5. Isakov V.A., Morozov S.V., Pilipenko V.I. Chapter 16. Clinical nutrition in diseases of the hepatobiliary system and pancreas. Nutrition and Clinical Dietology; ed. V.A. Tutelyan, D.B. Nikityuk. Moscow: GEOTAR-Media, 2021:415–435 (in Russ.).
6. Achkasov E.E., Vinnik Y.S., Dunaevskaya S.S. Immunopathogenesis of acute pancreatitis.M.: INFRA-M, 2021:162 (in Russ.).
7. Rau B., Poch B., Gansauge F. Pathophysiologic role of oxygen free radicals in acute pancreatitis: initiating event or mediator of tissue damage? *Ann. Surg.* 2000;231(3):352–360. DOI: 10.1097/00000658-200003000-00008.
8. Siegmund E., Weber H., Kasper M., Jonas L. Role of PGE2 in the development of pancreatic injury induced by chronic alcohol feeding in rats. *Pancreatology.* 2003;3(1):26–35. DOI: 10.1159/000069141.
9. Schneider A., Tögel S., Barmada M., Whitcomb D.C. Genetic analysis of the glutathione s-transferase genes MGST1, GSTM3, GSTT1, and GSTM1 in patients with hereditary pancreatitis. *Journal of Gastroenterology*. 2004;39:783–787. DOI: 10.1007/s00535-004-1389-7.
10. Kubyshkin V.A., Zatevahin I.I., Bagnenko S.F., Blagovestnov D.A., Vishnevskij V.A., Gal'perin E.I. National clinical guidelines for acute pancreatitis (in Russ.). URL: http://xn-9sbdbejx7bdduahou3a5d.xn-p1ai/stranica-pravlenija/unkr/urgentnaja-abdominalnaja-hirurgija/nacionalnye-klinicheskie-rekomendaci-po-ostromu-pankreatitu.html
11. Samgina T.A., Lazarenko V.A. The role of polymorphic variants rs11546155 and rs6119534 of the *GGT7* gene and some risk factors in the development of acute pancreatitis. *Voprosy Pitaniia.* 2022;91(2):43–50 (in Russ.). DOI: 10.33029/0042-8833-2022-91-2-43-50.
12. Kudryavtseva O.K., Barysheva E.M., Vdovina I.N., Klinovskaya A.A., Novikova E.A., Polonikov A.V., et al. Association of genetic variations in genes involved in glutathione metabolism with a risk of development of uterine fibroids. *Medical Genetics*. 2020;19(6):52–54 (in Russ.). DOI: 10.25557/2073-7998.2020.06.52-54.
13. Bocharova Y.A. Study of associations of three polymorphic variants of the glutathione synthase (*GSS*) gene with the risk of ischemic stroke. *Scientific Results of Biomedical Research*. 2020;6(4):476–487 (in Russ.). DOI: 10.18413/2658-6533-2020-6-4-0-4.
14. Azarova I., Klyosova E., Polonikov A. The link between type 2 diabetes mellitus and the polymorphisms of glutathione-metabolizing genes suggests a new hypothesis explaining disease initiation and progression. *Life*. 2021;11(9):886. DOI: 10.3390/life11090886.
15. Tang W., Basu S., Kong X., Pankow J.S., Aleksic N., Tan A. et al. Genome-wide association study identifies novel loci for plasma levels of protein C: The ARIC study. *Blood*. 2010;116:5032–5036. DOI: 10.1182/blood-2010-05-283739.

Authors' information

Samgina Tatiana A. – Cand. Sci. (Med.), Associate Professor, Department of Surgical Diseases No.2, Kursk State Medical University, Kursk, tass@list.ru, http://orcid.org/0000-0002-7781-3793

Kochetova Ludmila V. – Cand. Sci. (Med.), Associate Professor, Department of General Surgery, Krasnoyarsk State Medical University, Krasnoyarsk, kochetovalv@bk.ru, http://orcid.org/0000-0001-5784-7067

(✉) **Samgina Tatiana A.,** tass@list.ru

Received 01.05.2023;
approved after peer review 26.05.2023;
accepted 14.09.2023

УДК 616.127-005.8-036.8-037-073.43-8
https://doi.org/10.20538/1682-0363-2024-1-69-76

The role of 3D speckle-tracking echocardiography in predicting long-term outcomes after a first myocardial infarction

Timofeeva T. M.[1, 2], Efimova V.P.[2], Safarova A. F.[1, 2], Kobalava Zh.D.[1]

[1] *Peoples' Friendship University of Russia (RUDN University)*
8, Mikluho-Maklaya Str., Moscow, 117198, Russian Federation

[2] *Vinogradov City Clinical Hospital*
61, Vavilova Str., Moscow, 117292, Russian Federation

ABSTRACT

Aim. To determine the role of 3D echocardiography parameters in the prognosis of long-term cardiovascular complications in patients with a first acute myocardial infarction (AMI).

Materials and methods. A prospective, single-center, observational study included 46 patients with a first AMI and successful PCI without a history of heart failure (HF) and shortness of breath upon admission. The examination of patients was performed in accordance with the Russian standards of medical care provision. Additionally, 3D echocardiography was performed, and N-terminal pro-brain natriuretic peptide (NT-proBNP) was determined. The main outcomes assessed were hospitalization with HF, sudden cardiac death, and combined endpoint. Median follow-up was 554 days (IQR 550–785).

Results. During the follow-up period, 9 hospitalizations with HF, 3 sudden cardiac deaths, and 12 combined endpoints were registered. The effect of 3D echocardiography parameters on the development of sudden cardiac death and combined endpoint has not been revealed. The effect of the studied parameters on the development of HF during the follow-up period that required hospitalization was evaluated. A statistically significant increase in the LV sphericity index was revealed in the group of patients with the registered outcome. We found significant direct correlations of left ventricular volume indices with prescription of diuretics in the post-discharge period; hospitalization with HF in the post-infarction period with the level of NT-pro-BNP, left atrial volume with the duration of index hospitalization, duration of eventless survival with ST elevation. We found a negative correlation of radial strain with prescription of diuretics in the post-discharge period. Predictors of hospitalization with HF in the post-infarction period were identified – parameters of radial strain, area strain, and circumferential strain, which were included in the model for calculating the risk of the outcome under study.

Conclusion. In patients with the first AMI in the absence of clinical signs of HF, to calculate the risk of hospitalization with HF within 550 days after MI, it is advisable to take into account the level of radial strain and use a prognostic model (1), including parameters of circumferential and area strain (according to 3D echocardiography data).

Keywords: three-dimensional echocardiography, myocardial infarction, heart failure

Conflict of interest. The authors declare the absence of obvious or potential conflicts of interest related to the publication of this article.

Source of financing. The authors state that they received no funding for the study.

Conformity with the principles of ethics. All individuals signed an informed consent to participate in the study. The study was approved by the Ethics Committee at RUDN University.

For citation: Timofeeva T.M., Efimova V.P., Safarova A.F., Kobalava Zh.D. The role of 3D speckle-tracking echocardiography in predicting long-term outcomes after a first myocardial infarction. *Bulletin of Siberian Medicine.* 2024;23(1):69–76. https://doi.org/10.20538/1682-0363-2024-1-69-76.

✉ *Timofeeva Tatiana M.,* timtan@bk.ru

Роль спекл-трекинг эхокардиографии в трехмерном режиме для прогнозирования отдаленных исходов после первого инфаркта миокарда

Тимофеева Т.М.[1, 2], Ефимова В.П.[2], Сафарова А.Ф.[1, 2], Кобалава Ж.Д.[1]

[1] *Российский университет дружбы народов (РУДН)*
Россия, 117198, г. Москва, ул. Миклухо-Маклая, 8

[2] *Городская клиническая больница (ГКБ) им. В.В. Виноградова ДЗМ*
Россия, 117292, г. Москва, ул. Вавилова, 61

РЕЗЮМЕ

Цель: определение роли параметров эхокардиографии в 3D-режиме (3D-ЭхоКГ) в прогнозе развития сердечно-сосудистых осложнений в отдаленном периоде у пациентов с первым острым инфарктом миокарда (ОИМ).

Материалы и методы. В проспективное одноцентровое наблюдательное исследование включены 46 пациентов с первым ОИМ, успешным чрескожным коронарным вмешательством без анамнеза сердечной недостаточности (СН), одышки при поступлении. Обследование пациентов выполняли в соответствии с российскими стандартами оказания медицинской помощи, дополнительно выполняли трехмерную эхокардиографию и определяли мозговой натрийуретический гормон (NT-proBNP). Основными оцениваемыми исходами были госпитализация с СН, сердечно-сосудистая смерть и комбинированная конечная точка. Медиана периода наблюдения – 554 сут, IQR 550–785.

Результаты. За период наблюдения зарегистрировано девять госпитализаций с СН, три сердечно-сосудистые смерти, 12 комбинированных точек. Влияния параметров 3D-ЭхоКГ на развитие сердечно-сосудистой смерти и комбинированной конечной точки не получено. Оценивали влияние изучаемых параметров на развитие СН в течение периода наблюдения, потребовавшей госпитализации. Выявлено статистически значимое повышение индекса сферичности левого желудочка в группе пациентов с зарегистрированным исходом. Выявлены значимые прямые корреляционные связи объемных показателей левого желудочка с назначением диуретиков в постгоспитальном периоде; госпитализации с СН в постинфарктном периоде с уровнем NT-pro-BNP, объемом левого предсердия и продолжительностью индексной госпитализации, срока бессобытийной выживаемости с элевацией ST; отрицательная корреляционная связь радикальной деформации с назначением диуретиков в постгоспитальном периоде. Выявлены предикторы госпитализации с СН в постинфарктном периоде – показатели радиальной деформации, а также деформации площади и циркулярной деформации, которые вошли в модель расчета риска наступления изучаемого исхода.

Заключение. У пациентов с первым ОИМ при отсутствии клинических признаков СН для расчета риска госпитализации с СН в течение 550 сут после ИМ целесообразно учитывать уровень радиальной деформации и использовать прогностическую модель (1), включающую показатели циркулярной деформации и деформации площади (по данным 3D-ЭхоКГ).

Ключевые слова: трехмерная эхокардиография, инфаркт миокарда, сердечная недостаточность

Конфликт интересов. Авторы декларируют отсутствие явных и потенциальных конфликтов интересов, связанных с публикацией настоящей статьи.

Источник финансирования. Авторы заявляют об отсутствии финансирования при проведении исследования.

Соответствие принципам этики. Все пациенты подписали информированное согласие на участие в исследовании. Исследование одобрено комитетом по этике Медицинского института РУДН.

Для цитирования: Тимофеева Т.М., Ефимова В.П., Сафарова А.Ф., Кобалава Ж.Д. Роль спекл-трекинг эхокардиографии в трехмерном режиме для прогнозирования отдаленных исходов после первого инфаркта миокарда. *Бюллетень сибирской медицины.* 2024;23(1):69–76. https://doi.org/10.20538/1682-0363-2024-1-69-76.

INTRODUCTION

Acute myocardial infarction (AMI) is associated with a high risk of adverse outcomes: more than half of surviving patients require readmission within the same year [1]. One of the key factors in the unfavorable prognosis is reduction of left ventricular (LV) function [2], traditionally assessed by LV ejection fraction (EF) [3]. However, this generally accepted parameter has a number of significant limitations, including significant inter- and intraoperator variability and underestimation of subclinical LV dysfunction. At an early stage, weakening of some muscle layers in the heart is compensated by others, which contributes to relative preservation of LVEF. In recent decades, to more accurately assess the systolic function of the heart, three-dimensional echocardiography (3D Echo) with a speckle tracking assessment of longitudinal, circumferential, and radial strain and LV rotation parameters has been used. In addition, determination of LV volume and sphericity index with 3D Echo provides more correct data indicating early post-infarction remodeling [4–8].

Therefore, the aim of the study was to determine the role of 3D Echo parameters in the prognosis of long-term cardiovascular complications in patients with a first AMI.

MATERIALS AND METHODS

A prospective, single-center, observational study included 46 patients hospitalized in the ICU of Vinogradov City Clinical Hospital. Inclusion criteria: first AMI diagnosed according to the fourth universal definition of MI [3]; successful primary PCI in patients with ST-segment elevation MI (STEMI), early (within 24 hours) PCI in patients with non-ST-segment elevation MI (NSTEMI), i.e. achieving TIMI 3 flow in the affected vessel; no history of heart failure (HF), shortness of breath on admission, Killip 1.

Exclusion criteria: use of diuretics and vasopressors, pulmonary pathology, development of complications of AMI (rupture of the interventricular septum, separation of the papillary muscle), severe disturbances of cardiac rhythm and conduction at the time of inclusion, including atrial fibrillation / flutter.

The study complied with ethical standards set out in the WMA Declaration of Helsinki "Ethical Principles for Medical Research Involving Human Subjects" and the "Rules of Good Clinical Practice in the Russian Federation." All individuals participating in the study signed an informed consent to participate in the study. The study was approved by the Ethics Committee at RUDN University.

Upon admission, all patients included in the study underwent history taking, a standard physical examination, electrocardiography, chest X-ray, Echo, coronary angiography, and angioplasty with stent placement. Laboratory tests were performed in accordance with the Russian standards of medical care provision: complete blood count and blood biochemistry, including determination of the troponin I level upon admission and 6–12 hours after hospitalization, and additional determination of N-terminal pro-brain natriuretic peptide (NT-proBNP).

Echo was performed on the best-in-class Vivid E90 device (GE Healthcare, USA) upon discharge, followed by post-processing on the EchoPAC™ station (GE Healthcare, USA) with semi-automated assessment of LVEF. LV diastolic function was assessed in accordance with current recommendations [9].

All patients during the in-hospital period and for a year after discharge received standard dual antiplatelet therapy before and after the intervention.

The primary outcomes assessed were hospitalization for HF, sudden cardiac death, and a composite endpoint. Data were obtained from a unified medical information and analytical system, as well as from telephone contacts during the follow-up (fixed follow-up 550 days; median follow-up (random censoring) 554 days (IQR 550–785)).

Statistical data analysis was performed using the SPSS software (version 23.0). Quantitative variables were described as the arithmetic mean and the standard deviation ($M \pm SD$) (for normal distribution) or as the median and the interquartile range (*Me [IQR]*) (for non-normally distributed variables). The significance of differences between the two groups in quantitative variables was assessed using the Man – Whitney *U* test (for normal distribution) or the Student's *t*-test (for non-normally distributed variables). For qualitative variables, the significance of differences between the groups was assessed by the Pearson's chi-square ($\chi 2$) / Fisher exact test depending on the minimum expected number. The differences were considered statistically significant at $p < 0.05$. The direction and strength of a correlation between parameters were assessed using the Spearman's rank correlation coefficient. The dependence of binary parameters on quantitative and categorical ones was identified by the binary logistic regression (univariate and multivariate) analysis with determination of the odds ratio (OR). The ROC analysis was used to evaluate the prognostic value by

determining the area under the curve (AUC). The influence of the studied parameters on the risk of developing endpoints was assessed using the univariate and multivariate Cox regression analysis with determination of the hazard ratio (HR). Quantitative variables with negative values were analyzed by taking the modulo.

RESULTS

Clinical, demographic, laboratory, and Echo characteristics of patients are presented in Table 1.

Table 1

Characteristics of patients, *n* = 46	
Parameter	Value
Age, years, *M* ± *SD*	61.13 ± 8.84
Men, *n* (%)	32 (69.6)
Body mass index, kg / m², *M* ± *SD*	28.26 ± 3.99
Smoking, *n* (%)	18 (39.1)
SBP / DBP, mm Hg, *M* ± *SD*	141.10 ± 23.86 / 81.84 ± 12.76
History of atrial fibrillation, *n* (%)	3(6.5%)
STEMI, *n* (%)	12 (26.1)
Anterior MI, *n* (%)	22 (47.8)
Single-vessel disease, *n* (%)	14 (30.4)
Type 2 diabetes mellitus, *n* (%)	10 (21.7)
Dyslipidemia, *n* (%)	20 (43.5)
Glucose, mmol / l, *Me* [*IQR*]	6.89 [5.59; 8.70]
NT-proBNP, pg / ml, *Me* [*IQR*]	580.0 [264.60; 989.00]
Troponin I, ng / ml, *Me* [*IQR*]	0.26 [0.03; 4.65]
Troponin II, ng / ml, *Me* [*IQR*]	7.79 [1.54; 30.61]

Note. SBP – systolic blood pressure; DBP – diastolic blood pressure; Troponin I – the level upon admission to the intensive care unit; Troponin II – the level 6–12 hours after hospitalization.

To identify predictors of adverse outcomes, the patients were divided into groups with and without recorded outcomes. During the follow-up, 9 hospitalizations with HF, 3 sudden cardiac deaths, and 12 composite endpoints were registered. The influence of 3D Echo parameters on the development of sudden cardiac death and the composite endpoint was not identified. The influence of the studied parameters on the development of HF during the follow-up period requiring hospitalization was assessed. A statistically significant increase in the LV sphericity index was revealed in the group of patients with a registered outcome (Table 2).

The obtained associations of clinical data with 3D Echo parameters in the study group following the correlation analysis are presented in Table 3.

To identify predictors of the development of the studied endpoint using the binary logistic regression analysis, a prognostic model was developed using 3D Echo parameters (the analysis also included significant risk factors for HF, ST-segment elevation, MI localization, number of affected coronary arteries, levels of NT-proBNP, troponin, EFLV, LV diastolic function parameters, 2D-GLS, all 3D Echo parameters). The identified dependence is described by equation (1):

$$P\frac{1}{1+\text{e-z}\cdot}\times 100\%$$

$$z = 2.615 - 0.102 \times CS - 0.286 \times AS$$

where *P* is the probability of developing HF requiring hospitalization (%), *CS* is the index of circumferential strain, %, and *AS* is area strain, %.

Table 2

Comparative characteristics of patients with and without hospitalization with HF in the long-term period after MI, *n* = 46			
Parameter	Hospitalization with HF, *n* = 9	No outcome, *n* = 37	*p*
Age, years, *M* ± *SD*	63.0 [61.0; 73.0]	61.0 [57.0; 66.0]	0.146
Men, *n* (%)	6 (66.7)	26 (70.3)	0.975
Body mass index, kg / m², *M* ± *SD*	27.60 ± 3.27	28.48 ± 4.60	0.613
Smoking, *n* (%)	3 (33.3)	18 (48.6)	0.539
Hypertension, *n* (%)	9 (100.0)	27 (73.0)	0.172
Dyslipidemia, *n* (%)	7 (77.8)	13 (35.1)	0.290
Single-vessel disease, *n* (%)	3 (33.3)	11 (29.7)	0.833
Multivessel disease, *n* (%)	6 (66.7)	26 (70.3)	0.833
STEMI, *n* (%)	3 (33.3)	9 (24.3)	0.581
LVEF upon admission, %, *Me [IQR]*	47.0 [45.0; 54.0]	50.0 [45.0; 52.0]	0.845
LVEF at discharge, %, *Me* [*IQR*]	52.0 [45.0; 54.0]	54.0 [51.0; 58.0]	0.265
LAVI, ml / m², *Me* [*IQR*]	27.0 [22.0; 40.0]	28.0 [21.0; 31.0]	0.454
E/e', *Me* [*IQR*]	6.6 [5.6; 7.2]	6.5 [5.7; 7.9]	0.825
PASP, mm HG, *Me* [*IQR*]	28.0 [25.0; 36.0]	21.0 [14.0; 27.0]	0.108
3D LVEF, %, *Me* [*IQR*]	51.0 [47.0; 54.0]	51.0 [48.0; 55.0]	0.617
3D SpI, *M* ± *SD*	0.38 ± 0.04	0.33 ± 0.07	0.025*

Table 2 (continued)

Parameter	Hospitalization with HF, *n* = 9	No outcome, *n* = 37	*p*
3D LVEDV, ml, *Me* [*IQR*]	106.0 [99.0; 152.0]	113.0 [98.0; 140.0]	0.901
3D LVESV, ml, *Me* [*IQR*]	52.00 [46.0; 78.0]	57.0 [48.0; 66.0]	0.945
3D MBV/CO, l / min, *Me* [*IQR*]	4.5 [3.8; 4.6]	4.1 [3.6; 4.7]	0.438
2D-GLS, %, *Me* [*IQR*]	–14.0 [–14.0; –12.0]	–14.6 [–17.0; –11.0]	0.290
3D-GLS, %, *Me* [*IQR*]	–11.0 [–13.0; –7.0]	–9.0 [–13.0; –7.0]	0.738
3D circumferential strain, %, *Me* [*IQR*]	–11.0 [–13.0; –6.0]	–12.0 [–15.0; –10.0]	0.309
3D area strain, %, *Me* [*IQR*]	–18.84 ± 7.21	–18.8 ± 4.97	0.987
3D radial strain, %, *Me* [*IQR*]	28.00 ± 12.87	27.86 ± 9.26	0.971
3D torsion, º, *Me* [*IQR*]	3.56[1.3; 7.3]	4.30 [1.8; 8.1]	0.504
3D twist, º/cm, *Me* [*IQR*]	0.90 [0.30; 1.15]	1.10 [0.6; 1.4]	0.319

Note. BMI – body mass index; LAVI – left atrial volume index; E/e' – the ratio of peak early mitral inflow velocity (E) to the early diastolic mitral annular velocity; PASP – systolic pressure in the pulmonary artery; SpI – left ventricular sphericity index; LVEDV – left ventricular end-diastolic volume; LVESV – left ventricular end-systolic volume; MBV / CO – minute blood volume/cardiac output; GLS – global longitudinal strain
* differences in the parameters were statistically significant

Table 3

Associations of 3D echocardiography parameters

3D parameter	Parameter	*R*	*p**
3D LVEDV	BMI	0.324	0.028
	Mineralocorticoid antagonists in the post-hospital period	0.303	0.041
3D LVESV	2D-GLS	–0.520	<0.001
	Diuretics in the post-hospital period	0.370	0.011
3D SpI	History of hypertension	0.455	0.001
Radial strain	BMI	–0.303	0.040
	Diuretics in the post-hospital period	–0.469	0.001
Hospitalization with HF	NT-pro-BNP level	0.399	0.026
	LAVI > 34 ml / m^2	0.422	0.003
	Duration of index hospitalization	0.338	0.022
HF-free period	ST-segment elevation upon admission	–0.805	0.050

* correlation is statistically significant

The resulting regression model is statistically significant (p = 0.004). Based on the Nigelkirk's coefficient of determination, the model (1) determines 35.4% of the variance in the probability of hospitalization with HF.

According to the values of the regression coefficients, the parameters of circumferential strain and area strain have an inverse relationship with the probability of hospitalization with HF. Characteristics of the factors are presented in Table 4.

Thus, with an increase in the circumferential strain by 1%, the odds for hospitalization with HF within 1.5 years after the first AMI decrease by 2.49 times; with an increase in the area strain index by 1%, the odds for hospitalization with HF decrease by 1.67 times.

Table 4

Characteristics of the relationship between model predictors (1) and the probability of hospitalization with HF in the long-term follow-up period in patients after a first AMI

Predictors	OR; 95% CI	*p*
Circumferential strain, %	0.40; 0.20–0.80	0.010*
Area strain,%	0.60; 0.41–0.89	0.012*

Note. OR – odds ratio, CI – confidence interval.
* the influence of the predictor is statistically significant

Figure 1 compares the values of the adjusted hazard ratio with 95% CI for the studied factors included in model (1).

The cut-off value of the logistic probability function P (1) was determined using the ROC analysis. The resulting curve is shown in Figure 2.

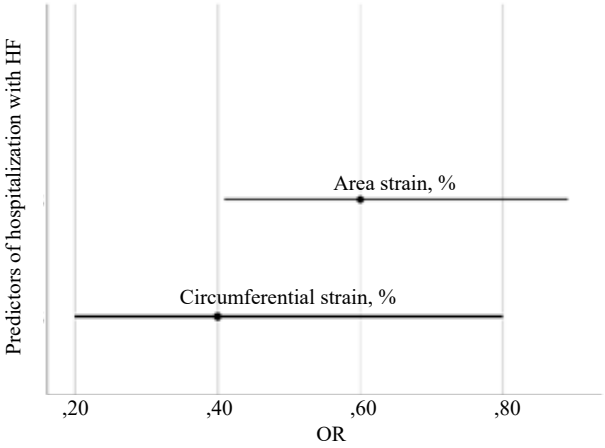

Fig. 1. Hazard ratio estimates with 95% CI for the studied predictors of the model (1) for hospitalization with HF

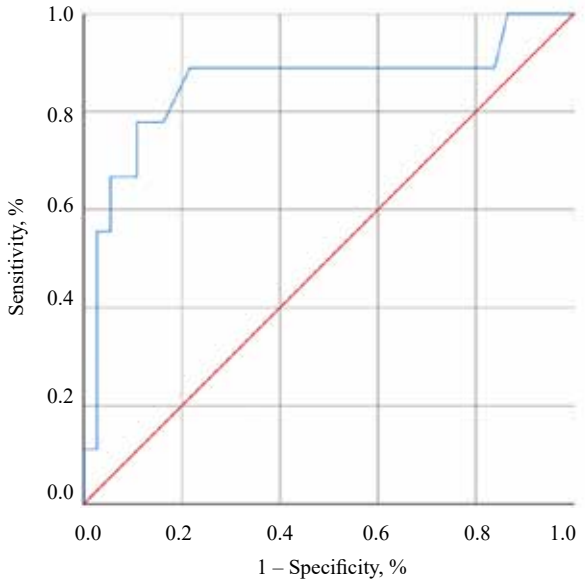

P_2 > 26.6%; Sensitivity 77.8%,
Specificity 89.2%, p = 0.026, AUC = 0.85

Fig. 2. The ROC curve characterizing the dependence of the probability of hospitalization with HF on the values of the prognostic function (1)

AUC was 0.85 ± 0.09 (95% CI: 0.68–1.00). The value of the logistic function (1) at the cut-off point was 26.6%. *P* (1) values greater than or equal to 26.6% were associated with a high risk of hospitalization with HF, and lower *P* (1) values were associated with a low risk. The sensitivity and specificity of the model (1) at the cut-off were 77.8 and 89.2%, respectively.

Table 5 shows an example of using the prognostic model (1) in two patients with a first AMI. We calculated logistic regression values *P* (1) taking into account the values of the predictors and inferred high and low risk. Patient 2, who was at high risk based on the model, was hospitalized with HF on day 291 of the follow-up.

Table 5

Example of using the prognostic model (1)

Patient	Patient 1 Woman, 64 years old, history of hypertension, STEMI, single-vessel disease	Patient 2 Woman, 58 years old, history of hypertension, STEMI, single-vessel disease
NTproBNP, pg / ml	556	630
Troponin I, II, ng / ml	0.98–1.46	0.76–1.72
Echocardiography	LAVI 29 ml / m^2 (< 34 ml / m^2) Baseline LVEF 44% 2D GLS 16% CS 12.2% AS 18.8%	LAVI 32 ml / m^2 (< 34 ml / m^2) Baseline LVEF 40% 2D GLS 10% CS 6% AS 9.8%
Index *P*	z = 2.615-0.102 × 12.2–0.286 × 18.8 = –4 $e^{-(-4)} = e^4 = 54.9$ *P* = 1/55.9 = 1.8% (<23.8%) Low risk	z = 2.615-0.102 × 6 – 0.286 x 9.8 = –0.8 $e^{-(-0,8)} = e^{0,8} = 2.23$ *P* = 1/3.23 = 31.0% (>23.8%) High risk
Hospitalization with HF	Not registered	Registered after 291 days

In the univariate analysis of the dependence of changes in the risk of hospitalization with HF on 3D Echo parameters using the Cox regression method, statistically significant predictors of the development of this endpoint were identified (Table 6).

Table 6

Characteristics of predictors of hospitalization with HF in the long-term follow-up period in patients after the first AMI

Predictors	HR; 95% CI	*p*
Circumferential strain, %	0.76; 0.597–0.968	0.026*
Radial strain, %	0.91; 0.831–0.995	0.039*

Note. HR – hazard ratio. * the influence of the predictor is statistically significant.

According to the data obtained, with an increase in circumferential strain by 1%, the risks of developing the starting point are reduced by 1.32 times, for radial strain – by 1.1 times.

DISCUSSION

In our study, in patients with first AMI with and without ST-segment elevation in the history of HF, non-invasive parameters of volumes, geometry and strain of the LV myocardium were studied according to 3D Echo data. Their prognostic value was established

in relation to the development of cardiovascular complications within 1.5 years.

In patients hospitalized with HF within 1.5 years after AMI, a significant increase in the LV sphericity index according to 3D Echo data was shown. This result is consistent with a study by H.F. Mannaerts et al., which included 33 patients with AMI. The follow-up lasted 12 months, and the sphericity index was shown to be the strongest echocardiography predictor of adverse post-infarction LV remodeling [6].

In a study by R.K. Ola et al., the information value of 3D parameters, such as LVEDV and sphericity index, as predictors of myocardial remodeling was also shown. These parameters were examined by the authors at 7 days and at 6 months after acute STEMI. The presence of adverse remodeling was defined as an increase in LVEDV, measured using 3D Echo, by 15% or more after 6 months. It was found, in particular, that the sphericity index in the group with adverse post-infarction remodeling was significantly higher than in the group with preserved LVEF (0.41 ± 0.05 and 31 ± 0.05, respectively; $p < 0.001$), but decreased in both groups after 6 months of follow-up (0.35 ± 0 .05 and 28 ± 0.05, respectively; $p < 0.001$). Thus, the authors concluded that determination of the sphericity index allows for early identification of patients at high risk of developing adverse myocardial remodeling after AMI [7]. Similar results were obtained in a study by M.L.Vieira et al. [10].

Predictors of the development of HF requiring hospitalization within 1.5 years of the post-infarction period, according to the multivariate binary regression analysis in our study, were parameters of circumferential strain and area strain. With an increase in circumferential strain by 1%, the chance of hospitalization with HF within 1.5 years after the first AMI decreases by 2.49 times; with an increase in the area strain by 1% – by 1.67 times; in radial strain – by 1.1 times. These factors were included in the prognostic model we developed ($p = 0.004$). According to the results of the univariate Cox regression analysis, with an increase in circumferential strain by 1%, the risks of developing the endpoint are reduced by 1.32 times ($p = 0.026$), in radial strain – by 1.1 times ($p = 0.039$).

A number of studies have also been published describing the use of strain indices measured by 3D Echo in post-AMI patients. The study by L. Xu et al. included 110 STEMI patients who underwent primary PCI. All patients underwent 3D Echo with the determination of longitudinal, radial, and circumferential strain in the three-dimensional mode, as well as longitudinal strain and routine Echo parameters in the two-dimensional mode. Similar to our results, it was found that 3D and 2D longitudinal strain, as well as 3D radial strain, are independent predictors of LV remodeling [11]. In a study by A. Sugano et al., it was confirmed that changes in circumferential strain were a predictor of adverse LV remodeling and showed that its decrease was associated with the presence of microvascular obstruction according to MRI in patients with STEMI who underwent primary PCI. This observation is of great importance, since it is known that the presence of microvascular obstruction is also an independent predictor of adverse LV remodeling [12].

In a study by N. Iwahashi et al. [13], as in our study, the prognosis for the development of cardiac death and hospitalization with HF in patients with STEMI and PCI was studied according to 3D Echo. It was found that 3D examination parameters were stronger predictors of outcomes compared to two-dimensional ones. Specifically, 3D longitudinal strain was the strongest predictor, followed by circumferential strain. 3D-GLS > –11.0% was an independent predictor of the studied outcomes ($\chi2 = 132.2$, $p < 0.001$). When combined with circumferential strain > –18.3%, patients were found to have an extremely high risk of adverse outcomes. Another study by this group of authors [14] examined the clinical and prognostic significance of 3D Echo parameters obtained over time in 272 patients with a first STEMI and PCI. Patients were followed-up for an average of 108 months. The primary endpoint was the occurrence of major cardiovascular events: sudden cardiac death and HF requiring hospitalization. It was shown that deterioration of 2D-GLS and 3D-GLS over 1 year was a significant prognostic factor ($\chi2=36.7$, $p < 0.001$).

CONCLUSION

In patients with a first AMI, regardless of LVEF upon admission in the absence of clinical signs of HF, to calculate the risk of hospitalization with HF within 550 days after MI, it is advisable to take into account the level of radial strain and use the prognostic model (1), including parameters of circumferential and area strain (by data from 3D Echo). *P* (1) values > 26.6% indicate a high risk of hospitalization with HF (sensitivity and specificity of 77.8 and 89.2%, respectively).

REFERENCES

1. Prakopchik I. V., Gurevich O. V. Methods for determining an unfavorable prognosis after myocardial infarction. *Bulletin of Smolensk Medical Academy*. 2008;2:50–52 (in Russ.).

2. Su W., Wang M., Zhu J., Li W., Ding X., Chen H. et al. Underweight predicts greater risk of cardiac mortality post acute myocardial infarction. *Int. Heart J.* 2020;61(4):658–664. DOI: 10.1536/ihj.19-635.
3. Ibanez B., James S., Agewall S., Antunes M.J., Bucciarelli-Ducci C., Bueno H. et al. 2017 ESC Guidelines for the management of acute myocardial infarction in patients presenting with ST-segment elevation: The Task Force for the management of acute myocardial infarction in patients presenting with ST-segment elevation of the European Society of Cardiology (ESC). *Eur. Heart J.* 2018;39(2):119–177. DOI: 10.1093/eurheartj/ehx393.
4. Benameur N., Arous Y., Ben Abdallah N., Kraiem T. Comparison between 3D echocardiography and cardiac magnetic resonance imaging (CMRI) in the measurement of left ventricular volumes and ejection fraction. *Curr. Med. Imaging Rev.* 2019;15(7):654–660. DOI: 10.2174/1573405614666180815115756.
5. Zhao L., Lu A., Tian J., Huang J., Ma X. Effects of different LVEF assessed by echocardiography and CMR on the diagnosis and therapeutic decisions of cardiovascular diseases. *Front. Physiol.* 2020;11:679. DOI: 10.3389/fphys.2020.00679.
6. Mannaerts H.F., van der Heide J.A., Kamp O., Stoel M.G., Twisk J., Visser C.A. Early identification of left ventricular remodelling after myocardial infarction, assessed by transthoracic 3D echocardiography. *Eur. Heart J.* 2004;25(8):680–687. DOI: 10.1016/j.ehj.2004.02.030.
7. Ola R.K., Meena C.B., Ramakrishnan S., Agarwal A., Bhargava S. Detection of left ventricular remodeling in acute ST elevation myocardial infarction after primary percutaneous coronary intervention by two dimensional and three dimensional echocardiography. *J. Cardiovasc. Echogr.* 2018;28(1):39–44. DOI: 10.4103/jcecho.jcecho_32_17.
8. Muraru D., Niero A., Rodriguez-Zanella H., Cherata D., Badano L. Three-dimensional speckle-tracking echocardiography: benefits and limitations of integrating myocardial mechanics with three-dimensional imaging. *Cardiovasc. Diagn. Ther.* 2018;8(1):101–117. DOI: 10.21037/cdt.2017.06.01.
9. Nagueh S.F., Smiseth O.A., Appleton C.P., Byrd B.F. 3rd., Dokainish H., Edvardsen T. et al. Recommendations for the evaluation of left ventricular diastolic function by echocardiography: an update from the American Society of Echocardiography and the European Association of cardiovascular imaging. *J. Am. Soc. Echocardiogr*. 2016;29(4):277–314. DOI: 10.1016/j.echo.2016.01.011.
10. Vieira M.L., Oliveira W.A., Cordovil A., Rodrigues A.C., Mônaco C.G., Afonso T. et al. 3D Echo pilot study of geometric left ventricular changes after acute myocardial infarction. *Arq Bras. Cardiol.* 2013;101(1):43–51. DOI: 10.5935/abc.20130112.
11. Xu L., Huang X., Ma J., Huang J., Fan Y., Li H. et al. Value of three-dimensional strain parameters for predicting left ventricular remodeling after ST-elevation myocardial infarction. *Int. J. Cardiovasc. Imaging.* 2017;33(5):663–673. DOI: 10.1007/s10554-016-1053-3.
12. Sugano A., Seo Y., Ishizu T., Watabe H., Yamamoto M., Machino-Ohtsuka T. et al. Value of 3-dimensional speckle tracking echocardiography in the prediction of microvascular obstruction and left ventricular remodeling in patients with ST-elevation myocardial infarction. *Circ. J.* 2017;81(3):353–360. DOI: 10.1253/circj.CJ-16-0944.
13. Iwahashi N., Kirigaya J., Gohbara M., Abe T., Horii M., Hanajima Y. et al. Global strain measured by three-dimensional speckle tracking echocardiography is a useful predictor for 10-year prognosis after a first ST-elevation acute myocardial infarction. *Circ. J.* 2021;85(10):1735–1743. DOI: 10.1253/circj.CJ-21-0183.
14. Iwahashi N., Horii M., Kirigaya J., Abe T., Gohbara M., Toya N. et al. Clinical usefulness of the serial examination of three-dimensional global longitudinal strain after the onset of ST-elevation acute myocardial infarction. *Circ. J.* 2022;86(4):611–619. DOI: 10.1253/circj.CJ-21-0815.

Authors' information

Timofeeva Tatiana M. – Cand. Sci. (Med.), Teaching Assistant, V.S. Moiseev Department of Internal Diseases with a Course in Cardiology and Functional Diagnostics, RUDN University; Physician, Department of Functional Diagnostics, Vinogradov City Clinical Hospital, Moscow, timtan@bk.ru, https://orcid.org/0000-0001-6586-7404

Efimova Victoria P. – Cand. Sci. (Med.), Head of the Department of Functional Diagnostics, Vinogradov City Clinical Hospital, Moscow, efimovavp@rambler.ru, https://orcid.org/0000-0002-4389-9752

Safarova Ayten F. – Dr. Sci. (Med.), Professor, V.S. Moiseev Department of Internal Diseases with a Course in Cardiology and Functional Diagnostics, RUDN University; Physician, Department of Functional Diagnostics, Vinogradov City Clinical Hospital, Moscow, aytensaf@mail.ru, https://orcid.org/0000-0003-2412-5986

Kobalava Zhanna D. – Dr. Sci. (Med.), Professor, Corresponding Member of RAS, Head of the V.S. Moiseev Department of Internal Diseases with a Course in Cardiology and Functional Diagnostics, RUDN University, Moscow, zkobalava@mail.ru, https://orcid.org/0000-0002-5873-1768

(✉) **Timofeeva Tatiana M.,** timtan@bk.ru

Received 22.08.2023;
approved after peer review 06.09.2023;
accepted 16.11.2023

УДК 616.24-002.592-071:616.15:577.15
https://doi.org/10.20538/1682-0363-2024-1-77-84

Parameters of the MMP / TIMP system in assessing the clinical course of pulmonary tuberculoma

Esmedlyaeva D.S.[1], Alekseeva N.P.[2], Dyakova M.Ye.[1], Karostik D.V.[1], Grigoriev I.V.[2], Sokolovich E.G.[3, 4, 5]

[1] *St. Petersburg Research Institute of Phthisiopulmonology*
2–4, Ligovsky Av., Saint Petersburg, 191036, Russian Federation

[2] *St. Petersburg University*
7/9, Universitetskaya Emb., Saint Petersburg, 199034, Russian Federation

[3] *N.N. Petrov National Medical Research Center of Oncology*
68, Leningradskaya Str., Saint Petersburg, 197758, Russian Federation

[4] *National Medical Research Center for Phthisiopulmonology and Infectious Diseases*
2/4, Dostoevskogo Str., Moscow, 127473, Russian Federation

[5] *Russian Medical Academy for Continuing Professional Education*
2/1 Barrikadnaya Str., Build. 1, Moscow, 125993, Russian Federation

ABSTRACT

Aim. To study the parameters of the matrix metalloproteinase (MMP) / tissue inhibitors of metalloproteinase (TIMP) system in assessing the clinical course of pulmonary tuberculoma.

Materials and methods. We examined 87 patients (55 men and 32 women), average age 33 [28; 43] years, with a morphologically and bacteriologically confirmed diagnosis of tuberculoma, who received treatment at St. Petersburg Research Institute of Phthisiopulmonology. In all patients, computed tomography of the chest, fiberoptic bronchoscopy, and lung function tests were performed. In the blood serum, concentrations of MMP-1, -8, -9, and their tissue inhibitor TIMP-1 were determined using ELISA (R&D Systems, USA), and the activity of α_2-macroglobulin (MG) was determined by the enzyme assays. For statistical data processing, Statistica 10.0 and R were used.

Results. In the study group, single and multiple tuberculomas were revealed in 37 and 63% of cases, respectively, necrotic areas – in 50% of patients, external respiration disorders – in 48% of cases, and catarrhal bronchitis (CB) – in 77% of cases. Tobacco smokers (TS) were identified in 69% of cases. Significant differences between MMP concentrations allowed us to distinguish four patterns from the characteristics adopted for the clinical and radiological assessment of disease intensity. It was shown that an increase in the levels of MMP-1 and MMP-9 can be a predictor of tuberculoma progression caused by a diffuse process with necrotic areas and bronchogenic dissemination (pattern 1, 2). Changes in the levels of MMP-8, TIMP-1 or MG (pattern 3, 4) were associated with permanent exposure to a non-specific component of inflammation (TS or CB).

Conclusion. Changes in the MMP / TIMP system parameters can be used as objective laboratory protein biomarkers to assess the clinical course of pulmonary tuberculoma.

Keywords: extracellular matrix, matrix metalloproteinases, tissue inhibitors of metalloproteinases, pulmonary tuberculoma

Conflict of interest. The authors declare the absence of obvious or potential conflicts of interest related to the publication of this article.

Source of financing. The authors state that hey received no funding for the study.

✉ *Esmedlyaeva Dilyara S.,* diljara-e@yandex.ru

Conformity with the principles of ethics. All individuals signed an informed consent to participate in the study. The study was approved by the Ethics Committee at St. Petersburg Research Institute of Phthisiopulmonology (Protocol No. 9 of 15.09.2016).

For citation: Esmedlyaeva D.S., Alekseeva N.P., Dyakova M.Ye., Karostik D.V., Grigoriev I.V., Sokolovich E.G. Parameters of the MMP / TIMP system in assessing the clinical course of pulmonary tuberculoma. *Bulletin of Siberian Medicine.* 2024;23(1):77–84. https://doi.org/10.20538/1682-0363-2024-1-77-84.

Показатели системы «матриксные металлопротеиназы и ингибиторы периферической крови» в оценке клинического течения туберкулемы легких

Эсмедляева Д.С.[1], Алексеева Н.П.[2], Дьякова М.Е.[1], Каростик Д.В.[1], Григорьев И.В.[2], Соколович Е.Г.[3, 4, 5]

[1] Санкт-Петербургский научно-исследовательский институт фтизиопульмонологии (СПб НИИФ)
Россия, 191036, г. Санкт-Петербург, Лиговский пр., 2-4

[2] Санкт-Петербургский государственный университет (СПбГУ)
Россия, 199034, г. Санкт-Петербург, Университетская наб., 7/9

[3] НМИЦ онкологии им. Н.Н. Петрова
Россия, 197758, г. Санкт-Петербург, ул. Ленинградская, 68

[4] Национальный медицинский исследовательский центр фтизиопульмонологии и инфекционных заболеваний (НМИЦФиИФ)
Россия, 127473, г. Москва, ул. Достоевского, 4/2

[5] Российская медицинская академия непрерывного профессионального образования
125993, г. Москва, ул. Баррикадная, 2/1, стр. 1

РЕЗЮМЕ

Цель. Изучить возможность использования показателей системы «матриксные металлопротеиназы (ММП) / ингибиторы периферической крови» в оценке клинического течения туберкулемы легкого.

Материалы и методы. Обследованы 87 больных (55 мужчин и 32 женщины), средний возраст 33 [28; 43] года, с бактериологически и морфологически верифицированным диагнозом «туберкулема», находившихся на лечении в ФГБУ «СПб НИИФ» Минздрава России. Всем пациентам выполнены компьютерная томография органов грудной клетки, фибробронхоскопия и оценка функции внешнего дыхания (ФВД). В сыворотке крови определяли концентрации ММП-1, -8, -9 и их тканевого ингибитора ТИМП-1 методом ELISA (R&D Systems, США), а также активность α2-макроглобулина (МГ) энзиматическим методом по торможению гидролиза N-бензоил-L-аргининэтилового эфира. Применяли Statistica 10.0 и R.

Результаты. В исследуемой группе единичные и множественные туберкулемы определены в 37 и 63% случаев соответственно, наличие распада – в 50%, нарушения ФВД – в 48% и неспецифические поражения трахеобронхиального дерева в виде катарального эндобронхита (КЭБ) – в 77% случаев. Табакокурильщики (ТК) выявлены в 69% случаев. Выделено четыре комбинации (паттерна) из характеристик, принятых для клинико-рентгенологической оценки активности специфического процесса, соответствующие различной степени повышения концентраций ММП в периферической крови. Показано, что повышение уровня ММП-1 и ММП-9 может являться предиктором прогрессирования туберкулемы, обусловленного распространенным процессом с наличием распада и бронхогенной диссеминации (паттерны № 1, 2). Изменения уровня ММП-8, ТИМП-1 или МГ отражают значимость вклада перманентного воздействия неспецифического компонента воспаления (ТК или КЭБ) в оценку тяжести специфического процесса и не исключают возможности его прогрессирования (паттерны № 3, 4).

Заключение. Изменения показателей системы «ММП / ингибиторы периферической крови» могут быть использованы в качестве объективных лабораторных белковых биомаркеров для оценки клинического течения специфического процесса при туберкулеме легких.

Ключевые слова: внеклеточный матрикс, матриксные металлопротеиназы, ингибиторы протеиназ, туберкулема легких

Конфликт интересов. Авторы декларируют отсутствие явных и потенциальных конфликтов интересов, связанных с публикацией настоящей статьи.

Источник финансирования. Авторы заявляют об отсутствии финансирования при проведении исследования.

Соответствие принципам этики. Все пациенты подписали информированное согласие на участие в исследовании. Исследование одобрено локальным этическим комитетом СПб НИИФ (протокол № 9 от 15.09.2016).

Для цитирования: Эсмедляева Д.С., Алексеева Н.П., Дьякова М.Е., Каростик Д.В., Григорьев И.В., Соколович Е.Г. Показатели системы «матриксные металлопротеиназы и ингибиторы периферической крови» в оценке клинического течения туберкулемы легких. *Бюллетень сибирской медицины.* 2024;23(1):77–84. https://doi.org/10.20538/1682-0363-2024-1-77-84.

INTRODUCTION

Pulmonary tuberculoma is a clinical form of tuberculosis that is presented by encapsulated caseous foci of more than 1.0 cm in diameter. These foci are different in genesis and are radiologically characterized by rounded shadows. Tuberculoma mainly originates from infiltrative and focal pulmonary tuberculosis [1]. In addition, tuberculoma can be imitated by a caseoma in cavernous tuberculosis. The proportion of tuberculoma in the tuberculosis prevalence in the Russian Federation is about 10%.

Clinical variants of the disease course reflect morphological differences in the development of specific inflammation. In case of a remitting course, tuberculoma results from resolution of an extensive pneumonic inflammatory infiltrate during its fading and demarcation. Caseous necrosis in this case has a homogenous nature, sometimes with foci of calcification (homogeneous tuberculomas). In case of a progressive course, on the contrary, tuberculoma is represented by a caseous pneumonic process growing from the center to the periphery, without grossly visible encapsulation and often without pronounced clinical manifestations (lamellar pattern of tuberculoma) [2, 3].

The assessment of the direction of specific inflammation in tuberculoma remains clinically relevant, as limited tuberculosis inflammation typically lacks signs of intoxication and bacterial excretion. The formed fibrous capsule prevents penetration of chemotherapy drugs into the focus of inflammation. Radiological signs of inflammation intensity in the presence of a fibrous capsule are limited and require a dynamic assessment of the size of tuberculoma for 2–3 months [4].

The potential danger of tuberculoma without bacterial excretion is determined by the probability of its progression due to possible drug resistance of the pathogen and the risk of treatment interruption by the patient due to subjective self-assessment of the condition. A morphological examination of the surgical material is the most objective method for predicting the direction of tuberculosis progression. At the same time, invasive methods for obtaining biological material have their limitations and contraindications, therefore, the search for protein biomarkers will contribute to expanding the arsenal of methods for objective assessment of the clinical course of the pathology [5].

Different phases of the clinical course of tuberculoma are based on changes in the lung parenchyma mediated by disturbances in the extracellular matrix (ECM) metabolism, characterized by an increase in the volume of the lesion, necrotic areas, thinning of the tuberculoma capsule, or its fibrotic transformation [5]. Matrix metalloproteinases (MMPs) belong to the family of extracellular zinc-dependent proteolytic enzymes involved in the ECM metabolism. They are end effectors of the innate immune response. The pathophysiological role of MMPs is associated with their involvement in the development and maintenance of inflammation and modeling of the effects of cytokines, growth factors, and hormones. This allows to consider MMPs not only as markers of tissue destruction and remodeling but also, possibly, as contributors to the inflammation intensity. According to the substrate specificity, various families of MMPs are distinguished: collagenases, gelatinases, stromelysins, etc. [6].

Infection of cells with *M. tuberculosis* leads to an increase in the expression of pro-MMPs, causing an imbalance between activated MMPs and their

inhibitors, contributing to the destruction of lung tissue and dissemination [7]. The imbalance in the MMP / tissue inhibitors of metalloproteinase (TIMP) system underlies structural changes in the lung parenchyma, determining external respiration disorders in various lung diseases, including tuberculosis [8, 9].

An important condition for obtaining significant prognostic data is an adequate choice of methods for statistical processing of the material. The use of symptom analysis is effective when it is necessary to evaluate a dataset that is informative only when considered as a whole [10]. An advantage of this method is the ability to form groups that differ in a combination of characteristics that are not revealed when assessed in isolation.

The aim of the study was to investigate the parameters of the MMP / TIMP system in assessing the clinical course of pulmonary tuberculoma.

MATERIALS AND METHODS

We examined 87 patients (55 men and 32 women), average age 33 [28; 43] years, with a morphologically and bacteriologically confirmed diagnosis of tuberculoma, who received treatment at St. Petersburg Research Institute of Phthisiopulmonology from 2017 to 2021. Exclusion criteria were: diabetes, pregnancy, and chronic obstructive pulmonary disease. The control group consisted of 20 apparently healthy age- and sex-matched individuals. In 95% of the cases, tuberculoma formed due to the involution of infiltrative pulmonary tuberculosis against the background of long-term chemotherapy for up to 1 year. In case of bacterial excretion before treatment initiation, in 90% of cases, strains with multi-drug resistance of the pathogen to anti-tuberculosis drugs were detected.

The enzyme-linked immunosorbent assay (ELISA) was used to measure the concentrations of MMPs in the blood serum: collagenases MMP-1 and MMP-8; gelatinase MMP-9; and their tissue inhibitor TIMP-1 using the ELISA reagent kit (R&D Systems, USA) according to the manufacturer's instructions. The activity of α_2-macroglobulin (MG) was assessed by the enzyme assays based on inhibition of alpha-N-benzoyl-L-arginine ethyl ester hydrolysis (ICN, Biomedicals Inc., USA).

In all patients, computed tomography (CT) of the chest was performed on the SOMATOM Sensation 64-slice CT scanner with the assessment of structural changes in the lung parenchyma (Nodule Analysis and Lung Volume Analysis software package (LUNA16) and Lung Volume Analysis (Canon Medical Informatics, Inc., USA)) [11]. Lung function tests (spirometry, body plethysmography) were performed using the MasterScreen PFT diagnostic system (VIASYS Healthcare, Germany) in accordance with the criteria established by the American Thoracic Society and European Respiratory Society (ATS / ERS) [12]. Fiberoptic bronchoscopy was performed using the BF-B2 flexible fiberoptic bronchoscope (Olympus, Japan).

For statistical data analysis, the Statistica 10.0. (StatSoft Inc., USA) and R (free software environment) software packages were used. The logarithmic scale (Log) was used for a number of metric variables (parameters of the MMP / TIMP system) to reduce the asymmetry of distribution. Data were presented as the median (*Me* or *MeLog*) and the interquartile range (Q_1; Q_3). We used the Fisher's exact test, the Mann – Whitney *U*-test, and the Spearman's rank correlation coefficient (r). The symptomatic analysis revealed the most significant patterns for the parameters of the MMP / TIMP system; they were represented as logical functions of categorical variables [10]. In this case, the pattern was considered as a combination of characteristics from radiological, functional, and endoscopic research methods, represented as a certain logical function described by the polynomial over the finite field of characteristic 2. All patients signed an informed consent to participate in the study. The study was approved by the local Ethics Committee at St. Petersburg Research Institute of Phthisiopulmonology (Protocol No. 9 of 15.09.2016).

RESULTS AND DISCUSSION

The study group of patients with tuberculoma was not homogeneous according to their radiological and functional characteristics. In half of the cases, necrotic areas were identified, in 54 (63%) of patients, X-ray revealed multiple necrotic foci. The median of the total volume of the foci was 5,700 mm^3 [2,920; 13,600], and the median of the total volume of necrotic areas was 192 mm^3 [0; 590]. The main parameters characterizing lung capacity were within acceptable ranges, although disturbances in airway patency were detected in every second patient (Table 1).

Among external respiration disorders, obstructive lung disease prevailed (60%). Restrictive lung disease was detected in isolated cases (7.1%), and no mixed patterns were found.

Non-specific changes in the bronchial mucosa with clinical manifestations of diffuse catarrhal bronchitis (CB) and a history of smoking were found in more than half of the patients. The median smoking index was 15 pack years [6.30; 22.50], with a smoking history of over 10 years in 87% of cases.

Table 1

Lung function parameters in patients with tuberculoma

Parameter	*Me* [Q_1; Q_3], *p*	Normal value
FVC, % from the predicted value	108.85 [95.80;121], >0.05	80–120
FEV_1, % from the predicted value	99.75 [93.0;100.2], >0.05	80–120
Gaensler index, %	78.6 [71.4;84], >0.05	>70
MMEF, % from the predicted value	77.0 [56.0;94.0], >0.05	>60

Note. FVC – forced vital capacity; FEV_1 – forced expiratory volume in one second, Gaensler index = FEV_1 / FVC (modified Tiffeneau index), MMEF – mean maximal expiratory flow between 25 and 75% of FVC; *p* – a statistical significance threshold compared to healthy individuals (Mann – Whitney *U*-test).

The intensity of the inflammation was characterised by a moderate increase in the levels of collagenases (MMP-1 and MMP-8) and a significant increase in gelatinase (MMP-9) against the background of decreased MG activity and the absence of significant changes in the TIMP-1 level in the peripheral blood (Table 2).

The binary analysis did not reveal any significant differences in metric variables (parameters of the MMP / TIMP system) for any of the selected categorical variables (Table 3).

The symptomatic analysis revealed that each of the biomarkers corresponded to certain combinations of the results (patterns). The formation of patterns is possible for any number of characteristics, but in this case, a combination of three of them was sufficient to obtain significant differences.

Table 2

Concentrations of the MMP / TIMP system parameters in patients with tuberculoma, *Me* [Q_1; Q_3]

Analytes	Patients with tuberculoma	Healthy controls	*p*
MMP-1Log, ng / ml	1.74 [1.31;2.30]	1.17 [0.89;1.72]	0.002
MMP-8Log, ng / ml	3.27 [2.64;3.94]	2.58 [2.22;2.70]	0.003
MMP-9, ng / ml	1,638.00 [50.80;2,557.69]	71.99 [51.33;73.94]	0.00004
TIMP-1Log, ng / ml	6.72 [6.58;6.89]	6.66 [6.55;6.80]	0.05
MG, nmol / min	1.70 [1.40;2.16]	3.00 [2.46;3.28]	0.00003

Note. The level of statistical significance compared to healthy controls – *p* (Mann–Whitney *U*-test).

Table 3

Concentration of the MMP / TIMP system parameters depending on the clinical and radiological characteristics of inflammation in patients with tuberculoma, *Me* and *MeLog* [Q_1; Q_3]

Pathological changes		Аналиты				
		MMP-1Log, ng / ml	MMP-8Log, ng / ml	MMP-9, ng / ml	TIMP-1Log, ng / ml	MG, nmol / min
Signs of necrosis	1	1.57 [1.02; 2.09]	3.15 [2.59; 3.83]	1721.00 [950.00; 2665.00]	6.68 [6.57; 6.84]	1.94 [1.35; 2.25]
	2	1.85 [1.46; 2.37]	3.50 [3.21; 3.93]	1771.00 [950.00; 2665.00]	6.77 [6.60; 6.93]	1.90 [1.57; 2.10]
Number of tuberculomas	1	1.84 [1.41; 2.23]	3.12 [2.73; 3.50]	1544.00 [924.00; 2343.00]	6.74 [6.61; 6.92]	1.84 [1.38; 2.10]
	2	1.96 [1.48; 2.46]	3.39 [3.07; 3.98]	1905.00 [1140.00; 2643.00]	6.71 [6.59; 6.89]	2.04 [1.43; 2.25]
External respiration disorders	1	1.54 [1.02; 1.96]	3.51 [3.36; 3.64]	1823.00 [1079.00; 2638.00]	6.74 [6.57; 6.98]	2.09 [1.35; 2.78]
	2	1.89 [1.38; 2.74]	3.49 [3.07; 3.89]	1769.00 [1100.00; 2185.00]	6.68 [6.59; 6.83]	1.96 [1.43; 2.16]
Catarrhal bronchitis	1	1.84 [1.41; 2.24]	3.60 [2.77; 4.44]	1355.00 [761.00; 2036.00]	6.58 [6.52; 6.82]	2.09 [1.35; 2.78]
	2	1.80 [1.36; 2.27]	3.21 [2.68; 3.76]	1778.00 [1058.00; 1778.00]	6.75 [6.65; 6.93]	1.96 [1.43; 2.16]
Tobacco smoking	1	1.74 [1.01; 2.46]	3.03 [2.72; 3.42]	1574.00 [651.00; 2447.00]	6.59 [6.54; 6.78]	2.30 [1.59; 2.99]
	2	1.85 [1.56; 2.26]	3.53 [3.05; 3.98]	1863.00 [1186.00; 2376.00]	6.73 [6.59; 6.93]	1.98 [1.50; 2.20]

Note. 1 – no signs of necrosis, single tuberculomas, no external respiration disorders, no catarrhal bronchitis, non-smoking patients; 2 – signs of necrosis, multiple tuberculomas, external respiration disorders, catarrhal bronchitis, smoking patients.

Stratified sampling based on the levels of collagenase MMP-1 and gelatinase MMP-9 allowed to identify pattern 1 – a combination of the number of tuberculomas, external respiration disorders, and CB ($p = 0.01$). Two-fold differences in MMP-1Log made it possible to differentiate a more severe subgroup of patients with multiple tuberculomas in combination with either external respiration disorders or CB. The median MMP-1 ($n = 37$) in the group of patients with severe disease reached 1.96 ng / ml (1.66; 1.9), while in the group with moderate disease ($n = 35$), it was 1.23 ng / ml (0.86; 1.56).

Similarly, in the group with severe disease, *Me* MMP-9 was 2,008 ng / ml (1,148; 2,648), while in the group with moderate disease, it was 1,351 ng / ml (874; 1,971).

It is assumed that the progression of tuberculoma increases as the volume of affected lung tissue enlarges. The formed pattern suggests that a conclusion about the progression of inflammation based solely on differences in its prevalence is not always correct According to pattern 1, an increase in the volume of morphological changes in the lung parenchyma becomes clinically significant when accompanied by external respiration disorders. The present study established a direct correlation between external respiration disorders and the volume of lung lesions (r = 0.27; p = 0.03, Spearman's rank correlation coefficient), which is consistent with literature data indicating a significant relationship between changes in ventilation and gas exchange parameters of the lungs in tuberculoma and the severity of such changes as the volume of the largest cavity, total volume of necrotic areas, presence of pleural involvement, and the prevalence of seeding foci [13].

The composition of pattern 1 also indicates a significant negative impact on the course of the primary infection in the lungs of non-specific inflammatory responses in the bronchial mucosa. CB, impairing the bronchial drainage function and changing the microcirculation in the affected bronchopulmonary segments, contributes to the aggravation of the process [14]. Differences in the concentration of MMP-1Log allowed to form pattern 2, which combined the characteristics of the total lesion volume, the total area of necrosis, and the presence of CB (p = 0.0017).

The group with a higher concentration of proteinase included patients (n = 42) who had multiple tuberculomas with the presence of CB or areas of necrosis. In this group, the median MMP-1Log was 6.63 ng / ml (3.62; 9.83). In the group of patients who had no areas of necrosis or no combination of multiple tuberculomas with CB (n = 19), the median MMP-1Log was 2.5 times lower, amounting to 2.56 ng / ml (1.56; 4.09). The significance of pattern 2 confirms the relevance of the dynamic assessment of changes in the volume of affected tissue used in clinical practice as one of the criteria for assessing the course of the disease.

It is known that tuberculomas with areas of necrosis progress more frequently than those without them (44.7 vs. 10.5%). Moreover, small foci tend to further decrease in size, while large tuberculomas are primarily characterized by the preservation of necrosis with an increase in its volume. The progression of tuberculomas is caused by lysis of caseous necrosis with subsequent cavernization of tuberculoma and bronchogenic dissemination of its contents [15]. Destruction of tuberculoma occurs as a result of its exposure to proteolytic enzymes, and the leading role in the formation of a caseous focus belongs to MMP-1 [16].

Thus, the composition of patterns formed during the analysis of subgroups associated with statistically significant differences in MMP-1Log and MMP-9 levels represents the most unfavourable combination of clinical and radiological characteristics of tuberculoma in terms of the clinical course of the disease. Such characteristics as the presence of multiple tuberculomas with external respiration disorders and inflammation of the tracheobronchial tree, as a rule, reflect the progression of specific inflammation.

Differences in the concentration of neutrophil collagenase (MMP-8) allowed for the formation of pattern 3, based on a combination of at least two of the characteristics discussed. For example, in the group of smoking patients with multiple foci (n = 39), the concentration of proteinase reached 3.83 ng / ml (3.21; 4.46) in contrast to a more favourable group (n = 9) where such factors were absent. MMP-8Log in this case was 1.2 times lower and amounted to 3.09 ng / ml (2.73;3.50).

Tobacco smoking is a risk factor that aggravates the severity of the disease, contributing to the prolongation of non-specific inflammation, and is one of the causes of irreversible external respiration disorders [17]. It was found that the patients of the subgroup with pattern 3 differed by 1.2 times from the rest of the patients in the Gaensler index (r = 0.27; p = 0.02), the main forced expiratory maneuver parameter, whose decrease is crucial in the diagnosis of lower airway obstruction.

The found relationship between the total volume of foci and the number of segmented neutrophils (r = 0.60; p = 0.04), which are the source of MMP-8, is in agreement with literature data on the increase in the number of peripheral blood neutrophils in patients with a progressive course of the disease as compared to its regressive and stable course [18].

Changes in the level of TIMP-1 and MG allowed for the formation of pattern 4, determined by the influence of a combination of CB and tobacco smoking (p = 0.004). It was found that in the presence of both characteristics, the level of TIMP-1Log was significantly higher (p = 0.004), amounting to 6.77 ng / ml (6.67;6.94), whereas in the absence of these factors, the concentration of TIMP-1Log was 6.52 ng / ml (6.47;6.67). A similar 1.5-fold decrease

was found for MG (p = 0.04). The activity of the inhibitor was reduced to 2.00 nmol / min (1.50; 2.25) in the more severe subgroup according to clinical and radiological characteristics, while in other patients, it remained at the reference level of 2.61 nmol / min (2.10; 3.09).

The validity of the composition of pattern 4 is explained by the literature data on the presence of bronchial pathology of a non-specific genesis in patients with smoking experience of more than 10 years, the so-called smoker's cough [19]. The revealed combination characterizes failure of inhibitory protection and corresponds to endoscopic presentation of non-specific CB of high prevalence.

Analyzing all 4 patterns, it should be noted that their composition characterizes both specific (necrosis, lesion volume) and non-specific (CB and tobacco smoking) components of inflammation, which indicates the nonlinear nature of the relationship between the MMP / TIMP system parameters and manifestations of the process intensity according to clinical and radiological criteria. Thus, changes in the parameters of the MMP / TIMP system can be considered as objective laboratory biomarkers for assessing the clinical course of specific inflammation in pulmonary tuberculoma.

CONCLUSION

The use of the symptomatic analysis made it possible to form four patterns, corresponding to different levels of MMPs in the blood, from the characteristics used to assess the clinical course of the disease. An increase in the concentration of MMP-1Log and MMP-9 in peripheral blood may be a predictor of the progression of multiple tuberculomas in the presence of necrosis and bronchogenic dissemination (patterns 1, 2). Changes in the levels of MMP-8, TIMP-1 or MG emphasize the significance of the permanent effect of non-specific inflammation components on the assessment of the process severity and do not exclude the possibility of its progression (patterns 3 and 4). The integrative approach combining the evaluation of serum protein biomarkers with the results of clinical and radiological studies is a highly promising non-invasive tool for predicting the direction of development of pulmonary tuberculoma without bacterial excretion.

REFERENCES

1. On improving anti-tuberculosis activities in the Russian Federation. Order of the Ministry of Healthcare of Russia No. 109 of 21.03.2003 (ed. 05.06.2017) (in Russ.). URL: http://www.pravo.gov.ru (access date: 27.02.2022).
2. Ariel B.M., Elkin A.V., Basek T.S., Ostashko O.M., Katser L.I. Morphological features of fibrous cavernous pulmonary tuberculosis through the example of biopsy material. *Archives of Pathology*. 2004;66(1):14–18 (in Russ.).
3. Kholodok O.A., Grigorenko A.A., Cheremkin M.I. Pulmonary tuberculoma as a form of tuberculosis. *Bulletin of Physiology and Pathology of Respiration.* 2014;(53):126–131 (in Russ.).
4. National Clinical Guidelines on the use of surgical methods for treating pulmonary tuberculosis. Thoracic surgery; ed. by P.K.Yablonskiy. M.: GEOTAR-Media, 2014:160 (in Russ.).
5. Valiev R.Sh., Valiev N.R., Iksanov I.Ya., Filatova M.S. Epidemiological significance of pulmonary tuberculosis, the results of surgical and non-surgical treatment in the Republic of Tatarstan. *Tuberculosis and Lung Diseases*. 2014;4:18–21 (in Russ.).
6. Lee H.S., Kim W.J. The role of matrix metalloproteinase in inflammation with a focus on infectious diseases. *Int. J. Mol. Sci*. 2022;23(18):10546. DOI: 10.3390/ijms231810546.
7. Krug S., Parveen S., Bishai W.R. Host-directed therapies: modulating inflammation to treat tuberculosis. *Front. Immunol*. 2021;12:660916. DOI: 10.3389/fimmu.2021.660916.
8. Uysal P., Uzun H. Relationship between circulating serpina3g, matrix metalloproteinase-9, and tissue inhibitor of metalloproteinase-1 and -2 with chronic obstructive pulmonary disease severity. *Biomolecules.* 2019;9:62–73. DOI: 10.3390/biom9020062.
9. Kumar N.P., Moideen K., Viswanathan V., Shruthi B.S., Sivakumar S., Menon P.A. et al. Elevated levels of matrix metalloproteinases reflect severity and extent of disease in tuberculosis-diabetes co-morbidity and are predominantly reversed following standard anti-tuberculosis or metformin treatment. *BMC Infect. Dis.* 2018;18:1–10. DOI: 10.1186/s12879-018-3246-y.
10. Alexeyeva N. P., Al-Juboori F.S., Skurat E.P. Symptom analysis of multidimensional categorical data with applications. *Periodicals of Engineering and Natural Sciences*. 2020;8(3):1517–1524. DOI: 10.21533/pen.v8i3.1539.
11. Gavrilov P.V., Baulin I.A., Lukina O.V. Standardized interpretation and control of detected isolated formations in the lungs using the lung imaging reporting and data system (Lung-Rads™). *Medical Alliance*. 2017;3:17–27 (in Russ.).
12. Pellegrino R., Viegi G., Brusasco V., Crapo R.O., Burgos F., Casaburi R. et al. Interpretative strategies for lung function tests. *Eur. Respir. J.* 2005;26(5):948–968. DOI: 10.1183/09031936.05.00035205.
13. Kiryukhina L.D., Gavrilov P.V., Savin I.B., Tamm O.A., Volodich O.S., Pavlova M.V., et al. Ventilation and gas exchange function of the lungs in patients with localized pulmonary tuberculosis. *Pulmonology.* 2013;(6):65 (in Russ.). DOI: 10.18093/0869-0189-2013-0-6-807-811.
14. Strelis A.A., Strelis A.K., Nekrasov E.V. Pre-operative treatment of patients with pulmonary tuberculomas and localized catarrhal bronchitis. *Bulletin of Siberian Medicine*. 2005;4(4):117–122 (in Russ.). DOI: 10.20538/1682-0363-2005-4-117-122.

15. Kholodok O.A., Cheremkin M.I. Morphological aspects of intensity of pulmonary tuberculomas. *Bulletin of Physiology and Pathology of Respiration.* 2013;(49):51–54 (in Russ.).
16. Kubler A., Luna B., Larsson C., Ammerman N.C., Andrade B.B., Orandle M. et al. Mycobacterium tuber-culosis dysregulates MMP/TIMP balance to drive rapid cavitation and unrestrained bacterial proliferation. *J. Pathol.* 2015;235(3):431–444. DOI: 10.1002/path.4432.
17. Valdez-Miramontes C.E., Trejo Martínez L.A., Torres-Juárez F., Rodríguez Carlos A., Marin- Luévano S.P., de Haro-Acosta J.P. et al. Nicotine modulates molecules of the innate immune response in epithelial cells and macrophages during infection with M. tuberculosis. *Clin. Exp. Immunol.* 2020;199(2):230–243. DOI: 10.1111/cei.13388.
18. Walker N.F., Karim F., Moosa M.Y.S., Moodley S., Mazibuko M., Khan K. et al. Elevated plasma mtrix metalloproteinase 8 associates with sputum culture positivity in pulmonary tuberculosis. *J. Infect. Dis.* 2022;226(5):928–932. DOI: 10.1093/infdis/jiac160.
19. Pavlova E.V. Morphological features of the bronchopulmonary system in patients with pulmonary tuberculosis. *Creative Surgery and Oncology*. 2012;3:67–70 (in Russ.). DOI: 10.24060/2076-3093-2012-0-3-67-70.

Authors' contribution

Esmedlyaeva D.S. – conception and design, preparation of the samples, collection of the material, carrying out biochemical studies; literature review; analysis and interpretation of the data; drafting of the manuscript. Alekseeva N.P. – statistical processing of the results; drafting of the article. Dyakova M.Ye. – carrying out biochemical studies. Karostik D.V. – carrying out radiological studies. Grigoriev I.V. – translation of the article, conception of the article. Sokolovich E.G. –generation of the idea of the study, conception and design of the study; scientific editing; final approval of the manuscript for publication.

Authors' information

Esmedlyaeva Dilyara S. – Cand. Sci. (Biology), Senior Researcher, St. Petersburg Research Institute of Phthisiopulmonology, Saint Petersburg, diljara-e@yandex.ru, http://orcid.org/0000-0002-9841-0061

Alekseeva Nina P. – Cand. Sci. (Physics and Mathematics). Associate Professor, Department of Statistical Modeling, St. Petersburg University, Saint Petersburg, ninaalexeyeva@mail.ru, http://orcid.org/0000-0001-8837-6739

Dyakova Marina Ye. – Dr. Sci. (Biology), Senior Researcher, St. Petersburg Research Institute of Phthisiopulmonology, Saint Petersburg, marinadyakova@yandex.ru, http://orcid.org/0000-0002-7810-880X

Karostik Denis V. – Post-Graduate Student, St. Petersburg Research Institute of Phthisiopulmonology, Saint Petersburg, d.karostik@mail.ru, http://orcid.org/0000-0003-3284-1421.

Grigoriev Ivan V. – Cand. Sci. (Philology), Associate Professor, Head of the Foreign Language Department in Philology and Arts, St. Petersburg University, Saint Petersburg, ivan_grigoriev@mail.ru, http://orcid.org/0000-0001-9865-0199

Sokolovich Evgeniy G. – Dr. Sci. (Med.), Professor, Deputy Head of the Department for Educational Work, N.N. Petrov National Medical Research Center of Oncology; Leading Researcher, Department of Surgery for Respiratory Tuberculosis, National Medical Research Center for Phthisiopulmonology and Infectious Diseases; Professor, Department of Thoracic Surgery, Russian Medical Academy for Continuing Professional Education, Saint Petersburg, sokole@mail.ru, http://orcid.org/0000-0003-4794-0588

(✉) **Esmedlyaeva Dilyara S.,** diljara-e@yandex.ru

Received 28.06.2023;
approved after peer review 24.07.2023;
accepted 14.09.2023

УДК 616.895.8:57.08
https://doi.org/10.20538/1682-0363-2024-1-85-93

Multifactorial, biomarker-based model for assessing the state of patients with schizophrenia

Cheremnykh E.G., Savushkina O.K., Prokhorova T.A., Zozulya S.A., Otman I.N., Pozdnyakova A.N., Karpova N.S., Shilov Yu.E., Klyushnik T.P.

Mental Health Research Center
34, Kashirskoe Highway, Moscow, 115522, Russian Federation

ABSTRACT

Relevance. Objective comparison of biological markers and real clinical presentation is especially difficult in mental disorders, which are classified according to a large number of diagnostic criteria and a wide variety of symptoms. Therefore, the development of an effective system of biochemical markers and assessment of their relationship to optimize the diagnosis and treatment of schizophrenia are relevant.

The aim of the study was to develop a statistical model that combines known and tested biochemical markers for mental illnesses in patients with schizophrenia.

Materials and methods. The study included 47 women aged 18–50 years (median age – 22 years) with the diagnosis of schizophrenia (ICD-10, F20) and 25 healthy women of the same age. The model was based on the functional activity of complement, thrombodynamics parameters, markers of inflammation, glutamate and energy metabolism, and antioxidant defense, which were shown to be associated with the severity of schizophrenia. The listed markers were evaluated in plasma, platelets, and erythrocytes of sick and healthy individuals.

Results. Statistical software found pair correlations and features of the distribution of all markers as random variables in the examined groups and evaluated correlations between pairs of markers. Ten biomarkers were identified and united into a system that was adequately described by the logistic regression model. The model was evaluated using the Pearson's test ($\chi 2(11) = 57.6$, $p = 0.001$) and calculation of correct predictions (91 and 80%) for samples of patients and healthy people, respectively.

Conclusion. Calculating the logistic equation resulted in the probability that the patient has schizophrenia involving the immune system, hemostasis, and oxidative stress. This model can be considered as a new formalized approach to the preclinical diagnosis of mental illnesses.

Keywords: schizophrenia, biomarker system, pair correlations, logistic regression model

Conflict of interest. The authors declare the absence of obvious or potential conflicts of interest related to the publication of this article.

Source of financing. The authors state that hey received no funding for the study.

Conformity with the principles of ethics. All individuals signed an informed consent to participate in the study. The study was approved by the Ethics Committee at Mental Health Research Center (Protocol No. 301 of 05.09.2016).

For citation: Cheremnykh E.G., Savushkina O.K., Prokhorova T.A., Zozulya S.A., Otman I.N., Pozdnyakova A.N., Karpova N.S., Shilov Yu.E., Klyushnik T.P. Multifactorial, biomarker-based model for assessing the state of patients with schizophrenia. *Bulletin of Siberian Medicine.* 2024;23(1):85–93. https://doi.org/10.20538/1682-0363-2024-1-85-93.

✉ *Cheremnykh Elena G.,* elcher10@yandex.ru

Многофакторная модель оценки состояния больных шизофренией на основе системы биомаркеров

Черемных Е.Г., Савушкина О.К., Прохорова Т.А., Зозуля С.А., Отман И.Н., Позднякова А.Н., Карпова Н.С., Шилов Ю.Е., Клюшник Т.П.

Научный центр психического здоровья (НЦПЗ)
Россия, 115522, г. Москва, Каширское шоссе, 34

РЕЗЮМЕ

Актуальность. Проблема объективного сопоставления биологических маркеров и реальной клинической картины особенно сложна при психических расстройствах, которые классифицируются по большому количеству диагностических критериев и большому разнообразию симптомов. Поэтому разработка эффективной системы биохимических маркеров и оценка их взаимосвязи для оптимизации диагностики и лечения шизофрении являются актуальной.

Цель исследования – разработать статистическую модель, объединяющую известные и проверенные для психических заболеваний биохимические маркеры для пациентов с шизофренией.

Материалы и методы. Обследовано 47 больных женщин в возрасте 18–50 лет (медианное значение – 22 года) с диагнозом «шизофрения» (МКБ-10, F20) и 25 здоровых женщин такого же возраста. В качестве основы модели были использованы функциональная активность комплемента, показатели тромбодинамики, маркеры воспаления, маркеры глутаматного и энергетического метаболизма и антиоксидантной защиты, связанные, как было показано ранее, с тяжестью течения шизофрении. Перечисленные маркеры оценивали в плазме, тромбоцитах и эритроцитах крови больных и здоровых.

Результаты. С помощью статистической программы выявлены парные корреляции и особенности распределения всех маркеров как случайных величин в обследованных группах, а также оценены зависимости между парами маркеров. Выявлены десять биомаркеров, объединенных в систему, которая адекватно описывается логистической моделью. Модель оценена с помощью критерия Пирсона ($\chi^2(11) = 57{,}6$; $p = 0{,}001$) и вычисления правильных предсказаний (91 и 80%) по выборкам больных и здоровых соответственно.

Заключение. Результатом вычисления логистического уравнения является вероятность наличия у пациента шизофренического процесса, в который вовлечены иммунная система, гемостаз и окислительный стресс. Эта модель может рассматриваться как новый формализованный подход к диагностике психических заболеваний на доклиническом этапе.

Ключевые слова: шизофрения, система биомаркеров, парные корреляции, логистическая регрессионная модель

Конфликт интересов. Авторы декларируют отсутствие явных и потенциальных конфликтов интересов, связанных с публикацией настоящей статьи.

Источник финансирования. Авторы заявляют об отсутствии финансирования при проведении исследования.

Соответствие принципам этики. Все пациенты подписали информированное согласие на участие в исследовании. Исследование одобрено этическим комитетом ФГБНУ НЦПЗ (протокол № 301 от 05.09.2016).

Для цитирования: Черемных Е.Г., Савушкина О.К., Прохорова Т.А., Зозуля С.А., Отман И.Н., Позднякова А.Н., Карпова Н.С., Шилов Ю.Е., Клюшник Т.П. Многофакторная модель оценки состояния больных шизофренией на основе системы биомаркеров. *Бюллетень сибирской медицины.* 2024;23(1):85–93. https://doi.org/10.20538/1682-0363-2024-1-85-93.

INTRODUCTION

Objective comparison of biological markers and real clinical presentation is especially difficult in mental disorders, which are classified according to a large number of diagnostic criteria and a wide variety of symptoms. The clinical status of patients with the same diagnosis may differ.

Schizophrenia is a heterogeneous mental illness with a wide variety of clinical manifestations caused by

different etiological factors and biological background. Therefore, the development of an effective system of biochemical markers and the assessment of their relationship to optimize the diagnosis and treatment of schizophrenia are relevant.

We suggest several groups of markers as a basis for such system.

1. Complement and hemostasis.

These two evolutionarily allied systems, complement system (CS) and hemostasis, have numerous connections that allow to consider them as a single system that regulates the entire set of immune interactions.

In recent years, special attention of researchers has been focused on the two processes – CS and coagulation in the fluid phase as tools for an instant response to external and internal threats and, at the same time, as sources of adverse pathological processes.

Coagulation may increase uncontrollably, and simultaneous amplification of the two systems contributes to critical complications of various pathologies. It is known that disseminated intravascular coagulation and multiple organ failure result from dysregulation of CS and increased positive feedbacks between CS and coagulation [1]. However, the interaction of these cascades contributes to the intensification of pathological processes not only in critical situations. A significant role of the CS – coagulation interaction in increasing resistance to therapy for atherosclerosis, cancer [2], mental illness [3], and diabetes was revealed [4]. The direction and overall level of interaction between CS and coagulation are determined by genetic conditions and the condition of the body at each time point.

2. Inflammatory markers

Among numerous pathogenetic hypotheses of schizophrenia, an important place is attributed to the study of the role of inflammation in the development of the disease. Due to the existence of neuroimmune relationships, activation of neuroinflammation in the brain [5] is associated with the development of systemic inflammatory responses, accompanied by an increase in the level of various inflammatory mediators in the patients' blood [6]. It was previously indicated that biomarkers which reflect the intensity of the ongoing pathological process in the brain in schizophrenia and interrelate with the severity of the disease and the clinical state of patients are: [7, 8]:

– activity of leukocyte elastase (LE), a serine protease released by activated neutrophils during degranulation at the site of inflammation;

– functional activity of the main endogenous inhibitor of LE – acute phase protein, **α**1-proteinase inhibitor (**α**1-**π**), synthesized in the liver;

– level of antibodies to protein S-100b (abS100-b) – a marker of astroglial activation, which also acts as a neurotrophic factor for serotonergic neurons.

3. Glutamate metabolism and antioxidant defense enzymes.

An important aspect of endogenous psychoses (schizophrenia) is the involvement of the glutamate system in the development of the pathological process [9]. The reduction of NMDA receptor (NMDAR) activity on inhibitory GABA interneurons leads to an increase in glutamatergic neurotransmission and various symptoms that occur in acute psychosis. Evidence has been obtained that NMDAR hypofunction is associated with oxidative stress which also contributes to the development of mental pathology associated with schizophrenia [10].

Pathophysiological processes associated with disorders in the glutamatergic system, glutamate metabolism, and oxidative stress, caused in particular by disturbances in the glutathione system, are involved in the formation of the acute phase response with the manifestation of positive symptoms, as well as in the emergence of negative symptoms and cognitive deficits.

Abnormalities of the glutamatergic system and glutamate metabolism have been detected in the studies on the brain [11] and blood of patients with psychosis [12].

Changes in the activity of the glutamate metabolic enzyme glutamate dehydrogenase (GDG), glutathione-dependent enzymes glutathione-S-transferase (GST) and glutathione reductase (GR), as well as mitochondrial complex IV – cytochrome c oxidase (COX) in platelets were detected for mental illnesses [13].

It is not possible to assess biochemical connections in the entire set of interactions between the markers due to the complexity of the overall system, which also has positive and negative feedbacks, thus complicating the decision-making process based on analytical data. So, as a model that combines all of the listed markers, we decided to consider a logistic regression model, whose synthesis is aimed at providing objective grounds for the psychiatric diagnosis of patients.

The aim of the study was to develop a statistical model that combines known and tested biochemical markers of mental illnesses in patients with schizophrenia.

MATERIALS AND METHODS

Clinical and biological research was carried out at Mental Health Research Center. The study was approved by the Ethics Committee at Mental Health Research Center (Protocol No. 301 of 05.09.2016) and was carried out in compliance with the current ethical standards and rules of biomedical research approved by the WMA Declaration of Helsinki (1975/2000 edition).

The study included 47 women aged 18–50 years (median age – 22 years) with the diagnosis of schizophrenia (ICD-10, F20) admitted to the hospital at the acute stage of the disease and 25 healthy women of the same age.

The listed markers were evaluated in plasma, platelets, and erythrocytes of patients and healthy people.

Inclusion criteria: verified diagnosis of schizophrenia (F20) according to the ICD-10 classification, acute psychotic state. Exclusion criteria: age under 18 and over 50 years, organic damage to the central nervous system, brain injury, severe somatic symptom disorders at the stage of decompensation, exacerbation of inflammatory or infectious diseases, use of psychoactive substances.

CS was assessed by the tailor-made method for assessing the functional activity of CS in test organisms – ciliates *Tetrahymena pyriformis,* the death of which when exposed to blood plasma is associated with activation of CS. The method described in [14] consists in cyclic counting of living protozoan cells in a blood plasma solution. The calculation is carried out on the BioLat device [15] using the AutoCiliata software developed by us.

The functional activity of the complement in the blood plasma was assessed using the calculated parameter: $faCS = 100 \times 1 / T_{50}$, where T_{50} is the time of death of half of the cells.

Coagulation markers – clot density (*D*) and initial speed of clot formation (*Vi*) were assessed by the thrombodynamics method [16]. Inflammation markers (*LE* activity and functional activity of *α1-π*, as well as the level of antibodies to the S-100b protein) were assessed in accordance with the methods presented in the work [7].

A marker of glutamate metabolism and a parameter of energy metabolism (the activity of GDH and COX, respectively) were assessed in platelets. Markers of antioxidant defense (the activity of glutathione-dependent enzymes) were assessed in platelets (*GST, GR*) and erythrocytes (*GSTer*, *GRer*) in accordance with the methods presented in the works [12, 13, 17].

The results of marker measurements in the examined groups were assessed using the Statistica.10 program tools, such as descriptive statistics, the Shapiro – Wilk test, the Spearman's rank correlation coefficients, the quantile regression model, and logistic equations.

RESULTS

In accordance with the Shapiro – Wilk test ($W \geq 0.946$; $p \leq 0.05$), only two predictors in the group of 47 patients (*COX* and *GDH*) and only one predictor in the group of 25 healthy people (*GDH*) ($W \geq 0.918$; $p \leq 0.05$) followed a normal distribution. Therefore, to analyze the statistical parameters in these groups, medians, coefficients of variation, and interquartile ranges were used (Table 1). To assess the relationship between the predictors, the nonparametric Spearman's rank correlation coefficient was used (Table 2, 3).

Table 1

Descriptive statistics of predictors in the group of patients and healthy controls

Parameter	Group of patients, *n* = 47		Group of healthy controls, *n* = 25	
	Me (Q_{25}; Q_{75})	Coefficient of variation	*Me* (Q_{25}; Q_{75})	Coefficient of variation
faCS	4.61 (3.12; 6.76)	50.9	6.75 (6; 7.5)	15.32
Vi	54.5 (51; 57)	8.92	52.6 (47; 55)	11.78
D	22,480 (20,743; 24,671)	14.04	22,029 (20,623; 23,627)	11.23
LE	234.4 (210.5; 265.7)	16.69	197 (187; 200)	5.91
α1-π	40.70 (33.7; 47.4)	20.31	33.7 (32; 35)	9.31
abS-100b	0.78 (0.69; 0.89)	17.86	0.77 (0.68; 0.79)	9.28
COX	5.10 (4.2; 5.71)	22.34	5.47 (5.05; 6.27)	18.85
GDH	5.93 (5.11; 6.86)	22.97	6.87 (5.77; 8.28)	19.04
GR	9.12 (7.54; 10.32)	30.85	10.50 (8.86; 11.78)	27.24
GST	14.73 (11.54; 17)	24.27	17.25 (13.96; 19.22)	18.68
GRer	2.10 (1.66; 2.37)	19.74	1.65 (1.41; 2)	27.71
GSTer	2.61 (2.23; 3.43)	35.69	2.09 (1.57; 2.74)	41.2

Table 2

Spearman's rank correlations (SRC) of 12 markers for the group of patients

Parameter	faCS	Vi	D	LE	α1- π	abS-100b	COX	GDG	GR	GST	GRer	GSTer
faCS	1	–0.41	–0.23	–0.04	0.08	–0.12	0.01	0.06	0.04	0.09	–0.05	0.01
Vi	–0.41	1	0.26	0.1	–0.06	0.05	–0.15	–0.23	0.03	–0.17	–0.17	–0.17
D	–0.23	0.26	1	0.05	0.23	–0.23	–0.01	–0.15	0.17	0.15	–0.01	0.08
LE	–0.04	0.1	0.05	1	–0.14	–0.08	–0.15	0.1	0.2	0.01	–0.07	–0.04
α1- π	0.08	–0.06	0.23	–0.14	1	–0.07	0.17	0.26	–0.01	0.12	0.12	0.21
abS-100b	–0.12	0.05	–0.23	–0.08	–0.07	1	0.15	0.04	0.01	–0.22	0.1	0.03
COX	0.01	–0.15	–0.01	–0.15	0.17	0.15	1	–0.13	–0.34	–0.13	0.13	0.01
GDG	0.06	–0.23	–0.15	0.1	0.26	0.04	–0.13	1	0.19	0.21	0.17	–0.12
GR	0.04	0.03	0.17	0.2	–0.01	0.01	–0.34	0.19	1	0.49	0.17	0.13
GST	0.09	–0.17	0.15	0.01	0.12	–0.22	–0.13	0.21	0.49	1	0.15	0.37
GRer	–0.05	–0.17	–0.01	–0.07	0.12	0.10	0.13	0.17	0.17	0.15	1	0.35
GSTer	0.01	–0.17	0.08	–0.04	0.21	0.04	0.01	–0.12	0.13	0.37	0.35	1

Note. Correlations in bold are significant at $p \leq 0.05$.

Table 3

Spearman's rank correlations (SRC) of 12 markers for the group of healthy controls

Parameter	faCS	Vi	D	LE	α1- π	abS-100b	COX	GDG	GR	GST	GRer	GSTer
faCS	1	0.25	–0.07	0.11	–0.35	0.19	–0.17	0.07	0.09	–0.04	0.15	0.13
Vi	0.25	1	0.15	0.04	–0.3	0.31	–0.32	–0.29	–0.26	–0.18	–0.04	0.11
D	–0.07	0.15	1	–0.1	–0.02	–0.16	0.14	–0.08	0.15	–0.22	–0.08	–0.28
LE	0.11	0.04	–0.1	1	0.07	–0.05	0.36	0.54	–0.43	0.14	0.09	0.05
α1- π	–0.35	–0.3	–0.02	0.07	1	–0.45	0.07	0.1	–0.28	–0.09	–0.1	0.01
abS-100b	0.19	0.31	–0.16	–0.05	–0.45	1	–0.15	–0.26	0.11	0.02	0.28	–0.05
COX	–0.17	–0.32	0.14	0.36	0.07	–0.15	1	0.47	0.13	0.68	–0.11	0.07
GDG	0.07	–0.29	–0.08	0.54	0.1	–0.26	0.47	1	0.18	0.55	–0.27	–0.3
GR	0.09	–0.26	0.15	–0.43	–0.28	0.11	0.13	0.18	1	0.25	–0.03	–0.36
GST	–0.04	–0.18	–0.22	0.14	–0.09	0.02	0.68	0.55	0.25	1	–0.19	0.08
GRer	0.15	–0.04	–0.08	0.09	–0.1	0.28	–0.11	–0.27	–0.03	–0.19	1	0.26
GSTer	0.15	0.11	–0.28	0.05	0.01	–0.05	0.07	–0.3	–0.36	0.08	0.26	1

Note. Correlations in bold are significant at $p \leq 0.05$.

Correlation modifications in the groups of patients and controls presumably reflect changes in the studied system, which can be assessed by the analysis of paired correlations due to numerous direct and indirect relationships between the markers.

To identify the fact of similar distribution of the predictor pairs for which at least a weak correlation (SRC ≥ 0.3) even in one group was detected, quantile regression plots were constructed (*Q–Q*). Figure shows *Q–Q* plots for pairs of predictors in the patient group with a detected correlation compared to *Q–Q* plots in the healthy controls. Each plot is accompanied by two equations – for a polynomial regression model and for a linear equation model using the least squares method.

All biochemical markers are in complex relationships, the strength of which can vary randomly. Quantile regression shows how strong /weak the correlation between pairs of markers is, and this correlation is usually nonlinear. Therefore, quadratic quantile regression plots make it possible to assess the strength of the relationship. When accumulated, this information can be the basis for constructing network models of biochemical interactions. Such models for each specific pathology will help identify critical points of therapeutic intervention, which optimization will reduce the number and side effects from medications.

After assessing the statistical characteristics of the two samples under study, an analytical equation (model) was obtained that will contribute to evaluation and classification of a set of markers characterizing whether an individual belongs to the group of patients or healthy controls.

For this purpose, we used the logistic regression model with the following features: the regression result was calculated as a probability of event occurrence. The dependent variable must be categorical, independent variables may not be normally distributed, or linearly related, or equally dispersed, which is typical of our measurement results (Table 1–3). The result of the logistic regression equation (1) is the probability of a person's attribution to the group of patients or healthy controls in accordance with the results of the study of predictor markers. The variable *P* was added as a binary variable, which is equal to "0" for the group of patients and "1" for the healthy group.

Group of patients (47)		Group of healthy controls (25)	
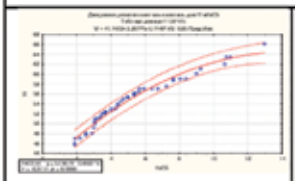	Vi = 41.15+3.27*(faCS) – 0.115*(faCS)^2 Vi = 57.96–0.68*(faCS); r = –0.3771; p = 0.0090 SRC = **–0.41**	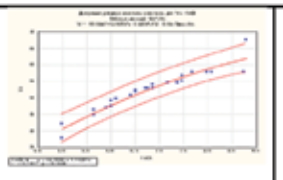	Vi = –10.86+12.94*(faCS) – 0.53*(faCS)^2 Vi = 44.1+1.14*(faCS); r = –0.1937; p = 0.3536 SRC = **0.25**
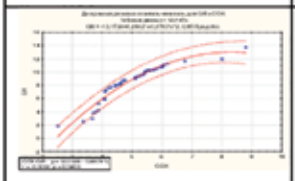	GR = –13.17+6.29*(COX) – –0.35*(COX)^2 GR = 12.033–0.7*(COX); r = –0.3002; p = 0.0403 SRC = **–0.34**	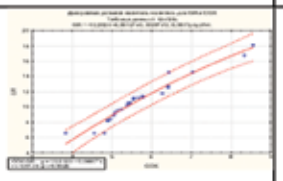	GR = –10.2+4.58*(COX) – 0.15*(COX)^2 GR = 10.51+0.05*(COX); r = 0.0178; p = 0.9326 SRC = **0.13**
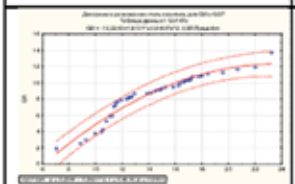	GR = –10.22+1.91*(GST) – 0.04*(GST)^2 GR = 3.23+0.36*(GST); r = 0.4876; p = 0.0005 SRC = **0.49**	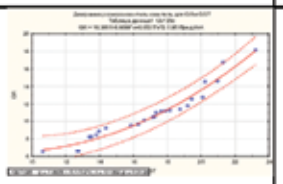	GR = 10.37– 0.91*(GST) + 0.05*(GST)^2 GR = 7.86 + 0.17*(GST); r = 0.1862; p = 0.3728 SRC = **0.25**
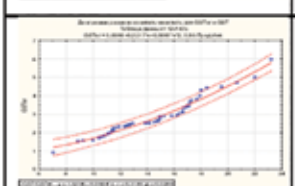	GSTer = 0.61+0.02*(GST) + 0.01*(GST)^2 GSTer = 1.52+0.09*(GST); r = 0.3189; p = 0.0289 SRC = **0.37**	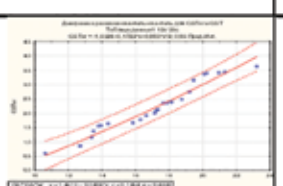	GSTer = –1.65+0.17*(GST) + 0.003*(GST)^2 GSTer = 1.46+0.04*(GST); r = 0.1415; p = 0.4880 SRC = **0.08**
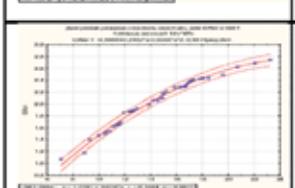	GRer = –0.6+0.26*(GST) – 0.004*(GST)^2 GRer = 1.77+0.02*(GST); r = 0.1584; p = 0.2877 SRC = **0.35**	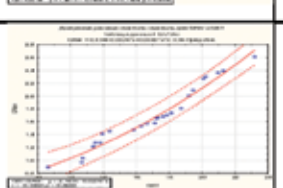	GRer = 0.44–0.003*(GST) + 0.004*(GST)^2 GRer = 2.14–0.03*(GST); r = –0.1880; p = 0.3680 SRC = **–0.19**
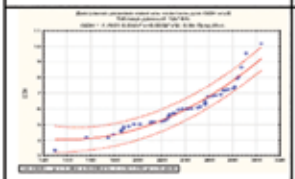	GDH = 7.79–0.05*(LE) + 0.0002*(GST)^2 GDH = 4.56+0.006*(LE); r = 0.1770; p = 0.2340 SRC = **0.1**	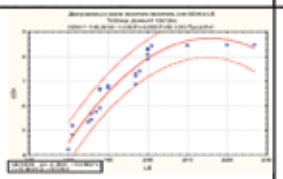	GDH = –146.06+1.44*(LE) – 0.003*(LE)^2 GDH = –2.49+0.05*(LE); r = 0.4226; p = 0.0353 SRC = **0.54**
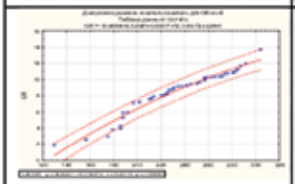	GR = –13.49+0.13*(LE) – 0.0001*(LE)^2 GR = 4.5527+0.02*(LE); r = 0.2513; p = 0.0883 SRC = **0.2**	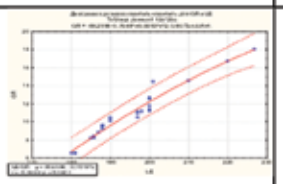	GR = –89.3+0.76*(LE) – 0.001*(LE)^2 GR = 30.66–0.1*(LE); r = –0.3999; p = 0.0477 SRC = **–0.43**
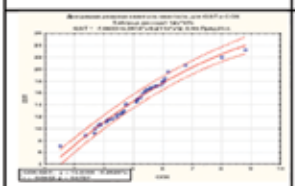	GST = –7.1+5.4*(COX) – 0.21*(COX)^2 GST = 15.85–0.26*(COX); r = –0.0842; p = 0.5737 SRC = **–0.13**	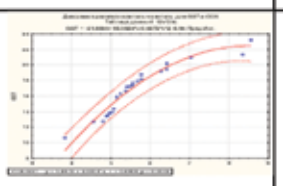	GST = –21.89+10.38*(COX) – 0.61*(COX)^2 GST = 5.5+2.0*(COX); r = 0.6808; p = 0.0002 SRC = **0.68**
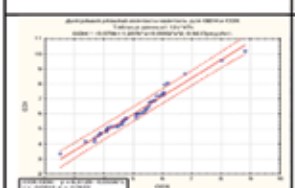	GDH = –0.08+1.21*(COX) + 0.0002*(COX)^2 GDH = 6.31–0.06*(COX); r = –0.0453; p = 0.7622 SRC = **–0.13**	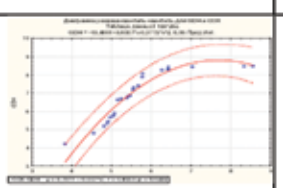	GDH = –13.49+5.8*(COX) – 0.378*(COX)^2 GDH = 3.73+0.56*(COX); r = 0.4553; p = 0.0222 SRC = **0.47**

Figure. Dependencies of pairs of predictors in two groups

$$P = 1 / (1 + e^{-Z}), \quad (1)$$

where $Z = a_0 + a_1 \times x_1 + a_n * x_n$

The coefficients a_0-a_1-..a_n were calculated using the Logit Regression procedure in the Statistica 10 software. The general logistic equation for all twelve markers is implausible:

$$x^2(13) = ---, p = 1.0 \text{ [18]}.$$

By removing one predictor at a time, a logistic model was built to find predictors that lead to an implausible result. Two parameters turned out to be such predictors: clot density (*D*), reflecting the state of the coagulation system, and leukocyte elastase (*LE*) activity which is a marker of neutrophil degranulation.

The resulting equation included 10 independent variables (*faCS, Vi, α1- π, abS-100b, COX, GDG,GR, GST, GRer , GSTer*) and the dependent binary variable *P* (2).

$$P = 1 / (1 + e^{-Z}), \quad (2)$$

where Z = 5.78 + 0.399 × (*faCS*) – 0.014 × *Vi* – 0.4 × (α1-π) – 8.24 × (*abS*-100b) + 1.9 × (*COX*) + 0.58 × (*GDG*) + 0.33 × (*GR*) – 0.17 × (*GST*) – 2.02 × (*GRer*) + 0.27 × (*GSTer*)

The value of the loss function was 17.7; it was the minimum value among all other variants of the equations. Pearson's criterion $\chi^2(11) = 57.6$, $p = 0.001$. The significance of regression coefficients was assessed using the Wald test (Table 4).

Table 4

Significance of regression coefficients

Parameter	Wald test	*p*
Intercept	1.84	0.175
faCS	5.49	0.019
Vi	3.95	0.046
α1-π	13.4	<0.001
abS-100b	0.54	0.462
COX	10.5	0.001
GDH	4.80	0.029
GR	6.01	0.014
GST	3.56	0.059
GRer	2.32	0.127
GSTer	0.87	0.350

Note. Correlations in bold are significant at $p \leq 0.05$.

Estimating the likelihood of a logistic equation gives a general idea of its coefficients. In accordance with this criterion, predictors with their own coefficients were identified, the equation for which had the smallest loss function value.

Correctly predicted value "0" (attribution to the group of patients) – 91,5%.

Correctly predicted value "1" (attribution to the group of healthy controls) – 80%.

DISCUSSION

Based on the coefficient of variation, it was revealed that the markers in the group of patients have greater variability than the markers in the healthy group (Table 1). There are 8 highly variable markers in the group of patients (*faCS, α1- π, GR, GST, COX, GDH, GSTer, GRer*), 3 moderately variable markers (*D, LE, abS-100b*), and only one weakly variable marker (*Vi*). In the healthy group, the variability of markers was as follows – only 3 markers (*GR, GRer, GSTer*) were highly variable, 6 markers (*faCS, Vi, D, COX, GDH, GST*) were moderately variable, and 3 markers (*α1- π, LE, abS-100b*) were weakly variable. The lower / upper quartile ranges also differed for all markers of the two groups. This result is quite typical of biochemical markers when comparing groups of patients and healthy controls.

Changes in the correlations in the patients and controls presumably reflect modifications in the system under consideration, which can be assessed using the analysis of paired correlations due to numerous direct and indirect relationships between the markers. Pairwise Spearman's rank correlation coefficient revealed only a few weak correlations in the group of patients and slightly stronger ones in the group of healthy people. Therefore, at the next stages of the study, the assessment of paired correlations together with the quantile regression will help identify critical correlations, which modifications are responsible for the development of the pathological process.

To evaluate paired correlations of random variables, quantile regression plots were constructed (*Q–Q*), since it is known that two random variables are distributed identically and have the dependence similar to that of their quantiles. Quadratic quantile regression plots make it possible to evaluate the strength of the correlations. When accumulated, this information may be the basis for constructing network models of biochemical interactions. Such models for each specific pathology will help identify critical points of therapeutic intervention, which optimization will reduce the number and side effects from medications.

For all pairs of predictors (Fig.), their dependencies are optimally approximated by the quadratic equation, while the nature of the equations for pairs from 2 groups is different.

The nonlinearity of dependencies of marker pairs is most likely a general law for describing the interactions of biochemical molecules. Thus, for *CS / Vi*, nonlinearity arises due to feedback in the entire complement – coagulation system. For *LE / GDG* and *LE /*

GR pairs, the relationship is nonlinear due to complex interactions of neutrophils and platelets, which serve as a source of model markers for assessing modeled brain cell enzymes.

When comparing individual markers in the patient group with those in healthy people, it is impossible to unambiguously determine whether an individual belongs to the group of patients, i.e. there are patients whose studied markers not always differ from the normal values. Therefore, the assessment by individual markers is not effective. A model that includes a set of markers and their correlations is of interest from a fundamental point of view, and the practical aspect of this issue is related to the possible use of the results obtained for early diagnosis of the disease.

The review of current literature showed that the creation of biomarker panels for schizophrenia is a relevant area for research. For example, models have been developed using proteins of the NMDA receptor signaling pathway and tryptophan metabolism [19], as well as inflammatory and immune biomarkers [20].

At this stage, the developed model can demonstrate a new formalized approach to the diagnosis of mental illnesses. In general, for the practical application of models, it is necessary to conduct studies on different clinical groups of patients with schizophrenia with a set of models that will be used for optimizing the diagnosis and therapy.

CONCLUSION

Applying statistical procedures, ten biochemical markers were identified and united into a system that is described by the logistic model and reflects the involvement of immune responses, hemostasis, and oxidative stress in the development of the pathological process in schizophrenia. These parameters are: the functional activity of the complement system, the initial rate of fibrin clot formation, the functional activity of α1-proteinase inhibitor, the level of antibodies to protein S-100b in the blood plasma, the activity of glutamate dehydrogenase and cytochrome c oxidase in platelets, and the activity of glutathione-S-transferase and glutathione reductase in platelets and erythrocytes. Two parameters (clot density when assessing coagulation and leukocyte elastase activity) were not included in this system, which is probably due to the peculiarities of the course of schizophrenia within the psychopathological syndrome considered in the present work.

The model was assessed by the Pearson's test ($\chi^2(11) = 57.6$, $p = 0.001$) and calculation of correct predictions (91 and 80%) for the entire sample consisting of two groups (patients and healthy controls).

This work can be considered as a new approach to the diagnosis of mental illnesses. As a rule, most biochemical markers are not specific; only their combination and identification of the most critical correlations will help create effective models demanded in clinical practice.

REFERENCES

1. Markiewski M.M., Nilsson B., Ekdahl K.N., Mollnes T.E., Lambris J.D. Complement and coagulation: strangers or partners in crime? *Trends in Immunology.* 2007;28(4):184–192. DOI: 10.1016/j.it.2007.02.0062.
2. Conway E.M. Reincarnation of ancient links between coagulation and complement. *Journal of Thrombosis and Haemostasis.* 2015;13(1):S121–S132. DOI: 10.1111/jth.12950.
3. Spivak B., Radwan M., Brandon J., Baruch Y., Stawski M., Tyano S. et al. Reduced total complement haemolytic activity in schizophrenic patients. *Psychological Medicine*. 1993;23(2): 315–318. DOI: 10.1017/s0033291700028397.
4. Cheremnykh E.G., Ivanov P.A., Factor M.I., Pozdnyakova A.N., Shilov Y.E., Brusov O.S. The role of the complement system in the pathogenesis of SARS-COV-2 viral infection in mental illness. *Psychiatry.* 2021;(19)4:76–89 (in Russ.). DOI: 10.30629/2618-6667-2021-19-4-76-89.
5. Buckley P.F. Neuroinflammation and schizophrenia. *Current Psychiatry Reports*. 2019;21(8):72. DOI: 10.1007/s11920-019-1050-z.
6. Müller N. Inflammation in schizophrenia: pathogenetic aspects and therapeutic considerations. *Schizophrenia Bulletin*. 2018;44(5):973–982. DOI: 10.1093/schbul/sby024.
7. Klyushnik T.P., Barkhatova A.N., Sheshenin V.S., Androsova L.V., Zozulya S.A., Otman I.N., et al. Specific features of immune responses in elderly and young patients with exacerbation of schizophrenia. *S.S. Korsakov Journal of Neurology and Psychiatry*. 2021;121(2): 53–59 (in Russ.). DOI: 10.17116/jnevro202112102153.
8. Zozulya S.A., Omelchenko M.A., Sarmanova Z.V., Migalina V.V., Kaleda V.G., Klyushnik T.P. Features of the inflammatory response in juvenile depression with attenuated symptoms of schizophrenic spectrum. *Psychiatry*. 2021;19(2):29–38 (in Russ.). DOI: 10.30629/2618-6667-2021-19-2-29-38.
9. McCutcheon R.A., Krystal J.H., Howes O.D. Dopamine and glutamate in schizophrenia: biology, symptoms and treatment. *World Psychiatry.* 2020;19(1):15–33. DOI: 10.1002/wps.20693.
10. Hardingham G.E., Do K.Q. Linking early-life NMDAR hypofunction and oxidative stress in schizophrenia pathogenesis. *Nature Reviews Neuroscience*. 2016;17(2):125–134. DOI: 10.1038/nrn.2015.19.
11. Hu W., MacDonald M.L., Elswick D.E., Sweet R.A. The glutamate hypothesis of schizophrenia: evidence from human brain tissue studies. *Annals of the New York Academy of Sciences*. 2015;1338(1):38–57. DOI: 10.1111/nyas.12547.
12. Prokhorova T.A., Boksha I.S., Savushkina O.K., Tereshkina E.B., Vorobyeva E.A., Pomytkin A.N., et al. Glutamate dehy-

drogenase activity in platelets of patients with endogenous psychosis. *S.S. Korsakov Journal of Neurology and Psychiatry*. 2016;116(3):44–48 (in Russ.). DOI: 10.17116/jnevro20161163144-48.
13. Tereshkina E.B., Savushkina O.K., Boksha I.S., Prokhorova T.A., Vorobeva E.A., Omel'chenko M.A., et al. Glutathione reductase and glutathione-S-transferase in blood cells in schizophrenia and schizophrenia spectrum disorders. *S.S. Korsakov Journal of Neurology and Psychiatry.* 2019;119(2):61–65 (in Russ.). DOI: 10.17116/jnevro201911902161.
14. Ivanov P.A., Factor M.I., Karpova N.S., Cheremnykh E.G., Brusov O.S. Complement-mediated death of ciliates *Tetrahymena pyriformis* under the influence of human blood serum. *Bulletin of Experimental Biology and Medicine*. 2015;160(12):739–743 (in Russ.).
15. Cheremnykh E.G., Pokataev A.S., Gridunova V.N. Device for biological studies. Patent No. 2361913C2 RU, Int. Cl. C12 M 1/00, C12 M 1/34, G01 N 33/02, G01 N 33/00, C12 Q 1/02, C12 Q 1/00, A23 K 1/00. No. 2006136885/13; Effective date for property rights: 18.10.06; Date of publication: 20.07.09, Bull. 20 (in Russ.).
16. Brusov O.S., Simashkova N.V., Karpova N.S., Factor M.I., Nikitina S.G. Thrombodynamics parameters of blood hypercoagulation in children with childhood autism and schizophrenia. *S.S. Korsakov Journal of Neurology and Psychiatry*. 2019;119(1):59–63 (in Russ.). DOI: 10.17116/jnevro201911901159.
17. Benecke R., Strümper P., Weiss H. Electron transfer complexes I and IV of platelets are abnormal in Parkinson's disease but normal in Parkinson-plus syndromes. *Brain.* 1993;116(6):1451–1463. DOI: 1093/brain/116.6.1451.
18. Royston T.P. Approximating the Shapiro – Wilk W-Test for non-normality. *Statistics and Computing.* 1992;2:117–119. DOI: 10.1007/BF01891203.
19. Lin E., Lin C.H., Hung C.C., Lane H.Y. An ensemble approach to predict schizophrenia using protein data in the N-Methyl-D-Aspartate Receptor (NMDAR) and tryptophan catabolic pathways. *Frontiers in Bioengineering and Biotechnology*. 2020;8:569. DOI: 10.3389/fbioe.2020.00569.
20. Li Y., Yolken R., Cowan D.N., Boivin M.R., Liu T., Niebuhr D.W. Biomarker identification and effect estimation on schizophrenia – a high dimensional data analysis. *Frontiers in Public Health.* 2015;3:75. DOI: 10.3389/fpubh.2015.00075.

Authors' contribution

Cheremnykh E.G. – conception and design of the study, analysis and interpretation of the data, statistical processing of the research results, drafting of the article. Savushkina O.K. – statistical processing of the results, selection of literature, editing of the article. Prokhorova T.A.,Zozulya S.A. – collection and processing of the material, carrying out of research, drafting of the article. Otman I.N. – collection and processing of the material, carrying out of research, drafting of the article. Pozdnyakova A.N. Karpova N.S., Shilov Yu.E. – collection and processing of the material, carrying out of research. Klyushnik T.P. – conception and design of the study, final approval of the article for publication.

Authors' information

Cheremnykh Elena G. – Cand. Sci. (Tech.), Senior Researcher, Laboratory of Biochemistry, Mental Health Research Center, Moscow, elcher10@yandex.ru, https://orcid.org/ 0000-0001-5166-4462

Savushkina Olga K. – Cand. Sci. (Biology), Leading Researcher, Laboratory of Neurochemistry, Mental Health Research Center, Moscow, osavushkina1@yandex.ru, https://orcid.org/ 0000-0002-5996-6606

Prokhorova Tatyana A. – Researcher, Laboratory of Neurochemistry, Mental Health Research Center, Moscow, gnidra@mail.ru, https://orcid.org/0000-0002-3574-2165

Zozulya Svetlana A. – Cand. Sci. (Biology), Leading Researcher, Laboratory of Neuroimmunology, Mental Health Research Center, Moscow, s.ermakova@mail.ru, https://orcid.org/0000-0001-5390-6007

Otman Irina N. – Cand. Sci. (Biology), Researcher, Laboratory of Neuroimmunology, Mental Health Research Center, Moscow, irinaot@mail.ru, https://orcid.org/0000-0003-3745-8413

Pozdnyakova Anastasia N. – Junior Researcher, Laboratory of Pathophysiology, Mental Health Research Center, Moscow, fanianastya@gmail.com, https://orcid.org/0000-0002-9137-0167

Karpova Natalya S. – Researcher, Laboratory of Biochemistry, Mental Health Research Center, Moscow, nat_karpova@mail.ru, https://orcid.org/0000-0003-2061-8097

Shilov Yuri E. – Cand. Sci. (Biology), Researcher, Laboratory of Biochemistry, Mental Health Research Center, Moscow, shilov-nl@yandex.ru, https://orcid.org/0000-0001-9301-2294

Klyushnik Tatyana P. – Dr. Sci. (Med.), Professor, Head of the Laboratory of Neuroimmunology, Mental Health Research Center, Moscow, klushnik2004@mail.ru, https://orcid.org/0000-0001-5148-3864

(✉) **Cheremnykh Elena G.,** elcher10@yandex.ru

Received 28.09.2023;
approved after peer review 03.10.2023;
accepted 16.11.2023

УДК 616.98:578.834.1]-06:616.24-002:616.127
https://doi.org/10.20538/1682-0363-2024-1-94-104

Changes in the cardiovascular profile in patients 3 and 12 months after COVID-19 pneumonia: parameters of arterial stiffness, global longitudinal strain, and diastolic function of the left ventricle

Yaroslavskaya E.I.[1], Shirokov N.E.[1], Krinochkin D.V.[1], Migacheva A.V.[1], Korovina I.O.[2], Osokina N.A.[1], Sapozhnikova A.D.[1], Petelina T.I.[1]

[1] *Tyumen Cardiology Research Center, Tomsk National Research Medical Center (NRMC) of the Russian Academy of Sciences*
111, Melnikaite Str., Tyumen, 625026, Russian Federation

[2] *Regional Clinical Hospital No. 1*
55, Kotovskogo Str., Tyumen, 625023, Russian Federation

ABSTRACT

Aim. To study changes in the brachial – ankle pulse wave velocity (baPWV), ankle – brachial index (ABI), diastolic function, and global longitudinal strain of the left ventricle (LV) 3 and 12 months after COVID-19 pneumonia.

Materials and methods. The dynamics of vascular age and LV global longitudinal strain was studied in 154 patients 3 and 12 months after COVID-19 pneumonia (51 ± 12 years, 48% were women). The control group consisted of 55 sex- and age-matched individuals.

Results. During the follow-up, the average baPWV decreased (13.2 [11.8; 15.1] cm / sec vs. 13.0 [11.8; 14.1] cm / s; $p < 0.001$), and the frequency of its elevated values declined (45.4 vs. 35.1%; $p = 0.008$). The average ABI increased (1.09 [1.04; 1.14] vs. 1.11 [1.06; 1.17]; $p = 0.012$), but remained within the normal range. LV global longitudinal strain (LV GLS) (–19.6 ± 2.2 and –19.7 ± 2.5%; $p = 0.854$) and the frequency of reduced LV GLS (21.4 and 26.6%; $p = 0.268$) did not change significantly and did not differ from values in the control group. Global longitudinal strain in the LV basal inferoseptal segment improved (–19.2 ± 3.6% vs. –20.1 ± 4.0%; $p = 0.032$). The early diastolic mitral annular velocity decreased (8.4 ± 3.0 cm / s vs. 8.0 ± 2.5 cm / s; $p = 0.023$). The LV isovolumic relaxation time was greater than in the control group (101.8 ± 22.3 ms at the 1st visit vs. 92.9 ± 21.5 ms; $p = 0.012$; 105.9 ± 21.9 ms vs. 92.9 ± 21.5 ms at the 2nd visit; $p < 0.001$). A positive correlation was found between baPWV ($r = 0.209$; $p = 0.009$) and ABI ($r = 0.190$; $p = 0.021$) and strain parameters of the LV basal segments 12 months after discharge.

Conclusion. Patients with optimal visualization on echocardiography at 12 months after COVID-19 pneumonia, compared to the results of the examination 3 months after the disease, had deteriorated parameters of LV diastolic function. LV GLS was within the grey zone and did not change significantly. An improvement in arterial stiffness was noted, associated with an improvement in the strain of basal LV segments.

Keywords: COVID-19, pulse wave velocity, ankle – brachial index, echocardiography, longitudinal myocardial strain

Conflict of interest. The authors declare the absence of obvious or potential conflicts of interest related to the publication of this article.

Source of financing. The authors state that hey received no funding for the study.

Conformity with the principles of ethics. All individuals signed an informed consent to participate in the study. The study was approved by the local Ethics Committee at Tyumen Cardiology Research Center, Tomsk NRMC of the Russian Academy of Sciences (Protocol No. 159 of 23.07.2020).

✉ *Yaroslavskaya Elena I.,* yaroslavskayae@gmail.com

Для цитирования: Yaroslavskaya E.I., Shirokov N.E., Krinochkin D.V., Migacheva A.V., Korovina I.O., Osokina N.A., Sapozhnikova A.D., Petelina T.I. Changes in the cardiovascular profile in patients 3 and 12 months after COVID-19 pneumonia: parameters of arterial stiffness, global longitudinal strain, and diastolic function of the left ventricle. *Bulletin of Siberian Medicine.* 2024;23(1):94–104. https://doi.org/10.20538/1682-0363-2024-1-94-104.

Динамика сердечно-сосудистого статуса пациентов через 3 и 12 месяцев после пневмонии COVID-19: показатели сосудистой жесткости, диастолической функции и продольной деформации левого желудочка

Ярославская Е.И.[1], Широков Н.Е.[1], Криночкин Д.В.[1], Мигачева А.В.[1], Коровина И.О.[2], Осокина Н.А.[1], Сапожникова А.Д.[1], Петелина Т.И.[1]

[1] Тюменский кардиологический научный центр, Томский национальный исследовательский медицинский центр (НИМЦ) Российской академии наук
Россия, 625026, г. Тюмень, ул. Мельникайте, 111

[2] Областная клиническая больница № 1
Россия, 625023, г. Тюмень, ул. Котовского, 55

РЕЗЮМЕ

Цель: изучить динамику скорости пульсовой волны (brachial-ankle pulsewave velocity, baPWV), лодыжечно-плечевого индекса (ankle-brachialindex, ABI), диастолической функции и продольной деформации левого желудочка (ЛЖ) через 3 и 12 мес после пневмонии COVID-19.

Материалы и методы. Динамика показателей сосудистого возрастаи продольной деформации ЛЖ изучена у 154 пациентов через 3 и 12 мес после пневмонии COVID-19 (51 ± 12 лет, 48% женщин). Группу контроля составили 55 сопоставимых по полу и возрасту пациентов.

Результаты. За время наблюдения снизилась усредненная baPWV (13,2 [11,8; 15,1] см/сек против 13,0 [11,8; 14,1] см/с, $p < 0,001$) и частота выявления ее повышенных значений (45,4 против 35,1%, $p = 0,008$). Усредненное значение ABI выросло, оставаясь в пределах нормы (1,09 [1,04; 1,14] против 1,11 [1,06; 1,17], $p = 0,012$). Глобальная продольная деформация ЛЖ (LV GLS) (19,6 ± 2,2% и –19,7 ± 2,5%; $p = 0,854$) и частота выявления сниженной LV GLS (21,4 и 26,6%; $p = 0,268$) значимо не изменились и не отличались от полученных в группе контроля. Продольная деформация базального нижне-перегородочного сегмента ЛЖ улучшилась (–19,2 ± 3,6% против –20,1 ± 4,0%; $p = 0,032$). Раннедиастолическая скорость септальной части митрального кольца снизилась (8,4 ± 3,0 см/с против 8,0 ± 2,5 см/с, $p = 0,023$). Время изоволюмического расслабления ЛЖ было больше, чем в группе контроля (на 1-м визите 101,8 ± 22,3 мс против 92,9 ± 21,5 мс; $p = 0,012$; на 2-м визите 105,9 ± 21,9 мс против 92,9 ± 21,5 мс; $p < 0,001$). Выявлена положительная корреляционная связь baPWV ($r = 0,209$; $p = 0,009$) и ABI ($r = 0,190$; $p = 0,021$)) с параметрами деформации сегментов базального уровня ЛЖ через год после выписки.

Заключение. У лиц с оптимальной визуализацией при эхокардиографии через год после пневмонии COVID-19 в сравнении с результатами обследования через 3 мес отмечается ухудшение параметров диастолической функции ЛЖ. LV GLS находилась в пределах «серой зоны» и значимо не изменилась. Отмечено улучшение показателей сосудистой жесткости, связанное с улучшением деформации сегментов базального уровня ЛЖ.

Ключевые слова: COVID-19, скорость распространения пульсовой волны, лодыжечно-плечевой индекс, эхокардиография, продольная деформация миокарда

Конфликт интересов. Авторы декларируют отсутствие явных и потенциальных конфликтов интересов, связанных с публикацией настоящей статьи.

Источник финансирования. Авторы заявляют об отсутствии финансирования при проведении исследования.

Соответствие принципам этики. Все пациенты подписали информированное согласие на участие в исследовании. Исследование одобрено локальным этическим комитетом Тюменского кардиологического научного центра, Томского НИМЦ (протокол № 159 от 23.07.2020).

Для цитирования: Ярославская Е.И., Широков Н.Е., Криночкин Д.В., Мигачева А.В., Коровина И.О., Осокина Н.А., Сапожникова А.Д., Петелина Т.И. Динамика сердечно-сосудистого статуса пациентов через 3 и 12 месяцев после пневмонии COVID-19: показатели сосудистой жесткости, диастолической функции и продольной деформации левого желудочка. *Бюллетень сибирской медицины.* 2024;23(1):94–104. https://doi.org/10.20538/1682-0363-2024-1-94-104.

INTRODUCTION

Increased arterial stiffness is known to impair myocardial relaxation and increase left ventricular (LV) end-diastolic pressure [1]. The study of the relationship between arterial stiffness and myocardial strain properties is of sustained interest. A chronic increase in afterload has been shown to accelerate LV remodeling and development of heart failure [2]. A study of 248 individuals without structural heart disease revealed an independent relationship between brachial – ankle pulse wave velocity (baPWV) and LV global longitudinal strain (GLS) [3]. J.W. Hwang et al. demonstrated that increased baPWV contributed to impaired LV GLS in patients with arterial hypertension (AH) and preserved LV ejection fraction (LVEF) [4].

Arterial stiffness is naturally associated with aging but may be accelerated by concomitant metabolic and cardiovascular pathology. One of the mechanisms that underlies changes in blood vessels during aging and cardiovascular diseases is a decrease in the number of elastic fibers and an increase in collagen content. Another mechanism is endothelial dysfunction, which develops as a result of inflammation, oxidative stress, and changes in smooth muscle tone in muscular arteries. COVID-19 is a multisystem disease with extensive damage to the cardiovascular system, causing increased arterial stiffness [5]. Today, complications of the experienced infectious process come to the forefront; most of these complications directly affect the vascular system. A significant number of COVID-19 survivors have been shown to develop persistent metabolic changes with vascular wall damage similar to that seen in AH, type 2 diabetes mellitus, and metabolic syndrome [6]. Mild inflammatory components play a role in the development of early vascular aging after COVID-19 [7, 8].

All of these may lead to the onset or progression of both AH and atherosclerotic vascular wall damage, especially after a complicated course of COVID-19. Considering that functional disorders develop faster than structural ones, the study of arterial stiffness after COVID-19 is very relevant, but such studies are still few. I. Ikonomidis et al. proposed to use the ratio of carotid – femoral pulse wave velocity (PWV) to LV GLS as a parameter for assessing ventricular – arterial coupling, which in turn affects LV diastolic function, the severity of concentric hypertrophy, and the degree of impairment of coronary flow reserve [9].

We hypothesized that in patients who have had a complicated course of COVID-19 in the long term after the disease, arterial stiffness increases, and LV GLS parameters worsen in comparison with the examination data in the early recovery period, which could be a reflection of early vascular aging.

The aim of the study was to determine changes in and relationships between baPWV, ankle – brachial index (ABI), and LV GLS 3 and 12 months after COVID-19 pneumonia.

MATERIALS AND METHODS

The study included patients of the “Prospective Registry of COVID-19-Associated Pneumonia Survivors” (state registration certificate No. 2021622535 of 18.11.2021). The study complied with the ethical standards of the Declaration of Helsinki as amended in 2000 and the “Rules of good clinical practice in the Russian Federation”, approved by Order of the Ministry of Health of the Russian Federation No. 266 of 19.06.2003. The study was approved by the local Ethics Committee (Protocol No. 159 of 23.07.2020) and registered in international clinical trials registry clinicaltrials.gov (No. NCT04501822). Patients were identified according to the 1C medical information system of infectious disease hospitals in the period from April 2020 to January 2021. Inclusion criteria: laboratory-confirmed diagnosis of COVID-19 pneumonia, age 18 years or older, and patient’s consent to participate in the study. Non-inclusion criteria: exacerbation of chronic diseases, hemodynamically significant heart defects, history of cancers younger than 5 years, tuberculosis, other diseases accompanied by pulmonary

fibrosis, chronic hepatitis, HIV. Exclusion criteria: pregnancy, cancer detected during the follow-up period, refusal to participate in the study, suboptimal echocardiography (Echo) imaging. All patients signed an informed consent to participate in the study.

An outpatient examination of 350 patients meeting all the criteria was performed 3 months ± 2 weeks (92 [82–99] days) and 12 months ± 3 weeks (367 [362–381] days) after discharge. Of the 380 patients included in the study, 28 were excluded for various reasons. At the first visit, 271 patients had optimal visualization quality during echocardiography, and at the second visit – 244 patients. Of the remaining examined subjects, vascular age parameters were assessed after 3 months (1st visit) in 339 (97%) subjects and after 12 months (2nd visit) in 286 (82%) subjects. The parameters of LV GLS and LV segmental longitudinal strain were studied 3 months after pneumonia in 271 (77%) patients with optimal visualization during echocardiography and after 12 months in 244 (70%) patients. Changes in vascular age indices and LV strain properties could be assessed in 154 (44%) patients (main group). The control group consisted of 55 sex- and age-matched patients with optimal visualization quality during echocardiography. They were included in the study at the same time as the main group and had neither a single positive result of the polymerase chain reaction identifying SARS-CoV-2 nor clinical manifestations of COVID-19.

Data from the acute phase of COVID-19 were assessed using discharge summaries from medical records. The average proportion of lung tissue damage in the examined patients according to computed tomography (CT) during hospitalization was 50.0%; 8.5% of patients were treated in intensive care units, 45.7% received hormonal therapy, 5.9% – biologically active therapy. 17.0% of patients had mild pneumonia, 31.3% – moderate, 38.1% – severe, and 13.6% – extremely severe pneumonia.

During the visits, all the study participants underwent determination of elastic properties of the peripheral arterial wall by volumetric sphygmography on the VaSera VS-1000 Series sphygmomanometer (Fukuda Denishi, Japan). We assessed baPWV on the right and left; ABI on the right and left as the ratio of systolic blood pressure (BP) at the ankle to systolic BP at the arm. The averaged values between the right and left sides were analyzed. In accordance with the specified hardware conditions for interpretation of the results, baPWV was considered to be normal at < 13.5 cm / sec; normal ABI values were considered to be $1.0 \leq \text{ABI} < 1.3$ (vascular age was not assessed in the control group, since it was determined in less than half of the patients in this group). Echo was performed on the best-in-class Vivid S70 ultrasound diagnostic system with data storage in DICOM format and subsequent data analysis on the Intelli Space Cardiovascular workstation using the TomTec software (Philips, USA). LV GLS > –18% was considered to be reduced [10, 11]. The symptoms of anxiety – depressive disorders (according to the GAD7 and PHQ9 scales), stress disorders (according to the Perceived Stress Scale (PSS-10)), and the quality of life (according to the SF-36 questionnaire) were assessed.

Statistical analysis was carried out using the SPSS 21 software application package (SPSS Inc., Chicago, IL, USA) and Statistica 12.0. The distribution of variables was assessed using the Kolmogorov – Smirnov test. For normal distribution of quantitative variables, parameters were presented as the mean and the standard deviation ($M \pm SD$). For distribution other than normal, parameters were presented as the median and the interquartile range Me [Q_{25}; Q_{75}]. The significance of differences in continuous variables was assessed depending on the data distribution using the Student's *t*-test for dependent variables or the Wilcoxon test. To compare qualitative variables, the McNemar test was used. Correlations between pairs of quantitative variables were assessed using the Pearson's chi-squared test for normal distribution, and Spearman's rank correlation coefficient for non-normal distribution. Comparison with the control group was performed using the Kruskal – Wallis test or one-way analysis of variance for quantitative variables, and by the $\chi 2$ test or Fisher's exact test for qualitative parameters. The results were considered statistically significant at $p < 0.05$.

RESULTS

The mean body mass index (BMI) in the main group corresponded to overweight at both visits and increased over the follow-up period (Table 1). The number of smokers decreased by 9.2%, but drinking alcohol several times a week increased by 5%. Symptoms of anxiety – depressive and stress disorders and subjectively perceived quality of life did not change significantly. The prevalence of cardiovascular diseases increased due to the newly identified 7 cases of AH and 6 cases of coronary artery disease (CAD). At the same time, no significant change in BP and heart rate was registered. The average baPWV decreased by 0.2 cm / sec, and the frequency of detection of its elevated values decreased by 10.3%. The average

value of ABI increased by 0.02, remaining within the normal range. The number of patients with normalization of lung CT data increased by 5.4%.

The main group did not differ from the control group in age and sex composition, significant differences in BMI appeared only at the end of the observation period. Individuals who had COVID-19 pneumonia in the early recovery period drank alcohol less frequently, more often showed symptoms of anxiety, and had worse physical characteristics of health than the control group. Patients of the main group did not differ from the control group in the frequency of AH, but 3 months after discharge, they showed a trend toward higher systolic BP than in the control group, and their diastolic BP was higher throughout the observation. In the control group, only one patient had diabetes mellitus, and there were no diagnosed cases of CAD.

Table 1

Changes in clinical parameters of patients after COVID-19 pneumonia and the control group

Parameter			Patients after COVID-19 pneumonia		*p*	Control group, *n* = 55	*p* *	*p***
			After 3 months, *n* = 154	After 12 months, *n* = 154				
Age, years, *M* ± *SD*			51.3 ± 11.5	–	–	51.8 ± 10.8	0.943	–
Female gender, %			48.1	–	–	56.4	0.290	–
Body mass index, kg / m², *M* ± *SD*			28.5 ± 4.4	29.3 ± 4.8	<0.001	27.4 ± 4.2	0.093	0.013
Smoking or recently quit, *n* (%)			62 (40.3)	46 (31.1)	0.002	15 (41.7)	0.877	0.266
Alcohol drinking, *n* (%)	do not drink		34 (22.4)	39 (26.7)	0.302	5 (13.9)	0.259	0.107
	several times a year		70 (46.1)	53 (36.3)	0.002	18 (50.0)	0.670	0.131
	several times a month		42 (27.6)	40 (27.4)	0.690	7 (19.4)	0.314	0.329
	once/several times a week		6 (3.9)	13 (8.9)	0.039	6 (16.7)	0.013	0.220
Identifying anxiety symptoms using the GAD7 scale, *n* (%)			47 (30.7)	36 (25.4)	0.185	4 (11.1)	0.017	0.067
Identifying depression symptoms using the PHQ9 scale, *n* (%)			49 (32.0)	36 (25.4)	0.262	8 (22.2)	0.249	0.697
Identifying stress symptoms using the Perceived Stress Scale-10, *n* (%)			16 (10.5)	12 (8.5)	1.000	2 (5.6)	0.533	0.738
Generalized scores of the SF-36 questionnaire, *Me* [Q_{25}; Q_{75}]	Physical component		48.5 [43.5; 51.6]	48.7 [44.1; 52.4]	0.143	50.0 [45.7; 52.7]	0.096	0.282
	Mental component		66.7 [59.7; 71.4]	67.7 [59.3; 71.9]	0.341	67.0 [60.9; 71.3]	0.855	0.879
Arterial hypertension, *n* (%)			111 (72.1)	118 (77.1)	0.039	38 (69.1)	0.671	0.238
Coronary artery disease, *n* (%)			21 (13.6)	27 (17.6)	0.031	0 (0.0)	0.004	0.001
Type 2 diabetes mellitus, *n* (%)			20 (13.0)	21 (13.6)	1.000	1 (1.8)	0.018	0.014
Congestive heart failure according to NYHA, *n* (%)		FC I	51 (71.8)	55 (72.4)	0.388	15 (88.2)	0.219	0.244
		FC II	17 (23.9)	18 (23.7)	1.000	2 (11.8)	0.344	0.348
		FC III	3 (4.2)	3 (3.9)	1.000	0 (0.0)	1.000	1.000
Office blood pressure, mm Hg, *Me* [Q_{25}; Q_{75}]	Systolic		129 [117; 140]	128 [116; 139]	0.511	120 [110; 135]	0.068	0.081
	Diastolic		82 [75; 92]	85 [80; 92]	0.164	80 [70; 81]	0.011	0.001
Heart rate per minute, *Me* [Q_{25}; Q_{75}]			63 [58; 70]	62 [56; 68]	0.400	72 [66;78]	0.857	0.183
Normalization of lung CT data, %			38.8	44.2	<0.001	–	–	–
Parameters of vascular wall elasticity								
Average baPWV value, cm / sec, *Me* [Q_{25}; Q_{75}]			13.2 [11.8; 15.1]	13.0 [11.8; 14.1]	<0.001	–	–	–
Frequency of detection of elevated baPWV (≥ 13.5 cm / sec), *n* (%)			69 (45.4)	54 (35.1)	0.008	–	–	–
Average ABI value, *Me* [Q_{25}; Q_{75}]			1.09 [1.04; 1.14]	1.11 [1.06; 1.17]	0.012	–	–	–
Detection of reduced ABI (less than 1), *n* (%)			44 (29.7)	35 (23.5)	0.451	–	–	–
Detection of increased ABI (1.3 and above), *n* (%)			3 (2.1)	3 (2.1)	1.000	–	–	–

Note. NYHA – New York Heart Association; FC – functional class; CT – computed tomography, *p* – level of statistical significance of differences between the groups of patients.

*p** – significance of differences between the control group and those who had COVID-19 pneumonia 3 months after discharge; *p*** – significance of differences between the control group and those who had COVID-19 pneumonia 12 months after discharge.

During hospitalization, the reference values of C-reactive protein (CRP), lactate dehydrogenase (LDH), aspartate aminotransferase (AST) (moderate increase), alanine aminotransferase (ALT) were significantly exceeded with subsequent normalization (with the exception of CRP: its average values after discharge decreased, but did not reach the normal value) (Table 2). At 12 months after discharge, there was a significant decrease in levels of total cholesterol (TC), triglycerides, and low-density lipoprotein cholesterol (LDL-C). At the same time, the mean values of these parameters in the outpatient setting were higher than the reference values except for triglycerides. During outpatient follow-up, the liver function tests worsened, the levels of creatine phosphokinase, creatinine, leukocytes, CRP, including high-sensitivity CRP, ferritin, and interleukin (IL) 1 and 6 increased. There was a trend toward a decrease in the level of glycated hemoglobin, its average value approached the normal ones. The N-terminal pro b-type natriuretic peptide (NT-proBNP) level decreased. The frequency of use of beta-blockers (34.0 vs. 42.5%; $p = 0.027$) and statins (46.9 vs. 59.5%; $p = 0.001$) increased over the follow-up period. The frequency of use of the following groups of drugs did not change: adenosine-converting enzyme inhibitors (26.5 and 30.1%; $p = 0.327$), antiplatelet agents (aspirin / clopidogrel) (19.0 and 19.6%; $p = 0.754$), diuretics (46.3 and 49.7%; $p = 0.458$), hypoglycemic agents (11.7 and 12.3%; $p = 1.000$).

Table 2

Changes in laboratory parameters of individuals with optimal Echo visualization after COVID-19 pneumonia

Parameter	Hospitalization period, n =154	3 months after discharge, n = 154	12 months after discharge, n = 154	p between 3 and 12 months
TC, mmol / l, *Me* [Q_{25}; Q_{75}], $M \pm SD$, N 0–5	4.0 [3.3; 4.8]	5.5 ± 1.4	5.1 ± 1.3	<0.001
TG, mmol / l, *Me* [Q_{25}; Q_{75}], N 0–1.7	–	1.3 [0.9; 1.7]	1.1 [0.8; 1.6]	0.039
HDL, mmol / l, $M \pm SD$ N males ≤40; females ≤31	–	1.4 ± 0.4	1.3 ± 0.3	0.514
LDL, mmol / l, $M \pm SD$ N 0–3	-	3.1 ± 1.2	3.1 ± 1.0	0.004
ALT, units / l, *Me* [Q_{25}; Q_{75}], N males ≤40; females ≤31	32.0 [17.3; 57.1]	21.0 [15.9; 27.5]	24.0 [18.6; 30.8]	0.008
AST, units/l, *Me* [Q_{25}; Q_{75}], N males ≤38; females ≤32	32.7 [23.9; 46.0]	19.4 [16.0; 24.2]	21.9 [18.6; 25.8]	0.002
Lactate dehydrogenase, units / l, *Me* [Q_{25}; Q_{75}], N 0–248	421.5 [292.0; 592.0]	183.9 [159.9; 204.3]	181.6 [159.0; 200.4]	0.064
Creatine phosphokinase, units/l, *Me* [Q_{25}; Q_{75}], N males ≤190; females ≤167	108.0 [63.0; 227.0]	100.0 [72.1; 139.6]	118.0 [84.1; 165.1]	<0.001
Creatinine, μmol/l, *Me* [Q_{25}; Q_{75}], N males 62–106; females 44–80	80.0 [69.0; 97.0]	74.5 [65.3; 83.2]	77.2 [67.4; 87.2]	<0.001
Fasting glucose, mmol / l, *Me* [Q_{25}; Q_{75}], N 3.3–6.1	7.2 [6.5; 9.1]	5.4 [5.0; 5.9]	5.4 [5.0; 6.0]	0.806
Glycated hemoglobin, %, *Me* [Q_{25}; Q_{75}], N 4.5–6.0	–	6.7 [5.7; 8.0]	5.8 [5.5; 6.2]	0.070
Leukocytes, 10^9 / l, *Me* [Q_{25}; Q_{75}], N 4.0–9.0	5.9 [4.4; 7.8]	5.2 [4.3; 6.4]	5.5 [4.6; 6.5]	0.001
Lymphocytes, %, $M \pm SD$, *Me* [Q_{25}; Q_{75}], N 19–37	23.0 ± 11.3	1.8 [1.5; 2.2]	1.9 [1.6; 2.2]	0.387
CRP, mg / l, *Me* [Q_{25}; Q_{75}], N ≤3	58.5 [15.9; 115.6]	3.5 [1.7; 6.2]	4.2 [2.9; 7.6]	<0.001
hsCRP, mg / l, *Me* [Q_{25}; Q_{75}], N ≤3	–	3.8 [1.7; 7.0]	4.1 [2.6; 7.5]	<0.001
Ferritin, mg / ml, *Me* [Q_{25}; Q_{75}], N males 20–300; females 10–120	–	67.8 [24.5; 151.6]	106.8 [37.9; 184.2]	0.002
D-dimer, μg/ml, *Me* [Q_{25}; Q_{75}], N 0.1–0.5	0.4 [0.2; 0.6]	0.3 [0.1; 0.4]	0.1 [0.1; 0.2]	0.527
NT-proBNP, pg/ml, *Me* [Q_{25}; Q_{75}], N under 75 years <125, over 75 years <400	–	67.4 [29.1; 155.8]	58.7 [30.9; 98.1]	0.007
Interleukin 8, pg / ml, *Me* [Q_{25}; Q_{75}], N≤8.11	–	13.7 [10.3; 17.3]	13.8 [10.3; 17.2]	0.739
Interleukin 1, pg / ml, *Me* [Q_{25}; Q_{75}], N 0–5 pkg/ml	–	2.0 [1.6; 2.8]	2.2 [1.6; 3.1]	0.001
Interleukin 6, pg / ml, $M \pm SD$, N ≤9.7	–	3.0 ± 1.2	3.5 ± 0.9	<0.001

Note. HDL – high-density lipoproteins; LDL – low-density lipoproteins; ALT – alanine aminotransferase; AST – aspartate aminotransferase; hsCRP – high-sensitivity C-reactive protein, N – normal values.

Larger values of LV volume during hospitalization can be explained by the infusion load, which was pathogenetically justified in the acute period of the disease. The larger anteroposterior dimension of the right ventricle (RV) can be explained by the load on the pulmonary circulation caused by pneumonia (Table 3). During the observation period, the area of RV decreased; the fraction of change in the area of RV increased, indicating structural and functional recovery of the RV. However, such parameters of RV function as tricuspid annular plane systolic excursion (TAPSE), peak tricuspid regurgitation velocity, S' tricuspid annular velocity, acceleration time of blood flow in the RV outflow tract in the main group, though being within the normal range, did not reach the values of the control group in dynamics, which indicates limitation of RV function after COVID-19 pneumonia.

In terms of LV parameters, COVID-19 pneumonia survivors showed a significant decrease in LV end-systolic volume and a slight increase in LV ejection fraction at one year after discharge, suggesting an improvement in LV systolic function in the late recovery period. However, the deterioration of LV diastolic function parameters draws attention: early diastolic mitral annular velocity at the septal annulus (e' sept) significantly decreased (and one year after discharge, it showed a trend toward a lower value than in the control group), there was a trend toward a decrease in LV early diastolic filling deceleration time (DT) and the ratio of the early diastolic velocity of transmittal flow to the early diastolic velocity of the mitral annulus (E/e'). The worse diastolic function compared to the control group is also evidenced by the longer LV isovolumic relaxation time (IVRT) during the whole observation period in the main group.

Table 3

Changes in the echocardiography parameters of persons after COVID-19 pneumonia and the control group, *M* ± *SD*

Parameter		Hospitalization period, *n* = 154	Patients after COVID-19 pneumonia		*p*	Control group, *n* = 55	*p* *	*p* **
			After 3 months, *n* = 154	After 12 months, *n* = 154				
LV end-diastolic volume (EDV)	ml	113.1±24.1	90.2±22.8	89.3±20.6	0.521	88.1±21.7	0.620	0.664
	ml / m²	–	46.5±9.9	45.6±8.6	0.167	46.2±9.1	0.950	0.585
LV end-systolic volume (ESV)	ml	36.4±12.3	29.3±10.7	27.4±7.3	0.031	28.6±10.1	0.608	0.849
	ml / m²	–	15.1±4.9	14.0±3.1	0.009	14.9±4.5	0.902	0.346
LV myocardial mass according to the area-length method	g	–	145.9±34.6	148.9±32.3	0.449	136.4±33.8	0.055	0.009
	g / m²		75.6±15.2	76.1±13.1	0.736	71.2±12.3	0.039	0.012
LV ejection fraction (2D Simpson), %		68.2±5.8	68.1±4.8	69.4±3.9	0.004	68.3±4.8	0.832	0.062
Time of blood flow deceleration in LV outflow tract, ms		–	215.0±32.2	215.7±30.9	0.889	209.7±29.5	0.292	0.217
LV isovolumic relaxation time, IVRT, ms		–	101.8±22.3	105.9±21.9	0.113	92.9±21.5	0.012	<0.001
DT, ms		–	216.6±61.9	205.8±51.5	0.054	194.4±39.7	0.123	0.338
LV early diastolic filling velocity, E, cm /s		–	71.2±15.5	69.4±14.6	0.137	71.8±16.2	0.823	0.313
LV late diastolic filling velocity, A, cm / s		–	68.8±16.3	68.4±15.4	0.731	66.2±14.2	0.284	0.476
Early diastolic velocity at the lateral part of the mitral annulus, e' later, cm/s		–	11.0±3.6	10.9±3.4	0.349	11.1±3.0	0.578	0.552
Early diastolic velocity at the septal part of the mitral annulus, e' sept, cm/s		–	8.4±3.0	8.0±2.5	0.023	8.8±2.6	0.272	0.076
E/e'		–	9.7±3.1	9.5±2.8	0.051	9.9±2.4	0.303	0.180
Maximum left atrial volume	ml	–	47.9±13.6	48.3±12.9	0.474	47.1±12.2	0.823	0.412
	ml / m²	–	24.8±6.6	24.7±5.9	0.953	24.7±5.2	0.674	0.895
Anteroposterior dimension of the RV	mm	26.9±3.3	25.5±2.4	25.8±2.7	0.539	25.3±2.4	0.631	0.440
	mm / m²	–	13.3±1.5	13.3±1.5	0.319	13.4±1.6	0.918	0.727
Diastolic area of the RV	cm²	–	15.7±4.0	14.8±3.3	<0.001	14.9±3.1	0.289	0.723
	cm² / m²	–	8.1±1.7	7.5±1.4	<0.001	7.9±1.5	0.354	0.129
Fraction of change in RV area, %		–	50.8±8.8	53.0±8.4	0.004	52.9±8.3	0.117	0.678
TAPSE, mm		–	22.7±2.5	22.7±2.3	0.973	24.2±2.4	<0.001	<0.001
Peak tricuspid regurgitation velocity, cm / s		–	2.1 [1.8; 2.3]	2.1 [1.9; 2.3]	0.553	1.9 [1.6; 2.1]	0.004	<0.001
Velocity S' of the tricuspid annulus, cm/s		–	9.8±2.6	9.7±2.7	0.289	12.6±1.8	<0.001	<0.001
Acceleration time of blood flow in RV outflow tract, ms		–	113.2±22.9	113.7±21.3	0.929	123.2±26.2	0.003	0.007

Note. DT – deceleration time of LV early diastolic filling.

The absence of significant differences in LV GLS in comparison with the control group and the frequency of detection of reduced LV GLS comparable to the control group (Table 4) allows to evaluate the state of LV systolic function in the main group as satisfactory. Improvement in segmental strain values was noted in the inferior and lateral segments of the LV basal level, with this improvement reaching statistical significance in the basal inferoseptal segment (Table 4). It is worth noting that the value of longitudinal strain in this particular segment 3 months after discharge tended to be lower than in the control group. There was some improvement in the values of segmental strain of LV middle level segments, but it did not reach statistical significance. The strain of the apical level segments worsened insignificantly.

Table 4

Changes in LV strain parameters in individuals 3 and 12 months after COVID-19 pneumonia and the control group, %, *M*±*SD*

Longitudinal strain parameter, %	Patients after COVID-19 pneumonia		*p*	Control group, *n* = 55	*p* *	*p* **
	After 3 months, *n* = 154	After 12 months, *n* = 154				
Global (LV GLS)	–19.6 ± 2.2	–19.7 ± 2.5	0.854	–19.9 ± 2.7	0.556	0.653
Global strain > –18%	33 (21.4)	41 (26.6)	0.268	15 (27.3)	0.376	0.926
Basal anterior segment	–17.3 ± 4.2	–16.7 ± 4.0	0.156	–17.3 ± 4.0	0.965	0.435
Basal anteroseptal segment	–16.8 ± 3.3	–16.7 ± 3.4	0.727	–17.3 ± 3.5	0.494	0.316
Basal inferoseptal segment	–19.2 ± 3.6	–20.1 ± 4.0	0.032	–20.1 ± 3.9	0.060	0.851
Basal inferior segment	–16.6 ± 3.0	–16.8 ± 3.2	0.596	–16.5 ± 3.2	0.728	0.435
Basal inferolateral segment	–17.3 ± 3.8	–17.7 ± 4.1	0.321	–17.5 ± 3.6	0.787	0.502
Basal anterolateral segment	–18.2 ± 4.2	–18.0 ± 4.0	0.459	–18.5 ± 4.6	0.484	0.474
Middle anterior segment	–17.6 ± 4.2	–17.4 ± 4.0	0.556	–17.8 ± 4.5	0.970	0.720
Middle anteroseptal segment	–20.8 ± 3.6	–20.5 ± 3.4	0.424	–20.8 ± 3.6	0.926	0.850
Middle inferoseptal segment	–21.2 ± 3.4	–21.9 ± 3.3	0.093	–22.2 ± 3.5	0.125	0.808
Middle inferior segment	–20.4 ± 3.0	–20.3 ± 3.1	0.925	–20.3 ± 3.0	0.699	0.984
Middle inferolateral segment	–17.9 ± 3.7	–18.0 ± 3.9	0.974	–17.7 ± 3.7	0.482	0.343
Middle anterolateral segment	–19.1 ± 3.4	–19.2 ± 3.7	0.838	–19.1 ± 3.9	0.664	0.787
Apical anterior segment	–21.3 ± 5.2	–21.3 ± 5.0	0.792	–21.8 ± 5.1	0.846	0.912
Apical septal segment	–24.0 ± 4.7	–23.9 ± 4.6	0.954	–24.3 ± 4.0	0.647	0.620
Apical inferior segment	–23.2 ± 4.6	–23.0 ± 4.5	0.472	–23.8 ± 4.1	0.658	0.701
Apical lateral segment	–21.2 ± 4.6	–20.9 ± 5.0	0.539	–21.1 ± 4.1	0.836	0.879
Apical segment	–22.5 ± 4.0	–22.3 ± 4.2	0.324	–22.8 ± 3.9	0.887	0.746
Basal level	-17.6 ± 2.2	–17.7 ± 2.6	0.448	–17.9 ± 2.7	0.400	0.627
Middle level	–19.5 ± 2.0	–19.6 ± 2.5	0.734	–19.6 ± 2.6	0.722	0.865
Apical level	–22.5 ± 4.0	–22.3 ± 4.2	0.693	–22.7 ± 3.8	0.639	0.489

Our study did not reveal the previously described [2, 3] associations of arterial stiffness parameters with LV GLS, which may be due to dysregulation of arterial – ventricular interaction caused by COVID-19. One year after discharge, arterial stiffness parameters (average baPWV (r = 0.209, p = 0.009) and average ABI (r = 0.190, p = 0.021) demonstrated a positive correlation with parameters of segmental strain of the LV basal level.

DISCUSSION

In the in-hospital period, CRP values were many times higher than the reference values, indicating extremely high activity of the inflammatory process and severity of tissue damage. In the recovery period, CRP values never reached the norm and, moreover, increased at one year after discharge, indicating a persistent potential for an increased inflammatory response in the late recovery period of the disease. High levels of high-sensitivity CRP and IL-8 during the recovery period, as well as increased levels of IL-1 and IL-6, indicate a persistent vascular inflammatory process, which may imply a threat of vascular complications.

The deterioration of the cardiovascular status during the observation period is evidenced by both the increase in the incidence of cardiovascular diseases (AH – by 5%, CAD – by 4%) and the need to prescribe beta-blockers, which increased by 8.5%, and statins – by 12.6%. The latter explains the fact that lipid profile values improved, but liver function tests worsened and the level of creatine phosphokinase increased.

The data on normalization of RV function obtained by us are in agreement with positive dynamics of CT lung data in our patients. The improvement of LV systolic function was indicated by the revealed decrease in LV end-systolic volume and a slight increase in LVEF, but the improvement of LV GLS was insignificant, and LV diastolic function deteriorated, as evidenced by the dynamics of tissue and pulse-wave Doppler parameters. Taking into account the worse parameters of LV diastolic function in the main group in comparison with the control group, COVID-19 can be considered as a pathogenetic factor of LV diastolic function disorders in our patients along with the progression of cardiovascular pathology.

Patients in the present study showed some improvement in arterial stiffness parameters during the follow-up period, as evidenced by a small but statistically significant decrease in baPWV, as well as a 10.3% decrease in the frequency of its elevated values. The increase in average ABI within normal values does not contradict this conclusion. These results can be interpreted as a return to baseline (before COVID-19) values of functional parameters of the vascular wall. However, the frequency of detection of abnormalities at the 2nd visit was still high (baPWV – 35.1%, ABI – 25.6%). Considering the negative dynamics we found in diastolic function parameters, as well as the high incidence of disturbances in arterial stiffness parameters one year after COVID-19 pneumonia, longer-term follow-up is necessary to study the degree of reversibility of vascular changes and their prognostic consequences.

The improvement of arterial stiffness parameters according to our results is associated with improvement of LV basal segmental strain. Since it was previously shown that in the early recovery period after COVID-19, a decrease in LV segmental strain is characteristic mainly for LV basal segments [12], this result can be interpreted as the restoration of LV strain properties, impaired in the acute period of COVID-19.

We found the only study with 1-year follow-up of arterial stiffness and LV GLS after COVID-19. Greek researchers I. Ikonomidis et al. examined 70 patients (54.5 years) 4 and 12 months after the diagnosis of COVID-19 and 70 individuals without COVID-19 matched by basic clinical characteristics [13]. The mean values of carotid – femoral PWV in the group after COVID-19 decreased insignificantly in the dynamics (12.09 and 11.19 m / s, $p = 0.883$), but still there was a trend toward higher values than in the control group (11.19 vs. 10.04 m / s, $p = 0.057$). Twelve months after COVID-19, LV GLS values showed a trend toward improvement compared to values at 4 months (–19.55 vs. –20.32%, $p = 0.069$), although they remained lower than in the control group (–20.32 vs. –21.98%, $p = 0.003$) [13].

We also found an insignificant improvement in LV GLS 12 months after COVID-19, and its value was closer to the data of group of I. Ikonomidis et al. 4 months after COVID-19 infection. This can probably be associated with a more severe course of COVID-19 in our patients: in the acute period, they all required hospitalization and 8.5% of them required mechanical ventilation, while in 34.3% of patients in the study by I. Ikonomidis et al., the course of the disease was mild and did not require hospitalization, and none of the Greek patients required mechanical ventilation. The LV GLS values obtained in our study can be attributed to the so-called grey zone, when the values can be regarded as both normal and pathological (LV GLS from –18% to –20%) [11]. It should be noted that according to the Greek researchers' data, the RV function parameters significantly improved, and one year after COVID-19 reached the parameters of the control group [13], which is fully consistent with our results.

The clinical significance of our study lies in identifying the negative dynamics of LV diastolic function in the long term after a complicated course of COVID-19. The assessment of arterial stiffness and LV diastolic function in this population may be an important prognostic factor and a marker of an increased risk of cardiovascular complications and thus will help identify a group of patients who need additional measures of secondary prevention.

A limitation of the study is the lack of data on arterial stiffness, LV longitudinal strain, and diastolic function before COVID-19 and during the acute period of the disease. It should be taken into account that the identified disorders, in addition to the direct effect of the virus, may be caused by its indirect effect through the development of new and aggravation of already existing cardiovascular diseases. In addition, our sample is limited to individuals with optimal Echo imaging.

CONCLUSION

Patients with optimal visualization on echocardiography one year after COVID-19 pneumonia, compared with the results of the examination after 3 months, have worsening parameters of LV diastolic

function. LV GLS was within the "grey zone" and did not change significantly. An improvement in vascular stiffness was noted, associated with an improvement in the longitudinal strain of LV basal segments.

REFERENCES

1. Mottram P.M., Haluska B.A., Leano R., Carlier S., Case C., Marwick T.H. Relation of arterial stiffness to diastolic dysfunction in hypertensive heart disease. *Heart*. 2005;91(12):1551–1556. DOI: 10.1136/hrt.2004.046805.
2. Çiftel M., Ateş N., Yılmaz O. Investigation of tndothelial dysfunction and arterial stiffness in multisystem inflammatory syndrome in children. *Eur. J. Pediatr*. 2022;181(1):91–97. DOI: 10.1007/s00431-021-04136-6.
3. Kim H.L., Seo J.B., Chung W.Y., Kim S.H., Kim M.A., Zo J.H. Independent association between brachial-ankle pulse wave velocity and global longitudinal strain of left ventricle. *Int. J. Cardiovasc. Imaging*. 2015;31(8):1563–1570. DOI: 10.1007/s10554-015-0744-5.
4. Hwang J.W., Kang S.J., Lim H.S., Choi B.J., Choi S.Y., Hwang G.S. et al. Impact of arterial stiffness on regional myocardial function assessed by speckle tracking echocardiography in patients with hypertension. *J. Cardiovasc Ultrasound*. 2012;20(2):90–96. DOI: 10.4250/jcu.2012.20.2.90.
5. Zota I.M., Stătescu C., Sascău R.A., Roca M., Anghel L., Maștaleru A. et al. Acute and Long-Term Consequences of COVID-19 on Arterial Stiffness-A Narrative Review. *Life (Basel)*. 2022;12(6):781. DOI: 10.3390/life12060781.
6. Ayres J.S. A metabolic handbook for the COVID-19 pandemic. *Nat. Metab*. 2020;2(7):572–585. DOI: 10.1038/s42255-020-0237-2.
7. Richardson S., Hirsch J.S., Narasimhan M., Crawford J.M., McGinn T., Davidson K.W. et al. Presenting characteristics, comorbidities, and outcomes among 5700 patients hospitalized with COVID-19 in the New York City Area. *JAMA*. 2020;323(20):2052–2059. DOI: 10.1001/jama.2020.6775.
8. Liberati A., Altman D.G., Tetzlaff J., Mulrow C., Gøtzsche P.C., Ioannidis J.P.A. et al. The PRISMA Statement for Reporting Systematic Reviews and Meta-Analyses of Studies That Evaluate Healthcare Interventions: Explanation and Elaboration. *BMJ*. 2009;339:b2700. DOI: 10.1136/bmj.b2700.
9. Ikonomidis I., Katsanos S., Triantafyllidi H., Parissis J., Tzortzis S., Pavlidis G. et al. Pulse wave velocity to global longitudinal strain ratio in hypertension. *Eur. J. Clin. Invest*. 2019;49(2):e13049. DOI: 10.1111/eci.13049.
10. Alcidi G.M., Esposito R., Evola V., Santoro C., Lembo M., Sorrentino R., Lo Iudice F. et al. Normal reference values of multilayer longitudinal strain according to age decades in a healthy population: A single-centre experience. *Eur. Heart J. Cardiovasc. Imaging*. 2018;19(12):1390–1396. DOI: 10.1093/ehjci/jex306.
11. Lang R.M., Badano L.P., Mor-Avi V., Afilalo J., Armstrong A., Ernande L. et al. Recommendations for cardiac chamber quantification by echocardiography in adults: an update from the American Society of Echocardiography and the European Association of Cardiovascular Imaging. *J. Am. Soc. Echocardiogr*. 2015;28(1):1–39.e14. DOI: 10.1016/j.echo.2014.10.003.
12. Shirokov N.E., Yaroslavskaya E.I., Krinochkin D.V., Musikhina N.A., Petelina T.I., Osokina N.A. Relationship between latent left ventricular contractile dysfunction and signs of immune inflammation in patients with COVID-19 pneumonia. *Cardiovascular Therapy and Prevention*. 2023;22(3):3434 (in Russ.).
13. Ikonomidis I., Lambadiari V., Mitrakou A., Kountouri A., Katogiannis K., Thymis J. et al. Myocardial work and vascular dysfunction are partially improved at 12 months after COVID-19 infection. *Eur. J. Heart Fail*. 2022;24(4):727–729. DOI: 10.1002/ejhf.2451.

Authors' contribution

Yaroslavskaya E.I. – conception and design, justification of the manuscript, critical revision of the manuscript for important intellectual content. Shirokov N.E., Krinochkin D.V. – analysis and interpretation of echocardiography data. Migacheva A.V. – analysis and interpretation of arterial stiffness parameters. Korovina I.O. – analysis and interpretation of the pulmonologist examination data, computed tomography of the lungs. Osokina N.A. – analysis and interpretation of the echocardiography data. Sapozhnikova A.D. – statistical data analysis. Petelina T.I. – final approval of the manuscript for publication.

Authors' information

Yaroslavskaya Elena I. – Dr. Sci. (Med.), Head of Instrumental Diagnostics Laboratory, Scientific Department of Instrumental Research Methods, Tyumen Cardiology Research Center, Tomsk NRMC, Tyumen, yaroslavskayae@gmail.com, http://orcid.org/0000-0003-1436-8853

Shirokov Nikita E. – Cand. Sci. (Med.), Researcher, Instrumental Diagnostics Laboratory, Scientific Department of Instrumental Research Methods, Tyumen Cardiology Research Center, Tomsk NRMC, Tyumen, shirokovne@infarkta.net, http://orcid.org/0000-0002-4325-2633

Krinochkin Dmitry V. – Cand. Sci. (Med.), Senior Researcher, Instrumental Diagnostics Laboratory, Scientific Department of Instrumental Research Methods, Tyumen Cardiology Research Center, Tomsk NRMC, Tyumen, krin@infarkta.net, http://orcid.org/0000-0003-4993-056X

Migacheva Anastasia V. – Research Assistant, Instrumental Diagnostics Laboratory, Scientific Department of Instrumental Research Methods, Tyumen Cardiology Research Center, Tomsk NRMC, Tyumen, MigachevaAV@infarkta.net, http://orcid.org/0000-0002-0793-2703

Korovina Irina O. – Pulmonologist, Tyumen Regional Clinical Hospital No. 1, Tyumen, ORCID: 0000-0002-8146-459X

Osokina Nadezhda A. – Junior Researcher, Instrumental Diagnostics Laboratory, Scientific Department of Instrumental Research Methods, Tyumen Cardiology Research Center, Tomsk NRMC, Tyumen, osokina569@gmail.com, http://orcid.org/0000-0002-3928-8238

Sapozhnikova Anastasia D. – Research Assistant, Instrumental Diagnostics Laboratory, Scientific Department of Instrumental Research Methods, Tyumen Cardiology Research Center, Tomsk NRMC, Tyumen, osokina569@gmail.com, http://orcid.org/0000-0003-0961-2348.

Petelina Tatiana I. – Dr. Sci. (Med.), Deputy Director for Research, Tyumen Cardiology Research Center, Tomsk NRMC, Tyumen, Petelina@infarkta.net, http://orcid.org/0000-0001-6251-4179.

(✉) **Yaroslavskaya Elena I.,** yaroslavskayae@gmail.com

Received 29.03.2023;
approved after peer review 28.09.2023;
accepted 16.11.2023

УДК 616.894-053.8-02:616.89-008.45/.48
https://doi.org/10.20538/1682-0363-2024-1-105-115

The role of neuropeptides (oxytocin, vasopressin, neuropeptide S) in the development of cognitive impairment in Alzheimer's disease

Avliyakulyeva A.M.[1], Kindyakova E.K.[1], Kuzmina S.V.[2], Gorina Y.V.[1, 3], Lopatina O.L.[1, 3]

[1] *V.F. Voino-Yasentsky Krasnoyarsk State Medical University*
1, Partizana Zheleznyaka Str., Krasnoyarsk, 660022, Russian Federation

[2] *Kazan State Medical University*
49, Butlerova Str., Kazan, 420012, Russian Federation

[3] *School of Fundamental Biology and Biotechnology, Siberian Federal University*
79, Svobodny Av., Krasnoyarsk, 660041, Russian Federation

ABSTRACT

Every year, the number of people diagnosed with Alzheimer's disease is rapidly increasing. Despite numerous studies, it was not possible to select a therapy that would reliably slow down the course of the disease and result in its complete cure. In this case, any consideration of the issue related to the search for drugs to eliminate cognitive and psychoemotional disorders in Alzheimer's disease is a pressing problem that deserves special attention.

We collected articles from the PubMed database published over the past 10 years. The aim of this review was to analyze the latest experimental data and results regarding the relationship between Alzheimer's disease and the activity of neuropeptides, such as oxytocin, vasopressin, and neuropeptide S, and describing the effects that occur upon their administration. This will allow for a more complete understanding of the problem and update information on this issue. The ability of neuropeptides to restore impaired cognitive functions in an animal model of Alzheimer's disease is examined in more detail.

Detailed information on the relationship and positive effect of the studied neuropeptides on Alzheimer's disease allows to consider these neuropeptides as potential drugs for the treatment of this disease.

Keywords: Alzheimer's disease, neuropeptides, oxytocin, vasopressin, neuropeptide S

Conflict of interest. The authors declare the absence of obvious or potential conflicts of interest related to the publication of this article.

Source of financing. The study was performed within the Mirror laboratories project at the National Research University "Higher School of Economics" (Saint Petersburg) (Research collaboration agreement between F. Voino-Yasentsky Krasnoyarsk State Medical University and Higher School of Economics No. cc/6.18.1-11.1/220922-33 of 22.09.2022).

For citation: Avliyakulyeva A.M., Kindyakova E.K., Kuzmina S.V., Gorina Y.V., Lopatina O.L. The role of neuropeptides (oxytocin, vasopressin, neuropeptide S)in the development of cognitive impairment in Alzheimer's disease. *Bulletin of Siberian Medicine.* 2024;23(1):105–115. https://doi.org/10.20538/1682-0363-2024-1-105-115.

✉ *Avliyakulyeva Aylar M.,* ailara@bk.ru

Роль нейропептидов (окситоцин, вазопрессин, нейропептид S) в развитии когнитивных нарушений при болезни Альцгеймера

Авлиякулыева А.М.[1], Киндякова Е.К.[1], Кузьмина С.В.[2], Горина Я.В.[1, 3], Лопатина О.Л.[1, 3]

[1] *Красноярский государственный медицинский университет (КрасГМУ) им. проф. В.Ф. Войно-Ясенецкого Россия, 660022, г. Красноярск, ул. Партизана Железняка, 1*

[2] *Казанский государственный медицинский университет (Казанский ГМУ) Россия, 420012, г. Казань, ул. Бутлерова, 49*

[3] *Институт фундаментальной биологии и биотехнологии (ИФБиБТ), Сибирский федеральный университет (СФУ) Россия, 660041, г. Красноярск, пр. Свободный, 79*

РЕЗЮМЕ

С каждым годом количество людей с диагностированной болезнью Альцгеймера стремительно увеличивается. Несмотря на многочисленные исследования, подобрать терапию, которая бы надежно замедляла течение болезни и приводила бы к полному излечению, не удалось. В таком случае любое рассмотрение вопроса, касающееся поиска лекарственных веществ для коррекции когнитивных и психоэмоциональных нарушений при развитии болезни Альцгеймера, является актуальной проблемой, заслуживающей особого внимания.

Проводился сбор статей из базы данных PubMed, опубликованных за последние 10 лет. Целью настоящего обзора является анализ последних экспериментальных данных и результатов, касающихся взаимосвязи между болезнью Альцгеймера и активностью таких нейропептидов, как окситоцин, вазопрессин и нейропептид S, а также описывающих эффекты, которые возникают при их введении. Это позволит более полно понять проблематику и обеспечит актуализацию сведений по данному вопросу. Наиболее подробно рассматривается способность нейропептидов восстанавливать нарушенные когнитивные функции у лабораторных животных с моделью болезни Альцгеймера.

Детально изложенная информация о наличии взаимосвязи и положительном влиянии изучаемых нейропептидов на болезнь Альцгеймера позволяет рассматривать данные нейропептиды в качестве потенциальных лекарственных препаратов для лечения данного заболевания.

Ключевые слова: болезнь Альцгеймера, нейропептиды, окситоцин, вазопрессин, нейропептид S

Конфликт интересов. Авторы заявляют об отсутствии явных и потенциальных конфликтов интересов при проведении исследования.

Источники финансирования. Работа выполнена в рамках проекта «Зеркальные лаборатории» Национального исследовательского университета «Высшая школа экономики» (Санкт-Петербург) (соглашение о научном сотрудничестве ФГБОУ ВО КрасГМУ им. проф. В.Ф. Войно-Ясенецкого Минздрава России с НИУ ВШЭ № сс/6.18.1-11.1/220922-33 от 22.09.2022).

Для цитирования: Авлиякулыева А.М., Киндякова Е.К., Кузьмина С.В., Горина Я.В., Лопатина О.Л. Роль нейропептидов (окситоцин, вазопрессин, нейропептид S) в развитии когнитивных нарушений при болезни Альцгеймера. *Бюллетень сибирской медицины.* 2024;23(1):105–115. https://doi.org/10.20538/1682-0363-2024-1-105-115.

INTRODUCTION

Alzheimer's disease (AD) is the most common neurodegenerative disorder. Current estimates indicate that 44 million people worldwide are diagnosed with dementia at present. It is predicted that by 2050, this number will increase by more than 3 times as the population ages. The prevalence of AD increases approximately twofold every 5 years after the age of 65 [1].

Although significant efforts have been made to study this disease, it is difficult to treat due to its complex multifactorial pathological physiology. To date, there is no therapy that has been proven to influence the pathology and course of the disease. Currently, approved drugs provide only temporary symptomatic relief, so the search and development of new drugs for the treatment of AD is underway [1, 2].

This disease is caused by hereditary mutations in the genes encoding the transmembrane amyloid precursor protein (APP), or the proteins presenilin 1 and presenilin 2 [3], associated with Abeta (Aβ) metabolism, which is the main biomarker of AD [4].

Early diagnosis and proper treatment of the disease can significantly improve the quality of life and functioning of patients, as well as reduce the severity of cognitive (memory loss, disorientation) and neurobehavioral disorders (depression, apathy, delusions, hallucinations, sleep disorders). Cholinesterase inhibitors (Donepezil, Galantamine, and Rivastigmine) and a glutamate NMDA receptor antagonist (Memantine) are drugs approved by clinical guidelines for the basic treatment of AD [5, 6]. Unfortunately, these drugs cannot provide a full recovery, but can only reduce the severity of cognitive and behavioral disorders. This is the reason for the active search for new medicinal substances that would not only slow down the development and severity of symptoms, but also provide targeted effects on key links in the pathogenesis of the disease.

HYPOTHALAMIC HORMONES: OXYTOCIN AND VASOPRESSIN

Vasopressin (AVP) and oxytocin (OXT) are two related neuropeptides that differ in only two amino acids. They are evolutionarily ancient and highly conserved neuropeptides in phylogeny that regulate a wide range of physiological functions [7].

Neuropeptides are produced mainly in the supraoptic nuclei (SON) and paraventricular nuclei (PVN) of the hypothalamus [8] and are transported to the posterior pituitary gland, where they are stored and ultimately released into the bloodstream, exerting an endocrine effect [9]. They are also synthesized in some other cells of the central nervous system and peripheral organs. Thus, AVP is additionally synthesized by cells of the suprachiasmatic nucleus, bed nucleus of the stria terminalis, and medial nucleus of the amygdala [10]. OXT is also produced by neurons of the peripheral nervous system: in osteoblasts of the bone marrow, liver, in nerve fibers of the gastrointestinal tract, subcutaneous adipose tissue [11], cardiomyocytes, adipose tissue, beta and alpha cells of the islets of Langerhans in the pancreas [12].

An interesting fact is that magnocellular neurons of the SON and PVN can release OXT and AVP from non-synaptic areas such as dendrites [13] via bulk transmission. This type of transmission results in a much more diffuse signal, which can potentially affect a large number of neurons within the intercellular space, since the distance over which such a signal propagates significantly exceeds the size of the synaptic cleft. The release of OXT and AVP is caused by various osmotic, reproductive, and social stimuli. The excretion of OXT and AVP occurs during childbirth as well as aggressive and social interactions. OXT is also released during mating, lactation, and in response to subtler social stimuli, including vocalization, eye contact, and touch [14].

When released into the systemic circulation, neuropeptides have an endocrine effect. Thus, AVP regulates salt and water balance, and OXT stimulates uterine contraction and lactation [9]. In addition to endocrine effects, these neuropeptides play an important role in the organization of central processes. The OXT/ A VP system is involved in the formation of social, working, spatial, and episodic memory, mediated by the CA2 and CA3 regions of the hippocampus, the amygdala, and the prefrontal cortex [15]. These neuropeptides model important processes in the hippocampus, such as neuronal excitability, synaptic plasticity, and social recognition memory. They influence not only memory formation, but also regulate social learning and behavior, including peer recognition, social attachment, and parental behavior (Fig. 1).

Currently, it is known that one receptor for OXT (OXTR) and three receptors for AVP (AVPR1A, AVPR1B, AVPR2) exist. These receptors, with the exception of AVPR2, are widely distributed in all regions of the hippocampus, especially in the CA2 region, which is involved in both encoding and retrieval of social memory and development of social aggression [16]. The OXT / AVP system is plastic, and its functions depend on the context, which includes life experience and the cause of stress or injury [17].

There is compelling evidence of the neurotropic effects of OXT. For example, administration of OXT stimulates neurogenesis in the hippocampus, whereas deletion of OXTR in mice causes irreversible pathological changes in the hippocampus. Selective removal of OXTR within adult-borne granule cells (abGCs) disrupts gene expression programs that influence dendritic growth and spine development. As a result, cells with underdeveloped synapses and impaired function are formed [18].

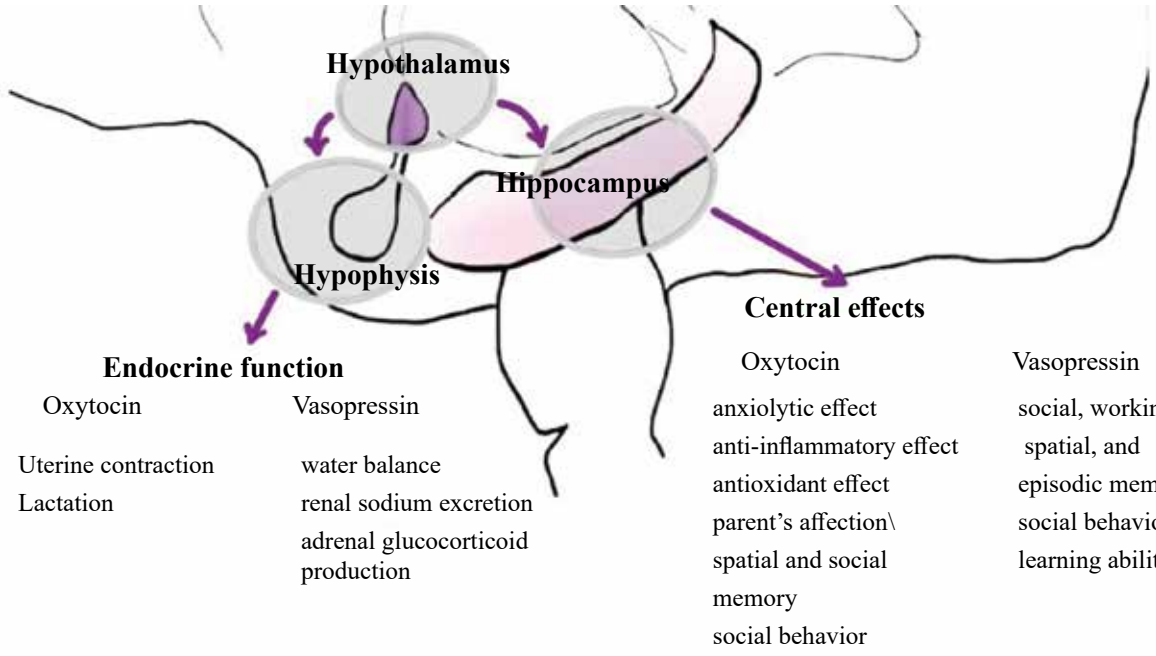

Fig. 1. Central and peripheral effects of oxytocin and vasopressin on the body

ALZHEIMER'S DISEASE AND SOCIAL COMMUNICATION DISORDERS

Characteristic signs of behavior during the development of AD and dementia are agitation and aggressive and impulsive behavior, whose manifestation only intensifies as the disease progresses. These symptoms are associated with disturbances in emotional processing, especially inability to perceive and recognize the emotions of others [19]. All this leads to impaired social cognition and difficulties in social interaction (Fig. 2).

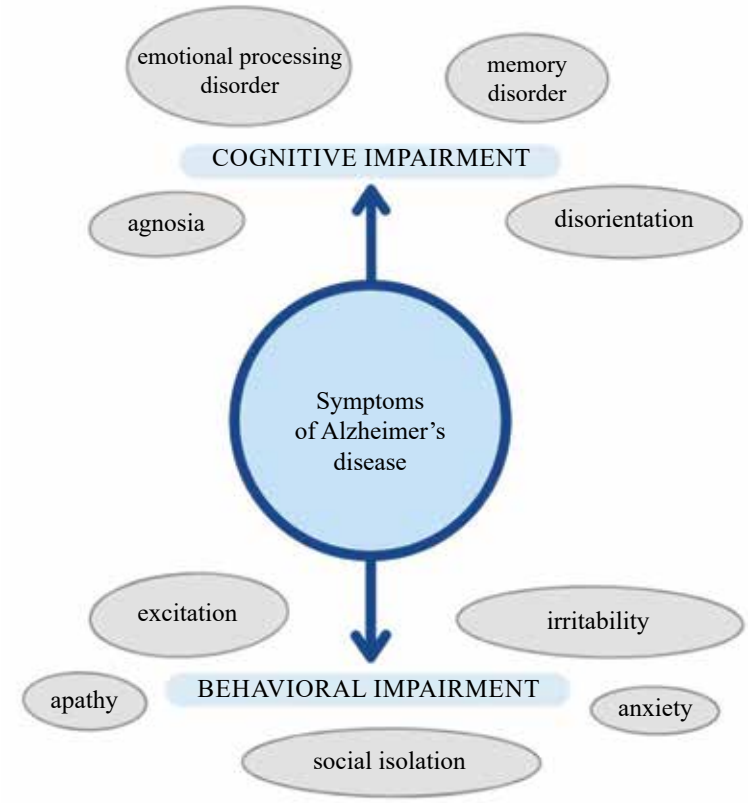

Fig. 2. Symptoms of Alzheimer's disease

Most studies were focused on assessing cognitive function, but the assessment of psychoemotional impairment may be a sensitive method for studying the clinical state in AD, which may lead to the introduction of new and effective treatment methods [20]. There are large-scale studies that support the effectiveness of psychosocial interventions to slow the progression of cognitive impairment in patients with AD. These psychosocial interventions include reminiscence therapy, art therapy, a walking program, and much more [21].

THE RELATIONSHIP BETWEEN ALZHEIMER'S DISEASE AND NEUROPEPTIDES

The functioning of the OXT / AVP system alters in neurodegenerative diseases. Based on this, it was suggested that these neuropeptides may play an important role in the development of social, emotional, and cognitive dysfunction in AD.

Oxytocin and Alzheimer's disease

OXT is considered to be a potential drug for the treatment of AD, since various studies have found that this neuropeptide has a wide range of effects that can lead to positive changes in the complex therapy of the disease. Social recognition memory allows a person to remember relatives and identify them as already familiar. This ability is important for normal social behavior and formation and stability of social interactions. One of the symptoms of AD is inability to recognize people patients know, which creates additional difficulties for patients and caregivers.

Newman's social behavior neural network (SBNN) hypothesis proposes interconnections between brain regions, such as the amygdala, bed nucleus of the stria terminalis, lateral septum, medial preoptic area, ventromedial hypothalamus, and anterior hypothalamus. The SBNN is believed to control various types of motivated social behavior, including defensive aggression, social recognition memory, parental behavior, and social communication. It is important to note that OXT / AVP and their receptors are found in all regions of the SBNN, which indicates their involvement in the regulation of social behavior [22].

OXT plays an important role in the regulation of social recognition memory during social interactions, whereas conditional deletion of OXTR in the CA2 / CA3a regions of the hippocampus impairs the formation of social recognition memory. In the experiment, Y. T. Lin et al. compared the performance of wild-type mice and OXTR knockout mice in a three-chamber sociability test. A group of knockout mice had a defect in retaining long-term social recognition memory, since 7 days after training their memory deteriorated significantly. The data obtained suggest that OXTR signaling is particularly important for maintaining long-term social recognition memory [23].

The results of another study show the importance of OXTR for the identification of various social stimuli, not only in the CA2 / CA3 region, but also in the dentate gyrus. When a Cre-expressing virus was injected into the anterior dentate gyrus of 8-week-old male mice with a conditional knockout of OXTR, an impairment in the ability to discriminate social stimuli was observed. The animals did not show preference for a new individual and had discrimination coefficients significantly lower than those in the control group [24].

Long-term potentiation (LTP) underlies learning and memory formation. In neurodegeneration and aging, LTP decreases, which is manifested by a decline in human cognitive abilities. Due to the accumulation of Aβ in the brain, suppression of LTP in the hippocampus is observed in AD. J. Takahashi et al. studied synaptic plasticity in hippocampal slices of male mice 5–7 weeks old. OXT was found to reverse the LTP impairment caused by perfusion of Aβ 25–35 into the hippocampus. This effect was mediated by OXTR, since LTP restoration was impaired when an OXTR antagonist was administered. The authors also associated this effect with phosphorylation of ERK kinase and the influx of Ca^{2+} ions through Ca^{2+}-permeable AMPA receptors, since the addition of their antagonists to the hippocampal slices impaired the ability of oxytocin to restore LTP [25].

A number of studies confirm the positive effect of OXT on spatial memory. Intracerebroventricular administration of native OXT into the ventricle and intranasal administration of an OXT derivative to mice (ddY line) contributed to the restoration of spatial memory in the Y-maze and the Morris water maze, impairments in which were caused by the administration of Aβ 25–35. This improvement was induced by OXT, since administration of the OXTR antagonist led to inhibition of improvements in spontaneous alternation and deterioration of spatial memory. The role of the neuropeptide may be associated with the restoration of spatial memory impairments specifically in neurodegenerative conditions [26].

Intracerebroventricular administration is impractical and somewhat traumatic, and neuropeptides administered in this way have a low ability to penetrate

the blood – brain barrier [26]. Due to these disadvantages, alternative intranasal administration appears to be more promising due to its non-invasive nature and ease of use.

A number of studies have proven that intranasal administration of OXT will facilitate the penetration of the peptide into the brain in the required amount. A study of the pharmacokinetics of the neuropeptide after intranasal administration showed that more than 95% of OXT was transported to the brain directly from the nasal cavity [27]. The peptide penetrates the brain by direct transport of the substance through the olfactory and trigeminal nerve fibers innervating the nasal cavity [28].

S.O. El-Ganainy et al. studied the effect of intranasal administration of OXT on rats (Sprague – Dawley line) with a model of AD. In the Morris water maze test, a decrease in the latent period was observed, which indicated that rats had a high ability of spatial learning after treatment with OXT. There was a decrease in Aβ 1–42 in the hippocampus in a group of rats that were treated with OXT in combination with galantamine. OXT treatment also suppressed the activation of caspase-3, which inhibited the process of apoptosis and prevented neuronal death and formation of neurofibrillary tangles. This was consistent with the results of a histopathological study, which noted orderly arrangement of hippocampal pyramidal cells and an improvement in their morphology [29].

Microglia are immune cells in the brain that play a key role in the occurrence of neuroinflammation [30]. Deposition of Aβ, tau protein, and neuronal damage leads to microglial activation, which contributes to the persistence of inflammation and the formation of reactive oxygen species [31]. Activated microglia stimulate neurons to overproduce Aβ, causing synaptic loss and the formation of extracellular plaques and neurofibrillary tangles. This leads to increased activation of microglia [32], and a positive feedback loop is formed that contributes to the development of AD.

Since activated microglia are considered one of the important components in the pathogenesis of AD, it is necessary to search for and study the ability of substances to inhibit their activation, which is what the authors of the following study did. IHC analysis of brain sections from old APP / PS1 mice (with mutations in the amyloid precursor protein and presenilin-1 genes) revealed increased lba-1 (lupus anticoagulant) immunoreactivity in the CA1 region of the hippocampus, which indicated activated microglia. Intranasal administration of OXT to control groups caused a decrease in lba-1 immunoreactivity around amyloid plaques compared to the controls receiving normal saline. When a purified culture of microglia was exposed to Aβ, its activation was observed, accompanied by an increase in lba-1 and CD68 immunoreactivity (cluster of differentiation 68). Treatment of the culture with OXT contributed to the attenuation of microglial activation induced by Aβ [33].

In AD, developing neuroinflammation is characterized by drastically increased production of proinflammatory cytokines (interleukin (IL)-1, IL-6, tumor necrosis factor alpha (TNFα)) and activation of enzymes that synthesize low-molecular inflammatory mediators [34]. It should be noted that there are data supported by experiments on the anti-inflammatory activity of OXT. Pretreatment of microglial cells suppressed the synthesis of proinflammatory cytokines provoked by the administration of lipopolysaccharide. The anti-inflammatory effects of OXT are associated with inhibition of eukaryotic initiation factor-2α (eIF-2α)-targeting kinases. It results in inhibition of the p/eIF2α/ATF4 pathway, decreased expression of TNFα and IL-6, and inhibited activation of inflammasomes, which suppresses the synthesis of IL-1β [35].

When the medial part of the hypothalamus is damaged, the level of OXT mRNA decreased, which led to increased activation of the nuclear factor-κB (NF-κB) pathway and increased expression of TNFα and IL-1β mRNA, which may be the reason for a decrease in anti-inflammatory protection [36]. Pretreatment of primary microglia and BV-2 microglia cells (cells isolated from C57/BL6 mice) with OXT resulted in significant inhibition of lipopolysaccharide-induced microglial activity, as reflected by suppression of the expression and release of cyclooxygenase-2 (COX-2) and inducible synthase nitric oxide (iNOS). During neuroinflammation, proinflammatory cytokines accumulate in glia, which can lead to neuronal damage and progression of neurodegenerative diseases [37]. Due to this, an important element of AD therapy is inhibition of neuroinflammation, which can be achieved through the use of OXT as a drug.

The results of a recent study that revealed the effect of OXT on the generation and deposition of amyloid plaques are worth noting. Mice (APP/PS1 strain) treated with OXT showed a decrease in plaque area and decreased Aβ immunoreactivity in the hippocampus. The neuropeptide also affected the morphology of amyloid plaques. The main groups of mice that received OXT had plaques with a denser core than the control groups [33]. There is a hypothesis that dense-

core plaques have a restriction mechanism, possibly similar to tuberculosis granulomas. With its help, microglia protect the brain from degeneration associated with AD. Highly polymerized and compacted Aβ in the nuclei has a less damaging effect and limits the spread of Aβ oligomers and protofibrils throughout the brain [38].

Since one of the symptoms of AD is increased anxiety, the presence of an anxiolytic effect in OXT makes this neuropeptide even more interesting. The effect of OXT on anxiety levels was studied using the light / dark box test. When the neuropeptide was administered into the PVN of male Wistar rats, a decrease in anxiety was observed. Preliminary infusion of the transient receptor potential channel antagonist SKF96365 into PVN blocked the anxiolytic effect of OXT [39].

Vasopressin and Alzheimer's disease

AVP is known to regulate water balance and blood pressure. It is also a neurotransmitter involved in the modulation of social communication, spatial memory and influencing memory consolidation and retrieval. One of the characteristic symptoms of AD is impaired spatial memory and social recognition memory, which manifest in the form of disorientation and inability to recognize familiar faces. As the results of the study showed, intranasal use of AVP (4–8) for 4 weeks (the main metabolic fragment of AVP, differing in chemical structure, but having a similar effect) significantly improved working and long-term memory in mice with a model of AD (APP/PS1 line), which was proven in the Y-maze test. In addition, a decrease in the latency period was found in the Morris water maze test, which indicates an improvement in spatial memory [40].

The study by C.J. Finton et al. shows the importance of the duration of AVP therapy for a significant effect on spatial memory. The significance of the effect on spatial memory depends on the duration of AVP therapy. Chronic intranasal administration of the neuropeptide showed a positive effect on spatial memory, while a single administration of AVP before testing had no significant effect [41].

The effect of a V1aR antagonist was studied to confirm the relationship between the AVP level and spatial memory. Intraperitoneal administration of SR49059 to Wistar rats prior to the Morris water maze test revealed the effect of AVP on spatial memory and learning. The results of Western blotting and ELISA showed a significant decrease in the expression of AVP and V1aR, which confirms the association between the level of the neuropeptide and spatial memory [42].

In addition to its ability to restore impaired spatial memory, AVP is also important for normal social recognition and formation of social memory. Studies show that blocking AVP receptors, as well as a decrease in the level of this neuropeptide, cause social memory impairment. Thus, mice with OXTR and AVPR1b knockout in hippocampal CA2 pyramidal neurons have impairments of social memory and impaired detection of social novelty [43]. When tested in AVP knockout rats (Brattleboro strain), impairments in recognition of new objects and conditional learning, as well as a decrease in the ability to social discrimination are observed [44].

The hippocampus is one of the key structures associated with learning, memory, and thinking, the activity of which depends on the rate of excitation of neurons in this part of the brain. The neuropeptide is able to modulate the electrophysiological changes caused by Aβ. AVP-induced changes in spontaneous discharges in the hippocampus in the CA1 region may help protect synaptic plasticity and cognitive functions, the impairment of which underlies many neurodegenerative diseases [45].

Social memories are formed partly as a result of information encoding by the hippocampus. The CA2 region of the hippocampus and in particular the AVPR1b expressed there are required for memory formation. In behavioral testing, mice (GENSAT QZ27 line) injected with adeno-associated virus (AAV) and wild-type mice were exposed to an unfamiliar female and re-exposed to the original or new female after a 2-hour retention interval. At the same time, optical stimulation of the nerve endings of PVN neurons innervating CA2 was present or absent in the tests. Optical stimulation during initial contact (memory acquisition) improved social recognition, i.e. the olfactory exploration of the female decreased upon repeated exposure. However, optical stimulation had no effect on the sociability of the mice. Stimulation during subsequent contact (memory recall) did not cause improvement. Administration of the AVPR1b antagonist to CA2 blocked the enhancement of social recognition. This suggests that the AVP $^{PVN \rightarrow CA2}$ pathway, which depends on AVPR1b signaling, promotes the acquisition of new memories, enhancing social memory. The authors of the study suggested that targeted therapy with AVPR1b agonists could become potential treatment for patients with dementia who have reduced social memory [46].

Neuropeptide S and Alzheimer's disease

Neuropeptide S (NPS) is an endogenous peptide in the central nervous system that selectively binds and activates NPS receptors. NPSR mRNA expression occurs throughout the central nervous system, with significant amounts expressed in the olfactory nuclei, thalamus, anterior and posterior hypothalamus, as well as the cortex, amygdala, and hippocampus. The NPS / NPSR system regulates many physiological and pathological functions, including arousal, wakefulness, learning and memory, anxiety, food intake and energy balance, drug addiction and pain. During experiments, it was found that in animals this neuropeptide promotes learning, improves memory, and also reduces anxiety [47].

Mice with AD (APP/PS1 line) showed a noticeable decrease in NPSR in the hippocampal region compared with wild-type mice. It can be assumed that the basis of AD symptoms is a lack of NPS effects, caused by a decrease in the amount of NPSR [48].

Increased anxiety is one of the symptoms of AD. NPS has a powerful anxiolytic effect, which makes it possible to consider it as a potential substance for the treatment of diseases accompanied by anxiety. Characteristic phenotypic features of NPS precursor knockout mouse models include learning and memory deficits, as well as increased anxiety [49]. NPS promotes anxiolysis in the amygdala and its mechanism of action depends on NPSR-mediated phospholipase C signaling. This ability of the neuropeptide is confirmed by the administration of a phospholipase C inhibitor (U73122), which prevents NPS-induced anxiolysis [50].

Scientists have found that the effects of NPS in the PVN are mediated by actions on local OXT neurons. NPS activates a subpopulation of OXT neurons in the PVN, which is confirmed by an increase in the intracellular concentration of Ca^{2+} ions in neurons of this subpopulation and an increase in the release of OXT by somatodendrites in the PVN. In turn, the activated OXT-PVN subpopulation mediates the anxiolytic effect of NPS, which is confirmed by the results of behavioral testing. Pre-administration of an OXTR antagonist blocks NPS-induced anxiolysis [51].

To study the effect of NPS on memory, this neuropeptide was administered once into the lateral ventricle of male Swiss Kunming mice 5 minutes after training. When tested on day 3 after training, the test group spent significantly more time with the new non-social object than the control group. Thus, the introduction of NPS made it possible to prolong object recognition memory.

As is known, AD is accompanied by a progressive decline in memory; when Aβ 1–42 was administered to test mice, a significant impairment in object recognition memory was observed. The progression of this condition was eliminated by the administration of NPS [52]. Research by R.W. Han et al. showed that infusion of NPS into the basolateral amygdala of Kunming mice after training improved long-term non-social object recognition memory, which was reduced by intraperitoneal administration of propranolol [53].

NPS plays a key role in the regulation of memory and learning in rodents [54]. Inhibition of NPSR activation causes impairment of olfactory spatial memory. Endogenous NPS plays an important role in the regulation of olfactory spatial memory, possibly due to the activation of NPSR-bearing neurons in the olfactory cortex and subicular complex of the hippocampus, but the precise mechanisms involved in olfactory spatial memory impaired by NPSR antagonists have yet to be determined [55].

P. Zhao et al. proved the influence of NPS on the key pathogenetic links of AD. The effect of NPS was analyzed in both wild-type mice and mice (APP/PS1 line) with a genetic model of AD. Eight-month-old mice were continuously injected intravenously with NPS for 2 weeks, and then hippocampal ELISA was performed. According to the results of the analysis, a decrease in the intensity of formation and subsequent deposition of Aβ plaques was observed due to a decrease in γ-secretase activity and APP phosphorylation at Thr668 compared to the ELISA results of the control group of mice that were intravenously injected with normal saline. Moreover, when performing the Morris water maze test, a gradual decrease in the latency period was noted during the five days of training. This suggests that NPS can not only improve spatial memory in wild-type mice, but also effectively restore cognitive impairment and significantly increase the number of active neurons in the hippocampus in mice.

The neuropeptide normalized the expression of synapsin I and PSD95 in the hippocampus, suggesting that NPS probably restores memory deficits by reversing impairments in hippocampal synaptic plasticity [48]. Together, these experimental data make it possible to consider NPS as a potential candidate for the treatment of AD.

CONCLUSION

All studies discussed in this review article have shown a relationship between the action of neuropeptides and the pathogenesis of AD. The exact mechanism of the potential therapeutic effect of neuropeptides has yet to be revealed, but the trend in the scientific field and the number of modern and fairly large publications suggest that this may happen in the nearest future.

When studying such a complex issue, it is important to conduct not one, but a series of studies, to compare the effects of treatment with neuropeptides and drugs that are currently included in clinical guidelines for the treatment of AD. It is also necessary to conduct a battery of behavioral tests for a more thorough understanding of the condition of the test animals and to perform tests at different periods of time with the possibility of further comparison of previously obtained and newer results with each other to determine the delayed effects of treatment.

REFERENCES

1. Lane C.A., Hardy J., Schott J.M. Alzheimer's disease. *Eur. J. Neurol*. 2018;25(1):59–70. DOI: 10.1111/ene.13439.
2. Athar T., Al Balushi K., Khan S.A. Recent advances on drug development and emerging therapeutic agents for Alzheimer's disease. *Mol. Biol. Rep.*2021;48(7):5629–5645. DOI: 10.1007/s11033-021-06512-9.
3. Breijyeh Z., Karaman R. Comprehensive Review on Alzheimer's Disease: Causes and Treatment. *Molecules.* 2020;25(24):5789. DOI: 10.3390/molecules25245789.
4. Mantzavinos V., Alexiou A. Biomarkers for Alzheimer's disease diagnosis. *Curr. Alzheimer Res.* 2017;14(11):1149–1154. DOI: 10.2174/1567205014666170203125942.
5. Grossberg G.T., Tong G., Burke A.D., Tariot P.N. Present algorithms and future treatments for Alzheimer's disease. *J. Alzheimers Dis*. 2019;67(4):1157–1171. DOI: 10.3233/JAD-180903.
6. Briggs R., Kennelly S.P., O'Neill D. Drug treatments in Alzheimer's disease. *Clin. Med. (Lond.).* 2016;16(3):247–253. DOI: 10.7861/clinmedicine.16-3-247.
7. Bordt E.A., Smith C.J., Demarest T.G., Bilbo S.D., Kingsbury M.A. Mitochondria, oxytocin, and vasopressin: unfolding the inflammatory protein response. *Neurotoxicity Res*. 2019;36(2):239–256. DOI: 10.1007/s12640-018-9962-7.
8. Szczepanska-Sadowska E., Wsol A., Cudnoch-Jedrzejewska A., Czarzasta K., Żera T. Multiple aspects of inappropriate action of renin-angiotensin, vasopressin, and oxytocin systems in neuropsychiatric and neurodegenerative diseases. *J. Clin. Med*. 2022;11(4):908. DOI: 10.3390/jcm11040908.
9. Caldwell H.K. Oxytocin and vasopressin: powerful regulators of social behavior. *Neuroscientist*. 2017;23(5):517–528. DOI: 10.1177/1073858417708284.
10. Dumais K.M., Veenema A.H. Vasopressin and oxytocin receptor systems in the brain: Sex differences and sex-specific regulation of social behavior. *Front. Neuroendocrinol*. 2016;40:1–23. DOI: 10.1016/j.yfrne.2015.04.003.
11. McCormack S.E., Blevins J.E., Lawson E.A. Metabolic Effects of oxytocin. *Endocr. Rev.* 2020;41(2):121–145. DOI: 10.1210/endrev/bnz012.
12. Kerem L., Lawson E.A. The effects of oxytocin on appetite regulation, food intake and metabolism in humans. *Int. J. Mol. Sci.* 2021;22(14):7737. DOI: 10.3390/ijms22147737.
13. Ludwig M., Apps D., Menzies J., Patel J.C., Rice M.E. Dendritic release of neurotransmitters. *Compr. Physiol.* 2016;7(1):235–252. DOI: 10.1002/cphy.c160007.
14. Johnson Z.V., Young L.J. Oxytocin and vasopressin neural networks: Implications for social behavioral diversity and translational neuroscience. *Neurosci. Biobehav. Rev*. 2017;76(Pt.A):87–98. DOI: 10.1016/j.neubiorev.2017.01.034.
15. Abramova O., Zorkina Y., Ushakova V., Zubkov E., Morozova A., Chekhonin V. The role of oxytocin and vasopressin dysfunction in cognitive impairment and mental disorders. *Neuropeptides*. 2020;83:102079. DOI: 10.1016/j.npep.2020.102079.
16. Cilz N.I., Cymerblit-Sabba A., Young W.S. Oxytocin and vasopressin in the rodent hippocampus. *Genes Brain Behav*. 2019;18(1):e12535.DOI: 10.1111/gbb.12535.
17. Carter C.S., Kenkel W.M., MacLean E.L., Wilson S.R., Perkeybile A.M., Yee J.R. et al. Is oxytocin "nature's medicine"? *Pharmacol. Rev.* 2020;72(4):829–861. DOI: 10.1124/pr.120.019398.
18. Pekarek B.T., Kochukov M., Lozzi B., Wu T., Hunt P.J., Tepe B. et al. Oxytocin signaling is necessary for synaptic maturation of adult-born neurons. *Genes Dev*. 2022;36(21-24):1100–1118. DOI: 10.1101/gad.349930.122.
19. Bidzan L., Bidzan M., Pąchalska M. Aggressive and impulsive behavior in Alzheimer's disease and progression of dementia. *Med. Sci. Monit.* 2012;18(3):CR182–189. DOI: 10.12659/msm.882523.
20. Cárdenas J., Blanca M.J., Carvajal F., Rubio S., Pedraza C. Emotional processing in healthy ageing, mild cognitive impairment, and Alzheimer's disease. *Int. J. Environ. Res. Public Health*. 2021;18(5):2770. DOI: 10.3390/ijerph18052770.
21. Duan Y., Lu L., Chen J., Wu C., Liang J., Zheng Y. et al. Psychosocial interventions for Alzheimer's disease cognitive symptoms: a Bayesian network meta-analysis. *BMC Geriatr*. 2018;18(1):175. DOI: 10.1186/s12877-018-0864-6.
22. Caldwell H.K., Albers H.E. Oxytocin, vasopressin, and the motivational forces that drive social behaviors. *Curr. Top Behav. Neurosci*. 2016;27:51–103. DOI: 10.1007/7854_2015_390.
23. Lin Y.T., Hsieh T.Y., Tsai T.C., Chen C.C., Huang C.C., Hsu K.S. Conditional deletion of hippocampal CA2/CA3a oxytocin receptors impairs the persistence of long-term social recognition memory in mice. *J. Neurosci*. 2018;38(5):1218–1231. DOI: 10.1523/JNEUROSCI.1896-17.2017.
24. Raam T., McAvoy K.M., Besnard A., Veenema A.H., Sahay A. Hippocampal oxytocin receptors are necessary for discrimination of social stimuli. *Nat. Commun*. 2017;8(1):2001. DOI: 10.1038/s41467-017-02173-0.
25. Takahashi J., Yamada D., Ueta Y., Iwai T., Koga E., Tanabe M. et al. Oxytocin reverses Aβ-induced impairment of hippocampal synaptic plasticity in mice. *Biochem. Bio-*

phys. Res. Commun. 2020;528(1):174–178. DOI: 10.1016/j.bbrc.2020.04.046.
26. Takahashi J., Ueta Y., Yamada D., Sasaki-Hamada S., Iwai T., Akita T. et al. Intracerebroventricular administration of oxytocin and intranasal administration of the oxytocin derivative improve β-amyloid peptide (25-35)-induced memory impairment in mice. *Neuropsychopharmacol. Rep*. 2022;42(4):492–501.DOI: 10.1002/npr2.12292.
27. Tanaka A., Furubayashi T., Arai M., Inoue D., Kimura S., Kiriyama A. et al. Delivery of oxytocin to the brain for the treatment of autism spectrum disorder by nasal application. *Mol. Pharm*. 2018;15(3):1105–1111. DOI: 10.1021/acs.molpharmaceut.7b00991.
28. Quintana D.S., Lischke A., Grace S., Scheele D., Ma Y., Becker B. Advances in the field of intranasal oxytocin research: lessons learned and future directions for clinical research. *Mol. Psychiatry*. 2021;26(1):80–91. DOI: 10.1038/s41380-020-00864-7.
29. El-Ganainy S.O., Soliman O.A., Ghazy A.A., Allam M., Elbahnasi A.I., Mansour A.M. et al. Intranasal oxytocin attenuates cognitive impairment, β-amyloid burden and tau deposition in female rats with Alzheimer's disease: interplay of ERK1/2/GSK3β/caspase-3. *Neurochem. Res*. 2022;47(8):2345–2356. DOI: 10.1007/s11064-022-03624-x.
30. Lemke G., Huang Y. The dense-core plaques of Alzheimer's disease are granulomas. *J. Exp. Med*. 2022;219(8):e20212477. DOI: 10.1084/jem.20212477.
31. Simpson D.S.A., Oliver P.L. ROS generation in microglia: understanding oxidative stress and inflammation in neurodegenerative disease. *Antioxidants (Basel)*. 2020;9(8):743. DOI: 10.3390/antiox9080743.
32. Edler M.K., Mhatre-Winters I., Richardson J.R. Microglia in Aging and Alzheimer's Disease: A Comparative Species Review. *Cells*. 2021;10(5):1138. DOI: 10.3390/cells10051138.
33. Selles M.C., Fortuna J.T.S., de Faria Y.P.R., Siqueira L.D., Lima-Filho R., Longo B.M. et al. Oxytocin attenuates microglial activation and restores social and non-social memory in APP/PS1 Alzheimer model mice. *iScience*. 2023;26(4):106545. DOI: 10.1016/j.isci.2023.106545.
34. Gorina Ya.V., Salmina A.B., Kuvacheva N.V., Komleva Yu.K., Morozova G.A., Demko I.V., Petrova M.M. Neuroinflammation and insulin resistance in Alzheimer's disease. *Sibirskmedobozr.* 2014;4:11–19 (in Russ.).
35. Inoue T., Yamakage H., Tanaka M., Kusakabe T., Shimatsu A., Satoh-Asahara N. Oxytocin suppresses inflammatory responses induced by lipopolysaccharide through inhibition of the eIF-2-ATF4 pathway in mouse microglia. *Cells*. 2019;8(6):527. DOI: 10.3390/cells8060527.
36. Roth C.L., D'Ambrosio G., Elfers C. Activation of nuclear factor kappa B pathway and reduction of hypothalamic oxytocin following hypothalamic lesions. *J. Syst. Integr. Neurosci*. 2016;2(1):79–84. DOI: 10.15761/JSIN.1000114.
37. Yuan L., Liu S., Bai X., Gao Y., Liu G., Wang X. et al. Oxytocin inhibits lipopolysaccharide-induced inflammation in microglial cells and attenuates microglial activation in lipopolysaccharide-treated mice. *J. Neuroinflammation*. 2016;13(1):77. DOI: 10.1186/s12974-016-0541-7.
38. Huang Y., Happonen K.E., Burrola P.G., O'Connor C., Hah N., Huang L. et al. Microglia use TAM receptors to detect and engulf amyloid β plaques. *Nat. Immunol.* 2021;22(5):586–594. DOI: 10.1038/s41590-021-00913-5.
39. Van den Burg E.H., Stindl J., Grund T., Neumann I.D., Strauss O. Oxytocin stimulates extracellular Ca2+ influx through TRPV2 channels in hypothalamic neurons to exert its anxiolytic effects. *Neuropsychopharmacology*. 2015;40(13):2938–2947. DOI: 10.1038/npp.2015.147.
40. Zhang X., Zhao F., Wang C., Zhang J., Bai Y., Zhou F. et al. AVP(4-8) Improves cognitive behaviors and hippocampal synaptic plasticity in the APP/PS1 mouse model of Alzheimer's disease. *Neurosci. Bull*. 2020;36(3):254–262. DOI: 10.1007/s12264-019-00434-0.
41. Finton C.J., Ophir A.G. Developmental exposure to intranasal vasopressin impacts adult prairie vole spatial memory. *Psychoneuroendocrinology*. 2022;141:105750. DOI: 10.1016/j.psyneuen.2022.105750.
42. Yang C., Zhang X., Gao J., Wang M., Yang Z. Arginine vasopressin ameliorates spatial learning impairments in chronic cerebral hypoperfusion via V1a receptor and autophagy signaling partially. *Transl. Psychiatry*. 2017;7(7):e1174. DOI: 10.1038/tp.2017.121.
43. Cymerblit-Sabba A., Walsh C., Duan K.Z., Song J., Holmes O., Young W.S. Simultaneous knockouts of the oxytocin and vasopressin 1b receptors in hippocampal CA2 impair social memory. *BioRxiv*. 2023;2023. DOI: 10.1101/2023.01.30.526271.
44. Varga J., Klausz B., Domokos Á., Kálmán S., Pákáski M., Szűcs S. et al. Increase in Alzheimer's related markers preceeds memory disturbances: studies in vasopressin-deficient Brattleboro rat. *Brain Res. Bull*. 2014;100:6–13. DOI: 10.1016/j.brainresbull.2013.10.010.
45. Pan Y.F., Jia X.T., Wang X.H., Chen X.R., Li Q.S., Gao X.P. et al. Arginine vasopressin remolds the spontaneous discharges disturbed by amyloid β protein in hippocampal CA1 region of rats. *Regul. Pept.* 2013;183:7–12. DOI: 10.1016/j.regpep.2013.03.003.
46. Smith A.S., Williams Avram S.K., Cymerblit-Sabba A., Song J., Young W.S. Targeted activation of the hippocampal CA2 area strongly enhances social memory. *Mol. Psychiatry*. 2016;21(8):1137–1144. DOI: 10.1038/mp.2015.189.
47. Lukas M., Neumann I.D. Nasal application of neuropeptide S reduces anxiety and prolongs memory in rats: social versus non-social effects. *Neuropharmacology*. 2012;62(1):398–405. DOI: 10.1016/j.neuropharm.2011.08.016.
48. Zhao P., Qian X., Nie Y., Sun E., Wang Z., Wu J. et al. Neuropeptide S ameliorates cognitive impairment of APP/PS1 transgenic mice by promoting synaptic plasticity and reducing Aβ deposition. *Front. Behav. Neurosci*. 2019;13:138. DOI: 10.3389/fnbeh.2019.00138.
49. Liu X., Si W., Garau C., Jüngling K., Pape H.C., Schulz S., Reinscheid R.K. Neuropeptide S precursor knockout mice display memory and arousal deficits. *Eur. J. Neurosci*. 2017;46(1):1689–1700. DOI: 10.1111/ejn.13613.
50. Grund T., Neumann I.D. Neuropeptide S induces acute anxiolysis by phospholipase C-dependent signaling within the medial amygdala. *Neuropsychopharmacology*. 2018;43(5):1156–1163. DOI: 10.1038/npp.2017.169.

51. Grund T., Goyon S., Li Y., Eliava M., Liu H., Charlet A. et al. Neuropeptide S activates paraventricular oxytocin neurons to induce anxiolysis. *J. Neurosci*. 2017;37(50):12214–12225. DOI: 10.1523/JNEUROSCI.2161-17.2017.
52. Han R.W., Zhang R.S., Xu H.J., Chang M., Peng Y.L., Wang R. Neuropeptide S enhances memory and mitigates memory impairment induced by MK801, scopolamine or $A\beta_{1-42}$ in mice novel object and object location recognition tasks. *Neuropharmacology*. 2013;70:261–267 .DOI: 10.1016/j.neuropharm.2013.02.002.
53. Han R.W., Xu H.J., Zhang R.S., Wang P., Chang M., Peng Y.L. et al. Neuropeptide S interacts with the basolateral amygdala noradrenergic system in facilitating object recognition memory consolidation. *Neurobiol. Learn Mem*. 2014;107:32–36. DOI: 10.1016/j.nlm.2013.10.010.
54. Li C., Wu X.J., Li W. Neuropeptide S promotes maintenance of newly formed dendritic spines and performance improvement after motor learning in mice. *Peptides*. 2022;156:170860. DOI: 10.1016/j.peptides.2022.170860.
55. Wang C., Xin L., Cai C.C., Cong C.Y., Xie J.F., Kong X.P. et al. Neuropeptide S displays as a key neuromodulator in olfactory spatial memory. *Chem. Senses*. 2020;45(3):195–202. DOI: 10.1093/chemse/bjaa003.

Authors' contribution

Avliyakulyeva A.M., Kindyakova E.K. – search and analysis of articles, manuscript design, creation of figures. Kuzmina S.V. – discussion of the concept of the article, final editing of the manuscript for publication. Gorina Ya.V., Lopatina O.L. – concept development, article search, manuscript editing.

Authors' information

Avliyakulyeva Aylar M. – Teaching Assistant, Department of Biological Chemistry with a Course in Medical, Pharmaceutical and Toxicological Chemistry, Junior Researcher, Laboratory of Social Neuroscience, V.F. Voino-Yasenetsky KrasSMU, Krasnoyarsk, ailara@bk.ru, https://orcid.org/0009-0009-8457-4581

Kindyakova Ekaterina K. – Teaching Assistant, Department of Biological Chemistry with a Course in Medical, Pharmaceutical and Toxicological Chemistry, Junior Researcher, Laboratory of Social Neuroscience, V.F. Voino-Yasenetsky KrasSMU, Krasnoyarsk, kindyakova13@mail.ru, https://orcid.org/0009-0008-3803-1490

Kuzmina Svetlana V. – Dr. Sci. (Med.), Associate Professor, Professor, Department of Psychiatry and Medical Psychology, Kazan State Medical University, Kazan, skouzmina21@list.ru, https://orcid.org/0000-0002-7330-1213

Gorina Yana V. – Dr. Sci. (Biology), Associate Professor, Department of Biological Chemistry with a Course in Medical, Pharmaceutical and Toxicological Chemistry, Senior Researcher, Laboratory of Social Neuroscience, V.F. Voino-Yasenetsky KrasSMU; Associate Professor, Department of Biophysics, Institute of Fundamental Biology and Biotechnology, Siberian Federal University, Krasnoyarsk, yana_20@bk.ru, https://orcid.org/0000-0002-3341-1557

Lopatina Olga L. – Dr. Sci. (Biology), Associate Professor, Professor, Department of Biological Chemistry with a Course in Medical, Pharmaceutical and Toxicological Chemistry, Head of the Laboratory of Social Neuroscience, V.F. Voino-Yasenetsky KrasSMU; Professor of the Department of Biophysics, Institute of Fundamental Biology and Biotechnology, Siberian Federal University, Krasnoyarsk, ol.lopatina@gmail.com, https://orcid.org/0000-0002-7884-2721

(✉) **Avliyakulyeva Aylar M.,** ailara@bk.ru

Received 10.11.2023;
approved after peer review 07.12.2023;
accepted 21.12.2023

УДК 616.832-004.2-073.86
https://doi.org/10.20538/1682-0363-2024-1-116-125

Modern possibilities of MRI-based diagnosis of multiple sclerosis. Literature review

Degtyarev I.Yu., Zavadovskaya V.D., Kurazhov A.P., Zorkaltsev M.A., Alifirova V.M., Sukhanova K.S.

Siberian State Medical University
2, Moscow Trakt, Tomsk, 634050, Russian Federation

ABSTRACT

Multiple sclerosis remains the most common demyelinating disease of the central nervous system and ranks first among neurological diseases that lead to disability in young people. The most important diagnostic and prognostic marker, especially at an early stage of the disease, is magnetic resonance imaging (MRI), which currently remains the only method that allows to explore the entire central nervous system *in vivo*.

The review presents literature data on modern achievements in MRI-based diagnosis of multiple sclerosis. Key attention is paid to such promising methods as assessment of brain and spinal cord atrophy, brain perfusion MRI, and diffusion tensor imaging. Implementation of these approaches in MRI can help solve the problem of early diagnosis of multiple sclerosis and determine more reliable markers of a response to ongoing therapy.

Keywords: magnetic resonance imaging, multiple sclerosis, DWI, MR perfusion

Conflict of interest. The authors declare the absence of obvious or potential conflicts of interest related to the publication of this article.

Source of financing. The authors state that they received no funding for the study.

For citation: Degtyarev I.Yu., Zavadovskaya V.D., Kurazhov A.P., Zorkaltsev M.A., Alifirova V.M., Sukhanova K.S. Modern possibilities of MRI-based diagnosis of multiple sclerosis. Literature review. *Bulletin of Siberian Medicine.* 2024;23(1):116–125. https://doi.org/10.20538/1682-0363-2024-1-116-125.

Современные возможности магнитно-резонансной диагностики рассеянного склероза. Обзор литературы

Дегтярев И.Ю., Завадовская В.Д., Куражов А.П., Зоркальцев М.А., Алифирова В.М., Суханова К.С.

Сибирский государственный медицинский университет (СибГМУ)
Россия, 634050, г. Томск, Московский тракт, 2

РЕЗЮМЕ

Рассеянный склероз остается наиболее часто встречаемым демиелинизирующим заболеванием центральной нервной системы и занимает первое место среди неврологических заболеваний, приводящих к инвалидизации лиц молодого возраста. Наиболее важной лучевой модальностью с диагностической и прогностической точек зрения, особенно на ранней стадии заболевания, является магнитно-резонансная томография (МРТ), которая в настоящее время остается единственным методом, позволяющим исследовать центральную нервную систему на всем протяжении *in vivo*.

✉ *Degtyarev Ilya Yu.,* ilya.degtyarev.4201@mail.ru

В настоящем обзоре приведены литературные данные о современных достижениях магнитно-резонансной диагностики рассеянного склероза. Ключевое внимание уделяется таким ее перспективным аспектам, как оценка атрофии головного и спинного мозга, оценка перфузии головного мозга и диффузионно-тензорная МРТ. Внедрение данных подходов в МРТ помогает приблизить решение проблемы ранней диагностики рассеянного склероза и повысить информативность оценки клинического ответа на проводимую терапию.

Ключевые слова: магнитно-резонансная томография, рассеянный склероз, DWI, МР-перфузия

Конфликт интересов. Авторы заявляют об отсутствии явных и потенциальных конфликтов интересов при проведении исследования.

Источники финансирования. Авторы заявляют об отсутствии финансирования при проведении исследования.

Для цитирования: Дегтярев И.Ю., Завадовская В.Д., Куражов А.П., Зоркальцев М.А., Алифирова В.М., Суханова К.С. Современные возможности магнитно-резонансной диагностики рассеянного склероза. Обзор литературы. *Бюллетень сибирской медицины.* 2024;23(1):116–125. https://doi.org/10.20538/1682-0363-2024-1-116-125.

INTRODUCTION

Multiple sclerosis (MS) is the most common autoimmune demyelinating disease of the central nervous system (CNS), characterized by the formation of multiple foci of demyelination and a variety of neurological symptoms. MS ranks first among neurological diseases leading to disability in young people. The disease is characterized by fully or partially reversible episodes of neurological disability that usually last from several days to several weeks [1].

More than 2.8 million people worldwide are diagnosed with MS [2]. MS is now more common in women, but this has not always been the case. Since the early 1900s, the sex ratio has been nearly equal, but since then it has steadily increased toward predominance of women, currently approaching 3:1 [3]. Although the first manifestation of the disease can occur at any age, in most patients with MS it occurs at the age of 20–40 years. The disease has a huge negative impact on their functional activity, financial security, and quality of life. The costs of medical care for MS are extremely high and increase as disability progresses [4].

PATHOGENESIS

To date, the pathogenesis of MS remains not fully understood, mainly due to limited understanding of the ethology of this disease. Various risk factors for the development of MS have been identified so far, such as serum vitamin D levels, genetic predisposition, and certain viral infections [5]. However, none of these factors has been recognized as etiological. This suggests that the etiopathogenesis of the disease is multifactorial [6].

Although the triggering mechanisms of MS remain unknown, the dominant scientific view on the pathogenesis of this disease is that the activation of autoaggression against myelin proteins, which form a multilayered sheath around the axons and cell bodies of neurons, plays a major role in its occurrence [7]. Thus, disruptions in immune mechanisms have been proposed as the main factors in the pathogenesis of MS. This is due to the fact that T and B lymphocytes are selectively sensitized by specific target antigens (probably autoantigens), which are expressed only in the central nervous system. This is indirectly confirmed by the discovery of a correlation between a decrease in the number and activity of circulating regulatory T cells in the peripheral blood with exacerbation of disease symptoms [8].

Currently, numerous forms of MS (cerebrospinal, spinal, cerebellar, optic, brainstem and others) are not separately identified and are not indicated in the diagnosis. To standardize terminology and increase the homogeneity of clinical studies, an internationally recognized and unified classification of MS was introduced, which distinguishes four variants of its clinical course (phenotype):

1. Relapsing remitting MS (RRMS) is characterized by the presence of periodic exacerbations with almost complete recovery or the presence of minimal residual neurological deficit and the absence of progression of symptoms in the period between relapses.

2. Primary progressive MS (PPMS) is characterized by the presence of steady progression

of neurological deficits from the onset of the disease in the absence of obvious exacerbations.

3. Secondary progressive MS (SPMS) is characterized by steady progression of the disease after a certain period of the relapsing remitting course.

4. Progressive MS with exacerbations is characterized by the presence of exacerbations of the disease with a steady aggravation of neurological symptoms.

Establishing the type of MS course in a particular patient is a key aspect in the diagnosis of this disease. An accurate description of the clinical course (phenotype) of the disease is important for predicting, planning, and clarifying the scope of necessary clinical trials, as well as for choosing the optimal treatment strategy [9].

This classification was partially revised in 2013 [10]. It now takes into account additional criteria for MS, such as its activity and progression (based on clinical presentation and MRI), thereby stratifying patient characteristics along two axes that can be assessed separately [11]. Thus, MS can be active or inactive, progressive or non-progressive. Distinguishing disease activity from disease progression has proven to be clinically meaningful, as MS treatment methods may be effective in actively progressive forms, but not in inactive progressive forms. The addition of MS classification to MRI data also reflects the understanding that, along with clinical observation, other parameters can be used to establish the characteristics of the course of this disease [11].

There is also clinically isolated syndrome (CIS), which is an early manifestation of MS. CIS involves an acute clinical attack affecting one or more areas of the central nervous system, which can lead to the onset of relapsing remitting MS. According to studies, CIS converts to RRMS after 20 years only in 21% of patients with a normal MRI image of the brain during CIS and in 82% of patients if MRI had one or more clinically asymptomatic lesions of the white matter of the brain [12].

At early stages of MS, clinical data alone are not enough to diagnose it accurately. On the other hand, instrumental and laboratory studies cannot always provide the necessary accuracy in diagnosing MS. It should also be noted that a large number of publications about numerous methods proposed for the diagnosis of MS do not reflect their real significance, since most of them do not analyze the assessment of their diagnostic effectiveness (primarily sensitivity and specificity). Unfortunately, the generally accepted magnetic resonance criteria for MS are used only as basic ones, making it impossible to conduct a reliable assessment of the risk of disease progression.

Another problem remains establishing the exact type of course of MS, as well as predictors of the transition of RRMS to SPMS, which must be taken into account for timely and effective correction of appropriate therapy. The development of various methods, including both imaging and laboratory diagnosis, to solve these problems is an extremely relevant area in the development of MS diagnosis.

CRITERIA FOR MAGNETIC RESONANCE MANIFESTATIONS OF LESIONS IN MULTIPLE SCLEROSIS

It is well known that the features of pathological processes in MS, including inflammation, demyelination, axonal loss, and gliosis, can be studied *in vivo* using both traditional and advanced medical imaging methods [13]. MRI is the most important radiation modality for MS from the point of view of its diagnosis and prognosis, especially at the early stage of the disease, which currently remains the only method that allows to study the entire central nervous system *in vivo.* Traditional MRI pulse sequences in the diagnosis of MS can determine the number, location, and activity of demyelinating lesions, although the sensitivity of these sequences is thought to be highly variable.

On the other hand, routine MRI has low sensitivity in detecting the heterogeneity of focal lesions and pathological changes observed in the tissue of the central nervous system outside the foci of demyelination. In addition, MRI is unable to separately quantify the level of damage to various CNS tissue components, such as myelin, axons, and glia [14].

It is preferable to visualize demyelinating processes on high-field MRI scanners (with a magnetic induction value equal to or greater than 1.0 T). T2-WI sequences with long TE (time echo) and TR (time repetition) are the most sensitive to damage to the brain matter in MS. This is due to the fact that demyelinating lesions in MS have a

longer T2 relaxation time compared to apparently unchanged white matter.

Numerous comparisons of neuroimaging data and histologic studies made it possible to identify a pathological substrate corresponding to changes in signal characteristics in various MRI modes. Thus, as a result of disruption of the protein – lipid bilayer, a decrease in the amount of lipids and an increase in water content, foci of demyelination in MS are visualized as areas of a magnetic resonance signal of increased intensity on T2-WI and decreased intensity on T1-WI. The MR signal from recently formed lesions is determined mainly by edema and from long-existing ones – by gliosis. Thus, MRI is capable of reflecting the polymorphism of pathological changes observed in the central nervous system in MS [15].

The currently accepted MRI criteria for MS are the McDonald criteria, first published in 2001 and then revised and updated in 2005 and 2010. The last revision was carried out in 2017. As with previous revisions of these criteria, the diagnosis of MS requires a combination of clinical and radiological signs. MS can be diagnosed if any of the following five groups of criteria are met, depending on the number of clinical attacks, the presence of dissemination in space and dissemination in time [16, 17].

Foci of demyelization in MS usually have a round or oval shape, and their diameter varies from a few millimeters to a centimeter or more [18]. To a certain degree, differences in the shape of the lesions is due to the passage of the tomographic slice at an angle to the cerebral venule, which often represents the center of the demyelination focus in MS. At the initial stage of the disease, the lesions appear elongated in the form of so-called Dawson's fingers, which is probably associated with inflammatory edema of the brain matter along the medullary venules [19].

It should be noted that the typical localization of lesions in MS is the periventricular white matter, including the corpus callosum, subcortical white matter, and infratentorial region. Isolated hyperintense lesions on T2- WI adjacent to the body or temporal horn of the lateral ventricle are very characteristic of MS and are rarely found in other pathologies [20].

The diagnostic potential of MRI is enhanced by the use of contrast enhancement, which involves intravenous administration of a contrast agent (CA). Firstly, contrast-enhanced MRI can determine the degree of disease activity, which has important prognostic value and great clinical value in choosing the most effective therapeutic strategy. Secondly, this method allows to obtain additional evidence of the dissemination of demyelination foci over time by simultaneous visualization of both active foci that accumulate CA and inactive ones that do not accumulate it. Thirdly, CA injection can help identify atypical lesions and detect latent structural lesions that are not visible on non-contrast images [21].

Contrast agents based on trivalent gadolinium, which belongs to the group of positive paramagnetic agents, do not normally penetrate the blood – brain barrier (BBB). It is believed that in MS it passes through the capillary walls and lingers for some time in the extracellular space [22].

Neuroimaging and pathomorphological comparisons confirm that the accumulation of CA occurs exclusively in active demyelination foci with pronounced inflammatory changes in the form of edema and cellular infiltration. At the same time, contrast-enhanced MRI may be more sensitive in detecting subclinical activity of RRMS than assessing the clinical status. With the accumulation of CA, pathological areas can change the shape and size. Usually, at first these are foci that evenly accumulate CAs, which subsequently, as the disease progresses, transform into foci that accumulate CAs in the "ring" or "semi-ring" type, after which the degree of CA capture by such foci decreases, since they become "chronic".

At the same time, there are known difficulties in the differential diagnosis of both typical and atypical forms of MS with tumor lesions of the central nervous system. Thus, lesions in MS in certain cases can be mistaken for hematogenous metastases accumulating CA, as well as primary brain tumors (in the so-called pseudotumor form of MS). At the same time, the "ring-shaped" type of their contrast is considered more characteristic of tumor lesions, while "ring-shaped-rupture" type is more typical of demyelination foci in MS [23].

MODERN POSSIBILITIES OF MRI-BASED DIAGNOSIS OF MULTIPLE SCLEROSIS

Effective treatment methods have made early diagnosis of MS highly desirable, and MRI criteria for MS have been revised to exclude conditions

that mimic the disease more accurately. However, identifying changes detected on MRI as clinically significant in MS still presents known difficulties due to the fact that traditional MRI data (total number and volume of lesions) poorly correlate with the degree of neurological deficit. This phenomenon called the clinico-radiological paradox led to the need to study pathological processes developing in the central nervous system along with demyelination and to develop new methods for assessing ultrastructural, biochemical, and functional changes in the central nervous system [24].

To date, there is no consensus on how to assess and monitor response to MS treatment. Currently, the concepts of "response" and "non-response", as well as the time frame for this criterion, are widely discussed in the scientific literature. Typically, failure to respond to treatment is determined based on three factors or a combination of factors, including increasing severity of neurological deficit, relapse rate, and the presence of active T2 lesions (defined as new lesions that increase the total number of lesions) or contrast-enhancing lesions on MRI. On the other hand, the clinical significance of detecting minimal MS activity using MRI data is controversial, which raises the issue of further development of guidelines regarding the determination and monitoring of the response to treatment [25].

It is now generally accepted that focal lesions detected by routine MRI represent only one aspect of the disease [26]. At the same time, advanced MRI technologies that have emerged over the past few decades have made it possible to detect microstructural changes in the brain in patients with MS, even in apparently normal white matter [27]. In addition, cortical lesions and atrophy of the gray matter of the brain may be important additional features of this disease [28].

It has been established that atrophy of the brain and spinal cord is becoming one of the main manifestations of MS and represents a very relevant finding [29]. In addition to tissue loss caused by locally destructive white matter lesions and secondary tissue loss due to tract-specific loss of axons and neurons, there are many other potential mechanisms for this process, including iron accumulation, mitochondrial damage, microglial activation, and oxidative stress [30]. Thus, brain atrophy begins at the early stages of MS and progresses annually in untreated patients at a rate of 0.5–1.0% per year, regardless of the clinical subtype of the disease [31]. It is worth noting that global brain atrophy can be observed not only during the onset of the first symptoms of MS, but even at its preclinical stages [32–34]. Atrophy has a stronger association with neurological deficits and cognitive impairment compared to traditional MRI criteria for nerve tissue damage in MS [35].

Brain atrophy can be easily measured using a wide range of MRI techniques. Qualitatively, atrophy can be established based on an increase in the cerebrospinal fluid spaces in combination with a decrease in the volume of brain tissue, as well as by measuring the width of the ventricles of the brain or the cross-sectional area of the corpus callosum. For more efficient and reproducible measurements in research and clinical trials, fully automated computer methods for segmenting diagnostic images based on high-resolution T1-WI are usually used, which allows for separate assessment of the white and gray matter of the brain and, by determining their ratio, identifying regional atrophy. However, the results of such studies should be interpreted carefully, as CNS volume is also influenced by non-MS factors, such as medications taken, daily fluctuations and hydration status, as well as MS-related edema, inflammation, and gliosis [36, 37].

Unfortunately, atrophy scoring criteria are not yet used in daily clinical practice due to many technical problems and a lack of consensus on the choice of a standardized method for their determination [38]. In this regard, the development of portable, fully automated methods for measuring atrophic changes in the brain, which are promising for widespread use in the future, continues [39].

In addition to the above data on morphological changes in the brain in MS, there are reports in the literature about changes in perfusion both in lesions and in tissues with a normal image of the brain [40]. Common MRI techniques for assessing cerebral perfusion include dynamic susceptibility contrast (DSC) magnetic resonance, dynamic contrast-enhanced (DCE) MRI, and arterial spin labeling (ASL) MRI. All of these methods can quantify cerebral blood flow velocity (CBF), cerebral blood volume (CBV), and mean cerebral transit time (MTT) of CA. The DSC and DCE methods involve visualization of the dynamic passage of a gadolinium-containing contrast agent bolus. The first one is

based on T2* weighted sequences, and the second one is based on T1-weighted sequences. Unlike DSC and DCE, the ASL method is based on the use of contrast properties of endogenous water molecules, which, being part of the blood, are marked using radiofrequency inversion pulses before they reach the brain [41].

It is still unclear whether changes in perfusion in MS are a primary process or simply an epiphenomenon caused by Wallerian degeneration or atrophy [38, 39]. However, accumulating evidence suggests that changes in cerebral perfusion in MS are an important part of this disease. Thus, there is evidence that a decrease in perfusion in the medulla can occur even in its apparently intact areas [42]. It has also been shown that hypoperfusion is not necessarily associated with demyelination areas. Moreover, it is assumed that changes in perfusion precede atrophy and lesion formation [43]. Additionally, a relationship between cerebral perfusion and the distribution of white matter lesions has been observed in a broad cohort of MS patients. In particular, white matter lesions in patients with secondary progressive MS were found in regions characterized by lower perfusion than in contralateral healthy regions. In contrast, in patients with RRMS, brain lesions were more common in areas with increased perfusion. This fact indicates that remyelination processes, which are more effective at the early stage of the disease, may be associated with changes in local perfusion [44].

Another study found a statistically significant decrease in CBF in the frontal cortex, thalamus, and caudate nucleus in patients with MS, without evidence of loss of gray matter volume and decrease in cortical thickness, and such abnormalities were more common in SPMS compared to RRMS [45]. The reasons for these changes in cerebral perfusion in MS are not fully understood, and today there are several hypotheses trying to explain them. Firstly, hypoperfusion may be associated with neuroaxonal loss. However, most studies did not find a relationship between perfusion and brain atrophy, while others reported only a partial relationship between changes in perfusion and the degree of brain damage detected on T2-weighted images.

In addition, decreased perfusion was also not associated with parameters of brain atrophy, supporting the idea that it may be driven by other mechanisms. Other possible explanations for the origin of cerebral atrophy include a decrease in energy requirements or a slowdown in tissue metabolism, primary ischemia, impaired cerebrovascular reactivity, mitochondrial dysfunction, and even a latent process of neurodegeneration before its manifestation at the macromorphological level. In this case, knowledge of the extent of atrophic changes in the brain may provide more therapeutic options than detection of a pronounced and widespread demyelination process.

The relationship between brain perfusion and contrast enhancement of lesions in MS is of considerable scientific interest. The literature provides data according to which in patients with RRMS, there is an increase in CBF and CBV by 20% compared to the baseline values 3 weeks before the accumulation of CA in lesions, a CBF and CBV increase by 25% during the period of CA accumulation, and a slow decrease in CA accumulation in the lesions in MS compared to baseline values within 20 weeks after initial gadolinium enhancement [46].

Patients need to undergo MRI repeatedly and frequently to monitor rapidly occurring changes in the central nervous system during periods of manifestation of MS and its increased activity. MR perfusion study is the mainstay for objectifying hemodynamic disorders in MS. However, this study is associated with an increased risk of dose-dependent deposition of gadolinium in brain tissue due to frequent repeated administration of CA.

Thus, impaired cerebral perfusion in MS is most likely one of the links in a complex cascade of pathophysiological processes occurring in this disease. However, it is yet to be determined whether the phenomena described above are closely related phenomena of the same order (possibly secondary to known immunological abnormalities in MS) or simply represent disparate aspects of MS. The identified correlations of changes in cerebral perfusion with various types of MS course raise the question of the advisability of using MRI perfusion parameters as markers for the early diagnosis of MS and the characteristics of its course.

Another promising advanced neuroimaging technique is diffusion tensor MRI (DTI), which allows for the assessment of the integrity of neural pathways. DTI can analyze and evaluate elements of the microstructural architecture of the brain that are not visualized using traditional pulse sequences.

Thus, DTI provides important additional information about the spatial organization of nerve fibers, directional coherence of axons, and the degree of integrity of a particular neural tract [47]. DTI has provided valuable insight into the pathogenesis of MS both within lesions and in the white matter of the brain, which appears intact according to routine MRI.

Animal models have shown that DTI can differentiate axonal damage caused by demyelination, suggesting that DTI can be used to evaluate neuroprotective treatments. Thus, DTI has a high diagnostic potential, making it possible to detect changes in MS lesions at the earliest stages of the disease, including in the white matter of the brain whose macromorphological characteristics are unchanged. DTI can also be used to describe the microstructures of biological tissues by quantifying water diffusion processes in affected brain regions in MS. Moreover, DTI makes it possible to determine the extent of white matter lesions more accurately than using T2-weighted images [48]. DTI parameters, including fractional anisotropy (FA), radial diffusivity (RD), and mean diffusivity (MD), can accurately characterize the state of neuronal structures and their disorders in patients suffering from MS [49].

This method is based on a non-invasive assessment of the molecular (Brownian) motion of water, which in biological tissues is limited by various cellular structures. In the white matter tracts of the brain, water mainly diffuses parallel to the direction of the axons (axial diffusivity), and visualization of this physical process allows for detailed mapping of the structural integrity of the white matter at the micro level. Using directional magnetic gradients in three planes within DTI, it is possible to evaluate water diffusion processes in directions perpendicular to the neural tracts (radial diffusivity). In this regard, axial diffusivity is thought to reflect the integrity of axons, and radial diffusivity reflects the degree of their myelination, while FA is an integral parameter characterizing the degree of the diffusion direction in a specific volume of the medulla. In this case, a low FA coefficient corresponds to a low degree of vectoriality of water diffusion, while a high FA coefficient is a consequence of highly directional movement of water along axons.

It has been established that lesions of the medulla in MS are associated with reduced values of the FA coefficient, which indicates that structural disorders of the nerve conduction tracts occur as part of this disease. It has been suggested that a decrease in the FA coefficient may act as a marker of acute brain lesions and, therefore, be one of the criteria for disease activity. RD represents the rate of water diffusion perpendicular to axons, which is largely related to the processes of demyelination and remyelination [50]. It was found that increased RD values are potentially associated with lesions detected on T2-weighted images, as well as with myelin damage. It was also shown that an increase in this coefficient can also be determined in the white matter of the brain, in which, according to traditional MRI, structural changes are completely absent. A relative increase in RD values was also observed in affected nerve fibers, which is consistent with Wallerian degeneration [51].

Unfortunately, obtaining high-quality diffusion tensor images is associated with technical difficulties, which limits the clinical use of DTI. However, recent advances in image post-processing technology have improved the reliability of DTI in assessing nerve fiber integrity, resulting in increased sensitivity for detecting changes in MS compared to standard MRI [52].

CONCLUSION

Thus, today there is no generally accepted and reliable neuroimaging technique for assessing the course of MS, and the diagnostic criteria used for this are based mainly on clinical relapses and the presence of brain changes detected on MRI. Although traditionally used MRI sequences provide high sensitivity for diagnosing MS, they do not reliably identify predictors of deterioration in the clinical course of MS, and the results of such studies poorly correlate with the clinical status of the patient.

The introduction of new technologies implemented within the framework of MR imaging can contribute to solving the problem of early diagnosis of MS and determining more reliable criteria for response to therapy. A better understanding of the relationship between perfusion changes, MS, and clinical outcomes may be important to obtain new potential markers to assess the effects of pharmacological and rehabilitation interventions.

In addition, the use of DTI for these purposes seems very promising. But the current body of research using DTI is relatively limited, indicating

that these studies are at an early stage. However, these data already indicate that the quantitative parameter of FA measured by DTI successfully correlates with impairments in MS. Low level of evidence suggests that FA indicates tissue damage in a range of disorders, but the evidence is insufficient to support its use as a diagnostic test or as a predictor of clinical outcomes.

Thus, data collection methods, data processing, and data interpretation require further improvement, followed by standardization and validation, before new technologies are ready for widespread clinical use.

REFERENCES

1. Brownlee W.J., Hardy T.A., Fazekas F., Miller D.H. Diagnosis of multiple sclerosis: progress and challenges. *Lancet*. 2017;389(10076):1336–1346. DOI: 10.1016/S0140-6736(16)30959-X.
2. Dobson R., Rice D.R., D'hooghe M., Horne R., Learmonth Y., Mateen F.J. et al. Social determinants of health in multiple sclerosis. *Nat. Rev. Neurol*. 2022;18(12):723–734. DOI: 10.1038/s41582-022-00735-5.
3. Dobson R., Giovannoni G. Multiple sclerosis – a review. *Eur. J. Neurol*. 2019;26(1):27–40. DOI: 10.1111/ene.13819
4. Gbaguidi B., Guillemin F., Soudant M., Debouverie M., Mathey G., Epstein J. Age-period-cohort analysis of the incidence of multiple sclerosis over twenty years in Lorraine, France. *Sci. Rep.* 2022;12(1):1001. DOI: 10.1038/s41598-022-04836-5.
5. Tarlinton R., Khaibullin T., Granatov E., Martynova E., Rizvanov A., Khaiboullina S. The interaction between viral and environmental risk factors in the pathogenesis of multiple sclerosis. *Int. J. Mol. Sci.* 2019;20(2):303. DOI: 10.3390/ijms20020303.
6. Liu R., Du S., Zhao L., Jain S., Sahay K., Rizvanov A. et al. Autoreactive lymphocytes in multiple sclerosis: Pathogenesis and treatment target. *Front. Immunol*. 2022;13:996469. DOI: 10.3389/fimmu.2022.996469.
7. Ttadelmann C., Timmler S., Barrantes-Freer A., Simons M. Myelin in the central nervous system: structure, function, and pathology. *Physiol. Rev.* 2019;99(3):1381–431. DOI: 10.1152/physrev.00031.2018.
8. Verma N.D., Lam A.D., Chiu C., Tran G.T., Hall B.M., Hodgkinson S.J. Multiple sclerosis patients have reduced resting and increased activated CD4+CD25+FOXP3+T regulatory cells. *Sci. Rep.* 2021;11(1):10476. DOI: 10.1038/s41598-021-88448-5.
9. Pitt D., Lo C.H., Gauthier S.A., Hickman R.A., Longbrake E., Airas L.M. et al. Toward precision phenotyping of multiple sclerosis. *Neurol. Neuroimmunol. Neuroinflamm*. 2022;9(6):e200025. DOI: 10.1212/NXI.0000000000200025.
10. Tartaglia M., Canevelli M., Malimpensa L., Belvisi D., Baione V., Ferrazzano G. et al. Neurophysiological and clinical biomarkers of secondary progressive multiple sclerosis: A cross-sectional study. *Front. Neurol*. 2023;14:1138600. DOI: 10.3389/fneur.2023.1138600.
11. Kappos L., Bar-Or A., Cree B.A.C., Fox R.J., Giovannoni G., Gold R. et al. EXPAND Clinical Investigators. Siponimod versus placebo in secondary progressive multiple sclerosis (EXPAND): a double-blind, randomised, phase 3 study. *Lancet*. 2018;391(10127):1263–1273. DOI: 10.1016/S0140-6736(18)30475-6.
12. Filippi M., Preziosa P., Meani A., Ciccarelli O., Mesaros S., Rovira A. et al. Prediction of a multiple sclerosis diagnosis in patients with clinically isolated syndrome using the 2016 MAGNIMS and 2010 McDonald criteria: a retrospective study. *Lancet Neurol*. 2018;17(2):133–142. DOI: 10.1016/S1474-4422(17)30469-6.
13. Eshaghi A., Prados F., Brownlee W.J., Altmann D.R., Tur C., Cardoso M.J. et al. MAGNIMS study group. Deep gray matter volume loss drives disability worsening in multiple sclerosis. *Ann. Neurol.* 2018;83(2):210–222. DOI: 10.1002/ana.25145.
14. Granziera C., Wuerfel J., Barkhof F., Calabrese M., De Stefano N., Enzinger C. et al. MAGNIMS Study Group. Quantitative magnetic resonance imaging towards clinical application in multiple sclerosis. *Brain*. 2021;144(5):1296–1311. DOI: 10.1093/brain/awab029.
15. Goischke H.K. Comorbidities in multiple sclerosis-a plea for interdisciplinary collaboration to improve the quality of life of MS patients. *Degener. Neurol. Neuromuscul. Dis*. 2019;9:39–53. DOI: 10.2147/DNND.S204555.
16. Lunde H.M.B., Assmus J., Myhr K.M., Bø L., Grytten N. Survival and cause of death in multiple sclerosis: a 60-year longitudinal population study. *J. Neurol. Neurosurg. Psychiatry*. 2017;88(8):621–625. DOI: 10.1136/jnnp-2016-315238.
17. Thompson A.J., Banwell B.L., Barkhof F., Carroll W.M., Coetzee T., Comi G. et al. Diagnosis of multiple sclerosis: 2017 revisions of the McDonald criteria (2017). *Lancet Neurol.* 2018;17(2):162–173. DOI: 10.1016/S1474-4422(17)30470-2.
18. Wang K.Y., Uribe T.A., Lincoln C.M. Comparing lesion detection of infratentorial multiple sclerosis lesions between T2-weighted spin-echo, 2D-FLAIR, and 3D-FLAIR sequences. *Clin. Imaging*. 2018;51:229–234. DOI: 10.1016/j.clinimag.2018.05.017.
19. Ineichen B.V., Cananau C., Platt N.M., Ouellette R., Moridi T., Frauenknecht K.B.M. et al. Dilated virchow-robin spaces are a marker for arterial disease in multiple sclerosis. *BioRxiv.* 2023;2023. DOI: 10.1101/2023.02.24.529871.
20. Filippi M., Preziosa P., Banwell B.L., Barkhof F., Ciccarelli O., De Stefano N. et al. Assessment of lesions on magnetic resonance imaging in multiple sclerosis: practical guidelines. *Brain*. 2019;142(7):1858–1875. DOI: 10.1093/brain/awz144.
21. Yarraguntla K., Seraji-Bozorgzad N., Lichtman-Mikol S., Razmjou S., Bao F., Sriwastava S. et al. Multiple Sclerosis Fatigue: A Longitudinal Structural MRI and Diffusion Tensor Imaging Study. *J. Neuroimaging*. 2018;28(6):650–655. DOI: 10.1111/jon.12548.
22. Oghabian M.A., Fatemidokht A., Haririchian M.H. Quantification of blood-brain-barrier permeability dysregulation and inflammatory activity in ms lesions by dynamic-contrast enhanced MR imaging. *Basic Clin. Neurosci*. 2022;13(1):117–128. DOI: 10.32598/bcn.2022.575.1.

23. Sun Y., Yu H., Guan Y. Glia connect inflammation and neurodegeneration in multiple sclerosis. *Neurosci. Bull*. 2023;39(3):466–478. DOI: 10.1007/s12264-023-01034-9.
24. Tanaka F., Umino M., Maeda M., Nakayama R., Inoue K., Kogue R. et al. Pseudocontinuous arterial spin labeling: clinical applications and usefulness in head and neck entities. *Cancers (Basel)*. 2022;14(16):3872. DOI: 10.3390/cancers14163872.
25. Gasperini C., Prosperini L., Tintoré M., Sormani M.P., Filippi M., Rio J. et al. MAGNIMS Study Group. Unraveling treatment response in multiple sclerosis: A clinical and MRI challenge. *Neurology*. 2019;92(4):180–192. DOI: 10.1212/WNL.0000000000006810.
26. Tommasin S., Gianni C., De Giglio L., Pantano P. Neuroimaging techniques to assess inflammation in Multiple sclerosis. *Neuroscience*. 2019;403:4–16. DOI: 10.1016/j.neuroscience.2017.07.055.
27. Granberg T., Fan Q., Treaba C.A., Ouellette R., Herranz E., Mangeat G. et al. *In vivo* characterization of cortical and white matter neuroaxonal pathology in early multiple sclerosis. *Brain*. 2017;140(11):2912–2926. DOI: 10.1093/brain/awx247.
28. Bergsland N., Horakova D., Dwyer M.G., Uher T., Vaneckova M., Tyblova M. et al. Gray matter atrophy patterns in multiple sclerosis: A 10-year source-based morphometry study. *Neuroimage Clin*. 2017;17:444–451. DOI: 10.1016/j.nicl.2017.11.002.
29. Tauhid S., Neema M., Healy B.C., Weiner H.L., Bakshi R. MRI phenotypes based on cerebral lesions and atrophy in patients with multiple sclerosis. *J. Neurol. Sci*. 2014;346(1-2):250–254. DOI: 10.1016/j.jns.2014.08.047.
30. Mahad D.H., Trapp B.D., Lassmann H. Pathological mechanisms in progressive multiple sclerosis. *Lancet Neurol*. 2015;14(2):183–193. DOI: 10.1016/S1474-4422(14)70256-X.
31. Rebsamen M., McKinley R., Radojewski P., Pistor M., Friedli C., Hoepner R. et al. Reliable brain morphometry from contrast-enhanced T1w-MRI in patients with multiple sclerosis. *Hum. Brain Mapp*. 2023;44(3):970–979. DOI: 10.1002/hbm.26117.
32. Tsagkas C., Geiter E., Gaetano L., Naegelin Y., Amann M., Parmar K. et al. Longitudinal changes of deep gray matter shape in multiple sclerosis. *Neuroimage Clin*. 2022;35:103137. DOI: 10.1016/j.nicl.2022.103137.
33. Yamout B., Al Khawajah M. Radiologically isolated syndrome and multiple sclerosis. *Mult. Scler. Relat. Disord*. 2017;17:234–237. DOI: 10.1016/j.msard.2017.08.016.
34. Labiano-Fontcuberta A., Mato-Abad V., Álvarez-Linera J., Hernández-Tamames J.A., Martínez-Ginés M.L., Aladro Y. et al. Gray matter involvement in radiologically isolated syndrome. *Medicine (Baltimore)*. 2016;95(13):e3208. DOI: 10.1097/MD.0000000000003208.
35. Cagol A., Schaedelin S., Barakovic M., Benkert P., Todea R.A., Rahmanzadeh R. et al. Association of brain atrophy with disease progression independent of relapse activity in patients with relapsing multiple sclerosis. *JAMA Neurol*. 2022;79(7):682–692. DOI: 10.1001/jamaneurol.2022.1025.
36. Krajnc N., Bsteh G., Berger T. Clinical and Paraclinical Biomarkers and the Hitches to Assess Conversion to Secondary Progressive Multiple Sclerosis: A Systematic Review. *Front. Neurol*. 2021;12:666868. DOI: 10.3389/fneur.2021.666868.
37. Hemond C.C., Bakshi R. Magnetic resonance imaging in multiple sclerosis. *Cold Spring Harb. Perspect. Med.* 2018;8(5):a028969. DOI: 10.1101/cshperspect.a028969.
38. Uher T., Krasensky J., Malpas C., Bergsland N., Dwyer M.G., KubalaHavrdova E. et al. Evolution of brain volume loss rates in early stages of multiple sclerosis. *Neurol. Neuroimmunol. Neuroinflamm*. 2021;8(3):e979. DOI: 10.1212/NXI.0000000000000979.
39. Wang C., Beadnall H.N., Hatton S.N., Bader G., Tomic D., Silva D.G. et al. Automated brain volumetrics in multiple sclerosis: a step closer to clinical application. *J. Neurol. Neurosurg. Psychiatry*. 2016;87(7):754–757. DOI: 10.1136/jnnp-2015-312304.
40. Lagana M.M., Pelizzari L., Baglio F. Relationship between MRI perfusion and clinical severity in multiple sclerosis. *Neural. Regen. Res*. 2020;15(4):646–652. DOI: 10.4103/1673-5374.266906.
41. Hernandez-Garcia L., Lahiri A., Schollenberger J. Recent progress in ASL. *Neuroimage*. 2019;187:3–16. DOI: 10.1016/j.neuroimage.2017.12.095.
42. Debernard L., Melzer T.R., Alla S., Eagle J., Van Stockum S., Graham C. et al. Deep grey matter MRI abnormalities and cognitive function in relapsing-remitting multiple sclerosis. *Psychiatry Res*. 2015;234(3):352–361. DOI: 10.1016/j.pscychresns.2015.10.004.
43. Ingrisch M., Sourbron S., Herberich S., Schneider M.J., Kümpfel T., Hohlfeld R. et al. Dynamic contrast-enhanced magnetic resonance imaging suggests normal perfusion in normal-appearing white matter in multiple sclerosis. *Invest. Radiol*. 2017;52(3):135–141. DOI: 10.1097/RLI.0000000000000320.
44. Lagana M.M., Pelizzari L., BaglioF. Relationship between MRI perfusion and clinical severity in multiple sclerosis. *Neural. Regen. Res*. 2020;15(4):646–652. DOI: 10.4103/1673-5374.266906.
45. De la Peña M.J., Peña I.C., García P.G., Gavilán M.L., Malpica N., Rubio M. et al. Early perfusion changes in multiple sclerosis patients as assessed by MRI using arterial spin labeling. *Acta Radiol. Open*. 2019;8(12):2058460119894214. DOI: 10.1177/2058460119894214.
46. Lapointe E., Li D.K.B., Traboulsee A.L., Rauscher A. What have we learned from perfusion mri in multiple sclerosis? *AJNR Am. J. Neuroradiol*. 2018;39(6):994–1000. DOI: 10.3174/ajnr.A5504.
47. Gharaylou Z., Sahraian M.A., Hadjighassem M., Kohanpour M., Doosti R., Nahardani S. et al. Widespread Disruptions of White Matter in Familial Multiple Sclerosis: DTI and NODDI Study. *Front. Neurol*. 2021;12:678245. DOI: 10.3389/fneur.2021.678245.
48. Oladosu O., Liu W.Q., Brown L., Pike B.G., Metz L.M., Zhang Y. Advanced diffusion MRI and image texture analysis detect widespread brain structural differences between relapsing-remitting and secondary progressive multiple sclerosis. *Front. Hum. Neurosci*. 2022;16:944908. DOI: 10.3389/fnhum.2022.944908.

49. Hori M., Maekawa T., Kamiya K., Hagiwara A., Goto M., Takemura M.Y. et al. Advanced diffusion MR imaging for multiple sclerosis in the brain and spinal cord. *Magn. Reson. Med. Sci*. 2022;21(1):58–70. DOI: 10.2463/mrms.rev.2021-0091.
50. Chen J., Zhou C., Zhu L. et al. Magnetic resonance diffusion tensor imaging for occult lesion detection in multiple sclerosis. *Exp. Ther. Med.* 2017;13(1):91–96. DOI: 10.3892/etm.2016.3950.
51. Tae W.S., Ham B.J., Pyun S.B., Kang S.H., Kim B.J. Current clinical applications of diffusion-tensor imaging in neurological disorders. *J. Clin. Neurol*. 2018;14(2):129–140. DOI: 10.3988/jcn.2018.14.2.129.
52. Granberg T., Fan Q., Treaba C.A., Ouellette R., Herranz E., Mangeat G. et al. *In vivo* characterization of cortical and white matter neuroaxonal pathology in early multiple sclerosis. *Brain*. 2017;140(11):2912–2926. DOI: 10.1093/brain/awx247.

Authors' information

Degtyarev Ilya Yu. – Teaching Assistant, Division of Diagnostic Radiology and Radiation Therapy, Siberian State Medical University, Tomsk, ilya. degtyarev.4201@mail.ru, https://orcid.org/0000-0002-8812-4168

Zavadovskaya Vera D. – Dr. Sci. (Med.), Professor, Head of the Division of Diagnostic Radiology and Radiation Therapy, Siberian State Medical University, Tomsk, wdzaw@mail.ru, https://orcid.org/0000-0001-6231-7650

Kurazhov Alexey P. – Dr. Sci. (Med.), Professor, Division of Diagnostic Radiology and Radiation Therapy, Siberian State Medical University, Tomsk, kurazhovap@mail.ru, https://orcid.org/0000-0003-1316-5421

Zorkaltsev Maksim A. – Dr. Sci. (Med.), Associate Professor, Division of Diagnostic Radiology and Radiation Therapy, Siberian State Medical University, Tomsk, zorkaltsev@mail.ru, https://orcid.org/0000-0003-0025-2147

Alifirova Valentina M. – Dr. Sci. (Med.), Professor, Head of the Neurology and Neurosurgery Division, Siberian State Medical University, Tomsk, v_alifirova@mail.ru , https://orcid.org/ 0000-0002-4140-3223

Sukhanova Kristina S. – Radiologist, Siberian State Medical University, Tomsk, athos227930@gmail.com , https://orcid.org/0000-0001- 9449-8564

(✉) **Degtyarev Ilya Yu.,** ilya.degtyarev.4201@mail.ru

Received 24.04.2023;
approved after peer review 25.05.2023;
accepted 14.09.2023

УДК 616.36-018.26:576.3
https://doi.org/10.20538/1682-0363-2024-1-126-133

Hepatic stellate cells and their role in the formation of the progenitor cell niche

Zhdanov V.V.[1], Chaikovskii A.V.[1], Pan E.S.[2]

[1] *Goldberg Research Institute of Pharmacology and Regenerative Medicine (GRIPRM), Tomsk National Research Medical Center (NRMC) of the Russian Academy of Sciences*
3, Lenina Av., Tomsk, 634028, Russian Federation

[2] *Research Institute of General Pathology and Pathophysiology*
8, Baltiyskaya Str., Moscow, 125315, Russian Federation

ABSTRACT

The processes of proliferation and differentiation of progenitor and stem cells in the body are ensured by a specific microenvironment, the stem cell niche. Universal components have been identified for all niches: supporting cells, extracellular matrix, and soluble biological factors. A niche is a dynamic system whose activity depends on regeneration needs.

The review presents data on the structure of the hepatic stem cell niche and one of its main components – stellate cells and their role in pathology.

Keywords: stem cell niche, stellate cells, progenitor cells, regeneration

Conflict of interest. The authors declare the absence of obvious and potential conflicts of interest related to the publication of this article.

Source of financing. The authors state that they received no funding for the study.

For citation: Zhdanov V.V., Chaikovskii A.V., Pan E.S. Hepatic stellate cells and their role in the formation of the progenitor cell niche. *Bulletin of Siberian Medicine.* 2024;23(1):126–133. https://doi.org/10.20538/1682-0363-2024-1-126-133.

Роль звездчатых клеток в формировании ниши прогениторных клеток печени

Жданов В.В[1]., Чайковский А.В[1]., Пан Э.С.[2]

[1] *Научно-исследовательский институт фармакологии и регенеративной медицины (НИИФиРМ) им. Е.Д. Гольдберга, Томский национальный исследовательский медицинский центр (НИМЦ) Российской академии наук*
Россия, 634028, г. Томск, пр. Ленина, 3

[2] *Научно-исследовательский институт общей патологии и патофизиологии (НИИОПП)*
Россия, 125315, г. Москва, ул. Балтийская, 8

РЕЗЮМЕ

Процессы пролиферации и дифференцировки прогениторных/стволовых клеток в организме обеспечиваются специфическим микроокружением – нишей стволовых клеток. Для всех ниш определены универсальные компоненты – поддерживающие клетки, внеклеточный матрикс и растворимые биологические факторы. Ниша является динамической системой, активность которой зависит от запросов регенерации.

✉ *Zhdanov Vadim V.,* hdanov_vv@pharmso.ru

В обзоре представлены данные о строении ниши стволовых клеток печени, одном из ее основных компонентов – звездчатых клетках и их роли в патологии.

Ключевые слова: ниша стволовой клетки, звездчатые клетки, прогениторные клетки, регенерация

Конфликт интересов. Авторы заявляют об отсутствии явных и потенциальных конфликтов интересов при проведении исследования.

Источники финансирования. Авторы заявляют об отсутствии финансирования при проведении исследования.

Для цитирования: Жданов В.В., Чайковский А.В., Пан Э.С. Роль звездчатых клеток в формировании ниши прогениторных клеток печени. *Бюллетень сибирской медицины.* 2024;23(1):126–133. https://doi.org/10.20538/1682-0363-2024-1-126-133.

THE CONCEPT OF A STEM CELL NICHE

For the first time, Wolf and Trentin proposed the concept of the existence of local mechanisms of tissue regulation that provide quantitative control over the structures of hematopoiesis. The concept of hematopoietic inductive microenvironment (HIM) was introduced – certain areas of hematopoietic tissue in which local regulation of blood stem cell maturation in a certain direction is carried out [1]. Later, Schofield proposed using the term "niche" to refer to the microenvironment of hematopoietic stem cells (HSCs), and the first concepts of regulation of the stem / progenitor cell population were formed [2].

According to modern concepts, a niche is a specialized local formation that has histologic and functional characteristics typical of various tissues, in which specific progenitor cells are located [3, 4]. A niche is a dynamic system that ensures tissue homeostasis by controlling the processes of proliferation, differentiation, mobilization and homing of progenitor cells, maintaining a balance between dormancy and self-renewal [5–7].

Thus, the stem cell (SC) niche can be considered an elementary functional unit of the regeneration process [3, 6, 8]. The interaction of neighboring regulatory cells with stem cells is critical for the establishment of the stem cell niche, both through secreted signaling factors and through direct cell – cell interactions [9].

NICHE TYPES

All SC niches can be divided into two types: stromal and epithelial [10].

The stromal niche. An example of this type of niche is the microenvironment of a hematopoietic stem cell. In the niche, there is a wide stromal zone containing progenitor cells. The interaction between cells is an important feature, as they have a paracrine and autocrine effect on each other [7, 11].

The epithelial niche. This niche type is characterized by cytoarchitectonics when the cells are arranged in the form of certain layers. In this case, stem / progenitor cells form direct contacts with other cells, including daughter cells, and, importantly, with the basement membrane [12].

NICHE COMPONENTS

In general, a niche is formed by the following components:

1) cells of the microenvironment;

2) extracellular matrix which is a mechanical framework for a niche, as well as a medium for storing and transmitting signaling molecules, hormones, and growth factors;

3) blood vessels;

4) nerve endings.

1. Cells of the microenvironment are represented by various types of cells that directly contact stem cells and also secrete various regulatory factors [3, 13]. The importance of cells in the SC microenvironment was first shown in the works by T.M. Dexter et al., who found that when hematopoietic stem cells are added to stromal non-hematopoietic cells, the lifespan of the HSC culture increases from 1–2 weeks to 14 weeks [2]. Common components of the stem cell niche, characteristic of niches in various organs and tissues, are fibroblasts, endothelial cells, and macrophages [3, 13–16]. These cellular elements determine the proliferation and differentiation status of progenitor cells through the synthesis of cytokines, chemokines, growth factors, other regulatory substances, and components of the extracellular matrix [6, 17]. In the liver, Kupffer cells (liver macrophages) can interact with hepatocyte precursor cells, influencing their proliferation and differentiation either through direct

contacts or through the production of certain humoral factors [16].

2. Extracellular matrix. For a long time, the extracellular matrix was considered a fairly inert component of tissues that does not take special part in the life of cells. However, over the past 25 years, research in this direction has allowed to obtain completely new data [18, 19]. The intercellular substance is a fairly dynamic element of the SC niche, influencing the production, degradation, and remodeling of its own components. Naturally, first of all, the extracellular matrix creates a platform or a framework for the functioning of progenitor cellular elements. The extracellular matrix is specific in biochemical composition for each tissue and reflects the characteristics of the cells present in this tissue [3, 18, 20].

It is known that rigidity is the main property of the extracellular matrix, through which cells sense external influence and respond to environmental changes accordingly. This phenomenon is known as mechanotransduction, which is the conversion of mechanical stimuli into an intracellular biochemical response. Moreover, the interaction between the cell and the extracellular matrix is reciprocal: cells constantly remodel the matrix in their microenvironment, and these dynamic modifications subsequently control cell behavior [18, 21].

NICHE INNERVATION, NERVE ENDINGS

In addition to the mentioned cellular elements of the SC niche (fibroblasts, macrophages, and endothelial cells), nerve fibers are important elements of the niche. The existence of myelinated and unmyelinated nerve fibers in the bone marrow has been shown, most of which are located next to the arterioles in the hematopoietic tissue [5, 6, 22]. The sympathetic and parasympathetic subsystems of the autonomic nervous system play an important role in regulating the HSC niche.

The release of mediators by terminals affects the production of hematopoietins and the activity of elements of the blood SC microenvironment [3, 19, 22]. The fibers of the sympathetic and parasympathetic nervous systems also end in synapses and various types of liver cells. By stimulating α1B-, α1D-, β1-, and β2-adrenergic receptors, proliferation of hepatic stellate cells and oval cells is activated (both cell types express adrenergic receptors) [23]. Oval cells also carry muscarinic M3 receptors, which, when stimulated by acetylcholine, increase their proliferation [24].

BLOOD VESSELS

Blood vessels of the microvasculature are an important element of any niche [2, 5]. Endothelial cells and pericytes are of particular importance. In the bone marrow, endothelial cells form a barrier between hematopoietic cells and blood and regulate the migration of blood cells into the bloodstream [25]. The endothelial cells lining the sinusoidal capillaries (sinusoidal endotheliocytes) are the basis of a unique capillary network present in the bone marrow and liver.

These elements contribute to the specialized perivascular microenvironment where the majority of HSCs are located [26]. Endothelial cells participate in the regulation of homeostasis and stimulation of tissue regeneration both through direct interaction with local stem and progenitor cells and through the secretion of angiocrine factors [27]. It is known that in adult animals, sinusoidal endothelial cells of the bone marrow largely ensure the regeneration of hematopoietic tissue [28]. Similar endothelial cells line the capillaries of the liver, with each hepatocyte located in close proximity to a sinusoidal endothelial cell in such a way that their plasma membranes contact. During liver regeneration, endothelial cells create a vascular niche with an instructive role. Through the production of angiocrine factors, it stimulates regenerative processes, similar to factors derived from endothelial cells that support hematopoiesis [29].

PROGENITOR CELLS OF VARIOUS TISSUES AND ORGANS. COMPOSITION AND FUNCTION OF STEM CELL NICHES IN DIFFERENT TISSUES

Identification and characterization of stem cell niches still remain a serious problem from the point of view of their biology. This is due to the difficulty in identifying cells in certain areas, including the limited number of known markers using which they could be distinguished from other cells of a particular tissue with which they have morphological similarity [3, 6]. To date, SC niches have been identified in hematopoietic tissue [14], skin [30], intestines [31], striated muscles [32], and the central nervous system [15]. The niche of hepatic [33] and pancreatic [34] progenitor cells is being actively studied.

LIVER

It is known that hepatocytes and cholangiocytes have a high regenerative potential and are able to ensure restoration of liver tissue with moderate cell death and local damage [35]. In addition to hepatocytes

and cholangiocytes, several types of progenitor cells located in different areas of the lobule play an important role in the process of liver regeneration. In cases where hepatocyte proliferation is impaired due to chronic pathology, such as chronic viral hepatitis or non-alcoholic fatty liver disease, hepatocytes cannot effectively mediate parenchymal regeneration [36]. In this case, hepatic progenitor cells are activated, that, as a rule, are sufficient for the regeneration of biliary and hepatocellular epithelium [37].

There are three known populations of progenitor cells in the liver [38]. The first group is located in the canals of Hering, hepatic stem cells (HpSCs, hepatic stem / progenitor cells), which participate in the regeneration of small biliary ducts and the liver parenchyma itself. Hepatic stem cells (HpSCs) are optional bipotent hepatoblast progenitor cells [38; 39]. They express a combination of epithelial cell adhesion molecules (EpCAM), neural cell adhesion molecules (NCAM), cytokeratin-19, albumin and are negative for alpha-fetoprotein (AFP) [37]. Progenitor cells of the biliary tract (BTSCs, biliary tree stem/progenitor cells) can be designated as the second group of hepatocyte precursors. It is a heterogeneous population of cells expressing various transcription factors (SOX9, SOX17 and PDX1), as well as surface (EpCAM, LGR5 and/or CD133) and cytoplasmic markers (CK7, CK19). Cells of this type also support the renewal of cholangiocytes in large intrahepatic and extrahepatic biliary ducts [40]. The third type of progenitor cells is a group of self-renewing Axin2+ hepatocyte cells adjacent to the central vein [38].

NICHE OF LIVER PROGENITOR CELLS

Like any other niche, the niche of progenitor cells in the liver contains a certain set of cells that directly contact SCs, form intercellular substance, and secrete regulatory factors [41], thus exerting both direct and indirect effects on progenitor elements [33]. SC niches in the liver are formed by different types of cells: hepatocytes; sinusoidal cells [16]; endothelial cells – line the hepatic sinusoids [42]; perisinusoidal cells – stellate cells of the liver (Ito cells) – are located in the space of Disse; leukocytes [43]; as well as connective tissue cells (fibroblasts, mast cells) and angioblasts [36].

All these cell types constantly interact with each other and with hepatocytes through the mediation of the extracellular matrix, constituting a single structural and functional system that ensures homeostasis of hepatic acini and is dependent on complex specialized functions of hepatocytes [44]. Kupffer cells maintain an adequate microenvironment for hepatocytes due to early activation of lysosomal hydrolases in them, activation of the N-acetylglycosamine, mannose and galactose receptor, which can mediate the pinocytosis of some glycoproteins of the extracellular matrix. Kupffer cells also participate in the remodeling of the extracellular matrix, locally secreting collagenase type 4, matrix metalloproteinases (MMP-1, MMP-13), gelatinases, and stromelysin [45].

The precursors of hepatic stellate cells and endothelial cells have almost the same phenotypic characteristics as their mature descendants (stellate cells and endothelial cells), however, there are differences. For example, stellate cell precursors minimally express retinoids, whereas they are found in abundance in mature Ito cells; endothelial cell progenitors do not express CD31 (PECAM), which is a hallmark of mature endothelium.

The products of microenvironment cells, such as fibroblasts and mesenchymal stem cells, include matrix factors (hyaluronans, collagen type III and IV) [42], minimally sulfated proteoglycans, and laminins [46]. These also include soluble signals, such as leukemia inhibitory factor (LIF), hepatocyte growth factor (HGF), and epidermal growth factor (EGF) [47]. In *in vitro* experiments, the addition of any of these factors, as well as hyaluronic acid substrates, to liver cell culture caused the differentiation of HpSCs into hepatoblasts [47, 48]. When the liver is damaged, stellate cells are activated, subsequently producing collagen type I, sulfated proteoglycans, as well as high levels of cytokines and growth factors [49]. In addition to signaling from the niche to stem / progenitor cells, there is also a feedback from stem / progenitor cells to the niche. HpSCs can activate stellate and endothelial cells through the Hedgehog signaling pathway, which leads to the synthesis of certain matrix components (collagen type IV, laminin, syndecans, and glypicans) that are associated with physiological liver regeneration [44].

Hepatic stellate cells (Ito cells, HSCs) were first described in 1876 by Kupffer, who named them “Sternzellen”. In the literature, hepatic stellate cells are found under various names (Ito cells, lipocytes, perisinusoidal cells or parasinusoidal cells, fat storing cells). Currently, the widely accepted and preferred term for these cells is hepatic stellate cells [50; 51]. Like Kupffer cells and liver endothelial cells, stellate cells are non-parenchymal cells located

perisinusoidally in the space of Disse, in the recesses between hepatocytes, limited by the basolateral surface of hepatocytes and the antiluminal side of sinusoidal endothelial cells (SECs) [52].

A series of studies revealed the ability of HSC to deposit retinoids and lipids. Liver stellate cells synthesize proteoglycans, which are the main component of the extracellular matrix of the liver tissue, and their synthesis is 6 times higher than that of hepatocytes. They also the main source of collagen types I, III, IV, V, VI, tenascin, laminin, and fibronectin. This type of cell also synthesizes four types of matrix metalloproteinases [50]. HSCs also closely interact with endothelial cells and nerve endings through their numerous processes passing through the space of Disse.

In the cytosol of stellate cells, there is a rough endoplasmic reticulum, a reduced perinuclear Golgi apparatus, and the cell itself has cytoplasmic processes, some of which are interhepatic, and others are subendothelial [50]. Cell processes have microspikes, with the help of which the Ito cell establishes contacts with hepatocytes, receiving from the latter chemotactic stimuli that cause contraction of the stellate cell [53]. Ito cells contain vacuoles of two types (sap and contractile). Sap vacuoles are cell membrane-bound structures of various sizes that have a diameter of no more than 2 μm, and lysosomes are their precursors. Contractile vacuoles are not connected to the membrane and are larger, exceeding 8 μm [50, 51, 54].

Stellate cells are of two types: resting and activated. Under normal physiological conditions, HSCs are in the so-called inactivated state, and their main function is to accumulate lipids and vitamin A [55]. Due to their plasticity (depending on their functional state) and ability to transdifferentiate, stellate cells perform various functions that are sometimes conflicting. With various types of damage (viral hepatitis, toxic hepatitis), HSCs receive signals from hepatocytes and immunocompetent cells, activate, and transform into myofibroblast-like cells [50, 51]. When activated, HSCs are modified, acquiring a flat shape, and lose their characteristic lipid vacuoles [55]. At the same time, the granular endoplasmic reticulum of the cells increases due to the activation of protein synthesis, and many contractile microfilaments appear in the cytoplasm.

Activation of stellate cells includes two phases: initiation (phase 1) and sustained activation (phase 2) [50]. The first phase is triggered by paracrine stimulation from damaged hepatocytes, Kupffer cells, and endothelial cells. In the second phase of activation, a number of morphofunctional changes occur in the cell: proliferation, chemotaxis, fibrogenesis are activated, contractility appears, matrix degradation and loss of retinoids occur, proinflammatory, profibrogenic, and promitogenic stimuli that act in an autocrine and paracrine manner are released [56].

The assumption about the important role of Ito cells in the process of liver regeneration was first put forward in the works by G. Kent et al. [57]. Their close anatomical location with hepatocytes in the space of Disse and around progenitor cells makes HSC perfect for the role of the main component in the niche of resident stem cells in the liver, as well as a stimulator of hepatocyte proliferation [35, 38, 40, 48].

Ito cells participate in the restoration of the liver parenchyma, both due to the synthesis of growth factors, chemokines, eicosanoids and other small molecules with paracrine, juxtacrine, autocrine functions or chemoattractant activity, and the synthesis of macromolecules of the extracellular matrix, as well as its remodeling [59]. Activated HSCs produce a significant number of cytokines: hepatocyte growth factor (HGF), epidermal growth factor (EGF), erythropoietin, neurotrophin and transforming growth factor alpha (TGFα). TGF-a and EGF act in the same way as autocrine factors, stimulating the proliferation of HSCs. Hepatic stellate cells are the only source of HGF in the liver. Hepatocytes are the main point of application of HGF [60]. When the liver is damaged, activated HSCs proliferate and migrate to areas of inflammation and necrosis of hepatocytes, producing large amounts of extracellular matrix components [50].

CONCLUSION

Our studies on a model of liver cirrhosis caused by the administration of carbon tetrachloride (CT) and a 5% ethanol solution showed that the content of Ito cells in the organ parenchyma (CD45-CD133+) in this pathology model increases by 267.2% compared to baseline values [61]. According to numerous data, in addition to the liver, stellate cells are present in other organs, including the pancreas [41], kidneys [62], and lungs [63].

Thus, we can conclude that stellate cells are the key elements of the tissue microenvironment and participate in the regulation of liver tissue regeneration. Moreover, there is evidence that stellate cells are

progenitor elements and are capable of differentiating into tissue-specific cells [41, 58, 60, 64].

REFERENCES

1. Goldberg E.D., Dygai A.M., Zhdanov V.V. The role of hematopoiesis-inducing microenvironment in the regulation of hematopoiesis in cytostatic myelosuppression. Tomsk: STT, 1999:128 (in Russ.).
2. Dygai A.M., Zhdanov V.V. Theory of hematopoiesis regulation. Moscow: Publishing House of the Russian Academy of Sciences, 2012:140 (in Russ.).
3. Fuchs E., Blau H.M. tissue stem cells: architects of their niches. *Cell Stem Cell.* 2020;27(4):532–556. DOI: 10.1016/j.stem.2020.09.011.
4. Martinez P., Ballarin L., Ereskovsky A.V.et al. Articulating the "stem cell niche" paradigm through the lens of non-model aquatic invertebrates. *BMC Biol.* 2022;(1): 20:23. DOI: 10.1186/s12915-022-01230-5.
5. Yushkov B.G., Klimin V.G. Damage and regeneration. Moscow, 2017:132 (in Russ.).
6. Mannino G., Russo C., Maugeri G.et al. Adult stem cell niches for tissue homeostasis. *J. Cell Physiol.* 2022;237(1):239–257. DOI: 10.1002/jcp.30562.
7. Hicks M.R., Pyle A.D. The emergence of the stem cell niche. *Trends Cell Biol.* 2023 33(2):112–123. DOI: 10.1016/j.tcb.2022.07.003.
8. Urbán N., Cheung T.H. Stem cell quiescence: the challenging path to activation. *Development.* 2021;148(3). DOI: 10.1242/dev.165084.
9. Brunet A., Goodell M.A., Rando T.A. Ageing and rejuvenation of tissue stem cells and their niches. *Nat. Rev. Mol. Cell Biol.* 2023;(1):45–62. DOI: 10.1038/s41580-022-00510-w.
10. Nimiritsky N.P., Sagaradze G.D., Efimenko A.Yu., Makarevich P.I., Tkachuk V.A. The niche of the stem cell. *Cell and Tissue Biology.* 2018;60(8):575–586 (in Russ.).
11. Ceafalan L.C., Enciu A.M., Fertig T.E. et al. Heterocellular molecular contacts in the mammalian stem cell niche. *Eur. J. Cell Biol.* 2018;97(6):442–461. DOI: 10.1016/j.ejcb.2018.07.001.
12. Fujiwara H., Ferreira M., Donati G. et al. The basement membrane of hair follicle stem cells is a muscle cell niche. *Cell.* 2011;144(4):577–589. DOI: 10.1016/j.cell.2011.01.014.
13. Sugiyama T., Omatsu Y., Nagasawa T. Niches for hematopoietic stem cells and immune cell progenitors. *Int. Immunol.* 2019;31(1):5–11. DOI: 10.1093/intimm/dxy058.
14. Raaijmakers M.H.G.P. Aging of the hematopoietic stem cell niche: an unnerving matter. *Cell Stem Cell.* 2019;25(3):301–303. DOI: 10.1016/j.stem.2019.08.008.
15. Segel M., Neumann B., Hill M.F.E. et al. Niche stiffness underlies the ageing of central nervous system progenitor cells. *Nature.* 2019;573(7772):130–134. DOI: 10.1038/s41586-019-1484-9.
16. Deng Y., Xia B., Chen Z. et al. Stem cell-based therapy strategy for hepatic fibrosis by targeting intrahepatic cells. *Stem Cell Rev. Rep.* 2022;18(1):77–93. DOI: 10.1007/s12015-021-10286-9.
17. Brizzi M.F., Tarone G., Defilippi P. Extracellular matrix, integrins, and growth factors as tailors of the stem cell niche. *Curr. Opin. Cell Biol.* 2012;24(5):645651. DOI: 10.1016/j.ceb.2012.07.001.
18. Stanton A.E., Tong X., Yang F. Extracellular matrix type modulates mechanotransduction of stem cells. *Acta Biomater.* 2019;96:310–320. DOI: 10.1016/j. actbio.2019.06.048.
19. Lee-Thedieck C., Schertl P., Klein G. The extracellular matrix of hematopoietic stem cell niches. *Adv. Drug Deliv. Rev.* 2022;181:114069. DOI: 10.1016/j.addr.2021.114069.
20. Sánchez-Romero N., Sainz-Arnal P., Pla-Palacín I. et al. The role of extracellular matrix on liver stem cell fate: A dynamic relationship in health and disease. *Differentiation.* 2019;106:49–56. DOI: 10.1016/j.diff.2019.03.001.
21. Humphrey J.D., Dufresne E.R., Schwartz M.A. Mechanotransduction and extracellular matrix homeostasis. *Nat. Rev. Mol. Cell Biol.* 2014;15(12):802–812. DOI: 10.1038/nrm3896.
22. Goldberg E.D., Dygai A.M., Khlusov I.A. The role of the autonomic nervous system in the regulation of hematopoiesis. Tomsk, 1997:218 (in Russ.).
23. Oben J.A., Diehl A.M. Sympathetic nervous system regulation of liver repair. *Anat. Rec. A Discov. Mol. Cell. Evol. Biol.* 2004;280(1):874–883. DOI: 10.1002/ar.a.20081.
24. Cassiman D., Denef C., Desmet V.J. et al. Human and rat hepatic stellate cells express neurotrophins and neurotrophin receptors. *Hepatology.* 2001;33(1):148–158. DOI: 10.1053/jhep.2001.20793.
25. Comazzetto S., Shen B., Morrison S.J. Niches that regulate stem cells and hematopoiesis in adult bone marrow. *Dev. Cell.* 2021;56(13):1848–1860. DOI: 10.1016/j.devcel.2021.05.018.
26. Hassanshahi M., Hassanshahi A., Khabbazi S.et al. Bone marrow sinusoidal endothelium: damage and potential regeneration following cancer radiotherapy or chemotherapy. *Angiogenesis.* 2017; 20(4):427–442. DOI: 10.1007/s10456-017-9577-2.
27. Poisson J., Lemoinne S., Boulanger C. et al. Liver sinusoidal endothelial cells: Physiology and role in liver diseases. *J. Hepatol.* 2017;66(1):212–227. DOI: 10.1016/j.jhep.2016.07.009.
28. Craig D.J., James A.W., Wang Y.et al. Blood vessel resident human stem cells in health and disease. *Stem Cells Transl. Med.* 2022;11(1):35–43. DOI: 10.1093/stcltm/szab001.
29. Lafoz E., Ruart M., Anton A. et al. The Endothelium as a driver of liver fibrosis and regeneration. *Cells.* 2020;9(4):929. DOI: 10.3390/cells9040929.
30. Li K.N, Tumbar T. Hair follicle stem cells as a skin-organizing signaling center during adult homeostasis. *EMBO J.* 2021;40(11):e107135. DOI: 10.15252/embj.2020107135.
31. Duckworth C.A. Identifying key regulators of the intestinal stem cell niche. *Biochem. Soc. Trans.* 2021;49(5):2163–2176. DOI: 10.1042/BST20210223.
32. Sousa-Victor P., García-Prat L., Muñoz-Cánoves P. Control of satellite cell function in muscle regeneration and its disruption in ageing. *Nat. Rev. Mol. Cell Biol.* 2022;23(3):204–226. DOI: 10.1038/s41580-021-00421-2.
33. Ge J.Y., Zheng Y.W., Tsuchida T. et al. Hepatic stellate cells contribute to liver regeneration through galectins in hepatic

stem cell niche. *Stem Cell Res. Ther.* 2020;11(1):425. DOI: 10.1186/s13287-020-01942-x.
34. Afelik S., Rovira M. Pancreatic β-cell regeneration: Facultative or dedicated progenitors? *Mol. Cell. Endocrinol.* 2017; 445:8594. DOI: 10.1016/j.mce.2016.11.008.
35. Li W., Li L., Hui L. Cell plasticity in liver regeneration. *Trends Cell Biol.* 2020;30(4):329–338. DOI: 10.1016/j.tcb.2020.01.007.
36. Michalopoulos G.K., Bhushan B. Liver regeneration: biological and pathological mechanisms and implications. *Nat. Rev. Gastroenterol. Hepatol.* 2021;18(1):40–55. DOI: 10.1038/s41575-020-0342-4.
37. Overi D., Carpino G., Franchitto A. et al. Hepatocyte injury and hepatic stem cell niche in the progression of non-alcoholicsteatohepatitis. *Cells.* 2020;9(3):590. DOI: 10.3390/cells9030590.
38. Lanzoni G., Cardinale V., Carpino G. The hepatic, biliary, and pancreatic network of stem/progenitor cell niches in humans: A new reference frame for disease and regeneration. *Hepatology.* 2016;64(1):277–286. DOI: 10.1002/hep.28326.
39. Miyajima A., Tanaka M., Itoh T. Stem/progenitor cells in liver development, homeostasis, regeneration, and reprogramming. *Stem Cell.* 2014;14(5):561–574. DOI: 10.1016/j.stem.2014.04.010.
40. Itoh T., Miyajima A. Liver regeneration by stem/progenitor cells. *Hepatology.* 2014;59(4):1617–1626. DOI: 10.1002/hep.26753.
41. Bynigeri R.R., Jakkampudi A., Jangala R. et al. Pancreatic stellate cell: Pandora's box for pancreatic disease biology. *World J. Gastroenterol.* 2017;23(3):382–405. DOI: 10.3748/wjg.v23.i3.382.
42. Kordes C., Bock H.H., Reichert D. Hepatic stellate cells: current state and open questions. *Biol. Chem.* 2021;402(9):1021–1032. DOI: 10.1515/hsz-2021-0180.
43. Gaça M.D., Pickering J.A., Arthur M.J. et al. Human and rat hepatic stellate cells produce stem cell factor: a possible mechanism for mast cell recruitment in liver fibrosis. *J. Hepatol.* 1999;30(5):850–858. DOI: 10.1016/s0168-8278(99)80139-1.
44. Lorenzini S., Bird T.G., Boulter L. et al. Characterisation of a stereotypical cellular and extracellular adult liver progenitor cell niche in rodents and diseased human liver. *Gut.* 2010;59(5):645–654. DOI: 10.1136/gut.2009.182345.
45. Kamm D.R., McCommis K.S. Hepatic stellate cells in physiology and pathology. *J. Physiol.* 2022;600(8):1825–1837. DOI: 10.1113/JP281061.
46. Hayes A.J., Tudor D., Nowell M.A. et al. Chondroitin sulfate sulfation motifs as putative biomarkers for isolation of articular cartilage progenitor cells. *J. Histochem. Cytochem.* 2008;56(2):125–138. DOI: 10.1369/jhc.7A7320.2007.
47. Wang Y., Cui C.-B., Yamauchi M. et al. Lineage restriction of human hepatic stem cells to mature fates is made efficient by tissue-specific biomatrix scaffolds. *Hepatology.* 2011;53(1):293–305. DOI: 10.1002/hep.24012.
48. Harrill J.A., Parks B.B., Wauthier E.et al. Lineage-dependent effects of aryl hydrocarbon receptor agonists contribute to liver tumorigenesis. *Hepatology.* 2015;61(2):548–560. DOI: 10.1002/hep.27547.
49. Lee Y.A., Wallace M.C., Friedman S.L. Pathobiology of liver fibrosis: a translational success story. *Gut.* 2015;64 (5):830–841. DOI: 10.1136/gutjnl-2014-306842.
50. Schönberger K., Tchorz J.S. Hepatic stellate cells: From bad reputation to mediators of liver homeostasis. *Sci. Signal.* 2023;16(787):eadh5460. DOI: 10.1126/scisignal.adh5460.
51. Blaner W.S., O'Byrne S.M., Wongsiriroj N. et al. Hepatic stellate cell lipid droplets: a specialized lipid droplet for retinoid storage. *Biochim. Biophys. Acta.* 2009;1791(6):467–473. DOI: 10.1016/j.bbalip.2008.11.001.
52. Gupta G., Khadem F., Uzonna J.E. Role of hepatic stellate cell (HSC)-derived cytokines in hepatic inflammation and immunity. *Cytokine.* 2019;124:154542–154542. DOI: 10.1016/j.cyto.2018.09.004.
53. Melton A.C., Yee H.F. Hepatic stellate cell protrusions couple platelet-derived growth factor-BB to chemotaxis. *Hepatology.* 2007;45(6):1446–1453. DOI: 10.1002/hep.21606.
54. Efremova N.A., Greshnyakova V.A., Goryacheva L.G. Modern ideas about the pathogenetic mechanisms of liver fibrosis. *Journal of Infectology.* 2023;15(1):16–24 (in Russ.). DOI: /10.22625/2072-6732-2023-15-1-16-24.
55. Tsuchida T., Friedman S.L. Mechanisms of hepatic stellate cell activation. *Nat. Rev. Gastroenterol. Hepatol.* 2017;14(7):397–411. DOI: 10.1038/nrgastro.2017.38.
56. Krizhanovsky V., Yon M., Dickins R.A. et al. Senescence of activated stellate cells limits liver fibrosis. *Cell.* 2008;134(4):657–667. DOI: 10.1016/j.cell.2008.06.049.
57. Kent G., Gay S., Inouye T., et al. Vitamin A-containing lipocytes and formation of type III collagen in liver injury. *Proc. Natl. Acad. Sci. USA.* 1976;73(10):3719–3722. DOI: 10.1073/pnas.73.10.3719.
58. Roskams T. Different types of liver progenitor cells and their niches. *J. Hepatol.* 2006;45(1):1–4. DOI: 10.1016/j.jhep.2006.05.002.
59. Chen L., Zhang W., Zhou Q. et al. HSCs play a distinct role in differentphases of oval cell-mediated liver regeneration. *Cell. Biochem. Funct.* 2012;30(7):588–596. DOI: 10.1002/cbf.2838.
60. Kitto L.J., Henderson N.C. Hepatic stellate cell regulation of liver regeneration and repair. *Hepatol. Commun.* 2021;5(3):358–370. DOI: 10.1002/hep4.1628.
61. Skurikhin E.G., Zhukova M.A., Pan E.S., Ermakova N.N., Pershina O.V., Pakhomova A.V., et al. Age-related features of the liver and stem cell reactions in the modeling of liver cirrhosis. *Cellular Technologies in Biology and Medicine*. 2021;1:24–30 (in Russ.).
62. Cha J.J., Mandal C., Ghee J.Y. et al. Inhibition of renal stellate cell activation reduces renal fibrosis. *Biomedicines.* 2020;8(10):431. DOI: 10.3390/biomedicines8100431.
63. Choi J., Son Y., Moon J.W., Park D.W., Kim Y.S., Oh J. Fusion protein of RBP and albumin domain III reduces lung fibrosis by inactivating lung stellate cells. *Biomedicines.* 2023;11(7):2007. DOI: 10.3390/biomedicines11072007.
64. Pintilie D.G., Shupe T.D., Oh S.H. et al. Hepatic stellate cells' involvement in progenitor-mediated liver regeneration. *Lab. Invest.* 2010;90(8):1199–1208. DOI: 10.1038/labinvest.2010.88.

Authors' information

Zhdanov Vadim V. – Dr. Sci. (Med.), Corresponding Member of RAS, Director of Goldberg Research Institute of Pharmacology and Regenerative Medicine, Tomsk NRMC, Tomsk, hdanov_vv@pharmso.ru, https://orcid.org/0000-0002-9516-0204

Chaikovskii Alexander V. – Cand. Sci. (Med.), Researcher, Laboratory of Pathophysiology and Experimental Therapy, Goldberg Research Institute of Pharmacology and Regenerative Medicine, Tomsk NRMC, Tomsk, thav_pharm@mail.ru, https://orcid.org/0000-0003-4398-9122

Pan Edgar S. – Cand. Sci. (Biology), Senior Researcher, Laboratory for Regulation of Reparative Processes, Research Institute of General Pathology and Pathophysiology, Moscow, artifexpan@gmail.com, https://orcid.org/0000-0002-2163-7647

(✉) **Zhdanov Vadim V.,** hdanov_vv@pharmso.ru

Received 11.08.2023;
approved after peer review 27.08.2023;
accepted 14.09.2023

УДК: 618.16-002.27-07-08(048.8)
https://doi.org/10.20538/1682-0363-2024-1-134-143

Vulvovaginal atrophy: current methods of diagnosis and treatment

Zainetdinova L.F., Telesheva L.F., Medvedev B.I., Khakhulina V.V.

South Ural State Medical University
64, Vorovskogo Str., Chelyabinsk, 454092, Russian Federation

ABSTRACT

Aim. To review modern methods of diagnosis and treatment of vulvovaginal atrophy (VVA), which is one of the manifestations of genitourinary syndrome of menopause in peri- and postmenopausal women.

Materials and methods. A review of domestic and foreign literature on the prevalence and modern methods of diagnosis and treatment of VVA was carried out.

Results. Unlike vasomotor symptoms, VVA progresses with age, causing a significant impairment in women's quality of life. Symptoms usually begin to bother perimenopausal patients, but their frequency and severity increase significantly in postmenopausal women. Diagnosis of VVA can present some difficulties, as many women perceive their condition as a natural manifestation of aging and do not seek medical care. Currently, drug and non-drug therapies for VVA have been proposed, each of which has its own characteristics, indications, and contraindications. However, the safety and effectiveness of some of them have not been fully proven.

Conclusion. VVA is common in peri- and postmenopausal women. Modern aspects of the diagnosis and treatment of this pathology can significantly improve the quality of life of patients with VVA symptoms. However, further research is needed to confirm safety of the proposed treatment methods, and search for new techniques is required.

Keywords: vulvovaginal atrophy, genitourinary syndrome of menopause, peri- and postmenopause

Conflict of interest. The authors declare the absence of obvious or potential conflicts of interest related to the publication of this article.

Source of financing. The authors state that they received no funding for the study.

For citation: Zainetdinova L.F., Telesheva L.F., Medvedev B.I., Khakhulina V.V. Vulvovaginal atrophy: current methods of diagnosis and treatment. *Bulletin of Siberian Medicine.* 2024;23(1):134–143. https://doi.org/10.20538/1682-0363-2024-1-134-143.

Вульвовагинальная атрофия: современные методы диагностики и лечения (обзор литературы)

Зайнетдинова Л.Ф., Телешева Л.Ф., Медведев Б.И., Хахулина В.В.

Южно-Уральский государственный медицинский университет (ЮУГМУ)
Россия, 454092, г. Челябинск, ул. Воровского, 64

РЕЗЮМЕ

Целью публикации является обзор современных методов диагностики и лечения вульво-вагинальной атрофии (ВВА), которая является одним из проявлений генитоуринарного менопаузального синдрома у женщин в пери- и постменопаузе.

✉ *Zainetdinova Larisa F.,* sea-gull6@yandex.ru

Материалы и методы. Проведен обзор отечественных и зарубежных источников, посвященных распространенности, диагностике и методам лечения ВВА.

Результаты. В отличие от вазомоторных симптомов, ВВА прогрессирует с возрастом, вызывая значительное нарушение качества жизни женщин. Симптомы, как правило, начинают беспокоить пациенток в перименопаузе, но их частота и выраженность значительно возрастают в постменопаузе. Диагностика ВВА может представлять некоторые трудности, так как многие женщины воспринимают свое состояние как естественное проявление старения организма и не обращаются за медицинской помощью. В настоящее время предложены медикаментозные и немедикаментозные методы лечения ВВА, каждый из которых имеет свои особенности, показания и противопоказания. Однако безопасность и эффективность некоторых из них полностью не доказана.

Заключение. Вульво-вагинальная атрофия часто встречается у женщин пери- и постменопаузального возраста. Современные аспекты диагностики и лечения данной патологии позволяют значительно повысить качество жизни пациенток с симптомами ВВА, однако необходимы дальнейшие исследования для подтверждения безопасности предлагаемых методов лечения и поиск новых.

Ключевые слова: вульво-вагинальная атрофия, генитоуринарный менопаузальный синдром, пери- и постменопауза

Конфликт интересов. Авторы декларируют отсутствие явных и потенциальных конфликтов интересов, связанных с публикацией настоящей статьи.

Источник финансирования. Авторы заявляют об отсутствии финансирования при проведении исследования.

Для цитирования: Зайнетдинова Л.Ф., Телешева Л.Ф., Медведев Б.И., Хахулина В.В. Вульвовагинальная атрофия: современные методы диагностики и лечения (обзор литературы). *Бюллетень сибирской медицины.* 2024;23(1):134–143. https://doi.org/10.20538/1682-0363-2024-1-134-143.

INTRODUCTION

One of the urgent problems in gynecology, which reduces the quality of life of women in menopause, is the genitourinary syndrome of menopause (GSM). The term GSM was proposed in 2014 by the North American Menopause Society (NAMS) and the International Society for the Study of Women's Sexual Health (ISSWSH), and was endorsed by the Russian Society of Gynecological Endocrinology and Menopause (ROSGEM) in 2015. This is a symptom complex associated with a decrease in estrogens and other sex steroids, including changes that occur in the external genitalia, perineum, vagina, urethra, and bladder [1, 2].

Symptoms of GSM typically begin in the perimenopause and progress into the postmenopausal period leading to functional and anatomical changes [3]. The incidence of GSM in perimenopausal women is 15–19%, and in postmenopausal women, it is 40–90% [4–9]. The prevalence of vulvovaginal atrophy (VVA), as one of the GSM manifestations, is 19% in women aged 40–45 years, in peri- and postmenopause, it ranges from 36 to 90% [5, 6, 10]. According to K. Levine et al. in sexually active women aged 40–65 years, symptoms corresponding to VVA occur in 57% [11]. However, despite the wide prevalence of VVA and GSM in general, this disease is often not diagnosed and treated [11–14].

Histologic changes in the vaginal epithelium in peri- and postmenopausal women include its thinning with signs of keratinization and a high nucleus-to-cytoplasmic ratio, the predominance of basal and parabasal cells, and a sharp decrease in the number of intermediate, surface cells and glycogen. This leads to a decrease in the number of lactobacilli and an increase in the pH of the vagina. Hypoestrogenic state of the vagina also includes smooth muscle atrophy, changes in the composition of the connective tissue with an imbalance in type I / III collagen, elastin, and hyaluronic acid, which leads to a decrease in tissue strength and elasticity and possibly fibrosis and obliteration of the vagina.

Thinning of the vaginal epithelium increases susceptibility to injury, which leads to bleeding, petechiae, ulceration, and inflammation [9, 15–19]. A small number of lactobacilli can cause vaginal colonization with anaerobic bacteria, inflammation,

and abnormal discharge and predispose to urinary tract infection. [20, 21]. According to the literature, in women with VVA, a microbiological examination of the vaginal discharge may show a pattern of normocenosis (44%), atrophic vaginitis (42%), bacterial vaginosis (12%), and non-specific vaginitis (1.7%). There is an increase in the number of neutrophils in atrophic vaginitis compared to vaginal atrophy [22–25]. According to some authors, an increase in anaerobic microflora can contribute to the appearance of VVA symptoms in peri- and postmenopausal women, but not all researchers agree with this [26–28].

VVA is manifested by such symptoms as dryness, burning, itching, irritation, discomfort and pain in the vagina, bloody discharge during and after sexual contact, sexual dysfunction, and superficial dyspareunia, unlike deep dyspareunia, which is characteristic of endometriosis [14]. This is a chronic pathology that progresses over the years. According to E. Moral et al., vaginal dryness is the most common and distressing symptom, affecting up to 93% of women. The severity of this symptom can be moderate or severe in 68% of cases [7].

Diagnosis of VVA is based on anamnestic data, assessment of the patient's complaints, gynecological examination with the determination of clinical signs, as well as laboratory tests. The medical history should include questions about the characteristics of sexual function, the presence of reduced libido and superficial dyspareunia [14]. On examination, the vaginal epithelium is thinned, pale, smooth due to impaired blood supply, there may be prolapse of the walls of the vagina. The thinned vaginal epithelium is easily injured during gynecological examination, and there may be subepithelial hemorrhages [29].

In addition, laboratory tests, such as vaginal pH assessment, vaginal maturation index (VMI), and vaginal health index (VHI), are used. With a decrease in estrogen levels, the vaginal environment becomes alkaline (pH > 4.5). With all these changes, the number of lactobacilli decreases and the growth of opportunictic and obligate anaerobes increases. VMI shows the degree of maturation of the vaginal epithelium by the balance between superficial, intermediate, and parabasal cells. With estrogen deficiency, the number of superficial cells sharply decreases or completely disappears, the number of cells in the intermediate layer decreases, and the number of cells in the parabasal and basal layers increases [29, 30].

VHI is one of the most commonly used parameters in the diagnosis of VVA. It allows specialists to evaluate the elasticity of the vagina, the nature and volume of secretions, pH, the presence of petechiae on the epithelium, and moisture. With vaginal atrophy, VHI does not exceed 15. However, clinical signs do not always correlate with laboratory data. [29, 31].

The Vulvovaginal Symptoms Questionnaire [32, 33], the Day-to-Day Impact of Vaginal Aging Questionnaire [34], and the Vaginal and Vulvar Assessment Scale Questionnaire [35] were highly effective for assessing VVA symptoms and GSM in general. However, despite its high prevalence, VVA is underdiagnosed and undertreated mainly due to the trend of many women to perceive it as a normal sign of natural aging [9, 16, 36–38].

Therapy for VVA and other manifestations of GSM should be started as early as possible, before the onset of irreversible atrophic manifestations, and continued for a long time, since symptoms may return [39–41]. The main goal of treatment is to relieve symptoms. Drug and non-drug treatments are used for this purpose. In 2020, the North American Menopause Society published updated guidelines [42]. For mild manifestations, lubricants and moisturizers are used at the first stage of treatment. They are devoid of side effects and can be used for a long time. This treatment option is recommended for women for whom the use of vaginal estrogen preparations is unacceptable [43, 44]. Vaginal lubricants are especially indicated for women who are concerned about vaginal dryness during sexual intercourse. They may be water soluble and at the same time tend to dry out. Silicone-based or oil-based lubricants are stronger but less lubricating.

Vaginal humectants are insoluble hydrophilic polymers with characteristic bioadhesiveness and the ability to retain moisture that is released locally, mimicking physiological vaginal discharge. They can also contain a large amount of excipients that affect the pH and osmolarity of the solution [43]. They can be used not only during sexual intercourse, but also regularly, as they have a fairly long-lasting effect, increasing the moisture content of the vaginal mucosa and lowering the pH. The frequency of use is directly proportional to the severity of vaginal atrophy. Topical use is recommended in the evening, at bedtime for 7–10 days, and then twice a week to maintain the effect.

Moisturizers most commonly contain hyaluronic acid, a glycosaminoglycan produced by fibroblasts, which is a major component of the extracellular

matrix found in connective and nervous tissue and epithelium, including the vagina. Hyaluronic acid is a strong antioxidant, increases the level of moisture in the cells, and reduces the symptoms of atrophy. When tissues are damaged, hyaluronic acid can stimulate fibroblast migration and proliferation, neoangiogenesis, tissue re-epithelialization, and collagen fiber deposition. With regular, daily or every 2–3-day use of a hyaluronic acid-based product, the severity of vaginal dryness is reduced, and this effect is comparable to the effect of topical estrogen therapy [45, 46]. Hyaluronic acid with phytoestrogens is part of the Estrogial preparation, which contains the sodium salt of hyaluronic acid, extracts of clover, calendula, and hops and can be used as monotherapy in patients with symptoms of vaginal atrophy in case of unwillingness or contraindication to the use of estrogens [47, 48].

The non-hormonal drug Multi-Gyn-Liqui-Gel, which is a gel based on the patented 2QR complex, betaine, glycerol, and xanthan gum, is used to eliminate vaginal dryness and stimulate natural hydration, prevent itching and the development of pathological conditions of the vagina and has the ability to neutralize pathogens and maintain vaginal hydration. This natural, safe agent protects the natural microflora and can be used in patients with breast cancer [49, 50].

A.G. Kedrova notes a good relief of VVA symptoms when Flamena is used in women after gynecological operations or in the process of combined treatment of tumors of the female reproductive system. Flamena is a gel containing active ingredients (dihydroquercetin, lecithin, glycine, and sangviritrin), which diffuses well through the walls of the vagina, moisturizing them and improving microcirculation. Treatment is carried out for 14–21 days until the symptoms of dryness, burning, itching, and irritation of the mucous membranes are relieved. Then it is possible to switch to maintenance therapy 2–3 times a week [51]. G. Capobianco et al. showed the effectiveness of the use of Lactobacillus acidophilus, estriol, and correction of the pelvic floor dysfunction to eliminate the symptoms of VVA in postmenopausal women [52].

Other possible components of vaginal moisturizers are ozonides, ozone intermediates that act as a biological reservoir that retains the therapeutic effect of the molecule. In connection with biological tissues, ozonides are rapidly activated, stimulating local microcirculation, inducing neoangiogenesis, promoting tissue repair, and inhibiting proinflammatory prostaglandins [53]. Fibroblasts are known to play an important role in re-epithelialization, synthesis of collagen fibers, regeneration of the extracellular matrix, tissue remodeling, and release of such endogenous growth factors as FGF, PDGF, TGF-β, and VEGF [54, 55]. Ozone stimulates the formation of collagen and fibroblasts in the wound, as well as growth factors PDGF, TGF-β, and VEGF [56]. Ozone promotes wound healing by activating the transcription factor NF-κB and regulating inflammatory responses [57, 58]. Ozone may influence the expression of proinflammatory cytokines, such as interleukin-1 (IL-1) and tumor necrosis factor α (TNFα), as well as adaptive immune responses, including cyclooxygenase-2 (*COX-2*) gene activation via activation of NF-κB [59, 60].

Non-hormonal VVA therapy provides relief of mild symptoms, while estrogen therapy is most effective in treating moderate and severe symptoms of vaginal atrophy [61]. Topical estrogen hormone therapy is used as the second step in case of failure of vaginal lubricants and moisturizers [62, 63].

Topical VVA therapy includes the use of natural estrogens in the form of tablets, creams, suppositories, or rings [64]. Estriol is the most effective and safest treatment for VVA symptoms, since it has the lowest affinity for estrogen receptors, does not convert to estradiol, and its systemic effects are extremely limited. The absence of a systemic effect of estriol is explained by the binding time to the receptor, which does not exceed 4 hours. [39].

The intravaginal administration of estriol has no age restrictions and can be prescribed to women over 60 years of age. At the beginning of treatment, drugs are prescribed daily at a therapeutic dose for 2–4 weeks (saturation therapy): estriol (vaginal suppositories) 0.5 mg, estriol (vaginal cream) – 1 mg / g; as there is improvement, 2 times a week for a year, then the duration of treatment is determined individually (maintenance therapy) [65]. The rationale for this regimen is that estrogen absorption is the highest during the first few days of treatment, when the vaginal epithelium is atrophic and highly vascularized. Once the epithelium matures, uptake of local estrogen decreases and therefore lower doses of estrogen are sufficient to prevent repeated atrophy [64].

Repeated intravaginal administration of estriol results in a small cumulative effect. However, doses of up to 0.5 mg of estriol twice a week are not associated with a significant increase in serum estrogen levels

after short-term (1 week) and long-term (12 months) treatment [42, 65]. The use of low-dose estriol in VVA does not require protection of the endometrium with progesterone. However, the systemic effects of estrogens are limited to low doses but not completely eliminated, especially at early stages of treatment [66]. Local estrogen therapy leads to a decrease in vaginal pH, an increase in the number of lactobacilli, maturation of the vaginal epithelium, and a decrease in the severity of dyspareunia and dryness symptoms [67–69].

One of the options for treating the symptoms of vaginal atrophy is the use of combined vaginal therapy: lyophilized culture of *Lactobacillus casei rhamnosus* (at least 2 x 10^7 CFU of viable lactobacilli), 0.2 mg estriol and 2.0 mg progesterone [70, 71], as well as an ultra-low dose of estriol (0.03 mg) and a lyophilized culture of *Lactobacillus acidophilus* KS400 (100×10^6 CFU of viable lactobacilli) [72]. Probiotic lactobacilli restore homeostasis in the vagina by enhancing the barrier function of the epithelium, affecting the secretion of antimicrobial peptides and mucosal immunity, and blocking the adhesion of pathogens. This allows not only to maintain the proliferation and maturation of the vaginal epithelium, but also to restore the lactobacillus microflora [70–72].

The presence of vasomotor symptoms is an indication for menopausal hormone therapy (MHT). However, up to 25% of women receiving MHT will continue to experience symptoms of urogenital atrophy. It is recommended that such women take vaginal estriol after reducing the severity or cessation of vasomotor disorders [62, 65].

Topical application of low doses of estrogen can cause side effects, such as burning sensation and swelling of the vaginal mucosa, which can reduce adherence to treatment [73]. There is also evidence that local estrogen therapy is not effective in 23–42% of treated women [74].

More than 60% of peri- and postmenopausal women with a history of breast cancer suffer from VVA symptoms. However, even topical estrogens present significant risks, especially in the estrogen-dependent histologic variant. Therefore, in the case of a history of estrogen-sensitive tumors, such as breast, endometrial, ovarian cancer, it is necessary to individually compare the risk and benefit together with an oncologist [36, 75]. Clinical data from large observational studies, such as Women's Health Initiative, Observational Study (WHI-OS), and the Nurses' Health Study, did not find an increased risk of endometrial cancer in women who used vaginal estrogens [76].

In February 2013, the US Food and Drug Administration (FDA) approved a selective estrogen receptor modulator, ospemifene, for the treatment of symptoms of VVA in menopausal women. It acts as an estrogen agonist in the vagina and has no clinically significant estrogenic effect on the endometrium or mammary glands. However, the safety of ospemifene has not been proven in women with a history of breast cancer or an increased risk of breast cancer or thromboembolism. The disadvantages of ospemifene compared to vaginal estrogens include the need for daily use and systemic side effects (flushing, potential risk of thromboembolism) [77].

Vaginal use of dehydroepiandrosterone sulfate (DHEA) for the treatment of GSM symptoms is due to the fact that DHEA is a precursor hormone and is converted into estrogen and androgens (testosterone, androstenedione and dihydrotestosterone) upon intravaginal administration [2]. The use of DHEA compared with placebo is an effective remedy for vaginal dryness, burning, itching, and dyspareunia and increases libido [78]. However, it has not yet been registered in the UK and Russia, and there are no data confirming its safety in patients with a history of breast cancer [79].

H.A. Torky et al. used oxytocin gel to treat symptoms of VVA in postmenopausal women. During treatment with oxytocin, there was an increase in the thickness of the vaginal epithelium and relief of VVA symptoms due to the ability of oxytocin to stimulate proliferation processes, increase the intensity of blood flow in the mucous membrane, and increase the secretion of growth factors [73].

The use of fractional laser and radiofrequency technologies is a new trend that is gaining popularity in the treatment of VVA. The most widely used technologies include fractional microablative CO_2 laser, non-ablative photothermal erbium-yttrium-aluminum garnet (YAG) laser and radio frequency (RF) energy devices. Laser or radiofrequency waves act by heating the connective tissue of the vaginal wall up to 40–42 °C. The effect of thermal energy on the walls of the vagina and vulva stimulates biological processes, such as proliferation, neovascularization, and synthesis of collagen and growth factors, which restores the elasticity and moisture of the vaginal mucosa and levels the symptoms of atrophy [80–82].

The effectiveness of laser therapy in the treatment of VVA has been assessed by VHI and the female

sexual function index (FSFI) in many studies and is comparable to that of topical estrogens [82–87]. Although the authors generally note that the procedure is well tolerated and proceeds quickly and painlessly, there have also been reports of increased pain in the vagina, scarring, fibrosis, impaired urination, and dyspareunia [88]. For the treatment of vaginal atrophy, three cycles are performed at an interval of 30–40 days, then once a year as maintenance therapy. However, the safety and efficacy of using a laser in vaginal atrophy has not been fully proven; it is not clear how long the effect of the treatment lasts [36, 88].

Temperature controlled transcutaneous radiofrequency (TTCRF) and, more recently, low-energy dynamic quadripolar radiofrequency (DQRF) can be used to treat VVA symptoms, sexual dysfunction, and urinary dysfunction [89–91]. No side effects, including burns or injury, have been reported. The treatment is well tolerated by patients. However, the number of patients is usually small, and the effectiveness of the method should be evaluated in larger studies [90].

Intramucosal (into the vaginal wall) injections of platelet-rich plasma is another direction in VVA treatment, which is under study. Injections are made once every 7–14 days, the course of treatment includes 2–6 procedures. Platelet-rich plasma (PRP) is an increased concentration of autologous platelets suspended in a small amount of plasma after centrifugation. The concept of PRP therapy lies in the ability of platelets to secrete numerous growth factors that are contained in platelet granules and are released from them during the process of platelet activation. Growth factors stimulate cell proliferation, differentiation, and migration to the injection site.

PRP therapy has a remodeling effect, supports tissue regeneration at the injection site, activates fibroblasts that create collagen and elastin, and also has antimicrobial and antifungal effects. PRP therapy is a safe and physiological method, since the patient's own blood components are used. PRP therapy is effective for treating dryness of the vaginal mucosa, burning, itching, discomfort, pain during sexual intercourse, discharge from the genital tract, inflammation of the vaginal mucosa when there is atrophy, as well as for restoring the microflora and, in general, occupies a leading position in anti-age medicine [92]. Stopping smoking may be an important factor in alleviating VVA symptoms, as smoking is associated with an increase in estrogen metabolism leading to vaginal atrophy [75].

Thus, VVA still remains a poorly understood and underdiagnosed disease. It affects the quality of life of millions of peri- and postmenopausal women. Over the past decade, various approaches have been developed to correct disorders of the urogenital tract associated with age-related estrogen deficiency, which create ample opportunities for the treatment of GSM symptoms. However, there is still no comprehensive data on the effectiveness and safety of many of the proposed drug and non-drug treatments.

REFERENCES

1. Yureneva S.V., Ermakova E.I., Glazunova A.V. Diagnosis and therapy of genitourinary menopausal syndrome in peri- and postmenopausal patients (brief clinical guidelines). *Obstetrics and Gynecology.* 2016;(5):138–144 (in Russ.). DOI: 10.18565/ aig.2016.5.138-144.
2. Brodman K.F. Genitourinary syndrome of menopause. in: mount sinai expert guides: obstetrics and gynecology. ed. R. Sperling. New York, NY, USA: John Wiley & Sons Ltd, 2020:210–217.
3. Sinha A., Ewies A.A.A. Non-hormonal topical treatment of vul-vovaginal atrophy: an up-to-date overview. *Climacteric*. 2013;16:305–331. DOI: 10.3109/13697137.2012.756466.
4. Palma F., Volpe A., Villa P., Cagnacci A. Vaginal atrophy of women in postmenopause. Results from a multicentric observational study: The AGATA study. *Maturitas*. 2016;83:40–44. DOI: 10.1016/j.maturitas.2015.09.001.
5. Kingsber S.A., Krychman M., Graham S., Bernick B., Mirkin S. The Women's EMPOWER Survey: Identifying women's perceptions on vulvar and vaginal atrophy and its treatment. *J. Sex Med*. 2017;14:413–424. DOI: 10.1016/j.jsxm.2017.01.010.
6. Nappi R.E., Seracchioli R., Salvatore S., Cagnacci A., Di Paolantonio T., Busacca M. Impact of vulvovaginal atrophy of menopause: Prevalence and symptoms in Italian women according to the EVES study. *Gynecol. Endocrinol*. 2019;35:453–459. DOI: 10.1080/09513590.2018.1563883.
7. Moral E., Delgado J.L., Carmona F., Caballero B., Guillán C., González P.M. et al. Genitourinary syndrome of menopause. Prevalence and quality of life in Spanish postmenopausal women. The GENISSE study. *Climacteric*. 2018;21:167–173. DOI: 10.1080/13697137.2017.1421921.
8. Cagnacci A., Xholli A., Sclauzero M., Venier M., Palma F., Gambacciani M. Vaginal atrophy across the menopausal age: Results from the ANGEL study. *Climacteric*. 2019;22:85–89. DOI: 10.1080/13697137.2018.1529748.
9. Gandhi J., Chen A., Dagur G., Suh Y., Smith N., Cali B. et al. Genitourinary syndrome of menopause: an overview of clinical manifestations, pathophysiology, etiology, evaluation, and management. *Am. J. Obstet. Gynecol*. 2016;215:704–711. DOI: 10.1016/j.ajog.2016.07.045.
10. Alvisi S., Gava G., Orsili I., Giacomelli G., Baldassarre M., Seracchioli R. et al. Review: vaginal health in menopausal women. *Medicina*. 2019;55:615. DOI: 10.3390/medicina55100615.

11. Levine K., Williams R., Hartmann K. Vulvovaginal atrophy is strongly associated with female sexual dysfunction among sexually active postmenopausal women. *Menopause*. 2008;15:661–666. DOI: 10.1097/gme.0b013e31815a5168.
12. Da Silva A.S., Baines G., Araklitis G., Robinson D., Cardozo L. Modern management of genitourinary syndrome of menopause. *Fac. Rev*. 2021;10:25. DOI: 10.12703/r/10-25.
13. Santoro N., Komi J. Prevalence and impact of vaginal symptoms among postmenopausal women. *J. Sex Med*. 2009;6:2133–2142. DOI: 10.1111/j.1743-6109.2009.01335.x.
14. Jannini E.A., Nappi R.E. Couplepause: a new paradigm in treating sexual dysfunction during menopause and andropause. *Sex Med. Rev*. 2018;6:384–395. DOI: 10.1016/j.sxmr.2017.11.002.
15. Miller E.A., Beasley D.E., Dunn R.R., Archie E.A. Lactobacilli dominance and vaginal pH: Why is the human vaginal microbiome unique? *Front. Microbiol*. 2016;7:1936. DOI: 10.3389/fmicb.2016.01936.
16. Briggs P. Genitourinary syndrome of menopause. *Post. Reprod. Health*. 2020;26(2):111–114. DOI: 10.1177/2053369119884144.
17. Portman D.J., Gass M.L. Genitourinary syndrome of menopause: new terminology for vulvovaginal atrophy from the International Society for the Study of Women's Sexual Health and the North American Menopause Society. *Menopause*. 2014;21:1063–1068. DOI: 10.1097/GME.0000000000000329.
18. Nappi R.E., Palacios S., Panay N., Particco M., Krychman M.L. Vulvar and vaginal atrophy in four European countries: Evidence from the European REVIVE Survey. *Climacteric*. 2016;19(2):188–197. DOI: 10.3109/13697137.2015.1107039.
19. Kim H., Kang S.Y., Chung Y.J., Kim J.H., Kim M.R. The recent review of the genitourinary syndrome of menopause. *J. Menopausal. Med*. 2015;21:65–71. DOI: 10.6118/jmm.2015.21.2.65.
20. Briggs P. Genitourinary syndrome of menopause. *Post. Reproductive Health*. 2020;26(2):111–114. DOI: 10.1177/2053369119884144.
21. K., Schneider G.M., Ridenhour B.J., Williams C.J., Song Y., Farage M.A. et al. Comparison of the vaginal microbiomes of premenopausal and postmenopausal women. *Front. Microbiol*. 2019;10:193. DOI: 10.3389/fmicb.2019.00193.
22. Stika C.S. Atrophic vaginitis. *Dermatol. Ther*. 2010;23(5):514–522. DOI: 10.1111/j.1529-8019.2010.01354.x.
23. Savelyeva G.M., Sukhoi G.T., Serov V.N., Radzinsky V.E., Manukhin I.B. (ed.) Gynecology. National guidelines. Moscow: GEOTAR-Media, 2017:1008 (in Russ.).
24. Ovsyannikova T.V., Makarov I.O., Borovkova E.I., Kulikov I.A. Local therapy of urogenital disorders in peri- and postmenopause. *Obstetrics, Gynecolog,y and Reproduction.* 2010;4(3):25–28 (in Russ.).
25. Rees M., Perez-Lopez F.R., Ceasu I., Depypere H., Erel T., Lambrinoudaki I. et al. EMAS clinical guide: low-dose vaginal estrogens for postmenopausal atrophy. *Maturitas.* 2012;73(2):171–174. DOI: 10.1016/j.maturitas.2012.06.009.
26. Hummelen R., Macklaim J.M., Bisanz J.E., Hammond J.A., McMillan A., Vongsa R. et al. Vaginal microbiome and epithelial gene array in post-menopausal women with moderate to severe dryness. *PLoS One.* 2011;6:e26602. DOI: 10.1371/journal.pone.0026602.
27. Brotman R.M., Shardell M.D., Gajer P., Fadrosh D., Chang K., Silver M.I. et al. Association between the vaginal microbiota, menopause status, and signs of vulvovaginal atrophy. *Menopause*. 2014;21:450–458. DOI: 10.1097/GME.0b013e3182a4690b.
28. Shen J., Song N., Williams C.J., Brown C.J., Yan Z., Xu C., Forney L.J. Effects of low dose estrogen therapy on the vaginal microbiomes of women with atrophic vaginitis. *Sci. Rep*. 2016;6:24380. DOI: 10.1038/srep24380.
29. Apolikhina I.A., Gorbunova E.A. Clinical and morphological aspects of vulvovaginal atrophy. *Medical Council*. 2014;(9):110–117 (in Russ.).
30. Hess R., Austin R.M., Dillon S., Chang C.C., Ness R.B. Vaginal maturation index self-sample collection in midlife women: Acceptability and correlation with physician-collected samples. *Menopause*. 2008;15:726–729. DOI: 10.1097/gme.0b013e31816c5541.
31. Bachmann G. Urogenital ageing: An old problem newly recognized. *Maturitas*. 1995;22:S1–S5. DOI: 10.1016/0378-5122(95)00956-6.
32. Fernandez-Alonso A.M., Cuerva M.J., Chedraui P., Pérez-López F.R. Screening and management of female sexual dysfunction during the second half of life. In: Pérez-López F.R. (ed.). Postmenopausal diseases and disorders. Switzerland: Springer International Publishing, 2019:165–185.
33. Erekson E.A., Yip S.O., Wedderburn T.S., Martin D.K., Li F.-Y., Choi J.N. et al. The vulvovaginal symptoms questionnaire: a questionnaire for measuring vulvovaginal symptoms in postmenopausal women. *Menopause*. 2013;20:973–979. DOI: 10.1097/GME.0b013e318282600b.
34. Huang A.J., Gregorich S.E., Kuppermann M., Nakagawa S., Van Den Eeden S.K., Brown J.C. et al. Daily impact of the vaginal aging questionnaire: a multivariate measure of the impact of vaginal symptoms on functioning and well-being in postmenopausal women. *Menopause*. 2015;22(2):144–154. DOI: 10.1097/GME.0000000000000281.
35. Eaton A.A., Baser R.E., Seidel B., Stabile C., Canty J.P., Goldfrank D.J. et al. Validation of clinical tools for vaginal and vulvar symptom assessment in cancer patients and survivors. *J. Sex Med*. 2017;14(1):144–151. DOI: 10.1016/j.jsxm.2016.11.317.
36. Alvisi S., Gava G., Orsili I., Giacomelli G., Baldassarre M., Seracchioli R. et al. Vaginal health in menopausal women. *Medicina*. 2019;55(10):615. DOI: 10.3390/medicina55100615.
37. Angelou K., Grigoriadis T., Diakosavvas M., Zacharakis D., Athanasiou S. The genitourinary syndrome of menopause: an overview of the recent data. Cureus. 2020;12(4):e7586. DOI: 10.7759/cureus.7586.

38. Mac Bride M.B., Rhodes D.J., Shuster L.T. Vulvovaginal atrophy. *Mayo Clin. Proc*. 2010;85:87–94. DOI: 10.4065/mcp.2009.0413.
39. Prilepskaya V.N. Genitourinary menopausal syndrome: the possibilities of estriol. *Gynecology*. 2018;20(1):5–8 (in Russ.). DOI: 10.26442/2079-5696_20.1.5-8.
40. Panay N., Palacios S., Bruyniks N., Particco M., Nappi R.E. Symptom severity and quality of life in the management of vulvovaginal atrophy in postmenopausal women. *Maturitas*. 2019;124:55–61. DOI: 10.1016/j.maturitas.2019.03.013.
41. Nappi R.E., Biglia N., Cagnacci A., Di Carlo C., Luisi S., Paoletti A.M. Diagnosis and management of symptoms associated with vulvovaginal atrophy: expert opinion on behalf of the Italian VVA study group. *Gynecol. Endocrinol*. 2016;32:602–606. DOI: 10.1080/09513590.2016.1183627.
42. The 2020 genitourinary syndrome of menopause position statement of The North American Menopause Society. *Menopause*. 2020;27(9):976–992. DOI: 10.1097/GME.0000000000001609.
43. Edwards D., Panay N. Treating vulvovaginal atrophy/genitourinary syndrome of menopause: How important is vaginal lubricant and moisturizer composition? Review. *Climacteric*. 2016;19(2):151–161. DOI: 10.3109/13697137.2015.1124259.
44. ACOG Practice Bulletin No. 141: management of menopausal symptoms. *Obstet. Gynecol*. 2014;123(1):202–216. DOI: 10.1097/01.AOG.0000441353.20693.78.
45. Salwowska N.M., Bebenek K.A., Żądło D.A., Wcisło-Dziadecka D.L. Physiochemical properties and application of hyaluronic acid: A systematic review. *J. Cosmet. Dermatol*. 2016;15(4):520–526. DOI: 10.1111/jocd.12237.
46. Mitchell C.M., Guthrie K.A., Larson J., Diem S., LaCroix A.Z., Caan B. et al. Sexual frequency and pain in a randomized clinical trial of vaginal estradiol tablets, moisturizer, and placebo in postmenopausal women. *Menopause*. 2019;26(8):816–822. DOI: 10.1097/GME.0000000000001341.
47. Shalina M.A., Lisyanskaya M.V., Nesterov I.M. Modern therapy of patients with peri- and postmenopausal vulvovaginal atrophy. (Clinical application experience). *Russian Bulletin of Obstetrician-Gynecologist*. 2022;22(5):100–103 (in Russ.). DOI: 10.17116/rosakush202222051100.
48. Tatarova N.A., Linde V.A., Gusev S.N. Non-hormonal therapy of genitourinary menopausal syndrome. *Gynecology, Obstetrics, and Perinatology.* 2021;20(2):141–146 (in Russ.). DOI: 10.20953/1726-1678-2021-2-141-146.
49. Tikhomirova E.V., Balan V.E., Titchenko Yu.P., Fomina-Nilova O.S. Possibilities of non-hormonal therapy in patients with vulvovaginal atrophy. *Russian Bulletin of Obstetrician-Gynecologist*. 2020;20(4):58–64 (in Russ.). DOI: 10.17116/rosakush20202004158.
50. Pestrikova T.Yu., Yurasova E.A., Shveeva M.A., Kovaleva T.D. A personalized approach to the management of patients with atrophic vulvovaginitis in postmenopause. *Russian Bulletin of Obstetrician-Gynecologist*. 2020;20(3):62–67 (in Russ.). DOI: 10.17116/rosakush20202003162.
51. Kedrova A.G. Prevention of vaginal atrophy after treatment of tumors of the organs of the female reproductive system. *Tumors of Female Reproductive System*. 2019;15(4):73–78 (in Russ.). DOI: 10.17650/1994-4098-2019-15-4-73-78.
52. Capobianco G., Wenger J.M., Meloni G.B., Dessole M., Cherchi P.L., Dessole S. Triple therapy with Lactobacilli acidophili, estriol plus pelvic floor rehabilitation for symptoms of urogenital aging in postmenopausal women. *Arch. Gynecol. Obstet*. 2014;289(3):601–608. DOI: 10.1007/s00404-013-3030-6.
53. Di Mauro R., Cantarella G., Bernardini R., Di Rosa M., Barbagallo I., Distefano A. et al. The biochemical and pharmacological properties of ozone: the smell of protection in acute and chronic diseases. *Int. J. Mol. Sci*. 2019;20:634. DOI: 10.3390/ijms20030634.
54. Werner S., Grose R. Regulation of wound healing by growth factors and cytokines. *Physiol. Rev*. 2003;83:835–870. DOI: 10.1152/physrev.2003.83.3.835.
55. Vincent F. Mechanisms of cutaneous wound repair. In: Freedberg I.M., Eisen A.Z., Wolff K., Austen K.F., Goldsmith L.A., Katz S.I. (eds) Fitzpatrick's dermatology in general medicine. 6th ed. New York: McGraw Hill, 2003:236–246.
56. Kim H.S., Noh S.U., Han Y.W., Kim K.M., Kang H., Kim H.O. et al. Therapeutic Effects of topical application of ozone on acute cutaneous wound healing. *J. Korean Med. Sci*. 2009;24(3):368–374. DOI: 10.3346/jkms.2009.24.3.368.
57. Valacchi G., Fortino V., Bocci V. The dual action of ozone on the skin. *Br. J. Dermatol.* 2005;153:1096–1100. DOI: 10.1111/j.1365-2133.2005.06939.x.
58. Janic B., Umstead T.M., Phelps D.S., Floros J. Modulatory effects of ozone on THP-1 cells in response to SP-A stimulation. *Am. J. Physiol. Lung Cell Mol. Physiol*. 2005;288:L317–L325. DOI: 10.1152/ajplung.00125.2004.
59. Fischer S.M. Is cyclooxygenase-2 important in skin carcinogenesis? *J. Environ. Pathol. Toxicol. Oncol*. 2002;21:183–191.
60. Valacchi G., Pagnin E., Corbacho A.M., Olano E., Davis P.A., Packer L. et al. *In vivo* ozone exposure induces antioxidant/stress-related responses in murine lung and skin. *Free Radic. Biol. Med*. 2004;36(5):673–681. DOI: 10.1016/j.freeradbiomed.2003.12.005.
61. Management of symptomatic vulvovaginal atrophy: 2013 position statement of The North American Menopause Society. Menopause. 2013;20(9):888–902. DOI: 10.1097/GME.0b013e3182a122c2.
62. The NAMS 2017 Hormone Therapy Position Statement Advisory Panel. The 2017 hormone therapy position statement of the North American menopause society. *Menopause*. 2017;24:728–753. DOI: 10.1097/GME.0000000000000921.
63. Phillips N.A., Bachmann G.A. Genitourinary syndrome of menopause: common problem, effective treatments. *Cleve Clin. J. Med*. 2018;85:390–398. DOI: 10.3949/ccjm.85a.15081.
64. Santen R.J. Vaginal administration of estradiol: effects of dose, preparation and timing on plasma estra-

diol levels. *Climacteric*. 2015;18(2):121–126. DOI: 10.3109/13697137.2014.947254.
65. Clinical guidelines. Menopause and menopause in women 2021. URL: https://geropharm.ru/uploads/file/menopauza-i-klimaktericheskoe-sostoyanie-u-ghenschiny-kr-2021.pdf [date of access: 03/29/2023] (in Russ.).
66. Jokar A., Davari T., Asadi N., Ahmadi F., Foruhari S. Comparison of the Hyaluronic Acid Vaginal Cream and Conjugated Estrogen Used in Treatment of Vaginal Atrophy of Menopause Women: A Randomized Controlled Clinical Trial. *Int. J. Community Based Nurs Midwifery*. 2016;4(1):6978.
67. Kozlov P.V., Dobrokhotova Yu.E., Ilyina I.Yu. Modern approaches to the drug correction of genitourinary menopausal syndrome. *General Medicine*. 2021;2:58–64 (in Russ.). DOI: 10.24412/2071-5315-2021-12331.
68. Oboskalova T.A., Lavrentieva I.V., Prokhorova O.V., Vorontsova A.V. Correction of symptoms of vaginal atrophy during therapy with gonadotropin-releasing hormone agonists. *Doctor.ru*. 2016;3(120):30–33 (in Russ.).
69. Biehl C., Plotsker O., Mirkin S. A systematic review of efficacy and safety of vaginal estrogen products for the treatment of genitourinary syndrome of menopause. *Menopause*. 2019;26(4):431–453. DOI: 10.1097/GME.0000000000001221.
70. Phillips N.A., Bachmann G.A. Genitourinary syndrome of menopause: Common problem, effective treatments. *Cleve Clin. J. Med*. 2018;85(5):390–398. DOI: 10.3949/ccjm.85a.15081.
71. Klinyshkova T.V., Samosudova I.B., Mironova O.N. Evaluation of cervical screening in the treatment of vulvovaginal atrophy in peri- and postmenopause. *Gynecology*. 2016;18(6):32–35 (in Russ.).
72. Muecka A.O., Ruana X., Prasauskasc V., Grobc P., Ortmann O. Treatment of vaginal atrophy with estriol and lactobacilli combination: a clinical review. *Climacteric*. 2018;21(2):140–147. DOI: 10.1080/13697137.2017.1421923.
73. Torky H.A., Taha A., Marie H., El-Desouky E., Raslan O., Moussa A.A. et al. Role of topical oxytocin in improving vaginal atrophy in postmenopausal women: a randomized, controlled trial. *Climacteric*. 2018;21(2):174–178. DOI: 10.1080/13697137.2017.1421924.
74. Kingsberg S.A., Wysocki S., Magnus L., Krychman M.L. Vulvar and vaginal atrophy in postmenopausal women: findings from the REVIVE (REal Women's VIews of Treatment Options for Menopausal Vaginal ChangEs) survey. *J. Sex Med*. 2013;10(7):1790–1799. DOI: 10.1111/jsm.12190.
75. Palacios S., Mejía A., Neyro J.L. Treatment of the genitourinary syndrome of menopause. *Climacteric*. 2015;18:23–29. DOI: 10.3109/13697137.2015.1079100.
76. Crandall C.J., Hovey K.M., Andrews C.A., Chlebowski R.T., Stefanick M.L., Lane D.S. et al. Breast cancer, endometrial cancer, and cardiovascular events in participants who used vaginal estrogen in the Women's Health Initiative Observational Study. *Menopause*. 2018;25(1):11–20. DOI: 10.1097/GME.0000000000000956.
77. Bachmann G., Santen R.J. Treatment of genitourinary syndrome of menopause (vulvovaginal atrophy). URL: https://uptodatefree.ir/topic.htm?path=treatment-of-genitourinary-syndrome-of-menopause-vulvovaginal-atrophy[updated 2023 Mar 29].
78. Labrie F., Archer D.F., Koltun W., Vachon A., Young D., Frenette L. et al.ur É. Efficacy of intravaginal dehydroepiandrosterone (DHEA) on moderate to severe dyspareunia and vaginal dryness, symptoms of vulvovaginal atrophy, and of the genitourinary syndrome of menopause. *Menopause*. 2018;25(11):1339–1353. DOI: 10.1097/GME.0000000000001238.
79. Tikhomirova E.V., Balan V.E., Fomina-Nilova O.S. Methods of treatment of genitourinary syndrome at the present stage. *Medical Council*. 2020;(13):91–96 (in Russ.). DOI: 10.21518/2079-701X-2020-13-91-96.
80. Apolikhina I.A., Ramazanova M.O. The first Russian experience of using ND:YAG laser (neodymium laser) for the treatment of symptoms of genitourinary menopausal syndrome. *Obstetrics and Gynecology: News, Opinions, Training*. 2021;10(1):6–10 (in Russ.). DOI: 10.33029/2303-9698-2022-10-1-6-10.
81. Wańczyk-Baszak J., Woźniak S., Milejski B., Paszkowski T. Genitourinary syndrome of menopause treatment using lasers and temperature-controlled radiofrequency. *Menopause Rev*. 2018;17(4):180–184. DOI: 10.5114/pm.2018.81743.
82. Salvatore S., Athanasiou S., Candiani M. The use of pulsed CO2 lasers for the treatment of vulvovaginal atrophy. *Curr. Opin. Obstet. Gynecol*. 2015;27:504–508. DOI: 10.1097/GCO.0000000000000230.
83. Gambacciani M., Levancini M., Russo E., Vacca L., Simoncini T., Cervigni M. Long-term effects of vaginal erbium laser in the treatment of genitourinary syndrome of menopause. *Climacteric*. 2018;21:148–152. DOI: 10.1080/13697137.2018.1436538.
84. Athanasiou S., Pitsouni E., Falagas M.E., Salvatore S., Grigoriadis T. CO2-laser for the genitourinary syndrome of menopause. How many laser sessions? *Maturitas*. 2017;104:24– 28. DOI: 10.1016/j.maturitas.2017.07.007.
85. Pitsouni E., Grigoriadis T., Falagas M.E., Salvatore S., Athanasiou S. Laser therapy for the genitourinary syndrome of menopause. A systematic review and meta-analysis. *Maturitas*. 2017;103:78–88. DOI: 10.1016/j.maturitas.2017.06.029.
86. Arroyo C. Fractional CO2 laser treatment for vulvovaginal atrophy symptoms and vaginal rejuvenation in perimenopausal women. *Int. J. Womens Health*. 2017;9:591–595. DOI: 10.2147/IJWH.S136857.
87. Eder S.E. Early effect of fractional CO_2 laser treatment in Post-menopausal women with vaginal atrophy. *Laser Ther.* 2018;27(1):41–47. DOI: 10.5978/islsm.18-OR-04.
88. Gordon C., Gonzales S., Krychman M.L. Rethinking the techno vagina: A case series of patient complications following vaginal laser treatment for atrophy. *Menopause*. 2019;26(4):423–427. DOI: 10.1097/GME.0000000000001293.

89. Caruth J.C. Evaluation of the safety and efficacy of a novel radiofrequency device for vaginal treatment. *Surg. Technol. Int*. 2018;32:145–149.
90. Vicariotto F., Raichi M. Technological evolution in the radiofrequency treatment of vaginal laxity and menopausal vulvo-vaginal atrophy and other genitourinary symptoms. First experiences with a novel dynamic quadripolar device. *Minerva Ginecol*. 2016;68:225–236.
91. Alinsod R.M. Temperature controlled radiofrequency for vulvovaginal laxity. *Prime*. 2015;3(4):16–21.
92. Apolikhina I.A., Urumagova A.T., Teterina T.A. Modern possibilities and prospects for the development of aesthetic gynecology. *Medical Opponent*. 2019;3(7):63-69 (in Russ.).

Authors' information

Zainetdinova Larisa F. – Dr. Sci. (Med.), Associate Professor, Professor of the Department of Obstetrics and Gynecology, South Ural State Medical University, Chelyabinsk, sea-gull6@yandex.ru, https://orcid.org/0000-0001-5256-843X

Telesheva Larisa F. – Dr. Sci. (Med.), Professor, Department of Microbiology, Virology, Immunology, South Ural State Medical University, Chelyabinsk, teleshevalarisa@mail.ru, https://orcid.org/0000-0002-7884-9675

Medvedev Boris I. – Dr. Sci. (Med.), Professor, Department of Obstetrics and Gynecology, South Ural State Medical University, Chelyabinsk, borismedvedev423@gmail.com, https://orcid.org/0009-0000-5633-6951

Khakhulina Victoria V. – Lecturer, Department of Obstetrics and Gynecology, South Ural State Medical University, Chelyabinsk, viktoriahahulina95@mail.ru.

(✉) **Zainetdinova Larisa F.,** sea-gull6@yandex.ru

Received 11.05.2023;
approved after peer review 01.06.2023;
accepted 14.09.2023

УДК 616.12-008.46-036.12-044.22
https://doi.org/10.20538/1682-0363-2024-1-144-155

New draft classification of chronic heart failure of the Russian Society of Cardiology: are there any obvious advantages over the current ones?

Kalyuzhin V.V.[1], Teplyakov A.T.[2], Bespalova I.D.[1], Kalyuzhina E.V.[1], Chernogoryuk G.E.[1], Terentyeva N.N.[3], Grakova E.V.[2], Kopeva K.V.[2], Garganeeva N.P.[1], Livshits I.K.[1], Ostanko V.L.[1], Shalovay A.A.[1], Pushnikova E.Yu.[2], Aptekar V.D.[2]

[1] *Siberian State Medical University*
2, Moscow Trakt, Tomsk, 634050, Russian Federation

[2] *Cardiology Research Institute, Tomsk National Research Medical Center (NRMC), of the Russian Academy of Sciences*
111, Kievskaya Str., Tomsk, 634012, Russian Federation

[3] *Surgut State University*
1, Lenina Av., Surgut, 628412, Russian Federation

ABSTRACT

In the interests of practical healthcare, routine classifications should be modified as rarely as possible. At the same time changes should be discarded only on sufficient grounds, for example, when there are no obvious advantages of a new classification over the existing ones or they can no longer be modified by introducing fundamental changes and amendments. In this regard, the evolution of approaches to the classification of chronic heart failure (CHF) is prominent. It becomes particularly relevant due to the fact that currently experts of the Russian Society of Cardiology (RSC) are actively discussing a new draft classification of CHF. The authors of the lecture gave a brief historical insight and reviewed the main classifications of CHF used in North America, Europe, and Russia. The new classification of CHF proposed by RSC experts, which is actually a modified classification of North American colleagues, does not have obvious advantages over the currently used CHF classification in Russia (since 2002). The latter is based on the classification by Vasilenko – Strazhesko which is familiar to domestic internists, since it has become an indispensable part of their clinical practice and has stood the test of time. In addition, its underlying principles provide the potential for its flexible modification.

Keywords: chronic heart failure, classification, stage, functional class, ejection fraction

Conflict of interest. The authors declare the absence of obvious or potential conflicts of interest related to the publication of this article.

Source of financing. The authors state that they received no funding for the study.

For citation: Kalyuzhin V.V., Teplyakov A.T., Bespalova I.D., Kalyuzhina E.V., Chernogoryuk G.E., Terentyeva N.N., Grakova E.V., Kopeva K.V., Garganeeva N.P., Livshits I.K., Ostanko V.L., Shalovay A.A., Pushnikova E.Yu., Aptekar V.D. New draft classification of chronic heart failure of the Russian Society of Cardiology: are there any obvious advantages over the current ones? *Bulletin of Siberian Medicine.* 2024;23(1):133–155. https://doi.org/10.20538/1682-0363-2024-1-144-155.

✉ *Kalyuzhin Vadim V.,* kalyuzhinvv@mail.ru

Проект новой классификации хронической сердечной недостаточности российского кардиологического общества: есть ли очевидные преимущества перед действующими?

Калюжин В.В.[1], Тепляков А.Т.[2], Беспалова И.Д.[1], Калюжина Е.В.[1], Черногорюк Г.Э.[1], Терентьева Н.Н.[3], Гракова Е.В.[2], Копьева К.В.[2], Гарганеева Н.П.[1], Лившиц И.К.[1], Останко В.Л.[1], Шаловай А.А.[1], Пушникова Е.Ю.[2], Аптекарь В.Д.[2]

[1] *Сибирский государственный медицинский университет (СибГМУ)*
Россия, 634050, г. Томск, Московский тракт, 2

[2] *Научно-исследовательский институт (НИИ) кардиологии, Томский национальный исследовательский медицинский центр (НИМЦ) Российской академии наук*
Россия, 634012, г. Томск, ул. Киевская, 111

[3] *Сургутский государственный университет (СурГУ)*
Россия, 628412, г. Сургут, пр. Ленина, 1

РЕЗЮМЕ

В интересах практического здравоохранения менять привычные классификации нужно как можно реже, хотя и отказываться от перемен следует только при достаточных основаниях, например, когда отсутствуют очевидные преимущества новой классификации перед действующими или неполностью исчерпаны возможности их модификации путем внесения принципиальных изменений и дополнений. В этом плане показательна эволюция подходов к классификации хронической сердечной недостаточности (ХСН), приобретающая особую актуальность в связи с тем, что в настоящее время экспертами Российского кардиологического общества (РКО) активно обсуждается проект новой классификации ХСН. Авторы лекции сделали краткий исторический экскурс и рассмотрели основные классификации ХСН, применяющиеся в Северной Америке, Европе и России.

Предлагаемая экспертами РКО новая классификация ХСН, представляющая собой фактически видоизмененную классификацию североамериканских коллег, не имеет очевидных преимуществ перед действующей в России с 2002 г. классификацией сердечной недостаточности, основанной на привычной для отечественных интернистов классификации Н.Д. Стражеско и В.Х. Василенко, которая вошла в плоть и кровь российских медиков и выдержала проверку временем. К тому же принципы, заложенные в её основу, обеспечивают потенциал для ее гибкой модификации, возможности которой не являются полностью исчерпанными.

Ключевые слова: хроническая сердечная недостаточность, классификация, стадия, функциональный класс, фракция выброса

Конфликт интересов. Авторы декларируют отсутствие явных и потенциальных конфликтов интересов, связанных с публикацией настоящей статьи.

Источник финансирования. Авторы заявляют об отсутствии финансирования при проведении исследования.

Для цитирования: Калюжин В.В., Тепляков А.Т., Беспалова И.Д., Калюжина Е.В., Черногорюк Г.Э., Терентьева Н.Н., Гракова Е.В., Копьева К.В., Гарганеева Н.П., Лившиц И.К., Останко В.Л., Шаловай А.А., Пушникова Е.Ю., Аптекарь В.Д. Проект новой классификации хронической сердечной недостаточности российского кардиологического общества: есть ли очевидные преимущества перед действующими? *Бюллетень сибирской медицины.* 2024;23(1):144–155. https://doi.org/10.20538/1682-0363-2024-1-144-155.

INTRODUCTION

The philosophical encyclopedic dictionary, published in 150,000 copies by the publishing house “Soviet Encyclopedia” in 1983, provides the following detailed definition of the term “classification” (Latin *classis* − rank, class and *facio* − to do, lay out): “a system of subordinate concepts (classes of objects) of any field of knowledge or human activity, often presented in the form of diagrams (tables) of various forms and used as a means to establish connections between these concepts or classes of objects, as well

as to navigate in the diversity of concepts or relevant objects" [1]. At the same time, the authors distinguish artificial and natural classifications. In the latter, the most essential features are taken as the basis, from which the maximum of derivatives follows, so that classification serves as a source of knowledge about the objects being classified. Artificial classifications lack these properties, since they are based on one or more insignificant, but easily distinguishable features. As an example, we can cite a primitive descriptive approach to classification based on a dichotomous division: sick – healthy; pregnant – not pregnant, heart failure +/-.

It is clear that in such an inexact science as medicine, it is almost impossible to construct a completely natural classification, similar to the periodic system of chemical elements by Mendeleev. But at all times many medical scientists have sought to create such a classification that would be as close as possible to a natural one in terms of this dichotomous division: natural − artificial.

A classification constructed in compliance with all logical requirements and being a convenient tool for clinical practice can be still used after more than one paradigm shift. At the same time, the dialectical nature of the development of scientific knowledge is clearly manifested in most classifications. At each stage of the development of scientific thought, the authors of one or another classification summarize the obtainted knowledge, marking the beginning of a new period of evolution, which almost inevitably results in a revision of the dominant paradigm, which can become an incentive to develop a more advanced classification [2].

We fully support the opinion of B.I. Shulutko [3] who stated that in the interests of practical healthcare, it is necessary to change habitual stereotypes (in particular, classifications) as rarely as possible. Although changes should be introduced only when reasons for them are sufficient, for example, when there are no obvious advantages of the new classification over the existing ones, or they cannot be modified by introducing fundamental changes and additions. In this regard, the evolution of approaches to the classification of chronic heart failure (CHF) is indicative, acquiring particular relevance due to the fact that currently experts of the Russian Society of Cardiology (RSC) are actively discussing a draft new classification of CHF, which, according to its authors, has advantages over existing ones [4, 5].

The aim of this lecture was to discuss the draft new classification of CHF proposed by RSC.

HISTORY OF THE ISSUE

Before we begin discussing the main issue of the lecture, let us give a brief historical insight into it. Researchers first attempted at creating a meaningful classification of CHF a long time ago. Even Jean-Nicolas Corvisart des Marets, determining the size of the heart intravitally using percussion, which he did perfectly, and comparing these data with the results of the autopsy, distinguished two types of cardiomegaly (he used the term "aneurysm"): active (with an increase in the thickness of the walls of heart chamber and an increase in its contractility) and passive (with thinning of the walls of the heart chamber and a decrease in its contractility) [6]. Having laid the foundations for the concept of cardiac remodeling, the pioneer of modern cardiology presented careful considerations about left and right ventricular (including secondary to left ventricular) heart failure. He insightfully described in the form of a 3-member formula the most common scenario of transformation of the size, shape, and function of the heart after its damaging overload. Pressure overload of the left ventricle (LV) – formation of an "active aneurysm" of the LV − development of a "passive aneurysm" of the left atrium and right ventricle, and also gave an excellent description of the three stages (periods) of a cardiac aneurysm of what would now be called CHF1[1].

At the first stage, which a competent physician may suspect due to the patient's predisposition to its development, the patient complains of weakness, shortness of breath, and palpitations upon exertion, without any findings during a physical examination, with the exception of cardiomegaly. At the second stage, the severity of symptoms increases: the patient instantly gets tired and often wants to rest, the heartbeat becomes stronger and faster, and breathing becomes extremely difficult with minimal physical exertion (*"The patient cannot climb three or four steps at once without being obliged to stop due to shortness of breath").* And even at rest, when the patient is unable to breathe freely lying and, to facilitate breathing, is forced to sit up, swelling of the feet and ankles appears in an upright position, which usually disappears during the night. At the third stage, the severity of symptoms and signs of CHF reaches a peak, at which the patient's life is in immediate danger

[1] Corvisart J.N. An essay on the organic diseases and lesions of the heart and great vessels. Translated by J. Gates. Boston: Bradford and Read, 1812: 344.

every minute (*"Death always intervenes to terminate the painful scene which this combination of symptoms presents")*. The severity of shortness of breath reaches the level of suffocation, edema syndrome progresses (up to anasarca), fluid accumulates in large cavities, diuresis decreases, a significant dilation of the veins in the neck and a painful enlargement of the liver are detected, the edge of which becomes dense. Thus, Jean-Nicolas Corvisart des Marets, albeit using general ideas, quite accurately outlined the continuum of heart failure (in fact, from risk factors to its terminal stage) which is a paradigm used in all modern classifications of CHF, without exception, based on identifying the stages of the pathological process.

We will not bore the reader for too long with an insight into the distant past; let us move on to the current classifications of CHF. The most time-tested classification is the one by New York Heart Association (NYHA[1]). P.D. White and M.M. Myers[2] convincingly substantiated more than 100 years ago that there is a need to supplement the diagnostic conclusion in patients with cardiovascular pathology with intranosological characteristics of their functional status, which is currently perceived as an axiom, and the NYHA classification of CHF based on this principle has received international recognition. This classification is used everywhere and is considered as a cornerstone in determining treatment strategies in all modern guidelines and recommendations on heart failure [7–9]. The discussed classification makes it possible to assess the level of decrease in physical activity and the degree of clinical manifestations of CHF. However, it cannot be used to assess the severity of heart disease, which is the cause of functional disorders, since the severity of symptoms (especially in the case of effective therapy) does not necessarily reflect the degree of myocardial dysfunction that causes them or correspond to it, which reduces the predictive power of the classification result [7, 10–14].

Another repeatedly noted limitation of the NYHA classification of CHF is its low reproducibility [8, 15], since when assessing the functional status of a patient with CHF, one should take into account the distinct subjectivity of both the doctor and the patient in determining which limitation of physical activity is slight or, conversely, significant, as well as what kind of physical exertion is habitual for the patient [16]. This subjectivity naturally leads to poor reproducibility of the results of functional class (FC) assessment in the same patient by different doctors [15, 16–18]. To objectify the FC assessment, it is most often proposed to evaluate exercise tolerance (distance covered in 6 minutes, threshold load, etc.) and the maximum volume of oxygen consumed in a functional test [9, 19]. However, this approach does not always provide a drastic increase in classification accuracy [20–22].

Medical scientists hoped that an approach based on additional identification of the stage of the pathological process could at least partially solve the problems with the above-mentioned shortcomings of the NYHA functional classification of CHF. This approach made it possible to more reliably and objectively classify patients with CHF during the development of heart and vascular disease, as well as prescribe treatment in strict accordance with the stage of development of the pathological condition. At the end of 2001, the medical journals Circulation and the Journal of the American College of Cardiology published further recommendations for the assessment and treatment of CHF in adults proposed by a working group of the American College of Cardiology (ACC) and the American Heart Association (AHA). The proposed recommendations for the first time divided the development CHF into 4 stages: from a threat of developing CHF with the presence of risk factors (stage A) to the terminal stage (stage D) [23]. The same stages were preserved in subsequent recommendations, including those of 2022 [8]. This classification complements, but does not replace, the NYHA functional classification, which reflects the severity of CHF symptoms in patients who can be classified as stage C or D [8].

As for the first part of the ACC and AHA classification, at stage A (allows to describe a patient at high risk of developing heart failure, but does not have structural or functional disorders of the pericardium, myocardium or heart valves) and B (diagnostic conclusion applicable to the patient with structural abnormalities of the heart, who has never had symptoms or signs of heart failure), there is no CHF as such, since the latter is defined as a complex clinical syndrome with corresponding symptoms and signs [8]. Thus, half of the heart failure classification

[1] New York Heart Association. Diseases of the heart and blood vessels: nomenclature and criteria for diagnosis, by the Criteria Committee of the New York Heart Association / Charles E. Kossmann chairman [and others]. Boston: Little, Brown, 1964:463.

[2] White P.D., Myers M.M. The classification of cardiac diagnosis. *JAMA*. 1921;77:1414–1415. DOI: 10.1001/jama.1921.02630440034013.

discussed is actually only applicable in a clinical situation without heart failure.

A reasonable question arises about the extent to which CHF is actually asymptomatic in a patient with so-called structural heart disease, which the classification suggests designating "stage B" in the diagnostic conclusion. For example, you are visiting a patient who seems not to have any symptoms and has been suffering from arterial hypertension for a long time, and a routine echocardiography revealed concentric myocardial hypertrophy and a type of LV diastolic dysfunction with impaired relaxation, as well as a high level of natriuretic peptides in the blood serum. Does anyone really think that, if asked in a straightforward way, such a patient is likely to deny the presence of shortness of breath, fatigue, and palpitations during intense and prolonged physical activity? Obviously, the vast majority of patients with so-called pre-heart failure will answer affirmatively. We will definitely interpret such complaints in this patient with isolated cardiovascular pathology as a manifestation of latent heart failure and not, for example, detraining.

American experts in the 2013 guideline [24] in patients with stage B CHF, who are essentially different from patients with stage C in that they have never had symptoms or signs of heart failure, still allowed the presence of such symptoms (even with physical activity exceeding normal), corresponding to FC I (Table 1). The choice of features that allow for dual interpretation as the basis for classification cannot but cause cognitive dissonance, since the members of the classification must be mutually exclusive. It is like at first they tried to prove to you that crocodiles do not fly, and then they say that they fly, only low. Taking into account the fact that Russian leading cardiologists have repeatedly expressed reasoned objections to the introduction of stage A CHF into the Russian classification [25, 26], it is not surprising that this approach was not adopted in Russia.

Table 1

Comparison of stages and functional classes of CHF [24]

Stage of CHF	Functional class according to NYHA classification
A	No heart failure
B	I
C	I II III
D	IV

In Russia, the approach to the classification of CHF which takes into account the division into stages and FC was different. The classification of stages of CHF by N.D. Strazhesko and V.H. Vasilenko (approved at the XII All-Union Congress of Therapists in 1935) which is continuously updated is well known to several generations of doctors who have successfully used it in their daily practice in diseases of the cardiovascular system with primary damage to the left side of the heart. It is quite simple to determine stages I and II of untreated CHF right at the patient's bedside: stage I is latent heart failure, which manifests itself only during physical activity; stage IIA is clinically pronounced monoventricular (left ventricular); stage IIB is severe biventricular (right ventricular, secondary to left ventricular) [15]. With the phenotype of treated CHF, when in a patient with compensated heart failure there is no information on the so-called hemodynamic changes (symptoms and signs of stagnation in the pulmonary and systemic circulation may be absent with full compensation), its stage I or II can be accurately established based on the results of an echocardiography assessment of remodeling (the presence and severity of spherification and thinning of the walls) and LV function (primarily diastolic). Asymptomatic LV dysfunction, adaptive LV remodeling or maladaptive LV remodeling should be diagnosed, which correspond to stages I, IIA or IIB CHF. The modification of the classification made in 2002 by Society of Experts in Heart Failure (SEHF) will be discussed below [27]. At the same time, the fundamental difference between stage III CHF and stage II B CHF is the presence of irreversible structural changes in target organs (heart, lungs, blood vessels, brain, kidneys) [27].

It should be admitted that a more detailed classification of the stages of CHF by N.D. Strazhesko and V.H.Vasilenko has significant advantages over the trivial approach proposed by American peers, who, as if taking the entire palette of achromatic shades to white and black, propose to distinguish only two stages of clinically pronounced CHF. The first one is conservative – curable stage C of symptomatic heart failure (the severity of clinical manifestations within this stage may differ greatly, ranging from latent left ventricular heart failure corresponding to FC I in the distant past to severe actual biventricular heart failure with anasarca). The second one is stage D which is referred to using different terms "terminal", "refractory" or "progressive" heart failure). At this stage, optimal pharmacotherapy, as

well as cardiac resynchronization therapy, are not effective, which causes repeated hospitalizations and justifies the need for such advanced treatments as heart transplantation and mechanical circulatory support, and/or transition to palliative care [8]. The attempt to describe the entire course of events in clinical heart failure using two stages is certainly better than the primitive dichotomous +/– approach (heart failure: present/absent). But it certainly represents a step back from the views that existed at the beginning of the last century, and even in the time of Jean-Nicolas Corvisart des Marets.

Classification by N.D. Strazhesko and V.H. Vasilenko also has some shortcomings, for which it is often criticized by heart failure specialists. The most common reason for criticism of the classification is its so-called rigidity, which consists in the fact that the authors use a staged approach as gradations, which excludes the transition from higher stages to lower ones [16, 28]. Indeed, the classification under discussion was approved back in 1935, when the possibilities for effective pharmacological or surgical correction of severe CHF were more than modest. The doctor actually observed the "natural" progressive course of heart failure, and therefore the classification did not provide for revising the established stage in the opposite direction [15]. But even at present, when no one doubts that the introduction into clinical practice of the achievements of clinical pharmacology and cardiac surgery often ensures positive changes in the parameters characterizing the process of cardiac remodeling, experts only allow for so-called step-up restaging ("the stage of CHF may worsen despite treatment") [29]. Taking into account the above, the possibility of repealing the provision excluding the transition from higher to lower stages should be discussed [15, 16].

The principles underlying the classification of CHF by N.D. Strazhesko and V.H. Vasilenko provide the potential for its flexible modification, the possibilities of which, in our opinion, still exist. This was the case in 2002, when SEHF proposed a combined classification that took into account the division by stages and FC for discussion. In the official commentary of the SEHF to the classification under discussion, attention is drawn to the continuity of this edition with the classifications by N.D. Strazhesko and V.H. Vasilenko, adopted in Russia, and NYHA, which is used worldwide [29]. At the same time, the classification no longer included all the additions to the 1935 original version that were made during its long history. But new concepts were introduced into it including "asymptomatic LV dysfunction", "adaptive remodeling of the heart and blood vessels", "maladaptive remodeling of the heart and blood vessels", "final stage of organ remodeling". The proposed modification of the classification ensured the accuracy of determining the stage of the pathological process, even when cardiac decompensation is effectively corrected, due to reliance on the results of an echocardiography examination, on the one hand, and when it is possible to objectify the change in the patient's functional status during treatment or the "natural" course of the disease by reflecting FC in the diagnostic conclusion, on the other.

Taking into account the fact that timely and correct recognition of heart failure, as well as the diagnosis of the notorious pre-heart failure (percussion should not be used to detect concentric LV hypertrophy or left atrial dilatation), is not conceivable without an ultrasound assessment of the structure and function of the heart, the ideas that echocardiography is not available or adaptive and maladaptive remodeling is difficult to asses should be rejected. Ensuring the universal availability of such an examination is the responsibility of regional and federal health care authorities.

On the other hand, the echocardiography examination in patients with heart failure is also necessary because, in accordance with all the latest recommendations of authoritative international and national cardiological organizations [7, 8], CHF should be classified depending on the value of the LV ejection fraction (EF). Let us recall that in the International Statistical Classification of Diseases and Related Health Problems, 11th revision (https://icd.who.int), different codes are used for left ventricular heart failure with preserved, mildly reduced, and reduced LVEF: BD11.0, BD11.1, and BD11.2, respectively.

We do not question the heuristic nature of discussing the important issue of the boundary between "normal" and "reduced" LVEF (apparently, it will not be possible without taking into account sexual dimorphism) [30–32]. Until a consensus is reached on this issue, a partial solution to the problem is to indicate a specific value for LVEF along with the CHF phenotype in the diagnostic conclusion. At the same time, we can discuss as much as we want reasonable doubts concerning the practical feasibility of identifying three CHF phenotypes based on the

initial ultrasound assessment of LVEF (with reduced, mildly reduced, and preserved LVEF), as well as reclassifying heart failure, based on the changes in the global contractile activity of the LV, established during subsequent echocardiography examinations. However, if Russian classification rejects such a division or simplification of establishing phenotypes to a dichotomy (with reduced and preserved LVEF), it would mean that we do not keep up with the rest of the world. In this regard (solely for the unification of terminology), we urge to stop simplifying CHF phenotyping to a dichotomy based on the value of LVEF.

Taking into account numerous experimental and clinical studies, the results of which cast doubt on the idea that systolic dysfunction of the heart is the main and only hemodynamic cause responsible for the occurrence and clinical manifestations of CHF, the characteristics of the state of LV diastolic function should be mentioned in the diagnostic conclusion as well (especially in patients with CHF and preserved LVEF) [15, 33–37]. Consequently, highlighting such a category in the classification is another direction of possible modifications of the current CHF classification.

DRAFT CLASSIFICATION OF CHF BY RSC

Holding the idea that the current classification of SEHF in 2002 is no longer consistent with modern ideas about the evolution of heart failure, strategies for its prevention and treatment, RSC experts initiated a discussion on the feasibility of making changes to the Russian classification of heart failure by stages [4]. The draft classification of CHF proposed by RSC was published in the ninth issue of the Russian Journal of Cardiology in 2023 (Table 2) [5].

Table 2

Classification of CHF proposed by RSC (draft, 2023) [5]
The risk of developing heart failure. The presence of diseases and conditions with a high risk of developing CHF.
Pre-heart failure. Absence of CHF symptoms and signs in the present and in the past. Presence of signs of structural and/or functional cardiac damage and/or increased levels of the brain natriuretic peptide.
Stage 1. Clinically manifested heart failure: the presence of CHF symptoms and signs in the present or in the past, caused by a disruption in the structure and/or function of the heart.
Stage 2. Advanced, clinically severe heart failure: severe symptoms and signs of CHF at rest, repeated hospitalizations due to CHF, despite attempts to optimize CHF therapy or intolerance to CHF therapy.

When getting acquainted with the project, it is impossible not to note the striking similarity of the proposed document with the classification of North American colleagues, which, as noted above, does not have obvious advantages over the Russian classification of 2002, which has not been actively used in our country for more than 20 years. On the Internet, you can find the brilliant saying "medical science has stepped far ahead, − our task is to catch up with", which accurately describes the continuous nature of the development of scientific knowledge. However, we do not understand what new scientific information on the etiology, pathogenesis, clinical presentation, and prevention of CHF has accumulated that has led to the fact that, after almost 25 years of the 21st century, an urgent paradoxical need has appeared to return to the ideas of the beginning of the century in order to keep up with progress.

In accordance with the international universal definition, which is cited by RSC experts [4], heart failure is a clinical syndrome with symptoms and/or signs caused by structural and/or functional disorders of the heart, confirmed by elevated levels of natriuretic peptides and/or objective signs of pulmonary or systemic stagnation [38]. However, in this project, when describing the clinical manifestations of heart failure, instead of writing "symptoms and/or signs", phrases with conjunction "and" are only used, for example, "symptom(s) and signs(s)" [5].

As for the initial stages of the cardiovascular disease continuum designated in the American prototype as stages (A and B), when there is essentially no heart failure (complex clinical syndrome with corresponding symptoms/signs), in the Russian project they are not referred to as stages, while preserving the first two lines of the CHF classification (classification of heart failure in patients without heart failure). The presence of sections of the CHF classification in which heart failure is denied (the so-called shift to the left) is explained by the need to focus on the initial stages of the cardiovascular disease continuum with an emphasis on those diseases and conditions in which the risk of developing CHF is especially high, which is extremely important for a physician to pay attention to preventive strategies that reduce cardiovascular risks [4].

There is no need to explain the importance of primary prevention, the measures of which are especially successful in high-risk groups to Russian internists, brought up on the ideas of S.P. Botkin and I.I. Mechnikov, who learned well from university

days that preventing diseases is much easier than treating them. All that is necessary to ensure the effectiveness of these measures, in addition to knowledge regarding specific risk factors for CHF and the perceived need to influence those that can be modified, is to promptly diagnose correctable factors, scrupulously record them in the diagnostic conclusion and do everything to control the situation with the help of non-drug methods and optimal pharmacotherapy in accordance with current guidelines [39–42]. Based on didactic considerations, the emphasis on preventive strategies can be put in a detailed scheme of the cardiovascular disease continuum, in which it is permissible to include its earliest links (even starting not with the major risk factors of CHF, but with the risk factors of the risk factors – the so-called primary risk factors). But the classification of heart failure, which, as we noted above, ideally serves as a source of knowledge about the objects being classified, should not go beyond its main function, which is to distinguish patients with CHF according to the stage of the syndrome. In light of what is stated in the classification of CHF, one can accept a "shift to the left" as no more than latent heart failure, which manifests itself only when more blood is needed from the circulatory system.

The work discussed also provides a brief description of the classification criteria relating only to CHF with reduced (< 50%) LVEF (Table 3). The latter causes confusion and a number of questions, one of which we will allow ourselves to ask. It is unclear whether the authors of this classification do not recognize the existence of "normal systolic" heart failure or maybe they postponed the development of classification criteria for CHF with preserved LVEF until better times.

Table 3

Classification signs of CHF with reduced LVEF

Parameter	Clinical	Laboratory (the level of natriuretic peptide is higher than normal)	Echocardio-graphic (LVEF < 50%)
The risk of CHF	Manifestations of existing diseases (arterial hypertension, coronary heart disease, diabetes mellitus, etc.)	–	–
Pre-heart failure	Manifestations of existing diseases + structural and/or functional changes of the heart (for example, left ventricular hypertrophy)	+	–
Stage 1 CHF	Shortness of breath, pasty shins	+	+
Stage 2 CHF	Shortness of breath, pastiness (swelling) of the shins + accumulation of fluid in the cavities (hydrothorax, hydropericardium, ascites)	+	+

Note. CHD – coronary heart disease.

In accordance with the data in Table 3, the presence or absence of structural changes in the heart (for example, LV hypertrophy) is supposed to be confirmed by the results of a clinical examination (apparently, palpation and percussion), since the analysis of echocardiography is used only to assess the value of LVEF. For the same reason, clinical signs (in particular, an attempt to distinguish swelling of the legs from their pastiness) will have to be used to distinguish between the first and second stages of CHF. We foresee great difficulties (for example, whether the presence of a minor right-sided hydrothorax would justify the conclusion about the terminal stage of the syndrome), which we encountered until the SEHF experts supplemented the classification criteria of the stages of CHF with a number of echocardiography parameters, introducing into the classification by N.D. Strazhesko and V.H. Vasilenko such concepts as "asymptomatic LV dysfunction", "adaptive remodeling of the heart and blood vessels", and "maladaptive remodeling of the heart and blood vessels".

In accordance with the project under discussion, RSC experts offer examples of how diagnostic conclusions are formed in order to allow for a better understanding of the practical meaning of the classification. It should be noted that examples of diagnosis formulation in any document require great courage from its authors, since any inaccuracy, including that associated with the imperfection of the classification itself, becomes the subject of criticism. Figuratively speaking, they step into the line of fire. This is probably why the authors of many clinical guidelines avoid such examples. We are convinced that examples of diagnosis formulation should become an integral part of clinical guidelines,

without which they should not be approved by the Scientific and Practical Council of the Ministry of Healthcare of the Russian Federation.

Let us consider examples of descriptions of each stage ("pre-stage") of CHF (Table 4), which are controversial and require feedback. To begin with, we should note that the uniform requirement for diagnosis classification has been violated. As is well known, a diagnosis that is not classified anywhere, regardless of its content, is regarded as incorrectly formulated [43, 44].

Table 4

Examples of clinical diagnosis formulation in a patient with CHF

Examples of clinical diagnosis formulation [5]	Questions and comments
Essential hypertension, stage II. Risk 3. Dyslipidemia. High risk of CHF	The high risk is reported twice in the diagnosis. May the risk of developing CHF be different (for example, low), with essential hypertension? If not, why is it mentioned in the diagnosis? The authors write in order to "make doctors focused at managing patients more thoroughly." However, we do not understand what "more thorough patient management" is. Is it even possible that a competent clinician will not prescribe optimal pharmacotherapy in accordance with current recommendations if high risk is not mentioned repeatedly in the diagnosis? Unfortunately, a bad doctor will not do this even after having described a high risk three times in the diagnostic conclusion. Is arterial hypertension a risk factor only for CHF or also for CHD, cardiac arrhythmias, peripheral artery pathology, cerebrovascular diseases, and chronic kidney disease? It is unclear to us if a clinician should describe each high risk separately in the diagnosis ("High risk of CHF. High risk of coronary heart disease. High risk...") or enumerate the risks? In the presence of comorbid pathology, in a combined clinical diagnosis, the practitioner should re-describe high risk after each disease and condition in which the likelihood of developing CHF is especially high (the list is quite extensive: arterial hypertension, obesity, coronary heart disease, atrial fibrillation, cardiomyopathy, diabetes mellitus, chronic kidney disease, chronic obstructive pulmonary disease, antitumor therapy) [4]?
Type 2 diabetes mellitus. CKD, stage 3a. Pre-heart failure.	Let us ignore the fact that the diagnosis of diabetes mellitus and chronic kidney disease is not complete, but it is unknown what structural and /or functional changes in the heart allowed to justify "atrial insufficiency" (we can only call such terminology a mockery of the "great, verbose and mighty" Russian language). If there is LV hypertrophy, then the diagnosis apparently did not include information about symptomatic arterial hypertension in a patient with diabetic nephropathy (which should also be classified). Would not it be better to specifically describe these structural and/or functional changes in the heart in the diagnosis (for example, the shape and severity of LV hypertrophy), without replacing it with an elaborate and vague term?
Coronary heart disease: stable angina pectoris FC 2. Coronary artery bypass grafting in 2018 CHF, stage 1. FC 2. Coronary heart disease: postinfarction cardiosclerosis (myocardial infarction in 2020). CHF, stage 2. FC 3. LV aneurysm. Right-hand hydrothorax.	The use of a dichotomous classification of the stages of CHF leads to the fact that such a diagnosis makes it more difficult to understand that this is a patient with multiple heart failure than when using the current classification of CHF (this has already been mentioned above). The authors refused to distinguish CHF phenotypes according to the value of LVEF.

CONCLUSION

The new classification of CHF proposed by RSC experts, which is actually a modified classification of North American colleagues, does not have obvious advantages over the heart failure classification that has been adopted in Russia since 2002 and is based on the classification by N.D. Strazhesko and V.H. Vasilenko, which is familiar to Russian internists. The latter, in the figurative expression of V.Yu. Mareev [45], has become an integral part of the knowledge of Russian internists and has stood the test of time. In addition, the principles underlying it provide the potential for its modification, which is possible to carry out.

REFERENCES

1. Philosophical Encyclopedic Dictionary; edited by L.F. Ilyicheva, P.N. Fedoseeva, S.M. Kovaleva, V.G. Panova, M.: Soviet Encyclopedia, 1983:840 (in Russ.).
2. Meyen S.V., Schrader Yu.A. Methodological aspects of classification theory. *Lethaea Rossica. The Russian Journal of Palaeobotany*. 2017;14:101−110 (in Russ.).
3. Shulutko B.I. Nephrology 2002. The current state of the problem. St. Petersburg: Renkor, 2002:780 (in Russ.).
4. Shlyakhto E.V. Classification of heart failure: focus on pre-

vention. *Russian Journal of Cardiology.* 2023;28(1):7−8 (in Russ.). DOI: 10.15829/1560-4071-2023-5351.
5. Galyavich A.S., Nedogoda S.V., Arutyunov G.P., Belenkov Yu.N. On the classification of chronic heart failure. *Russian Journal of Cardiology.* 2023;28(9):13−18 (in Russ.). DOI: 10.15829/1560-4071-2023-5584.
6. Karamanou M., Vlachopoulos C., Stefanadis C., Androutsos G. Professor Jean-Nicolas Corvisart des Marets (1755-1821): founder of modern cardiology. *Hellenic J. Cardiol.* 2010;51(4):290−293.
7. McDonagh T.A., Metra M., Adamo M., Gardner R.S., Baumbach A., Böhm M. et al. 2021 ESC Guidelines for the diagnosis and treatment of acute and chronic heart failure. *Eur. Heart J.* 2021;42(36):3599−3726. DOI: 10.1093/eurheartj/ehab368
8. Heidenreich P.A., Bozkurt B., Aguilar D., Allen L.A., Byun J.J., Colvin M.M. et al. 2022 AHA/ACC/HFSA Guideline for the Management of Heart Failure: Executive Summary: A Report of the American College of Cardiology/American Heart Association Joint Committee on Clinical Practice Guidelines. *Circulation*. 2022;145(18):e895−e1032. DOI: 10.1161/CIR.0000000000001063.
9. Mareev V.Yu., Fomin I.V., Ageev F.T., Begrambekova Yu.L., Vasyuk Yu.A., Garganeeva A.A., et al. Clinical guidelines of the Society of Experts in Heart Failure– Russian Society of Cardiology – Russian Scientific Medical Society of Internal Medicine. Heart failure: chronic (CHF) and acute decompensated (ADHF). Diagnosis, prevention and treatment. *Kardiologiia*. 2018;58(S6):8−161 (in Russ.). DOI: 10.18087 / cardio. 2475.
10. International Guidelines on Heart Failure; edited by S.J. Ball, R.V.F. Campbell, G.S. Francis; translated from English. Moscow: MEDIA SPHERE, 1995:89 (in Russ.).
11. Kalyuzhin V.V., Teplyakov A.T., Kalyuzhin O.V. Heart failure. Moscow: Medical Information Agency, 2018:376 (in Russ.).
12. Caraballo C., Desai N.R., Mulder H., Alhanti B., Wilson F.P., Fiuzat M. et al. Clinical Implications of the New York Heart Association Classification. *J. Am. Heart Assoc.* 2019;8(23): e014240. DOI: 10.1161/JAHA.119.014240.
13. Rohde L.E., Zimerman A., Vaduganathan M., Claggett B.L., Packer M., Desai A.S. et al. Associations Between New York Heart Association Classification, Objective Measures, and Long-term Prognosis in Mild Heart Failure: A Secondary Analysis of the PARADIGM-HF Trial. *JAMA Cardiol.* 2023;8(2):150−158. DOI: 10.1001/jamacardio.2022.4427.
14. Lindberg F., Tomasoni D., Savarese G. What Role for New York Heart Association Class in Heart Failure Clinical Trials? *JAMA Cardiol.* 2023;8(8):793. DOI: 10.1001/jamacardio.2023.1638.
15. Kalyuzhin V.V., Teplyakov A.T., Bespalova I.D., Kalyuzhina E.V., Ostanko V.L., Terentyeva N.N., et al. Correct diagnostic conclusion in patients with chronic heart failure: a reality or a pipe dream? *Bulletin of Siberian Medicine*. 2020;19(3):128−136 (in Russ.). DOI: 10.20538/1682-0363-2020-3-128-136.
16. Sidorenko B.A., Preobrazhensky D.V. Diagnosis and treatment of chronic heart failure. 3rd ed., corr. Moscow: Miklos, 2004: 352 (in Russ.).
17. Caraballo C., Desai N.R., Mulder H., Alhanti B., Wilson F.P., Fiuzat M. et al. Clinical Implications of the New York Heart Association Classification. *J. Am. Heart Assoc.* 2019;8(23): e014240. DOI: 10.1161/JAHA.119.014240.
18. Cosiano M.F., Vista A., Sun J.L., Alhanti B., Harrington J., Butler J. et al. Comparing New York Heart Association Class and patient-reported outcomes among patients hospitalized for heart failure. *Circ. Heart Fail.* 2023;16(1):e010107. DOI: 10.1161/CIRCHEARTFAILURE.122.010107.
19. Agdamag A.C., Van Iterson E.H., Tang W.H.W., Finet J.E. Prognostic role of metabolic exercise testing in heart failure. *J. Clin. Med.* 2023;12(13):4438. DOI: 10.3390/jcm12134438.
20. Lim F.Y., Yap J., Gao F., Teo L.L., Lam C.S.P., Yeo K.K. Correlation of the New York Heart Association classification and the cardiopulmonary exercise test: A systematic review. *Int. J. Cardiol.* 2018;263:88−93. DOI: 10.1016/j.ijcard.2018.04.021.
21. Ritt L.E.F., Ribeiro R.S., Souza I.P.M.A., Ramos J.V.S.P., Ribeiro D.S., Feitosa G.F. et al. Low concordance between NYHA Classification and Cardiopulmonary Exercise Test Variables in Patients with Heart Failure and Reduced Ejection Fraction. *Arq. Bras. Cardiol.* 2022;118(6):1118–1123. DOI: 10.36660/abc.20210222.
22. Zimerman A., da Silveira A.D., Solomon S.D., Rohde L.E. NYHA classification for decision-making in heart failure: Time to reassess? *Eur. J. Heart Fail.* 2023;25(7):929−932. DOI: 10.1002/ejhf.2923.
23. Hunt S.A., Baker D.W., Chin M.H., Cinquegrani M.P., Feldman A.M., Francis G.S. et al. A report of the American College of Cardiology/American Heart Association Task Force on Practice Guidelines (Committee to revise the 1995 Guidelines for the Evaluation and Management of Heart Failure). *J. Am. Coll. Cardiol.* 2001;38(7):2101−2113. DOI: 10.1016/s0735-1097(01)01683-7.
24. Yancy C.W., Jessup M., Bozkurt B., Butler J., Casey D.E. Jr., Drazner M.H. et al. 2013 ACCF/AHA guideline for the management of heart failure: a report of the American College of Cardiology Foundation/American Heart Association Task Force on practice guidelines. *Circulation.* 2013; 128 (16): e240−327. DOI: 10.1161/CIR.0b013e31829e8776.
25. Sitnikova M.Yu. Do we need stage A in the classification of chronic heart failure? *Journal of Heart Failure*. 2009;10(4):237−238 (in Russ.).
26. Samorodskaya I.V., Larina V.N., Chernyavskaya T.K., Kakorina E.P. Comparison of classifications and justification of the need for a transdisciplinary consensus to account for morbidity and mortality associated with chronic heart failure. *Complex Issues of Cardiovascular Diseases.* 2022;11(1):6−16 (in Russ.). DOI: 10.17802/2306-1278-2022-11-1-6-16.
27. Mareev V.Yu., Ageev F.T., Arutyunov G.P., Koroteev A.V., Mareev Yu.V., Ovchinnikov A.G. National guidelines for the diagnosis and treatment of CHF (fourth edition). *Journal of Heart Failure*. 2013;81(7):379−472 (in Russ.).
28. Mukharlyamov N.M., Mareev V.Yu. Treatment of chronic heart failure. M.: Medicine, 1985:208 (in Russ.).
29. The official comments of the Society of Experts in Heart Failureon the discussed classification of CHF. *Journal of Heart Failure*. 2002;3(2):62 (in Russ.).

30. The Russian Society of Cardiology (RSC). Chronic heart failure. 2020 Clinical guidelines. *Russian Journal of Cardiology*. 2020;25(11): 311−374 (in Russ.). DOI: 10.15829/1560-4071-2020-4083.
31. Salem J.E., Nguyen L.S., Hammoudi N., Preud'homme G., Hulot J.S., Leban M. et al. Complex association of sex hormones on left ventricular systolic function: insight into sexual dimorphism. *J. Am. Soc. Echocardiogr.* 2018;31(2):231−240. e1. DOI: 10.1016/j.echo.2017.10.017.
32. Ageev F.T., Ovchinnikov A.G., Ageeva S.F., Mareev V.Yu. What is "normal left ventricular ejection fraction" and its relationship with the pathogenesis and effectiveness of the treatment of heart failure. *Kardiologiia*. 2023;63(6):69−74 (in Russ.). DOI: 10.18087/cardio.2023.6.n2404.
33. Belenkov Yu.N., Ageev F.T., Mareev V.Yu. Meet diastolic heart failure. *Journal of Heart Failure*. 2000;1(2):40−44 (in Russ.).
34. Kalyuzhin V.V., Teplyakov A.T., Solovtsov M.A. The role of systolic and diastolic dysfunction of the left ventricle in the clinical manifestation of chronic heart failure in patients with myocardial infarction. *Therapeutic Archive*. 2002;74 (12):15-18 (in Russ.).
35. Kalyuzhin V.V., Teplyakov A.T., Ryazantseva N.V., Vechersky Yu.Yu., Khlapov A.P., Kolesnikov R.N. Diastole of the heart. Physiology and clinical pathological physiology. Tomsk: TPU Publishing House, 2007:212 (in Russ.).
36. Obokata M., Reddy Y.N.V., Borlaug B.A. Diastolic Dysfunction and Heart Failure With Preserved Ejection Fraction: Understanding Mechanisms by Using Noninvasive Methods. *JACC Cardiovasc. Imaging.* 2020;13(1−2):245−257. DOI: 10.1016/j.jcmg.2018.12.034.
37. Kalyuzhin V.B., Teplyakov A.T., Bespalova I.D., Kalyuzhina E.V., Chernogoryuk G.E., Terentyeva N.N., et al. Diastolic heart failure: the limits of the use of the term. *Bulletin of Siberian Medicine*. 2023;22(1):113−120 (in Russ.). DOI: 10.20538/1682-0363-2023-1-113-120.
38. Bozkurt B., Coats A.J.S., Tsutsui H., Abdelhamid C.M., Adamopoulos S., Albert N. et al. Universal definition and classification of heart failure: a report of the Heart Failure Society of America, Heart Failure Association of the European Society of Cardiology, Japanese Heart Failure Society and Writing Committee of the Universal Definition of Heart Failure: Endorsed by the Canadian Heart Failure Society, Heart Failure Association of India, Cardiac Society of Australia and New Zealand, and Chinese Heart Failure Association. *Eur. J. Heart Fail.* 2021;23(3):352−380. DOI: 10.1002/ejhf.2115.
39. Visseren F.L.J., Mach F., Smulders Y.M., Carballo D., Koskinas K.C., Bäck M. et al. 2021 ESC Guidelines on cardiovascular disease prevention in clinical practice. *Eur. J. Prev. Cardiol.* 2022;29(1):5−115. DOI: 10.1093/eurjpc/zwab154.
40. Piepoli M.F., Adamo M., Barison A., Bestetti R.B., Biegus J., Böhm M. et al. Preventing heart failure: a position paper of the Heart Failure Association in collaboration with the European Association of Preventive Cardiology. *Eur. J. Heart Fail.* 2022;24(1):143−168. DOI: 10.1002/ejhf.2351.
41. Wong N.D., Sattar N. Cardiovascular risk in diabetes mellitus: epidemiology, assessment and prevention. *Nat. Rev. Cardiol.* 2023;20(10):685−695. DOI: 10.1038/s41569-023-00877-z.
42. Handelsman Y., Butler J., Bakris G.L., DeFronzo R.A., Fonarow G.C., Green J.B. et al. Early intervention and intensive management of patients with diabetes, cardiorenal, and metabolic diseases. *J. Diabetes Complications.* 2023;37(2):108389. DOI: 10.1016/j.jdiacomp.2022.108389.
43. Zabozlaev F.G., Zairatiants O.V., Kaktursky L.V., Klevno V.A., Kuchuk S.A., Maksimov A.V. Methodological guidelines for comparing the final clinical and pathoanatomic / forensic diagnoses. *Forensic Medicine*. 2019;5(4):48−56 (in Russ.). DOI: 10.19048/2411-8729-2019-5-4-48-56.
44. Klevno V.A., Zairatiants O.V., Zabozlaev F.G., Kaktursky L.V., Kakorina E.P., Lysenko O.V., et al. Rules for the formulation of forensic and pathoanatomical diagnoses, selection and coding of causes of death according to ICD-10. A guide for doctors. Moscow: GEOTAR-Media, 2023:656 (in Russ.).
45. Mareev V.Yu. Guidelines for the rational treatment of patients with heart failure Section 2. Definition of CHF, causes of development, pathogenesis, classification and goals of therapy. *Consilium Medicum***.** 1999;1(3):111−115 (in Russ.).

Authors' information

Kalyuzhin Vadim V. − Dr. Sci. (Med.), Professor, Head of the Advanced Therapy Division with Rehabilitation, Physiotherapy and Sports Medicine Course, Siberian State Medical University, Tomsk, kalyuzhinvv@mail.ru, http://orcid.org/0000-0001-9640-2028

Teplyakov Alexander T. − Dr. Sci. (Med.), Professor, Principal Researcher, Cardiology Research Institute, Tomsk NRMC, Tomsk, Vgelen1970@gmail.com, http://orcid.org/0000-0003-0721-0038

Bespalova Inna D. − Dr. Sci. (Med.), Head of the Propaedeutics of Internal Diseases Division with Therapy Course of the Pediatrics Department, Siberian State Medical University, Tomsk, innadave@mail2000.ru, http://orcid.org/0000-0002-4513-6329

Kalyuzhina Elena V. − Dr. Sci. (Med.), Professor, Advanced Therapy Division with Rehabilitation, Physiotherapy and Sports Medicine Course, Physiotherapy and Sports Medicine, Siberian State Medical University, Tomsk, kalyuzhina.e@mail.ru, http://orcid.org/0000-0002-7978-5327

Chernogoryuk Georgy E. − Dr. Sci. (Med.), Professor, Advanced Therapy Division with Rehabilitation, Physiotherapy and Sports Medicine Course, Siberian State Medical University, Tomsk, chernogoryuk@yandex.ru, http://orcid.org/0000-0001-5780-6660

T**erentyeva Nadezhda N.** − Cand. Sci. (Med.), Associate Professor, the Department of Internal Diseases of Surgut State University, Surgut, nadiater@mail.ru, http://orcid.org/0000-0002-0462-3526

Grakova Elena V. − Dr. Sci. (Med.), Leading Researcher, Department of Myocardial Pathology, Cardiology Research Institute, Tomsk NRMC, Tomsk, gev@cardio-tomsk.ru, http://orcid.org/0000-0003-4019-3735

Kopeva Kristina V. − Cand. Sci. (Med.), Researcher, Department of Myocardial Pathology, Cardiology Research Institute, Tomsk NRMC, Tomsk, kristin-kop@inbox.ru, http://orcid.org/0000-0002-2285-6438

Garganeeva Natalia P. − Dr. Sci. (Med.), Professor, General Medical Practice and Outpatient Therapy Division, Siberian State Medical University, Tomsk, garganeeva@gmail.com, http://orcid.org/0000-0002-7353-7154

Livshits Inna K. − Cand. Sci. (Med.), Associate Professor, Advanced Therapy Division with Rehabilitation, Physiotherapy and Sports Medicine Course, Siberian State Medical University, Tomsk, lik78.78@mail.ru, http://orcid.org/0000-0003-2357-6910

Ostanko Valentina L. − Cand.Sci. (Med.), Associate Professor, Advanced Therapy Division with Rehabilitation, Physiotherapy and Sports Medicine Course, Siberian State Medical University, Tomsk, valentina209@yandex.ru, http://orcid.org/0000-0002-9950-721X

Shalovay Alla A. − Cand. Sci. (Med.), Associate Professor, Advanced Therapy Division with Rehabilitation, Physiotherapy and Sports Medicine Course, Siberian State Medical University, Tomsk, allashalovay.2708@yandex.ru, http://orcid.org/0000-0001-7258-4883 .

Pushnikova Elena Yu. − Cand. Sci. (Med.), Cardiologist, Department of Myocardial Pathology, Cardiology Research Institute, Tomsk NRMC, Tomsk, peu@cardio-tomsk.ru, http://orcid.org/0000-0002-0456-9398

Aptekar Vladimir D. − Dr. Sci. (Med.), Head of the Cardiology Department No. 4, Cardiology Research Institute, Tomsk NRMC, Tomsk, avd@cardio-tomsk.ru, http://orcid.org/0009-0001-1167-0814

(✉) **Kalyuzhin Vadim V.,** kalyuzhinvv@mail.ru

Received 08.12.2023;
approved after peer review 15.12.2023;
accepted 23.12.2023

УДК 616.74-009.7:575.21:616.127
https://doi.org/10.20538/1682-0363-2024-1-156-165

Monogenic diseases associated with cardiomyopathy genes and their phenotypic manifestations

Kucher A.N., Nazarenko M.S.

Research Institute of Medical Genetics, Tomsk National Research Medical Center (NRMC) of the Russian Academy of Sciences
10, Naberezhnaya Ushayki Str., Tomsk, 634050, Russian Federation

ABSTRACT

The aim of the present study was to summarize the data on the spectrum of genetic diseases and their phenotypic manifestations in case of structural and functional defects in 75 genes, pathogenic variants of which are associated with the formation of different types of cardiomyopathy (CMP). The search for scientific publications was carried out in foreign (PubMed) and Russian (eLibrary) digital libraries. The data analysis was performed using the Simple ClinVar, An Online Catalog of Human Genes and Genetic Disorders, and STRING databases.

It was shown that the vast majority of CMP genes are pleiotropic. Monogenic diseases caused by mutations in CMP genes are characterized by a wide range of pathological manifestations in various organs and systems (cardiovascular, nervous, endocrine, musculoskeletal systems, connective tissue, skin and appendages, organs of vision and hearing, kidneys) as well as by metabolic and immune disorders. Therefore, if a patient (regardless of the primary diagnosis) has pathogenic / likely pathogenic variants or variants of uncertain significance in the CMP genes, we recommend a detailed and comprehensive clinical examination. This is important for clarifying the effects of rare genetic variants, identifying significant clinical and prognostic features for CMP and monogenic diseases associated with CMP genes, and identifying risk groups and controllable triggers that contribute to the manifestation of pathogenic genetic variants.

Keywords: cardiomyopathy genes, monogenic diseases, phenotypic manifestations

Conflict of interest. The authors declare the absence of obvious and potential conflicts of interest related to the publication of this article.

Source of financing. The study was supported by the state assignment from the Ministry of Science and Higher Education (No. 122020300041-7).

For citation: Kucher A.N., Nazarenko M.S. Monogenic diseases associated with cardiomyopathy genes and their phenotypic manifestations. *Bulletin of Siberian Medicine.* 2024;23(1):156–165. https://doi.org/10.20538/1682-0363-2024-1-156-165.

Спектр фенотипических проявлений моногенных заболеваний, связанных с генами кардиомиопатий

Кучер А.Н., Назаренко М.С.

Научно-исследовательский институт (НИИ) медицинской генетики, Томский национальный исследовательский медицинский центр (НИМЦ) Российской академии наук
634050, г. Томск, ул. Набережная Ушайки, 10

✉ *Nazarenko Maria S.,* maria.nazarenko@medgenetics.ru

РЕЗЮМЕ

Цель настоящего исследования заключалась в обобщении данных о спектре наследственных заболеваний и их фенотипических проявлениях при структурно-функциональных нарушениях в 75 генах, патогенные варианты которых связаны с формированием различных типов кардиомиопатий (КМП). Поиск научных публикаций проведен в зарубежных (PubMed) и отечественных (eLibrary) электронных библиотеках. Анализ данных выполнен с использованием баз Simple ClinVar, An Online Catalog of Human Genes and Genetic Disorders, а также интернет-ресурса STRING.

Показано, что подавляющее большинство генов КМП обладают плейотропизмом и при моногенных заболеваниях, вызванных мутациями в данных генах, регистрируют широкий спектр патологических проявлений в различных системах органов (сердечно-сосудистой, нервной, эндокринной, костно-мышечной системы и соединительной ткани, кожи и придатков, органов зрения и слуха, почек), а также нарушения метаболизма и иммунитета. В связи с этим вне зависимости от первичного диагноза при выявлении у пациентов в генах КМП патогенных / вероятно патогенных вариантов или вариантов с неопределенной значимостью рекомендуется проведение детального и комплексного клинического обследования. Это имеет важное значение для уточнения эффектов редких вариантов генов, выделения клинически и прогностически значимых признаков для КМП и моногенных заболеваний, связанных с генами КМП, а также выявления групп риска и управляемых триггеров, способствующих проявлению патогенных генетических вариантов.

Ключевые слова: гены кардиомиопатий, моногенные заболевания, фенотипические проявления

Конфликт интересов. Авторы заявляют отсутствие явных и потенциальных конфликтов интересов, связанных с публикацией данной статьи.

Источник финансирования. Работа выполнена при финансировании Госзадания Министерства науки и высшего образования (№ 122020300041-7).

Для цитирования: Кучер А.Н., Назаренко М.С. Спектр фенотипических проявлений моногенных заболеваний, связанных с генами кардиомиопатий. *Бюллетень сибирской медицины.* 2024;23(1):156–165. https://doi.org/10.20538/1682-0363-2024-1-156-165.

INTRODUCTION

One of the key problems of modern biomedical research is to understand the regularities of implementation of the genetic program and identify the mechanisms of formation of genetically determined phenotypes, including pathological ones [1, 2]. Advances in the field of molecular genetic research, systems biology, and systems medicine allow to take a fresh look at the issue of transformation from genotype to phenotype [3].

Cardiomyopathies (CMPs) represent a clinically and etiologically heterogeneous group of myocardial pathologies and are a remarkable example of the complexity of pathological phenotype formation. CMPs can have a monogenic, oligogenic or polygenic basis [4–6], which develops into a pathological phenotype over decades (and is manifested more often in adults) and in some cases only under certain environmental triggers [5, 6]. Clinically, CMPs can be separated into hypertrophic (HCM), dilated (DCM), restrictive (RCM) and arrhythmogenic right ventricular cardiomyopathy (ARVC); dysfunctions of certain genes are often considered to be their causes [6–8].

However, similar myocardial disorders can be caused by both external and internal environmental factors (for example, drug-induced, diabetic, peripartum, stress-induced, inflammatory (myocarditis) CMP, etc.), and pathogenic variants in genes thought to cause CMPs are also detected in patients with these conditions [9–11]. In some cases, there is a combination of several types of CMP or a transition from one form to another as the disease progresses [12–14], and CMPs can also represent a symptom of other complex pathological phenotypes [11, 15].

Dozens of genes are known, pathogenic / likely pathogenic variants of which can lead to one of the types of CMP. The number and spectrum of causative genes vary for different CMPs, but negative variants in the same genes (and even the same variants) can lead to both different and same types of CMPs [16]. There is a growing body of evidence that, on the one hand, mutations in different genes can lead to the development of similar phenotypes (in particular, to CMP), and, on the other hand, pathological variants in the same gene can contribute to the formation of different clinical phenotypes and traits, even not associated with the

underlying pathology [4, 6, 17, 18]. Identification of phenotype features, as well as clarification of the spectrum of possible disorders in the presence of pathogenic gene variants is of interest not only from a fundamental point of view (to determine the scope of specific genes), but also has clinical significance, in particular for translational medicine [3, 19]. The aim of this study was to summarize the data on the spectrum of genetic diseases and their phenotypic manifestations in structural and functional defects of the CMP genes.

DATA SOURCE AND ANALYTICAL TOOLS

Information about the genes of primary CMPs does not completely match in different sources (ClinGen, SimpleClinVar, Online Mendelian Inheritance in Man (OMIM) databases, etc.), which is due to differences in the criteria used for classifying genes as significant. In the present study, the Simple ClinVar database (https://simple-clinvar.broadinstitute.org/, accessed on February 2023), was used as a source of information on CMP genes.

The analysis of the scope of the CMP genes was performed on the basis of Online Mendelian Inheritance in Man (OMIM) (https://www.omim.org/) data on monogenic diseases that can be caused by mutations in the CMP genes under discussion. To describe the features of phenotypic manifestations of monogenic diseases caused by mutations in the CMP genes, we used MeSH, a vocabulary thesaurus used for indexing citations in MEDLINE (https://www.ncbi.nlm.nih.gov/mesh/). The online STRING (https://string-db.org/) resource was also used to characterize the CMP genes. The search for scientific publications was carried out in foreign (PubMed) and Russian (eLibrary) digital libraries.

CHARACTERISTICS OF THE PRIMARY CARDIOMYOPATHY GENES

According to Simple ClinVar, pathogenic / likely pathogenic variants of 75 genes can lead to one of the forms of primary CMPs; 40 of these genes are reported for HCM, 50 genes for DCM, 11 genes for ARVC, and 7 genes for RCM (Figure). Most of the CMPs genes are protein-coding genes, *FLNC-AS1* and *TTN-AS1* belong to non-coding RNA genes. Along with specific genes (which are characterized as causal to one type of CMP), there are genes variants of which can lead to different types of CMPs. For example, variants in the *ACTN2*, *DES*, *LMNA*, and *TMEM43* genes are considered causal for HCM, DCM, and ARVC; variants in the *MYH7*, *TNNI3*, *TNNT2*, and *TTN* are considered causal for HCM, DCM, and RCM (Figure). In other words, pathogenic variants in the same CMP genes can lead to different pathological phenotypes affecting the functioning of the heart.

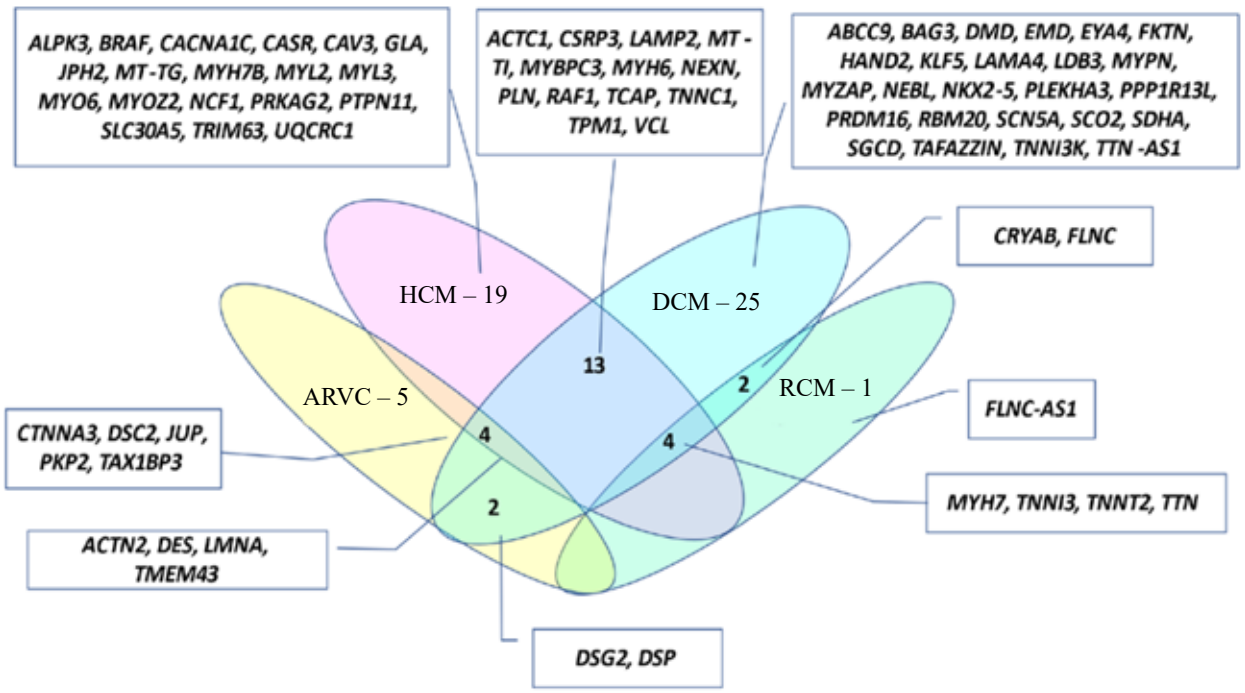

Figure. Common and specific genes for different monogenic CMPs

According to the Tissue Expression Database (https://tissues.jensenlab.org/) and STRING [20, 21], the CMP genes under discussion are expressed in many tissues, including various parts of the heart (right ventricle, cardiac muscle, left and right atrium, ventricle, atrium), embryonic tissues (21 genes), tissues of the female reproductive system (17 genes), testicles (9 genes), fetus (13 genes), sensory organs (6 genes), rectum (5 genes), gallbladder (3 genes), in adipocytes (2 genes), platelets (4 genes), etc. [20, 21]. In particular, the *PKP2*, *UQCRC1*, *VCL*, *RAF1*, *MYH7B*, *SDHA*, *DSC2*, *NCF1*, *TMEM43*, *FLNC*, *PTPN11*, *MYPN*, *HAND2*, *DMD*, *LMNA*, *BAG3*, *EMD*, *KLF5*, *JUP*, *MYH6*, *LAMP2* genes are expressed in embryonic structures (BTO:0000174 according to [20]), the *BAG3*, *DMD*, *VCL*, *SDHA*, *NCF1*, *PTPN11* genes are expressed in the sensory organs, etc. Expression in different types of tissues and at different stages of ontogenesis suggests that dysfunction in CMP genes can affect the functioning of not only the cardiovascular, but also other organ systems.

According to STRING [21], 71 proteins encoded by the CMP genes were functionally related (the average local clustering coefficient is 0.656), a total of 683 functional or physical interactions were registered (on average, 19.2 per protein) with the expected 35 interactions (protein-protein interactions enrichment $p < 1.0e\text{-}16$). The protein products of only 7 genes were not included into the network: *NCF1*, *TAX1BP3*, *KLF5*, *SLC30A5*, *PLEKHA3*, *PRDM16* and *CASR*. The integration of proteins encoded by the CMP genes into a single network is expected due to criteria for their selection for analysis, but this also implies the possibility of involvement of these genes in common pathological conditions when other organ systems are affected.

THE SPECTRUM OF MONOGENIC DISEASES ASSOCIATED WITH THE CMP GENES (ACCORDING TO OMIM) AND THEIR CLINICAL MANIFESTATIONS

Monogenic diseases are not indicated for 13 genes in the Online Mendelian Inheritance in Man (OMIM) database: for the *HAND2*, *KLF5*, *MT-TG*, *MT-TI*, *MYH7B*, *MYZAP*, *NEBL*, *PLEKHA3*, *PPP1R13L*, *SLC30A5*, *TAX1BP3*, *TRIM63*, *TTN-AS1* genes [22]. For the 62 remaining genes, a total of 191 diseases are listed, with only two pathologies being reported as predisposition (the *CASR* gene – to idiopathic generalized epilepsy; *SCN5A* gene – to sudden infant death syndrome). In most cases, autosomal dominant (72.8%) or autosomal recessive (17.3%) inheritance is noted, less frequently – mixed autosomal dominant / autosomal recessive (4.0%), autosomal dominant / digenic dominant (1.2%), and X-linked (4.6%) inheritance of the disease in the presence of pathological variants are observed. In five cases, somatic mutations are considered as the cause of the pathology (for cancers).

The CMP genes are characterized both by a different number of monogenic diseases and by their diversity. The largest number of diseases (from 5 to 11) was registered for *LMNA*, *SCN5A*, *MYH7*, *BRAF*, *NKX2-5*, *DSP*, *TTN, CASR*, *CAV3* genes (Table 1).

Table 1

CMP genes characterized by the largest number of monogenic diseases according to OMIM

Gene	Monogenic diseases
LMNA	DCM, 1A; Charcot – Marie – Tooth disease, type 2B1; Emery– Dreifuss muscular dystrophy type 2, (AD); Emery – Dreifuss muscular dystrophy type 3, (AR); heart – hand syndrome, Slovenian type; Hutchinson – Gilford progeria syndrome; familial partial lipodystrophy, type 2; Malouf syndrome; mandibuloacral dysplasia; muscular dystrophy, congenital; restrictive dermopathy 2 – **11 diseases in total**
SCN5A	Atrial fibrillation, familial, 10; Brugada syndrome 1; DCM, 1E; heart block, nonprogressive; heart block, progressive, type IA; long QT syndrome 3; sick sinus syndrome 1; ventricular fibrillation, familial, 1; susceptibility to sudden infant death syndrome **– 9 diseases in total**
MYH7	DCM, 1S; HCM, 1; Laing distal myopathy; left ventricular noncompaction 5; myosin storage congenital myopathy (AD and AR); scapuloperoneal myopathy **– 7 diseases in total**
BRAF	Lung adenocarcinoma, somatic; cardiofaciocutaneous syndrome; colorectal cancer, somatic; LEOPARD syndrome 3; melanoma, malignant, somatic; non-small cell lung cancer, somatic; Noonan syndrome 7 – **7 diseases in total**
NKX2-5	Atrial septal defect 7, with or without AV conduction defects; conotruncal heart malformations, variable; hypoplastic left heart syndrome 2; hypothyroidism, congenital nongoitrous, 5; tetralogy of Fallot; ventricular septal defect 3 **– 7 diseases in total**
DSP	Arrhythmogenic right ventricular dysplasia 8; DCM with woolly hair and keratoderma; dilated cardiomyopathy with woolly hair, keratoderma, and tooth agenesis; epidermolysis bullosa, lethal acantholytic; palmoplantar keratodermas striata II; woolly hair-skin fragility syndrome **– 6 diseases in total**

Table 1 (continued)

Gene	Monogenic diseases
TTN	DCM, 1G; HCM, 9; muscular dystrophy, limb-girdle, (AR) 10; myopathy, myofibrillar, 9, with early respiratory failure; congenital myopathy-5 with cardiomyopathy; tardive tibial muscular dystrophy – **6 diseases in total**
CASR	Hyperparathyroidism, neonatal; hypocalcemia (AD); hypocalcemia (AD) with Bartter syndrome; hypocalciuric hypercalcemia, type I; predisposition to idiopathic generalized epilepsy 8, late onset – **5 diseases in total**
CAV3	HCM, familial; creatine phosphokinase, elevated serum; long QT syndrome 9; distal myopathy, Tateyama type; rippling muscle disease 2 – **5 diseases in total**

Note. AD and AR designate autosomal dominant and autosomal recessive inheritance, respectively.

Four monogenic diseases were associated with 14 genes (*ABCC9*, *ACTC1*, *ACTN2*, *CACNA1C*, *CRYAB*, *FKTN*, *FLNC*, *LDB3*, *MYH6*, *MYO6*, *MYPN*, *PTPN11*, *SDHA*, *TNNT2*), and the number of diseases indicated in OMIM does not exceed three for the remaining genes.

From the above list of monogenic diseases for the CMP genes (Table 1), it is obvious that pathological manifestations of mutations in these genes are detected not only in the cardiovascular system, but also in other organs. In MeSH terminology, genetic diseases caused by pathogenic variants in the CMP genes can manifest as symptoms of damage to various organ systems (Table 2). According to OMIM and MeSH data, damage to the cardiovascular system accompanies monogenic diseases caused by 56 CMP genes, damage to the musculoskeletal system and connective tissue is caused by 24 CMP genes, skin and appendages, and metabolic disorders – by 8 genes each, pathology of the central nervous system is associated with 6 CMP genes. In addition, endocrine system disorders, pathology of the kidneys, eyes, immunity, hearing, and some other disorders were recorded with mutations in 4 or less genes.

It is worth noting that the "ranking" of CMP genes by the number of nosologies indicated in OMIM is not fully consistent with the that in relation to the organ systems in which such disorders occur. Full accordance is observed only for the *LMNA* gene (maximum number of inherited diseases and the number of affected systems) and a number of genes with a small number of monogenic diseases indicated in OMIM (for example, for the *ALPK3*, *CSRP3*, *JPH2*, *LAMA4*, *CTNNA3* and some others genes, only cardiovascular system is indicated). Similar estimates were obtained for the *BRAF*, *CASR*, and *CAV3* genes, which have a high "ranking" both in terms of the number of nosologies and the number of disorders in monogenic diseases of affected organ systems (Table 1, 2). It is important to emphasize that the list of disorders presented in MeSH that are characteristic of monogenic diseases caused by pathogenic variants in the CMP genes is not complete and does not take into account all pathological features that are characteristic of the respective diseases.

The table does not include the MeSH "Immune System Diseases" category, which is found only for the *NCF1* gene (characterized by Phagocyte bactericidal dysfunction).

A variety of clinical manifestations in monogenic diseases caused by pathogenic variants in the CMP genes is also registered within individual organ systems (Table 2) [22]. CMP genes dysfunction can lead to other heart pathologies (various arrhythmias, heart and vascular defects, etc.). Thus, variants in the *ABCC9* and *SCN5A* genes lead to atrial or ventricular fibrillation. A number of CMP genes (*CTNNA3*, *DSC2*, *DSG2*, *DSP*, *PKP2*, *TMEM43*) act as causative factors for the development of arrhythmogenic right ventricular dysplasia or arrhythmias among symptoms, syndromes, and diseases. For example, tachycardia is caused by *SCN5A* and *CACNA1C* in Brugada syndrome, and by *PRKAG2* gene in Wolff – Parkinson – White syndrome [22].

According to clinical observations, atrial fibrillation may represent the initial stage of cardiomyopathy manifestation (in particular in carriers of pathogenic / likely pathogenic variants in CMP genes) [23], and the phenotype of arrhythmogenic CMP may occur in other genetically determined cardiomyopathies [24]. However, arrhythmias do not always manifest in patients with monogenic CMPs even in the presence of the same pathogenic variant, as was observed, in particular, in patients with HCM caused by the p.Gln1233Ter substitution in the *MYBPC3* gene [25].

It should be highlighted that out of 62 CMP genes associated with monogenic diseases according to OMIM, no diseases manifested by the pathology of the cardiovascular system are mentioned for 6 genes – *CASR*, *SCO2*, *EMD*, *LAMP2*, *NCF1,* and *UQCRC1*. This indicates that information in the OMIM database about possible monogenic diseases caused by pathogenic variants in the CMP genes is incomplete.

Table 2

Examples of phenotypic manifestations* of monogenic diseases caused by pathogenic variants in the CMP genes according to MeSH

Genes	OMIM {total nosologies}	CVD	Musculoskeletal / connective tissue diseases	Nervous system diseases	Skin and appendages	Neoplasia	Traits	Metabolism	Endocrine system diseases	Kidney diseases	Eye diseases	Hearing disorders	Total MeSH Terms
LMNA	115200, 605588, 181350, 616516, 610140, 176670, 151660, 212112, 248370, 613205, 619793 **{11}**	CMP, CHD	MD, hand deformities, mandibuloacral dysplasia	Motor and sensory neuropathy	Restrictive dermopathy	–	–	Progeria, lipid metabolism D.	Gonadal dysgenesis	Urogenital A.	–	–	7
BRAF	211980, 115150, 114500, 613707, 155600, 211980, 613706 **{7}**	CHD	Muscle and skeletal A. Connective tissue A.	–	Ectodermal dysplasia, pigmentation D.	Lung Cr, Colorectal Cr, melanoma	Feeding difficulties, face and skull A.	–	–	–	–	–	5
PTPN11	151100, 607785, 156250, 163950 **{4}**	CHD	Muscle and skeletal A. Connective tissue A.	–	Ectodermal dysplasia, pigmentation D.	Bone and cartilage Cr.; leukemia	Feeding difficulties, face and skull A.	–	–	–	–	–	5
SDHA	613642, 252011, 619259, 614165 **{4}**	CMP	–	Neurodegeneration, ataxia	–	Paraganglioma	–	Mitochondrial diseases	–	–	ONA	–	5
RAF1	615916, 611554, 611553 **{3}**	CMP, CHD	Muscle and skeletal A. Connective tissue A.	–	Ectodermal dysplasia, pigmentation D.	–	Feeding difficulties, face and skull A.	–	–	–	–	–	4
CACNA1C	611875, 618447, 620029, 601005 **{4}**	Ar.	Skeletal A.	Seizures, autism	–	–	Neuromuscular manifestations	–	–	–	–	–	4

Table 2 (continued)

Genes	OMIM {total nosologies}	CVD	Musculoskeletal / connective tissue diseases	Nervous system diseases	Skin and appendages	Neoplasia	Traits	Metabolism	Endocrine system diseases	Kidney diseases	Eye diseases	Hearing disorders	Total MeSH Terms
CASR	239200, 601198, 601198, 145980, 612899 **{5}**	–	–	Epilepsy	–	–	–	Calcium metabolism P.	P. of parathyroid and adrenal glands	D. of transport in tubules	–	–	4
FKTN	611615, 253800, 613152, 611588 **{4}**	CMP	MD	Brain A.	–	–	–	–	–	–	Eye A.	–	4
ABCC9	614050, 608569, 239850, 619719 **{4}**	CMP, Ar., cardiomegaly	MP, osteochondrodysplasia	–	Hypertrichosis	–	–	–	–	–	–	–	3
CAV3	192600, 123320, 611818, 614321, 606072 **{5}**	CMP, Ar.	MD	–	–	–	CPK level	–	–	–	–	–	3
CRYAB	615184, 613763, 608810, 613869 **{4}**	CMP	MP	–	–	–	–	–	–	–	Cataract	–	3
TMEM43	604400, 619832, 614302 **{3}**	CMP	MD	–	–	–	–	–	–	–	–	Auditory neuropathy	3

Note. CMP – cardiomyopathy; CHD – congenital heart disorder; Ar. – arrhythmia; MD – muscular dystrophy; MP – myopathy; CPK – creatine phosphokinase; ONA – optic nerve atrophy, A. – anomalies; P. – pathology; Cr. – cancer; D.– disorders.

The musculoskeletal system and connective tissue are the second most frequently affected tissues by the presence of pathogenic variants in the CMP genes. Anomalies of the muscles, skeleton, and connective tissue, muscular dystrophy, myopathies, and some other disorders were registered for mutations in 24 genes (Table 2). In particular, various forms of myopathy are caused by mutations in the *ACTN2* gene (congenital myopathy with structured cores and Z-line abnormalities; distal myopathy, type 6, with adult onset), *BAG3* (myofibrillar myopathy, type 6), etc. [22].

Pathogenic variants in the CMP genes are also associated with the development of other monogenic diseases, manifested by pathological changes in the skin and hair (including restrictive dermopathy, skin pigmentation disorders, keratosis, woolly hair, etc.), cancers (melanoma, leukemia and other cancers), neurological disorders (neurodegenerative changes, seizures, epilepsy, ataxia, autism, etc.), metabolic (changes in lipid metabolism, mitochondrial pathology, storage diseases, etc.) and endocrine disorders (pathology of the parathyroid gland and adrenal glands) (Table 2), as well as various syndromes characterized by a wide range of structural and functional disorders. At the same time, on the one hand, complex clinical phenotypes are registered in some types of CMP, and, on the other hand, cardiomyopathies (or other myocardial disorders) can act as a symptom of a genetic disease or syndrome [22].

Thus, DCM caused by pathogenic variants in the *DSP* gene is combined with woolly hair and keratoderma; a left ventricular noncompaction can be registered in DCM and HCM (in both cases, the causative variant is localized in the *ACTN2* gene). CMP as a symptom is observed in Barth syndrome (DCM, neutropenia, proximal myopathy, physical and motor development delay are registered; the causative gene is *TAFAZZIN*); Danon disease (HCM, myopathy, mental retardation, the causative gene is *LAMP2*), LEOPARD syndrome (characterized by myocardial hypertrophy, multiple lentigines, electrocardiography conduction abnormalities, hypertelorism, pulmonary stenosis, abnormal genitalia, growth retardation, and sensorineural deafness; pathogenic variants of *PTPN11*, *RAF1*, *BRAF* can act as causative genes); Malouf syndrome (DCM, skeletal anomalies, reproductive disorders, mental retardation, where the causative gene is *LMNA*), Naxos disease (arrhythmogenic right ventricular dysplasia, palmoplantar keratoderma and woolly hair, the causative gene is *JUP*) and others [22].

It is worth noting that damage to other organ systems is observed in monogenic diseases caused by different CMP genes. Thus, skin and hair structure disorders were detected in arrhythmogenic right ventricular dysplasia (the causative gene is *DSC2*); cardiofaciocutaneous syndrome (*BRAF*); lethal acantholytic epidermolysis bullosa, striate palmoplantar keratoderma II (*DSP* gene), Cantú syndrome (*ABCC9* gene), restrictive dermopathy 2 (*LMNA* gene), etc. Mutations in the CMP genes can lead to sensory organ damage both as isolated phenotypes (*EYA4*, *MYO6* cause deafness; *CRYAB* causes cataract) and as individual symptoms (mutations in the *GLA*, *PTPN11*, *RAF1*, *BRAF*, *FKTN* genes) [22].

Cancers are caused by somatic mutations in the *BRAF* gene (adenocarcinoma, colorectal cancer, melanoma, non-small cell lung cancer) and the *PTPN11* gene (juvenile myelomonocytic leukemia), and pathogenic variants in the *SDHA* gene lead to paraganglioma 5. In addition, it should be noted that for syndromes caused by mutations in the CMP genes, malformations of various organ systems, physical and mental retardation, and disorders in the reproductive system are observed [22].

As already noted, the data provided in MeSH on phenotypic manifestations in monogenic diseases caused by mutations in the CMP genes cannot be considered complete, and as these patients are described in more detail, their phenotypic features and, accordingly, the scope of the genes will be refined. Thus, significant associations were found between pathogenic variants in the *PTPN11* gene and pulmonary stenosis (both valvular and supravalvular) and pulmonary valve dysplasia [2]. It has been shown that children and young adults with Noonan syndrome, who have pathogenic variants in the *PTPN11* gene, despite their slim build, are characterized by an unfavorable metabolic profile (low level of high-density lipoproteins, a trend toward higher triglyceride levels, higher HOMA-IR median, impaired glucose metabolism according to glucose tolerance test) [17]. Rare cases of early-onset cardiomyopathy associated with pathogenic variants in the *ALPK3* gene (DCM, HCM, mixed DCM/HCM phenotype with progression to HCM) combined with craniofacial anomalies have been described [13].

The spectrum of monogenic diseases caused by pathogenic variants in CMP genes is expanding. Thus, based on the expression patterns and study of protein - protein interaction networks using *in silico* tools, the *TTN* gene is considered as a candidate for arthrogryposis type 10 (a congenital disease of the musculoskeletal system manifested by joint

contractures, muscle underdevelopment, and changes in the spinal cord) [26].

In general, based on the summarized data on the phenotypic features of monogenic diseases caused by pathogenic variants in the CMP genes and taking into account the functional connectivity of the proteins encoded by these genes, we can expect the involvement of CMP genes in normal variability and formation of predisposition to pathological conditions of the cardiovascular, musculoskeletal, nervous, endocrine, and other organ systems. The traits associated with these organ systems may be of interest for a more detailed study in patients with various CMPs, including monogenic forms.

CONCLUSION

Despite the fact that the data are incomplete (due to the peculiarities of formation of any information resources), the information above allows to make several generalizations. Firstly, it is obvious that the CMP genes are pleiotropic, and pathogenic variants localized in these genes can lead to disorders in various organ systems. Secondly, the expression in various organs and the functional connectivity of the proteins encoded by CMP genes suggest the involvement of many genes in determining the structural and functional features of organ systems for which changes were registered in the already known monogenic diseases. Thirdly, monogenic diseases are caused by pathogenic gene variants with a strong effect, and, accordingly, monogenic diseases are characterized by extreme phenotypic manifestations (even in the case of incomplete penetrance and expressivity). Therefore, that polymorphic variants of these genes can make a certain contribution to the normal variability of traits of the relevant organ systems and take part in the formation of a polygenic basis of various disease determinations.

This statement is confirmed by the data of genome-wide association studies (GWAS), according to which polymorphic variants of the CMP genes are involved in the formation of variability not only of parameters reflecting the functional state of cardiovascular system (ECG and Echo parameters, blood pressure, etc.), but also in disorders of various organ systems (endocrine, urogenital, musculoskeletal, organs of vision and hearing, etc.), biochemical parameters and blood cell composition [27]. In our opinion, taking into account the complexity of genetic determination (from monogenic to polygenic component), incomplete penetrance and expressivity of genetic variants, and the possible modifying effect of various genetic factors on the clinical presentation of CMP [25, 28, 29], this aspect requires more detailed consideration.

In addition, the data above also define some important areas of research that may have significant clinical relevance in the future. First of all, this concerns a detailed clinical examination of patients with a diagnosed genetic disease, which is or may be caused by CMP genes. The examination should be comprehensive and not limited to the detailed characterization of previously described symptoms and traditionally examined parameters or systems of organs. So, V. Lodato et al. [3] note that physicians observing CMP in children “can face the most bizarre scenarios”. And the diagnostic process requires knowledge in cardiology, pediatrics, metabolism, radiology, and genetics (both clinical and molecular) and personalized management. As such data accumulate, it will be possible to identify clinically and prognostically significant traits for CMPs and other monogenic diseases associated with CMP genes, as well as markers that may contribute to the phenotypic manifestation of the pathogenic genetic variant. A detailed phenotypic description of patients is important to clarify the effects of rare variants of the CMP genes detected by molecular genetic testing, as well as variants of uncertain significance (VUS). This approach may allow for early identification of risk groups and manageable triggers that contribute to the manifestation of pathogenic gene variants.

This study was based on the analysis of CMP genes. At the same time, it seems appropriate to assess the scope of the genes of other monogenic diseases, as well as a to perform a deeper, comprehensive examination of individuals with an established or suspected diagnosis of various hereditary diseases.

REFERENCES

1. Nussinov R., Tsai C.J., Jang H. Protein ensembles link genotype to phenotype. *PLoS Comput. Biol*. 2019;15 (6):e1006648. DOI: 10.1371/journal.pcbi.1006648.
2. Leoni C., Blandino R., Delogu A.B., De Rosa G., Onesimo R., Verusio V. et al. Genotype-cardiac phenotype correlations in a large single-center cohort of patients affected by RASopathies: Clinical implications and literature review. *Am. J. Med. Gene.t A*. 2022;188(2):431–445. DOI: 10.1002/ajmg.a.62529.
3. Lodato V., Parlapiano G., Calì F., Silvetti M.S., Adorisio R., Armando M. et al. Cardiomyopathies in children and systemic disorders when is it useful to jook beyond the heart? *J. Cardiovasc. Dev. Dis*. 2022;9(2):47. DOI: 10.3390/jcdd9020047.
4. Cerrone M., Remme C.A., Tadros R., Bezzina C.R., Delmar M. Beyond the one gene-one disease paradigm: complex genetics and pleiotropy in inheritable cardiac disorders. *Circulation*.

2019;140(7):595–610. DOI: 10.1161/CIRCULATIONAHA.118.035954.
5. Hershberger R.E., Cowan J., Jordan E., Kinnamon D.D. The complex and diverse genetic architecture of dilated cardiomyopathy. *Circ Res*. 2021; 128 (10): 1514–1532. DOI: 10.1161/CIRCRESAHA.121.318157.
6. McKenna W.J., Judge D.P. Epidemiology of the inherited cardiomyopathies. *Nat. Rev. Cardiol*. 2021;18(1):22–36. DOI: 10.1038/s41569-020-0428-2.
7. Brieler J., Breeden M.A., Tucker J. Cardiomyopathy: an overview. *Am. Fam. Physician*. 2017;96(10):640–646.
8. El Hadi H., Freund A., Desch S., Thiele H., Majunke N. Hypertrophic, dilated, and arrhythmogenic cardiomyopathy: Where are we? *Biomedicines*. 2023;11(2):524. DOI: 10.3390/biomedicines11020524.
9. Povysil G., Chazara O., Carss K.J., Deevi S.V.V., Wang Q., Armisen J. et al. Assessing the role of rare genetic variation in patients with heart failure. *JAMA Cardiol*. 2021;6(4):379–386. DOI: 10.1001/jamacardio.2020.6500.
10. Koziol K.J., Aronow W.S. Peripartum cardiomyopathy: current understanding of pathophysiology, diagnostic work-up, management, and outcomes. *Curr. Probl. Cardiol*. 2023;48 (8):101716. DOI: 10.1016/j.cpcardiol.2023.101716.
11. Paul C., Peters S., Perrin M., Fatkin D., Amerena J. Non-ischaemic dilated cardiomyopathy: recognising the genetic links. *Intern. Med. J*. 2023;53(2):178–185. DOI: 10.1111/imj.15921.
12. Komissarova S.M., Rineyskaya N.M., Chakova N.N., Niyazova S.S. Overlapping Phenotype: Left Ventricular non-Compaction and Hypertrophic Cardiomyopathy. *Kardiologiia*. 2020; 60 (4): 137–145 (in Russ.). DOI: 10.18087/cardio.2020.4.n728.
13. Ding W.W., Wang B.Z., Han L., Li Z.P., Zhang W., Wang H. et al. ALPK3 gene-related pediatric cardiomyopathy with craniofacial-skeletal features: a report and literature review. *Zhonghua Er Ke Za Zhi – Chinese Journal of Pediatrics*. 2021;59(9):787–792. [Chinese]. DOI: 10.3760/cma.j.cn112140-20210222-00150.
14. Gonçalves L., Pires I., Santos J., Correia J., Neto V., Moreira D. et alOne genotype, two phenotype: Hypertrophic cardiomyopathy with left ventricular non-compaction. *Cardiol. J*. 2022;29 (2):366–367. DOI: 10.5603/Cj.2022.0020.
15. Joury A., Faaborg-Andersen C., Quintana R.A., da Silva-de-Abreu A., Nativi-Nicolau J. Diagnostic tools for cardiac amyloidosis: a pragmatic comparison of pathology, imaging and laboratories. *Curr. Probl. Cardiol*. 2023;48(5):101106. DOI: 10.1016/j.cpcardiol.2022.101106.
16. Simple ClinVar. URL: https://simple-clinvar.broadinstitute.org/
17. Noronha R.M., Villares S.M.F., Torres N., Quedas E.P.S., Homma T.K., Albuquerque E.V.A. et al. Noonan syndrome patients beyond the obvious phenotype: A potential unfavorable metabolic profile. *Am. J. Med. Genet. A*. 2021;185(3):774–780. DOI: 10.1002/ajmg.a.62039.
18. Rimskaya E.M., Novikov P.S., Salami H.F., Golitsyn S.P. Brugada syndrome and early repolarization syndrome: various clinical forms of J-wave syndrome in one family. *Russian Cardiology Bulletin*. 2022;17(2):81–87 (in Russ.). DOI: 10.17116/Cardiobulletin20221702181.
19. Yu C., Deng X.J., Xu D. Gene mutations in comorbidity of epilepsy and arrhythmia. *J.* Neurol. 2023;270(3):1229–1248. DOI: 10.1007/s00415-022-11430-2.
20. Tissue expression database. URL: https://tissues.jensenlab.org/
21. STRING. URL: https://string-db.org/
22. Online Mendelian Inheritance in Man. URL: https://omim.org/
23. Yoneda Z.T., Anderson K.C., Quintana J.A., O'Neill M.J., Sims R.A., Glazer A.M. et al. Early-onset atrial fibrillation and the prevalence of rare variants in cardiomyopathy and arrhythmia genes. *JAMA Cardiol*. 2021;6(12):1371–1379. DOI: 10.1001/jamacardio.2021.3370.
24. Cipriani A., Perazzolo Marra M., Bariani R., Mattesi G., Vio R., Bettella N. et al. Differential diagnosis of arrhythmogenic cardiomyopathy: phenocopies versus disease variants. *Minerva Med*. 2021;112(2):269–280. DOI: 10.23736/S0026-4806.20.06782-8.
25. Salakhov R.R., Golubenko M.V., Valiakhmetov N.R., Pavlyukova E.N., Zarubin A.A., Babushkina N.P. et al. Application of long-read nanopore sequencing to the search for mutations in hypertrophic cardiomyopathy. *Int. J. Mol. Sci*. 2022;23(24):15845. DOI: 10.3390/ijms232415845.
26. Biswas A., Nath S.D., Ahsan T., Hossain M.M., Akhteruzzaman S., Sajib A.A. *TTN* as a candidate gene for distal arthrogryposis type 10 pathogenesis. *J. Genet. Eng. Biotechnol*. 2022;20(1):119. DOI: 10.1186/s43141-022-00405-5.
27. GWAS Catalog. The NHGRI-EBI Catalog of human genome-wide association studies. URL: https://www.ebi.ac.uk/gwas/
28. Kucher A.N., Valiakhmetov N.R., Salakhov R.R., Golubenko M.V., Pavlyukova E.N., Nazarenko M.S. Phenotype variation of hypertrophic cardiomyopathy in carriers of the p.Arg870His pathogenic variant in the *MYH7* gene. *Bulletin of Siberian Medicine*. 2022;21(3):205–216 (in Russ.). DOI: 10.20538/1682-0363-2022-3-205-216. DOI: 10.20538/1682-0363-2022-3-205-216.
29. Kucher A.N., Sleptsov A.A., Nazarenko M.S. The genetic landscape of dilated cardiomyopathy. *Russian Journal of Genetics*. 2022;58(4):371–387 (in Russ.). DOI: 10.31857/S0016675822030080. DOI: 10.1134/S1022795422030085.

Authors' information

Kucher Aksana N. – Dr. Sci. (Biology), Leading Researcher, Laboratory of Population Genetics, Research Institute of Medical Genetics, Tomsk NRMC, Tomsk, aksana-kucher@medgenetics.ru, http://orcid.org/0000-0003-3824-3641

Nazarenko Maria S. – Dr. Sci. (Med.), Head of the Laboratory of Population Genetics, Research Institute of Medical Genetics, Tomsk NRMC, Tomsk, maria.nazarenko@medgenetics.ru, http://orcid.org/0000-0002-0673-4094

(✉) **Nazarenko Maria S.,** maria.nazarenko@medgenetics.ru

Received 11.05.2023;
approved after peer review 20.06.2023;
accepted 14.09.2023

УДК 616.24-002.5-092:579.61
https://doi.org/10.20538/1682-0363-2024-1-166-175

Features of the lung microbiota in tuberculosis infection

Orlova E.A., Ogarkov O.B., Kolesnikova L.I.

Research Center for Family Health and Human Reproduction Problems (RC FHHRP)
16, Timiryazeva Str., Irkutsk, 664003, Russian Federation

ABSTRACT

Normal lung microbiota is a small number of transient microbes; however, respiratory pathology may be associated with persistent microbial colonization of the lungs. It remains a poorly understood and mysterious part of the pathogenesis of tuberculosis infection.

The review considers the general pathogenetic mechanisms of the effect of lung microbiota in respiratory pathology and presents the main methodological difficulties in the study of the lung microbiome. This review is aimed at analyzing the results of the available studies on diverse microbial composition of human lungs in tuberculosis using metagenomic sequencing methods. Despite high variability of the presented data, we can conclude that dysbiosis in tuberculosis is more often characterized by a decrease in bacterial diversity and enrichment of lung microbiota with anaerobic bacteria. *Acinetobacter*, *Campylobacter*, *Moraxella*, *Pseudomonas*, *Staphylococcus,* and *Streptococcus*, as well as some other microorganisms are indicated as important pathogenetic factors of dysbiosis in pulmonary tuberculosis, the role of which is yet to be elucidated.

Keywords: microbiota, microbiome, lungs, tuberculosis, metagenomics

Conflict of interest. The authors declare the absence of obvious or potential conflicts of interest related to the publication of this article.

Source of financing. The study was carried out within state assignment No. 121022500179-0.

For citation: Orlova E.A., Ogarkov O.B., Kolesnikova L.I. Features of the lung microbiota in tuberculosis infection. *Bulletin of Siberian Medicine.* 2024;23(1):166–175. https://doi.org/10.20538/1682-0363-2024-1-166-175.

Особенности микробиоты легких при туберкулезной инфекции

Орлова Е.А., Огарков О.Б., Колесникова Л.И.

Научный центр проблем здоровья семьи и репродукции человека (НЦ ПЗСРЧ)
Россия, 664003, г. Иркутск, ул. Тимирязева, 16

РЕЗЮМЕ

Микробиота легких представляет собой маятник, который колеблется между двумя статическими состояниями – от небольшого количества транзиторных микробов в норме до моделей устойчивой микробной колонизации при патологии. Микробиота легких остается малоизученной и загадочной частью патогенеза туберкулезной инфекции.

В настоящем обзоре отражены общие патогенетические механизмы влияния микробиоты легких при респираторной патологии и представлены основные методологические трудности в изучении легочного

✉ *Orlova Elizaveta A.,* elizaveta.a.orlova@gmail.com

микробиома. Рассмотрены результаты доступных исследований, посвященных изучению особенностей микробного разнообразия легких человека при туберкулезе с применением методов метагеномного секвенирования. Несмотря на высокую вариабельность представленных данных, дисбиоз при туберкулезе чаще характеризуется снижением бактериального разнообразия и обогащением легочной микробиоты анаэробными представителями. *Acinetobacter*, *Campylobacter*, *Moraxella*, *Pseudomonas*, *Staphylococcus* и *Streptococcus*, а также некоторые другие микроорганизмы указываются как важные патогенетические факторы дисбиоза при туберкулезе легких, роль которых еще предстоит выяснить.

Ключевые слова: микробиота, микробиом, легкие, туберкулез, метагеномика

Конфликт интересов. Авторы декларируют отсутствие явных и потенциальных конфликтов интересов,связанных с публикацией настоящей статьи.

Источник финансирования. Работа выполнена в рамках темы государственного задания № 121022500179-0.

Для цитирования: Орлова Е.А., Огарков О.Б., Колесникова Л.И. Особенности микробиоты легких при туберкулезной инфекции. *Бюллетень сибирской медицины.* 2024;23(1):166–175. https://doi.org/10.20538/1682-0363-2024-1-166-175.

INTRODUCTION

Modern approaches, including studies based on metagenomic sequencing, have confirmed the existence of lung *microbiota*, a community of microorganisms that colonize lung tissue. It differs from the microbiota of other biotopes of the human body in its low biomass and dynamic diversity of composition because the respiratory tract is a heterogeneous environment with a low nutrient content and high levels of phospholipids, antimicrobial peptides, and immune system cells that prevent microbial colonization [1]. A low bacterial load in the lungs is physiologically maintained to ensure efficient gas exchange.

Lung microbiota, along with the microbiota of the gastrointestinal tract (GIT), significantly contributes to the development of respiratory diseases and can thus be considered a pathogenetic factor. In this case, the balance between microbial immigration and elimination is disrupted, and the composition of the lung microbiota varies depending on the pathology. The most studied changes in lung microbiota are associated with exacerbation of chronic obstructive pulmonary disease (COPD) [2], asthma [3], cystic fibrosis [4], obstructive apnea [5], and pulmonary infections [6]. Less studied are pulmonary dysbiosis in HIV [7] and various forms of lung cancer [8].

Although tuberculosis (TB) remains one of the leading infectious diseases of the lungs, the number of studies on the lung microbiota in TB remains very limited, in contrast to changes in the intestinal, skin, and urogenital microbiomes. Previously, we discovered saprophytic *Bacillus licheniformis* and *Brevibacillus spp.* in the composition of biofilms when inoculating sputum from patients with pulmonary TB [9, 10]. Using DNA sequencing, the microbial diversity of caseous necrosis of surgically excised TB lesions was studied [11]. In addition, domestic research has been devoted to the bacteriological analysis of the bronchial microbiota in patients with TB [12] and the lung microbiota in mice in a model of experimental TB [13].

Currently, next-generation sequencing and metagenomic analysis are the gold standards in the study of infectious lung diseases and human microbiota [14–16]. A systematic search identified 20 original studies that examined the composition and structure of lung microbial diversity in human TB using metagenomic sequencing. The aim of this review was to summarize the pathogenetic mechanisms underlying the influence of respiratory microbiota on lung health and to analyze the available studies on human lung microbiota in the context of pulmonary TB. Special attention is paid to the unique methodological difficulties that arise when analyzing the lung *microbiome* (the genetic component of the microbiota).

LUNG MICROBIOTA AS A PATHOGENETIC FACTOR

Currently, the microbiota is considered to be a factor supporting the immune homeostasis of the lungs and a participant in the pathological process in respiratory diseases. The general pattern of the pathological process in lung diseases is a disruption of the biocenosis of the lung, which is usually unfavorable for the proliferation of bacteria. The

conditions for microbial growth in the lungs radically change due to the influx of nutrient-rich mucus and edema, the establishment of oxygen gradients [17], an increase in the concentration of proinflammatory molecules that promote bacterial growth [18], and disruption of local immune defense mechanisms [19]. The lower respiratory tract (trachea and lungs) is not a homogeneous tissue but consists of regions with varying oxygen levels, pH, temperature, mucus content, and immune cell populations. Pathological changes in the lungs are rarely homogeneous. Much more often, areas of damaged tissue are formed in which local inflammation and changes in microenvironmental conditions occur. In turn, a positive feedback loop is established between microbiota dysbiosis and lung disease. Such changes give a differential advantage in survival to some types of bacteria and impair the growth of others; therefore, the composition of the lung microbiota differs in different diseases [20].

Although the lungs are highly aerated organs, their microbiota contains species with different oxygen requirements. Members of the Bacteroidota (*Prevotella* and *Porphyromonas*) and Fusobacteriota phyla are obligate anaerobes, whereas Bacillota, Pseudomonadota, and Actinomycetota consist of both obligate aerobic (*Pseudomonas* and *Neisseria*) and facultative (*Streptococcus* and *Haemophilus*) and obligate anaerobic (*Veillonella*) genera. A decrease in oxygen levels in the lungs occurs with irreversible airway obstruction when the surface area available for gas exchange decreases by 90 %, which promotes the growth of anaerobic microorganisms [21]. An anaerobic or oxygen-depleted microenvironment that is optimal for the enhanced growth of anaerobic microorganisms is formed in COPD, emphysema, pulmonary fibrosis, and caseous necrosis in a TB focus [22]. During inflammation, the local pH in the lungs can decrease, which promotes the development of acidophilic microorganisms, such as *Lactobacillus* (phylum Bacillota) infection in COPD. The general ratio between Bacteroidota and Bacillota changes in favor of the latter because most Bacteroidota are pH sensitive and cannot develop in an acidic environment [20]. Numerous inflammatory metabolites (catecholamines, inflammatory cytokines), elevated temperature, and free ATP are also growth factors for some bacterial species [21].

Healthy airways produce relatively little protective mucus (about 100 ml per day). To avoid the protective properties of the mucous layer, some microorganisms use specific mechanisms, for example, the formation of biofilms – bacterial populations enclosed in a secreted polymer matrix, attached to each other and the biotic surface [23]. Although the growth of biofilms in healthy lungs remains questionable because of the very low bacterial load and mucociliary clearance, biofilms may have pathogenetic significance in many diseases. In patients with cystic fibrosis, high mucus production and impaired mucociliary clearance are observed in the respiratory tract. Its increased production leads to local foci of anoxia, increased temperature, and promotes persistent bacterial colonization [21]. For example, areas with high mucus levels provide an additional competitive niche for *Pseudomonas aeruginosa* [24] and the nontypeable *Haemophilus influenzae* [25]. This form additionally helps pathogenic bacteria to become more resistant to antibiotics [23]. However, according to our observations, modern clinical strains of *Mycobacterium tuberculosis* (MTB) in most cases do not form biofilms *in vitro* but are capable of producing them in mixed cultures [9]. Drug resistance factors or the host environment surrounding the pathogen may interfere with the production of MTB biofilms [10].

Thus, lung dysbiosis does not always play the role of a leading link in the pathogenesis of respiratory diseases, and cause-and-effect relationships can be multidirectional depending on the pathology. General pathogenetic mechanisms of the influence of microbiota on lung health can be described as an imbalance between immigration and elimination of microorganisms, changes in the composition of the microbiota due to microanatomical differentiation of biotic and abiotic conditions, and the use of specific pathogen-associated mechanisms by microorganisms.

LUNG MICROBIOTA IN TUBERCULOSIS

Despite more than a century of studies on MTB, gaps remain in the understanding of the factors determining the pathogenesis and clinical outcome of pulmonary TB. Multidirectional interactions of immune cells with MTB [26, 27] and probably with lung commensals [28–30] play an important role. A systematic search identified 20 studies aimed at analyzing the characteristics of lung microbiota in humans with TB using metagenomic sequencing methods. More than half of them were published in the previous 3 years and are not included in the latest available reviews [30, 31]. An analysis of the data obtained from these studies is briefly presented in Table. Most studies have been conducted on sputum samples using 16S rRNA gene amplification and

sequencing. Bronchoalveolar lavage (BAL) fluid was used less frequently, as shotgun metagenomic sequencing. Thus, the design of the conducted studies imposes certain limitations on the interpretation of the data obtained. In some cases, the study results are highly variable and contradictory.

The works by Z. Cui et al. [32] and F. Valdez-Palomares et al. [33] showed that active TB is associated with higher taxonomic diversity in lung microbiota. On the contrary, most other studies report a decrease [34–39] or an insignificant change [40–43]. Many studies have found differences in the relative abundance of taxa between patients with TB and controls, sometimes down to the species level. Although it is difficult to compare the general view between different studies, several studies have shown that in TB patients, the microbiota is enriched in members of the phyla Actinomycetota (presumably due to the detection of MTB) [37, 43] and Pseudomonadota [35, 40, 43], the family *Bacillaceae* [36, 44], the genera *Acinetobacter* [39, 44], *Campylobacter* [45, 46], *Moraxella* [33, 44], *Pseudomonas* [34, 39], and the species *Staphylococcus aureus* [38, 47]. Regarding the occurrence of the phyla Bacteroidota [37, 40] and Bacillota [35, 37], the genera *Rothia* [42, 44] and *Streptococcus* [35, 41, 48], controversial results that are directly opposite to each other have been obtained. Many other microorganisms, such as *Cupriavidus*, *Porphyromonas*, *Neisseria*, *Haemophilus*, *Selenomonas*, and *Fusobacterium*, have been considered by various authors to be likely important pathogenetic factors in TB infection.

The enrichment of the pulmonary microbiota with anaerobes (*Prevotella*, *Campylobacter*, *Staphylococcus*, *Streptococcus*, *Selenomonas*, *Fusobacterium*, *Porphyromonas*) and the accumulation of various metabolites of anaerobic fermentation in the lungs observed in TB are associated with changes in pulmonary immunity and the progression of TB infection. Thus, an increase in the proportion of *Prevotella* in the lungs correlates with the concentrations of short-chain fatty acids (propionate and butyrate) [52]. These compounds suppress the production of interferon (IFN)**γ and** interleukin (IL)-17A in response to stimulation of peripheral human blood mononuclear cells by MTB antigens. This immunological effect increases the susceptibility of HIV-infected patients to TB and possibly contributes to the progression of latent TB to active disease. Elevated pulmonary short-chain fatty acid levels are also associated with Treg cell induction [53]. Their population increases significantly in the blood of patients with active TB and suppresses the production of IFNγ [54] and proliferation of MTB-specific effector T cells [55].

Anti-tuberculosis treatment is long-term (at least six months) and includes a combination of narrow- and broad-spectrum anti-tuberculosis drugs. Long-term antibiotic treatment is considered to have deleterious effects on the structure and composition of microbial communities coexisting in the host. Only one of the analyzed studies did not confirm the effect of anti-tuberculosis drugs on the lung microbiota [50]. Other studies have shown a significant decrease in microbial diversity during treatment with anti-tuberculosis drugs [43, 51]. G. Xiao et al. demonstrated a differential effect of treatment on the composition of the lung microbial community with decreased abundances of *S. aureus*, *Pasteurella multocida*, *E. coli*, and *N. gonorrhoeae* and an increase in the number of *Prevotella melaninogenica*, *P. jejuni*, *Ralstonia pickettii*, *Neisseria subflava*, and *Prevotella intermedia* [38].

Some studies have noted low relative abundance of mycobacteria (the percentage of single reads from the total metagenome) [36, 40]. We also obtained a similar result during a pilot study of the microbial diversity of caseous necrosis in several tuberculomas [11]. In addition, Y. Hu et al. showed that there are differences in lung bacterial communities between smear-positive (MTB^+) and smear-negative TB patients (MTB^-) [37]. Such changes in the satellite microbiota of the lung appear to play a significant role in the pathophysiology of TB, which remains to be elucidated.

LIMITATIONS IN LUNG MICROBIOME STUDIES

It must be emphasized that researchers of lung microbiome (both normal and pathological) are faced with methodological difficulties unique to this niche. Almost all studies on lung microbiota have focused on sputum or BAL fluid samples, and there are significant technical difficulties in collecting samples from the lower respiratory tract. Although some studies have generally found minimal contamination of bronchoscopy specimens with upper respiratory tract microbiota [56], others have demonstrated that specimens may be significantly contaminated with nasopharyngeal bacteria [57]. This imposes significant limitations in differentiating the microbiota of the lungs from that of the upper respiratory tract. Invasive methods, such as open lung biopsy, allow one to obtain more reliable material for research [11,

Table

Studies conducted on lung microbiota in human TB

Reference	Sample type and size (TB) / (Control)	Method	Dominant microbiota in TB	Taxa that differ significantly in abundance in TB
Z. Cui et al. [32], 2012	Sputum (31) / Oropharynx samples (24)	16S rRNA	Pseudomonadota (*Phenylobacterium*, *Stenotrophomonas*, *Cupriavidus*, *Pseudomonas*), Actinomycetota, Crenarchaeota	↑ *Sphingomonas*, *Brevundimonas*, *Diaphorobacter*, *Mobilicoccus*, *Brevibacillus*
M. K. Cheung et al. [40], 2013	Sputum (22) / (14)	16S rRNA	Bacillota (*Streptococcus*), Pseudomonadota (*Neisseria*), Bacteroidota (*Prevotella*), Actinomycetota (*Actinomyces*), Fusobacteriota (*Fusobacterium*, *Leptotrichia*)	↑ Pseudomonadota, Bacteroidota, *Mogibacterium, Moryella, Oribacterium*
J. Wu et al. [34], 2013	Sputum (75) / Oropharynx samples (20)	16S rRNA	Bacillota (*Streptococcus*, *Gramulicatella*), Pseudomonadota (*Pseudomonas*)	↑ *Pseudomonas*
L. E. Botero et al. [41], 2014	Nasal, oropharynx, and sputum samples (6) / (6)	16S rRNA	Bacillota, Bacteroidota, Pseudomonadota, Actinomycetota, Fusobacteriota	↑ Streptococcaceae
Y. Zhou et al. [49]P, 2015	BAL (32) / Saliva (24)	16S rRNA	Pseudomonadota (*Cupriavidus*, *Acinetobacter*), Actinomycetota (*Mycobacterium*), Bacteroidota (*Prevotella*, *Porphyromonas*)	↑ *Mycobacterium, Porphyromonas*
P. Krishna et al. [44], 2016	Sputum (25) / (16)	16S rRNA	Pseudomonadota (*Neisseria*), Bacillota (*Streptococcus*, *Veillonella*), Fusobacteriota, Actinomycetota, Bacteroidota	↑ *Corynebacterium*, *Atopobium, Rothia mucilaginosa, Bacillus, Enterococcus, Megasphaera, Veillonella dispar, Lautropia, Acinetobacter, Moraxella*
J. A. Vázquez-Pérez et al. [35], 2020	BAL (6) / (10)	16S rRNA	Bacillota, Pseudomonadota, Bacteroidota, Actinomycetota, Fusobacteriota, Cyanobacteriota	↑ Pseudomonadota, Bacillota ↓↓ *Streptococcus* Only in TB *Lactococcus* and *Leuconostoc* were found
Y. Hu et al. [37], 2020	BAL (6 MTB^{+}-TB) / (6 MTB^{-}-TB)	Shotgun, 16S rRNA	Actinomycetota (*Mycobacterium*, *Rothia*, *Actinomyces*), Bacillota (*Streptococcus*, *Staphylococcus*), Pseudomonadota (*Pseudomonas*), Bacteroidota, Fusobacteriota	↑ Actinomycetota, especially *Mycobacterium* ↓ Bacillota, Bacteroidota
Y. Hu et al. [36], 2020	BAL (12) / –	16S rRNA	Bacillota	↑ *Mycobacterium*, *Bacillaceae*, especially *Anoxybacillus*
C. Sala et al. [50], 2020	Sputum (30) / (30)	16S rRNA	Actinomycetota, Bacteroidota, Bacillota, Fusobacteriota, Pseudomonadota	Not found
E. A. Orlova et al. [11], 2021	Biopsy (12) / –	PCR, 16S rRNA	Bacillota (*Streptococcus*), Actinomycetota (*Mycobacterium*), Pseudomonadota (*Pseudomonas, Brevundimonas*, *Pelomonas*)	Not carried out

D. P. Kateete et al. [51], 2021	Sputum (120) / –	16S rRNA	Bacteroidota (*Prevotella*, *Alloprevotella*, *Porphyromonas*), Bacillota (*Streptococcus*, *Veillonella*, *Gemella*), Pseudomonadota (*Haemophilus*, *Neisseria*), Fusobacteriota (*Fusobacterium*), Actinomycetota (*Rothia*)	Not carried out
M. HaileMariam et al. [42], 2021	Sputum (72) / (54)	16S rRNA	Bacillota (*Streptococcus*), Pseudomonadota (*Haemophilus*), Actinomycetota (*Rothia, Atopobium*)	↑ *Haemophilus* ↓ *Rothia*
F. Valdez-Palomares et al. [33], 2021	Sputum (39) / (6)	16S rRNA	Bacillota (*Streptococcus*, *Veillonella*), Bacteroidota (*Prevotella*), Pseudomonadota (*Neisseria*, *Moraxella*), Fusobacteriota, Actinomycetota	↑ *Ralstonia*, *Moraxella*
L. Ding et al. [47], 2021	BAL (101) / –	Shotgun	Pseudomonadota, Bacillota, Bacteroidota, Actinomycetota	↑ *Staphylococcus aureus*
M. R. Ticlla et al. [46], 2021	Sputum (334) / –	16S rRNA, Shotgun	Bacillota (*Streptococcus*, *Veillonella*), Pseudomonadota (*Neisseria*, *Haemophilus*, *Lautropia*), Bacteroidota (*Prevotella*, *Porphyromonas*), Fusobacteriota (*Fusobacterium*), Actinomycetota (*Rothia*), Saccharibacteria, Spirochaetes, Gracilibacteria, Absconditabacteria, Tenericutes	↑ *Campylobacter*
G. Xiao et al. [38], 2022	BAL (38) / BAL, oropharynx samples (15)	Shotgun	Pseudomonadota (*K. pneumoniae*, *Pasteurella multocida*, *Escherichia coli*, *Neisseria gonorrhoeae*), Bacillota (*S. aureus*)	↑ *S. aureus*, *N. gonorrhoeae*
V. Ueckermann et al. [39], 2022	Sputum, BAL (20) / (51)	16S rRNA	Pseudomonadota (*Burkholderiaceae*, *Enterobacteriaceae*, *Neisseriaceae*), Bacillota (*Lachnospiraceae*, *Veilonellaceae*, *Peptostreptococcaceae*, *Staphylococcaceae*), Actinomycetota (*Micrococcaceae*, *Microbacteriaceae*, *Bifidobacteriaceae*, *Norcardia*, *Actinomycetaceae*), Bacteroidota (*Prevotellaceae*)	↑ *Achromobacter*, *Acinetobacter*, *Stenotrophomonas*, *Pseudomonas*, *Mycobacterium*
M. Zhang et al. [43], 2022	BAL (23) / (13)	16S rRNA	Bacteroidota, Bacillota, Pseudomonadota, Actinomycetota	↑ Pseudomonadota, Actinomycetota, Acidobacteria, Chloroflexi, AD3
X. Xia et al. [45], 2022	BAL (21) / (57)	16S rRNA	Bacillota, Bacteroidota, Pseudomonadota, Actinomycetota, Fusobacteriota	↑ *Mycobacterium*, *Selenomonas, Lactobacillus, Leptotrichia*, *Campylobacter*

Note: ↑ – taxon abundance increased, ↓ – taxon abundance decreased, ↓↓ – taxon abundance significantly decreased.

58, 59] but are almost always difficult to access. In this way, unaffected areas of the lungs from patients with various forms of cancer obtained during surgical operations were studied as healthy tissue [58], but even these samples can be considered as "conditionally healthy", since patients before surgery received potent immunosuppressive and antibacterial therapy, which can influence the lung microbiota of patients [60].

It is also worth noting that the extremely low bacterial load in healthy lungs leads to a suboptimal signal-to-noise ratio [61], and methods for subtracting the noise component have not yet been standardized and differ between studies. Noise refers to the signal from bacterial DNA, which is the background in endoscopic and surgical sterile equipment, in solutions for nucleic acid extraction, etc. [62]. Specimens with low absolute abundance of bacterial DNA are subject to some degree of stochastic results, named sequencing stochasticity [63].

In shotgun metagenome studies, human DNA is also sequenced; therefore, in respiratory samples with low microbial biomass, the vast majority of sequenced reads are from human genomic DNA [64]. Although 16S rRNA gene sequencing allows for the analysis of taxonomic composition to the species level in some cases [65], the underlying DNA amplification also limits the general view of the microbiome to taxa with inherently high abundances. In addition, the cell walls of some microorganisms (for example, mycobacteria, fungi, capsular forms of bacteria) are resistant to standard DNA extraction techniques [66]. For these reasons, Y. Hu et al. considered that the 16S approach is not the best way to study the TB-associated microbiome, since it is associated with technical limitations in amplification and sequencing of mycobacterial 16S rRNA gene [37].

Lung biogeography – microanatomical differences in microbial diversity – can be a source of bias in studies depending on the method of BAL collection (invasive or noninvasive) and the location of collection. The studies conducted contain controversial results [56, 67]. Based on this, when planning an experiment, careful selection of conditions for all stages of sample preparation of biological material and special caution when interpreting the results are required.

CONCLUSION

Metagenomics is becoming an increasingly actively used approach for studying the characteristics of the pathogenesis and diagnosis of respiratory diseases. Although the study of the lung microbiome was not initially included in the Human Microbiome Project, sufficient evidence has accumulated over the past 10 years indicating the involvement of a dynamic oligobacterial community of the lung in the pathogenesis of TB. However, differences in the study groups, types of clinical samples, and analysis methods still do not allow to definitely conclude about changes in the composition and structure of the lung microbiota during the disease. Each study makes a trade-off between the sensitivity and specificity of the applied methods. More systematic and detailed work, for example, combining metagenomics with *in vitro* cultivation and phenotyping of microorganisms, will likely reveal the complex interactions between MTB and the satellite microbiota of the lung and will also help to determine the specific changes that affect the prognosis of patients with TB.

REFERENCES

1. Rogan M.P., Geraghty P., Greene C.M., O'Neill S.J., Taggart C.C., McElvaney N.G. Antimicrobial proteins and polypeptides in pulmonary innate defence. *Respir .Res*. 2006;7(1):29. DOI: 10.1186/1465-9921-7-29.
2. Cvejic L., Harding R., Churchward T., Turton A., Finlay P., Massey D. et al. Laryngeal penetration and aspiration in individuals with stable COPD. *Respirology*. 2011;16(2):269–275. DOI: 10.1111/j.1440-1843.2010.01875.x.
3. Field S.K., Underwood M., Brant R., Cowie R.L. Prevalence of gastroesophageal reflux symptoms in asthma. *Chest*. 1996;109(2):316–322. DOI: 10.1378/CHEST.109.2.316.
4. Scott R.B., O'Loughlin E. V., Gall D.G. Gastroesophageal reflux in patients with cystic fibrosis. *J. Pediatr*. 1985;106(2):223–227. DOI: 10.1016/s0022-3476(85)80291-2.
5. Morse C.A., Quan S.F., Mays M.Z., Green C., Stephen G., Fass R. Is there a relationship between obstructive sleep apnea and gastroesophageal reflux disease? *Clin. Gastroenterol. Hepatol*. 2004;2(9):761–768. DOI: 10.1016/s1542-3565(04)00347-7.
6. Koh W.J., Lee J.H., Kwon Y.S., Lee K.S., Suh G.Y., Chung M.P. et al. Prevalence of gastroesophageal reflux disease in patients with nontuberculous mycobacterial lung disease. *Chest*. 2007;131(6):1825–1830. DOI: 10.1378/chest.06-2280.
7. Beck J.M., Schloss P.D., Venkataraman A., Twigg H., Jablonski K.A., Bushman F.D. et al. Multicenter comparison of lung and oral microbiomes of HIV-infected and HIV-uninfected individuals. *Am. J. Respir. Crit. Care Med*. 2015;192(11):1335–1344. DOI: 10.1164/rccm.201501-0128OC.
8. Kovaleva O.V., Kushlinskii N.E., Podlesnaya P.A., Stilidi I.S., Gratchev A.N. Diagnostic and prognostic potential of the resident non-small cell lung cancer microbiome. *Klin. Lab. Diagn*. 2022;67(8):458–62. DOI: 10.51620/0869-2084-2022-67-8-458-462.
9. Ogarkov O.B., Badleeva M.V., Belkova N.L., Adelshin R.V., Tsyrenova T.A., Khromova P.A., et al. The phenomenon of the formation of biofilms by *Brevibacillus* spp. and *Bacillus*

spp. in the presence of clinical strains of *Mycobacterium tuberculosis*. *Molecular Genetics, Microbiology and Virology*. 2017;35(3):103 (in Russ.). DOI: 10.18821/0208-0613-2017-35-3-98-103.

10. Ogarkov O.B., Suzdalnitsky A.E., Khromova P.A., Tsyrenova T.A., Sokolnikova N.A., Zhdanova S.N., et al. Biofilm formation induced by clinical isolates of *Mycobacterium tuberculosis*. *Russian Journal of Infection and Immunity*. 2018;8(4):435–440 (in Russ.). DOI: 10.15789/2220-7619-2018.
11. Orlova E.A., Ogarkov O.B., Suzdalnitskiy A.E., Khromova P.A., Sinkov V.V., Plotnikov A.O., et al. Analysis of microbial diversity in caseous necrosis of tuberculosis foci. *Molecular Genetics, Microbiology and Virology*. 2021;39(3):18–24 (in Russ.). DOI: 10.17116/molgen20213903118.
12. Puzanov V.A., Komissarova O.G., Nikonenko B.V. Bacterial microbiota of lower gut and bronchi in tuberculosis patients. *Tuberculosis and Lung Diseases*. 2020;98(5):37–43 (in Russ.). DOI: 10.21292/2075-1230-2020-98-5-37-43.
13. Kayukova S.I., Panova A.E., Averbakh M.M., Nikonenko B.V., Gracheva A.N., Kompantseva N.I., et al. State of the lung microbiota in C57bl/6 mice in the experimental tuberculosis model. *Tuberculosis and Lung Diseases*. 2023;101(2):94–99 (in Russ.). DOI: 10.58838/2075-1230-2023-101-2-94-99. 14.
15. Sinkov V.V., Ogarkov O.B., Plotnikov A.O., Gogoleva N.E., Zhdanova S.N., Pervanchuk V.L. et al. Metagenomic analysis of mycobacterial transrenal DNA in patients with HIV and tuberculosis coinfection. *Infect. Genet. Evol*. 2020;77:104057. DOI: 10.1016/j.meegid.2019.104057.
16. Galeeva J., Babenko V., Bakhtyev R., Baklaushev V., Balykova L., Bashkirov P. et al. 16S rRNA gene sequencing data of the upper respiratory tract microbiome in the SARS-CoV-2 infected patients. *Data Br*. 2022;40. DOI: 10.1016/j.dib.2021.107770.
17. Worlitzsch D., Tarran R., Ulrich M., Schwab U., Cekici A., Meyer K.C. et al. Effects of reduced mucus oxygen concentration in airway *Pseudomonas infections* of cystic fibrosis patients. *J. Clin. Invest*. 2002;109(3):317–325. DOI: 10.1172/jci13870.
18. Kanangat S., Meduri G.U., Tolley E.A., Patterson D.R., Meduri C.U., Pak C. et al. Effects of cytokines and endotoxin on the intracellular growth of bacteria. *Infect. Immun*. 1999;67(6):2834–2840. DOI: 10.1128/iai.67.6.2834-2840.1999.
19. Segal L.N., Clemente J.C., Tsay J.C.J., Koralov S.B., Keller B.C., Wu B.G. et al. Enrichment of the lung microbiome with oral taxa is associated with lung inflammation of a Th17 phenotype. *Nat. Microbiol.* 2016;1:16031. DOI: 10.1038/nmicrobiol.2016.31.
20. Marsland B.J., Gollwitzer E.S. Host-microorganism interactions in lung diseases. *Nat. Rev. Immunol*. 2014;14(12):827–835. DOI: 10.1038/nri3769.
21. Dickson R.P., Erb-Downward J.R., Martinez F.J., Huffnagle G.B. The microbiome and the respiratory tract. *Annu. Rev. Physiol*. 2016;78:481–504. DOI: 10.1146/annurev-physiol-021115-105238.
22. Ulrichs T., Kaufmann S.H.E. New insights into the function of granulomas in human tuberculosis. *J. Pathol*. 2006;208(2):261–269. DOI: 10.1002/path.1906.
23. Domingue J.C., Drewes J.L., Merlo C.A., Housseau F., Sears C.L. Host responses to mucosal biofilms in the lung and gut. *Mucosal. Immunol*. 2020;13(3):413–422. DOI: 10.1038/s41385-020-0270-1.
24. Bjarnsholt T., Jensen P.Ø., Fiandaca M.J., Pedersen J., Hansen C.R., Andersen C.B. et al. *Pseudomonas aeruginosa* biofilms in the respiratory tract of cystic fibrosis patients. *Pediatr. Pulmonol*. 2009;44(6):547–558. DOI: 10.1002/ppul.21011.
25. Starner T.D., Zhang N., Kim G.H., Apicella M.A., McCray P.B. *Haemophilus influenzae* forms biofilms on airway epithelia: implications in cystic fibrosis. *Am. J. Respir. Crit. Care Med*. 2006;174(2):213–220. DOI: 10.1164/rccm.200509-1459OC.
26. Voronkova O.V., Urazova O.I., Novitsky V.V., Churina Ye.G., Khasanova R.R., Naslednikova I.O., et al. Features of the immune imbalance during various clinico-pathogenetic variants of acute progressive pulmonary tuberculosis. *Bulletin of Siberian Medicine*. 2010;9(3):42–50 (in Russ.). DOI: 10.20538/1682-0363-2010-3-42-50 27.
28. Naidoo C.C., Nyawo G.R., Wu B.G., Walzl G., Warren R.M., Segal L.N. et al. The microbiome and tuberculosis: state of the art, potential applications, and defining the clinical research agenda. *Lancet Respir. Med*. 2019;7(10):892–906. DOI: 10.1016/s2213-2600(18)30501-0.
29. Balcells M.E., Yokobori N., Hong B., Corbett J., Cervantes J. The lung microbiome, vitamin D, and the tuberculous granuloma: A balance triangle. *Microb.Pathog*. 2019;131:158–163. DOI: 10.1016/j.micpath.2019.03.041.
30. Shah T., Shah Z., Baloch Z., Cui X.M. The role of microbiota in respiratory health and diseases, particularly in tuberculosis. *Biomed. Pharmacother*. 2021;143:112108. DOI: 10.1016/j.biopha.2021.112108.
31. Comberiati P., Di Cicco M., Paravati F., Pelosi U., Di Gangi A., Arasi S. et al. The role of gut and lung microbiota in susceptibility to tuberculosis. *Int. J. Environ. Res. Public Health*. 2021;18(22):12220. DOI: 10.3390/ijerph182212220.
32. Cui Z., Zhou Y., Li H., Zhang Y., Zhang S., Tang S. et al. Complex sputum microbial composition in patients with pulmonary tuberculosis. *BMC Microbiol*. 2012;12:276. DOI: 10.1186/1471-2180-12-276.
33. Valdez-Palomares F., Torrico M.M., Palacios-González B., Soberón X., Silva-Herzog E. Altered microbial composition of drug-sensitive and drug-resistant TB patients compared with healthy volunteers. *Microorganisms.* 2021;9(8):1762. DOI: 10.3390/microorganisms9081762.
34. Wu J., Liu W., He L., Huang F., Chen J., Cui P. et al. Sputum microbiota associated with new, recurrent and treatment failure tuberculosis. *PLoS One*. 2013;8(12):83445. DOI: 10.1371/journal.pone.0083445.
35. Vázquez-Pérez J.A., Carrillo C.O., Iñiguez-García M.A., Romero-Espinoza I., Márquez-García J.E. et al. Alveolar microbiota profile in patients with human pulmonary tuberculosis and interstitial pneumonia. *Microb. Pathog*. 2020;139:103851. DOI: 10.1016/j.micpath.2019.103851.
36. Hu Y., Kang Y., Liu X., Cheng M., Dong J., Sun L. et al. Distinct lung microbial community states in patients with pulmonary tuberculosis. *Sci. China Life Sci*. 2020;63(10):1522–1533. DOI: 10.1007/s11427-019-1614-0.

37. Hu Y., Cheng M., Liu B., Dong J., Sun L., Yang J. et al. Metagenomic analysis of the lung microbiome in pulmonary tuberculosis – a pilot study. *Emerg. Microbes Infect*. 2020;9(1):1444–1452. DOI: 10.1080/22221751.2020.1783188.
38. Xiao G., Cai Z., Guo Q., Ye T., Tang Y., Guan P. et al. Insights into the unique lung microbiota profile of pulmonary tuberculosis patients using metagenomic next-generation sequencing. *Microbiol .Spectr*. 2022;10(1):e01901-21. DOI: 10.1128/spectrum.01901-21.
39. Ueckermann V., Lebre P., Geldenhuys J., Hoosien E., Cowan D., van Rensburg L.J. et al. The lung microbiome in HIV-positive patients with active pulmonary tuberculosis. *Sci. Rep*. 2022;12(1):8975. DOI: 10.1038/s41598-022-12970-3.
40. Cheung M.K., Lam W.Y., Fung W.Y.W., Law P.T.W., Au C.H., Nong W. et al. Sputum microbiota in tuberculosis as revealed by 16S rRNApyrosequencing. *PLoS One*. 2013;8(1):e54574. DOI: 10.1371/journal.pone.0054574.
41. Botero L.E., Delgado-Serrano L., Cepeda M.L., Bustos J.R., Anzola J.M., Del Portillo P. et al. Respiratory tract clinical sample selection for microbiota analysis in patients with pulmonary tuberculosis. *Microbiome*. 2014;2:29. DOI: 10.1186/2049-2618-2-29.
42. HaileMariam M., Yu Y., Singh H., Teklu T., Wondale B., Worku A. et al. Protein and microbial biomarkers in sputum discern acute and latent tuberculosis in investigation of pastoral ethiopian cohort. *Front. Cell. Infect.Microbiol*. 2021;11:595554. DOI: 10.3389/fcimb.2021.595554.
43. Zhang M., Shen L., Zhou X., Chen H. The microbiota of human lung of pulmonary tuberculosis and the alteration caused by anti-tuberculosis drugs. *Curr. Microbiol*. 2022;79(11):321. DOI: 10.1007/s00284-022-03019-9.
44. Krishna P., Jain A., Bisen P.S. Microbiome diversity in the sputum of patients with pulmonary tuberculosis. *Eur. J. Clin. Microbiol. Infect. Dis*. 2016;35(7):1205–1210. DOI: 10.1007/s10096-016-2654-4.
45. Xia X., Chen J., Cheng Y., Chen F., Lu H., Liu J. et al. Comparative analysis of the lung microbiota in patients with respiratory infections, tuberculosis, and lung cancer: A preliminary study. *Front. Cell. Infect. Microbiol*. 2022;12:1024867. DOI: 10.3389/fcimb.2022.1024867.
46. Ticlla M.R., Hella J., Hiza H., Sasamalo M., Mhimbira F., Rutaihwa L.K. et al. The sputum microbiome in pulmonary tuberculosis and its association with disease manifestations: A cross-sectional study. *Front. Microbiol*. 2021;12:633396. DOI: 10.3389/fmicb.2021.633396.
47. Ding L., Liu Y., Wu X., Wu M., Luo X., Ouyang H. et al. Pathogen metagenomics reveals distinct lung microbiota signatures between bacteriologically confirmed and negative tuberculosis patients. *Front. Cell. Infect. Microbiol*. 2021;11:708827. DOI: 10.3389/fcimb.2021.708827.
48. Nakhaee M., Rezaee A., Basiri R., Soleimanpour S., Ghazvini K. Relation between lower respiratory tract microbiota and type of immune response against tuberculosis. *Microb. Pathog*.2018;120:161–165. DOI: 10.1016/j.micpath.2018.04.054.
49. Zhou Y., Lin F., Cui Z., Zhang X., Hu C., Shen T. et al. Correlation between either *Cupriavidus* or *Porphyromonas* and primary pulmonary tuberculosis found by analysing the microbiota in patients' bronchoalveolar lavage fluid. *PloS One*. 2015;10(5):e0124194. DOI: 10.1371/journal.pone.0124194.
50. Sala C., Benjak A., Goletti D., Banu S., Mazza-Stadler J., Jaton K. et alMulticenter analysis of sputum microbiota in tuberculosis patients. *PLoS One*. 2020;15(10):e0240250. DOI: 10.1371/journal.pone.0240250.
51. Kateete D.P., Mbabazi M.M., Nakazzi F., Katabazi F.A., Kigozi E., Ssengooba W. et al. Sputum microbiota profiles of treatment-naïve TB patients in Uganda before and during first-line therapy. *Sci. Rep*. 2021;11(1):24486. DOI: 10.1038/s41598-021-04271-y.
52. Segal L.N., Clemente J.C., Li Y., Ruan C., Cao J., Danckers M. et alAnaerobic bacterial fermentation products increase tuberculosis risk in antiretroviral treated HIV-patients. *Cell. Host. Microbe*. 2017;21(4): 530–537. DOI: 10.1016/j.chom.2017.03.003.
53. Trompette A., Gollwitzer E.S., Yadava K., Sichelstiel A.K., Sprenger N., Ngom-Bru C. et al. Gut microbiota metabolism of dietary fiber influences allergic airway disease and hematopoiesis. *Nat. Med*. 2014;2 (2):159–166. DOI: 10.1038/nm.3444.
54. Ribeiro-Rodrigues R., Resende Co T., Rojas R., Toossi Z., Dietze R., Boom W.H. et al. A role for CD4+CD25+ T cells in regulation of the immune response during human tuberculosis. *Clin. Exp. Immunol*. 2006;144(1):25–34. DOI: 10.1111/j.1365-2249.2006.03027.x.
55. Sharma P.K., Saha P.K., Singh A., Sharma S.K., Ghosh B., Mitra D.K. FoxP3+ regulatory T cells suppress effector T-cell function at pathologic site in miliary tuberculosis. *Am. J. Respir. Crit. Care Med*. 2009;179(11):1061–1070. DOI: 10.1164/rccm.200804-529oc.
56. Dickson R.P., Erb-Downward J.R., Freeman C.M., McCloskey L., Beck J.M., Huffnagle G.B. et al. Spatial variation in the healthy human lung microbiome and the adapted island model of lung biogeography. *Ann. Am. Thorac. Soc*. 2015;12(6):821–830. DOI: 10.1513/annalsats.201501-029oc.
57. Berger G., Wunderink R.G. Lung microbiota: Genuine or artifact? *Isr. Med. Assoc. J.* 2013;15(12):731–733.
58. Kovaleva O., Podlesnaya P., Rashidova M., Samoilova D., Petrenko A., Zborovskaya I. et al. Lung microbiome differentially impacts survival of patients with non-small cell lung cancer depending on tumor stroma phenotype. *Biomedicines*. 2020;8(9):349. DOI: 10.3390/biomedicines8090349.
59. Yu G., Gail M.H., Consonni D., Carugno M., Humphrys M., Pesatori A.C. et al. Characterizing human lung tissue microbiota and its relationship to epidemiological and clinical features. *Genome Biol*. 2016;17(1):163. DOI: 10.1186/s13059-016-1021-1.
60. Carney S.M., Clemente J.C., Cox M.J., Dickson R.P., Huang Y.J., Kitsios G.D. et al. Methods in lung microbiome research. *Am. J. Respir. Cell. Mol. Biol*. 2020;62(3):283–299. DOI: 10.1165/rcmb.2019-0273tr.
61. Twigg H.L., Morris A., Ghedin E., Curtis J.L., Huffnagle G.B., Crothers K. et al. Use of bronchoalveolar lavage to assess the respiratory microbiome: signal in the noise. *Lancet Respir. Med*. 2013;1(5):354–356. DOI: 10.1016/s2213-2600(13)70117-6.
62. Salter S.J., Cox M.J., Turek E.M., Calus S.T., Cookson W.O., Moffatt M.F. et al. Reagent and laboratory contam-

ination can critically impact sequence-based microbiome analyses. *BMC Biol*. 2014;12:87. DOI: 10.1186/s12915-014-0087-z.
63. Charlson E.S., Bittinger K., Haas A.R., Fitzgerald A.S., Frank I., Yadav A. et al. Topographical continuity of bacterial populations in the healthy human respiratory tract. *Am. J.Respir. Crit. Care Med*. 2012;184(8):957–963. DOI: 10.1164/rccm.201104-0655oc.
64. Marotz C.A., Sanders J.G., Zuniga C., Zaramela L.S., Knight R., Zengler K. Improving saliva shotgun metagenomics by chemical host DNA depletion. *Microbiome*.2018;6(1):42. DOI: 10.1186/s40168-018-0426-3.
65. Klimenko E.S., Pogodina A.V., Rychkova L.V., Belkova N.L. The ability of taxonomic identification of *Bifidobacteria* based on the variable regions of 16S rRNA gene. *Russian Journal of Genetics*. 2020;56(8):904–914 (in Russ.). DOI: 10.31857/s001667582008007x.
66. Sulaiman I., Wu B.G., Li Y., Scott A.S., Malecha P., Scaglione B. et al. Evaluation of the airway microbiome in nontuberculous mycobacteria disease. *Eur. Respir. J*. 2018;52(4):1800810. DOI: 10.1183/13993003.00810-2018.
67. Erb-Downward J.R., Thompson D.L., Han M.K., Freeman C.M., McCloskey L., Schmidt L.A. et al. Analysis of the lung microbiome in the "healthy" smoker and in COPD. *PLoS One*. 2011;6(2):e16384. DOI: 10.1371/journal.pone.0016384.

Authors' information

Orlova Elizaveta A. – Post-Graduate Student, Junior Researcher, Laboratory for Epidemic and Social Infections, Institute of Epidemiology and Microbiology, RC FHHRP, Irkutsk, elizaveta.a.orlova@gmail.com, http://orcid.org/0000-0003-2169-0242

Ogarkov Oleg B. – Dr. Sci. (Med.), Head of the Institute of Epidemiology and Microbiology, RC FHHRP, Irkutsk, obogarkov@mail.ru, https://orcid.org/0000-0002-3168-1983

Kolesnikova Lyubov I. – Dr. Sci. (Med.), Professor, Academician of RAS, Scientific Supervisor, RC FHHRP, Irkutsk, iphr@sbamsr.irk.ru, https://orcid.org/0000-0003-3354-2992

(✉) **Orlova Elizaveta A.,** elizaveta.a.orlova@gmail.com

Received 07.09.2023;
approved after peer review 22.09.2023;
accepted 16.11.2023

300 ЛЕТ РОССИЙСКОЙ АКАДЕМИИ НАУК

Праздничный вечер, посвященный 300-летию Российской академии наук, состоялся в Государственном Кремлевском дворце 8 февраля 2024 года. Событие собрало ведущих ученых страны. Отечественных исследователей поздравили с юбилеем президент России Владимир Владимирович Путин и президент РАН Геннадий Яковлевич Красников.

В ходе официальной части праздника состоялось вручение государственных наград выдающимся академикам и премий президента в области науки и инноваций для молодых ученых. Вечер продолжился масштабным праздничным концертом, отразившим историю развития Российской академии наук и отечественной культуры в музыке, танцах, балете и костюмированных постановках.

Президент страны перечислил важнейшие планируемые преобразования в деятельности Российской академии наук. В первую очередь РАН должна активно участвовать в принятии ключевых государственных решений — именно с этой целью ее глава был включен в Совет безопасности Российской Федерации. Планируется, что академия наук будет проводить экспертизу значимых научно-технологических проектов страны, а также школьных и вузовских учебников.

В.В. Путин отметил, что Российской академии наук будет отведена ведущая роль в исследовательских программах по ключевым направлениям, таким как космос, микроэлектроника, квантовые и биотехнологии, генетика. Помимо этого, на РАН возлагается ответственность за деятельность Высшей аттестационной комиссии и диссертационных советов. Президент добавил, что для реализации общих целей академии должны сплоченно работать все региональные отделения и центры РАН. Еще одно важное преобразование — увеличение роли академии наук в проведении фундаментальных исследований. В состав Российской академии наук должны войти Российский центр научной информации и издательство «Наука», основанное в 1727 г. «Отмечу, что общий объем госрасходов на научные исследования и разработки гражданского назначения в ближайшие три года превысит полтора триллиона рублей», — заявил В.В. Путин.

bulletin.ssmu.ru

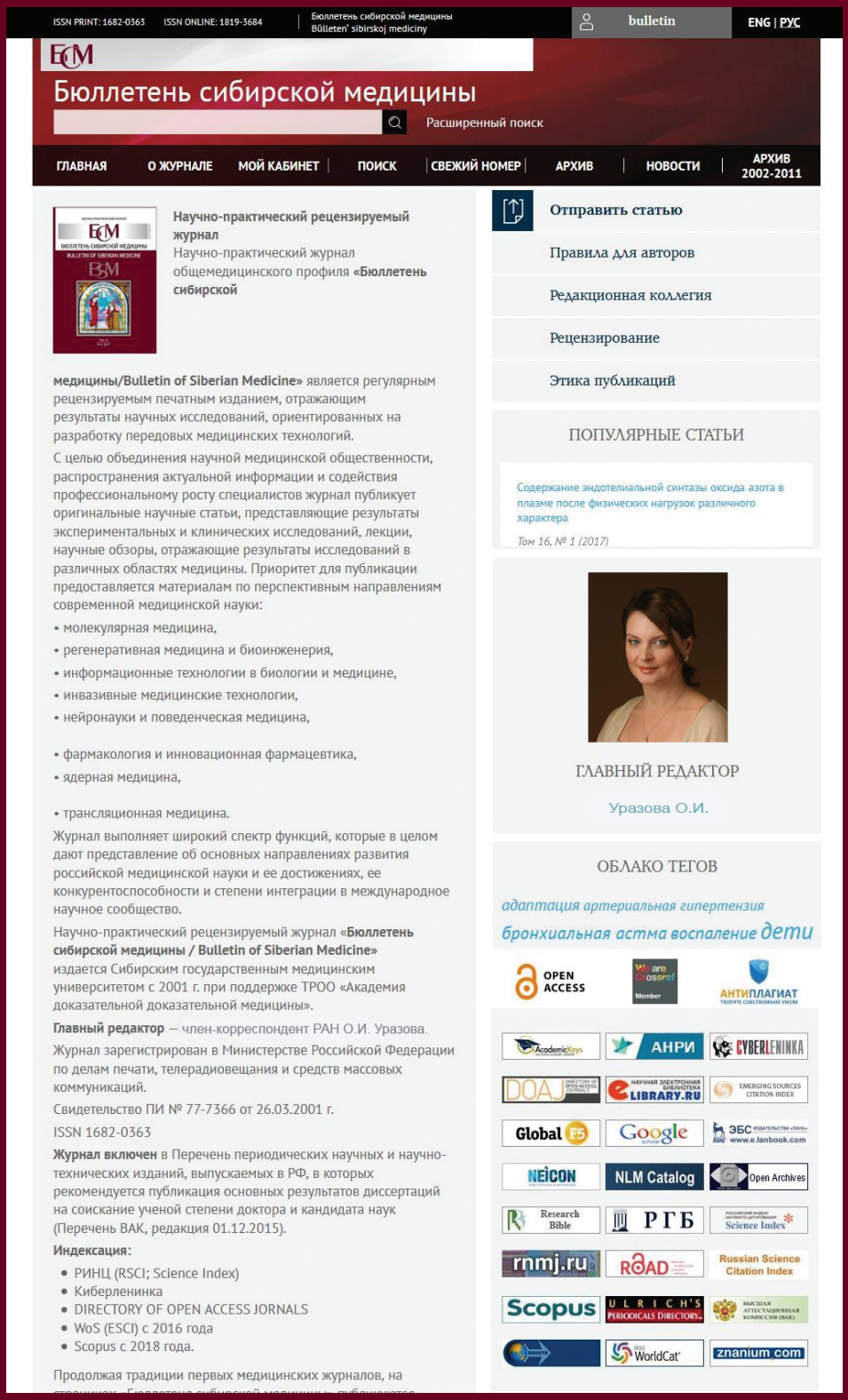

ISSN 1682-0363 (print)
ISSN 1819-3684 (online)
БЮЛЛЕТЕНЬ СИБИРСКОЙ МЕДИЦИНЫ
2024. Т. 23. № 1. 1–175